Controls on mineralisation in the Cadeby formation (lower magnesian linestone)

Thesis

CONTROLS ON MINERALISATION IN THE CADEBY FORMATION (LOWER MAGNESIAN LIMESTONE)

by

Gillian Margaret Harwood

Thesis submitted to the Open University for the Degree of Doctor of Philosophy

December 1981

ACKNOWLEDGMENTS

I would like to thank the many people who made this thesis possible particularly Denys Smith for suggesting the original project and making numerous constructive comments on this manuscript and my two supervisors, Ian Gass and George Hornung. Ian has made many helpful comments and has helped to provide an indirect source of finance.

Many people in the departments at Leeds and the Open University have helped; Finlay Johnstone co-ordinated services at Leeds, Andy Tindle at the Open University spent considerable time calibrating the probe for carbonates. Tony Dickson at Nottingham introduced me to cathodoluminescence and helped with th techniques and instrument time. Rick Smith showed me the Durham localities and has spent much time in discussions of Permian mineralisation. Jan Kramers first suggested lead isotope determinations and helped with sample preparation and isotope measurements; Max Coleman did the stable isotope determinations. Many others at Leeds and the Open University have helped in discussion and encouragement.

Paula Reece spent many hours typing this thesis in a very short period; without her hard work this thesis would never have been finished on time. Kirsty, Joe and Malcolm have helped (and hindered!) throughout this research but found that rocks were not always boring. Martin Bigland helped with some photography. Finally I should like to thank Bryan for his support in many ways over the last few months.

"I find it astonishing that you can be so enthusiastic about such grotty rocks".

I.G. Gass, written comm., 1981

THE UNIVERSITY OF NEWCASTLE UPON TYNE

HEAD OF DEPARTMENT:
PROFESSOR D. G. MURCHISON, F.R.S.E.

DEPARTMENT OF GEOLOGY
THE UNIVERSITY NEWCASTLE UPON TYNE NE1 7RU
TELEPHONE NEWCASTLE 328511

12th October, 1983

I hearby state that I am willing to let my Ph.D. thesis, 'Controls on mineralization in the Cadeby Formation', be made available to readers and to be photocopied subject to the discretion of the Librarian.

Gill M. Harwood.

CONTROLS OF MINERALIZATION IN THE PERMIAN CADEBY FORMATION

G.M. HARWOOD

Short Abstract

Several distinct low grade assemblages of baryte and/or base metal sulphides are present within the Cadeby Formation at outcrop, each assemblage being restricted to a certain geographical area and, sometimes, one stratigraphic horizon. Although some occurrences are fault controlled, the majority have a stratigraphic control related to both carbonate facies and diagenetic history. High energy carbonate facies and bryozoan patch reefs are devoid of mineralization, whereas lower energy facies may host stratiform sulphides and baryte. Mineralization is also related to former displacive evaporites, either by direct replacement or by precipitation in voids resultant from evaporite dissolution. Diagenesis is complex with different mechanisms of dolomitization, evaporite replacement and dedolomitization; mineralization is related to early diagenesis at some localities. The spatial occurrences of mineralized localities suggests an underlying structural control linked with basement tectonics. Although isotope determinations indicate most sulphur has derived from interbedded evaporites, metals may have been introduced through basement fractures, be derived from within the formation or related to Kupferschiefer/Marl Slate mineralization. No common origin for the Permian mineral occurrences therefore exists.

Controls of Mineralisation in the Cadeby Formation (Lower Magnesian Limestone)

G.M. HARWOOD

Long Abstract

An initial summary of mineralisation near the top of the Cadeby Formation at outcrop demonstrated that both sedimentology and diagenesis act to control mineralised occurrences within the dolomitised carbonates. Mineralisation was not directly related to open fractures.

A brief sedimentological study defined a variety of facies which developed on a broad shallow carbonate platform. Siliciclastic carbonates were confined to the southern part of the outcrop. In the Lower Member, low energy lagoon facies were developed in two areas. Both these areas contain evidence for the existence of penecontemporaneous displacive evaporites. Moderate energy facies in the Lower Member are represented by a zone of shallow water to intertidal peloid packstones with skeletal packstones and wackestones near the base of the formation. Patch reefs occur further from the palaeoshore in slightly deeper water. Peloid grainstone barriers protect lagoon environments. A slight regression formed the crypt algal laminites and intertidal/supratidal carbonates of the Hampole Beds.

The Upper Member at outcrop is dominated by peloid grainstones and packstones which form a major barrier facies of large dune and shoal forms over the sub-horizontal surface of the Hampole Beds. Crypt algal laminites, present in a few localities near the top of the Upper Member, contain evidence

of palaeo-sabkha formation. Breccias, from penecontemporaneous erosion of peloid grainstones, are found in one area.

Diagenesis in the Cadeby Formation is complex. Dolomitisation is demonstrated to be penecontemporaneous, eogenetic and mesogenetic. Penecontemporaneous dolomitisation is restricted to lagoon facies; in places it is associated with calcitisation of evaporites. Penecontemporaneous dolomitisation results from storm recharge and subsequent evaporation and desiccation of the lagoons. Later large scale seepage reflux caused pervasive dolomitisation throughout most of the formation. Evaporite-saturated pore fluids subsequently formed replacive evaporite aggregates and evaporite porosity-occluding cements. In the southern region evaporites were not so prevalent and coarse subhedral sucrose dolomite rhombs formed in the mixing zone between hypersaline marine brines and continental groundwaters. During mesogenesis some of the evaporites were leached; limpid dolomite crystals partially occluded some resultant vugs. In other zones ferroan dolomite formation and anhedral dolomite remobilisation to sub- or eu-hedral dolomites occurred. Subsequent ferroan-dedolomitisation was patchy.

During telogenesis anhydrite was converted to gypsum which was later mostly leached by fluctuating groundwaters. The resultant calcium-rich waters precipitated calcite-spar cements or caused dedolomitisation. Large areas were partially leached and contain dispersed dedolomite.

Mineralisation comprises baryte and/or galena and/or sphalerite. Baryte forms large replacive flats in two areas.

Copper mineralisation is only known in two districts. Occurrences of mineralisation fall into distinct districts, many of which overly prominent basement structures. Metals in penecontemporaneous mineralisation come from surrounding sediments; penecontemporaneous mineralisation is low grade and restricted to lagoon facies. Metals in mesogenetic mineralisation may be derived from the underlying basement; alternatively, the basement structures may play an important role in stimulating mineralising fluid circulation without supplying the metals themselves. Sulphur comes largely from the interbedded or overlying evaporites; some may come from later (Jurassic) sea water sulphate.

In the Cadeby Formation sedimentology and diagenesis combine in areas to form a porous carbonate which could be an excellent host for mineralisation or hydrocarbons. Its future economic potential should not be overlooked.

CONTENTS

LIST OF CONTENTS

REFERENCES

Attached in pocket:

Reprints: Calcitised anhydrite and associated sulphides in the English Zechstein First Cycle Carbonate (EZ1 Ca).

Baryte mineralisation related to hydraulic fracturing in English Permian Z1 carbonates

Isotopic evidence for Controls of mineralisation in the Permian lower Magnesian Limestone

PART I

INTRODUCTION AND SEDIMENTOLOGY

CHAPTER 1

Introduction and previous research

1.1 Introduction

In eastern England the Upper Permian is represented by Zechstein strata, a series of carbonates and evaporites. The lowest carbonate, the Cadeby Formation or Lower Magnesian Limestone, was known to contain several occurences of base metal sulphide and baryte mineralisation (e.g. Sedgwick, 1829; Marshall, 1856, Fowler, 1943, Deans, 1961). The uppermost bed of the Cadeby Formation is mineralised at several localities (Deans, 1961) and the original objective of this thesis was to investigate these occurences along the southern section of the Permian outcrop in eastern England between Catterick and Nottingham, using a geochemical approach. A combination of reasons led to the broadening of the project into investigating mineralised localities throughout the Cadeby Formation. Some core material was also examined. This thesis attempts to describe the main mineral assemblages in the Cadeby Formation and to relate their occurence and distribution to sedimentology; diagenesis and basement features.

The Cadeby Formation produces good quality arable land and is intensely farmed. Abandoned quarries and railway cuttings are rapidly in-filled by refuse

from large towns near the outcrop. Working quarries have inaccessible quarry facies and access is prevented in many due to the policy of certain roadstone companies. Accessible exposure is therefore poor and it is often impossible to correlate exactly from one outcrop, or series of outcrops, to the next.

1.2 Previous research

1.2.1 Stratigraphy of the Upper Permian

The pioneering work on the Permian strata at outcrop was done by Sedgwick (1829) who recognised two major carbonates, the Upper and Lower Magnesian Limestones, and, at the end of his paper, compared them to strata of similar age in Germany. Other early workers included Wilson (1881), particularly in the south of the outcrop, Phillips (1875), and Marshall (1856). Their work was extended in the late nineteenth and early twentieth centuries by Geological Survey Memoirs (notable authors Fox-Strangeways and Aveline) and by local amateur geologists (Tute, 1868; 1884; Trechmann, 1914; 1931). Sherlock (1911) postulated a southerly transition of the carbonates into the continental series of sands, marls and pebble beds, hitherto considered Triassic in age. He also

correlated the Upper Permian carbonates with the Zechstein carbonates of Northern Europe.

By the commencement of the First World War the main lithological boundaries of the Upper Permian strata at outcrop in Yorkshire and Nottinghamshire were established (Fig 1.1) and many of the fossils contained described. The patchy nature of the basal sands and breccias and the irregularity of the underlying carboniferous surface, confused by Sedgwick, was also established.

Until the 1940s, with the exception of some Geological Survey Memoirs, little more information was pub-lished on the Permian strata and, although evaporites were known to be present in the subsurface at Teeside (Marley 1864; Trenchmann, 1913) and were extracted at Billingham in 1930 (Smith, 1974b), there was no indication of the extent of evaporites at depth in East Yorkshire. Colliery shafts sunk through the Permian at this period were in South Yorkshire and Nottinghamshire (Edwards, 1951; Wilcockson, 1951) where evaporites are not well developed. Records of Thorne colliery shaft, however, show over 7.25 metres of anhydrite in the 'Permian Middle marl' (Wilcockson, 1951, p. 486-7).

Hydrocarbon exploration and I.G.S. boreholes revealed the extent of the evaporites. Discovery

Figure 1.1 Permian stratigraphy in Yorkshire (1914)

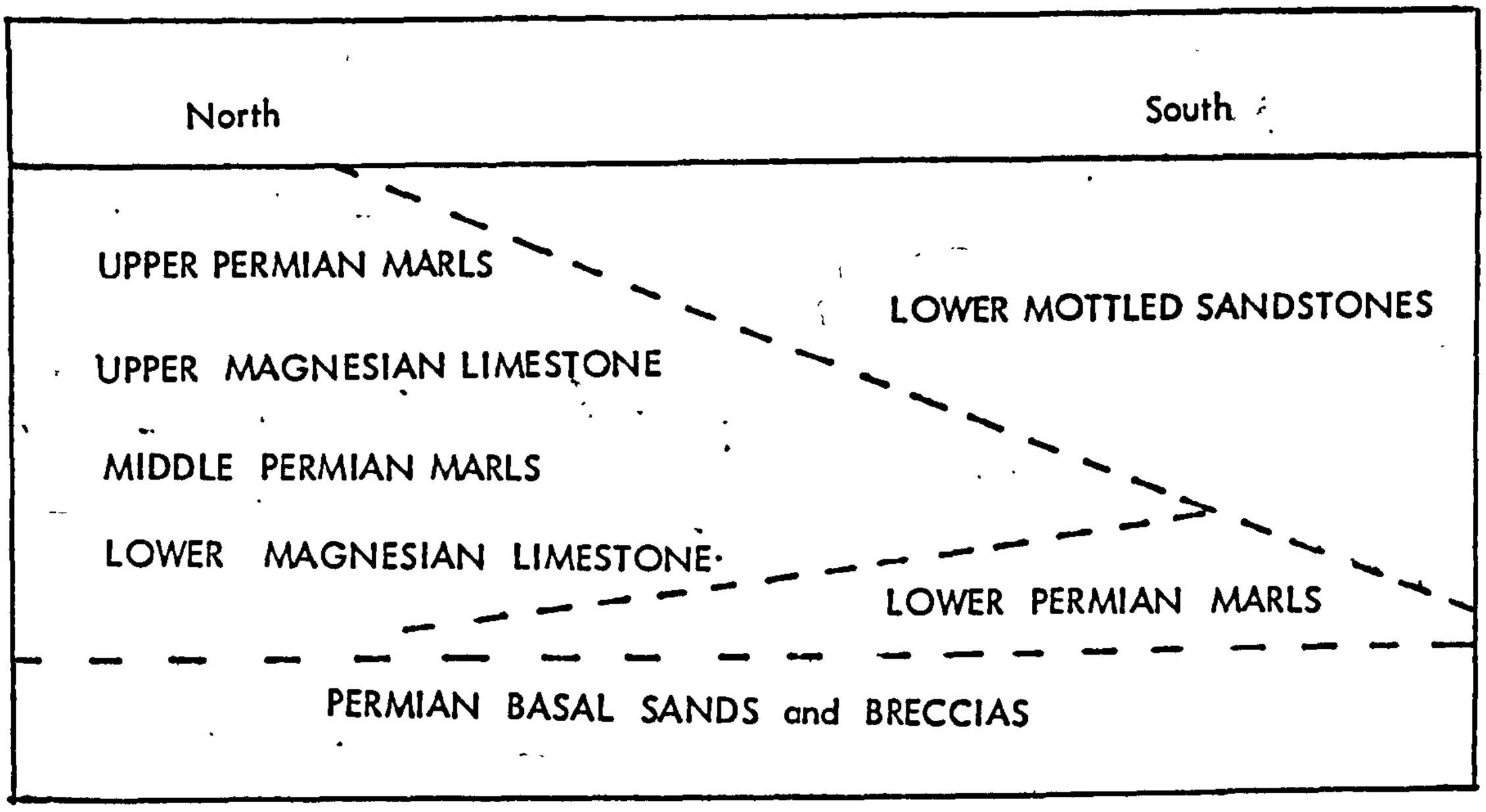
North
South
UPPER PERMIAN MARLS
UPPER MAGNESIAN LIMESTONE
MIDDLE PERMIAN MARLS
LOWER MAGNESIAN LIMESTONE
LOWER MOTTLED SANDSTONES
LOWER PERMIAN MARLS
PERMIAN BASAL SANDS and BRECCIAS

of gas in Permian carbonates at Hayton and Eskdale led to further wildcat exploration holes and realisation of the presence of hundreds of metres of anhydrite and halite (Falcon and Kent, 1953) and proved the existence of a further carbonate, the Kirkham Abbey Formation, which does not extend as far west as the present outcrop. Upper Permian isopachs for the carbonates and evaporites were constructed by Taylor and Colter (1975); core descriptions of individual boreholes are reported by Fowler (1944), Stewart (1949, 1951a, 1951b, 1963), Raymond (1953) and Brunstrom (1962). The wealth of recent information on subsurface strata, both onshore and offshore, has enabled broad correlation between Durham and Yorkshire (commenced by Sherlock, 1926; Taylor and Fong, 1969) and across the North Sea Basin into the Netherlands, Germany, Poland and Denmark (Figs. 1.2 and 1.3).

Five separate cycles are now recognised throughout most of the Zechstein Basin (Fig 1.2). German terminology is used throughout the North Sea Basin as the stimulus for development was the Groningen Gas Field in the north-east Netherlands. Correlation between England and Germany is not exact; the prefix E is therefore used before the English Zechstein cycles (Fig 1.2). Recent drilling has shown that there were two major

Figure 1.2 Permian stratigraphy (1981)

	Yorkshire	Durham	Germany	
EZ5	Saliferous Marl Formation* / Permian Upper Marls*	Saliferous marl* / Top Anhydrite	Zechsteinletten / Grenzanhydrit	Z5
		Sleights siltstone*		
EZ4		Upper anhydrite	Aller halite / Pegmatitanhydrit	Z4
		Carnallitic Marl*	Roter salzton*	
EZ3	Brotherton Formation / Upper Magnesian Limestone	Boulby halite / Billingham main anhydrite / Seaham Formation	Leine halite / Hauptanhydrit / Plattendolomit / Grauer salzton*	Z3
EZ2	Ripon Formation* / Permian Middle Marls*	Fordon evaporites / Kirkham Abbey Formation	Stassfurt series / Hauptdolomit / Roker Formation / Upper Magnesian Limestone	Z2
EZ1	Cadeby Formation / Lower Magnesian Limestone	Hayton anhydrite / Upper Member / Lower Member / Marl Slate	Werra anhydrit / Ford Formation / Middle Magnesian Limestone / Zechsteinkalk / Raisby Formation / Lower Magnesian Limestone / Marl Slate / Kupferschiefer	Z1
	Permian Basal Sands*		Rotliegendes*	

*continental facies

Figure 1.3 Map showing the probable extent of the Zechstein Basin and north North Sea Basin during the first Zechstein cycle (modified from Ziegler, 1981).

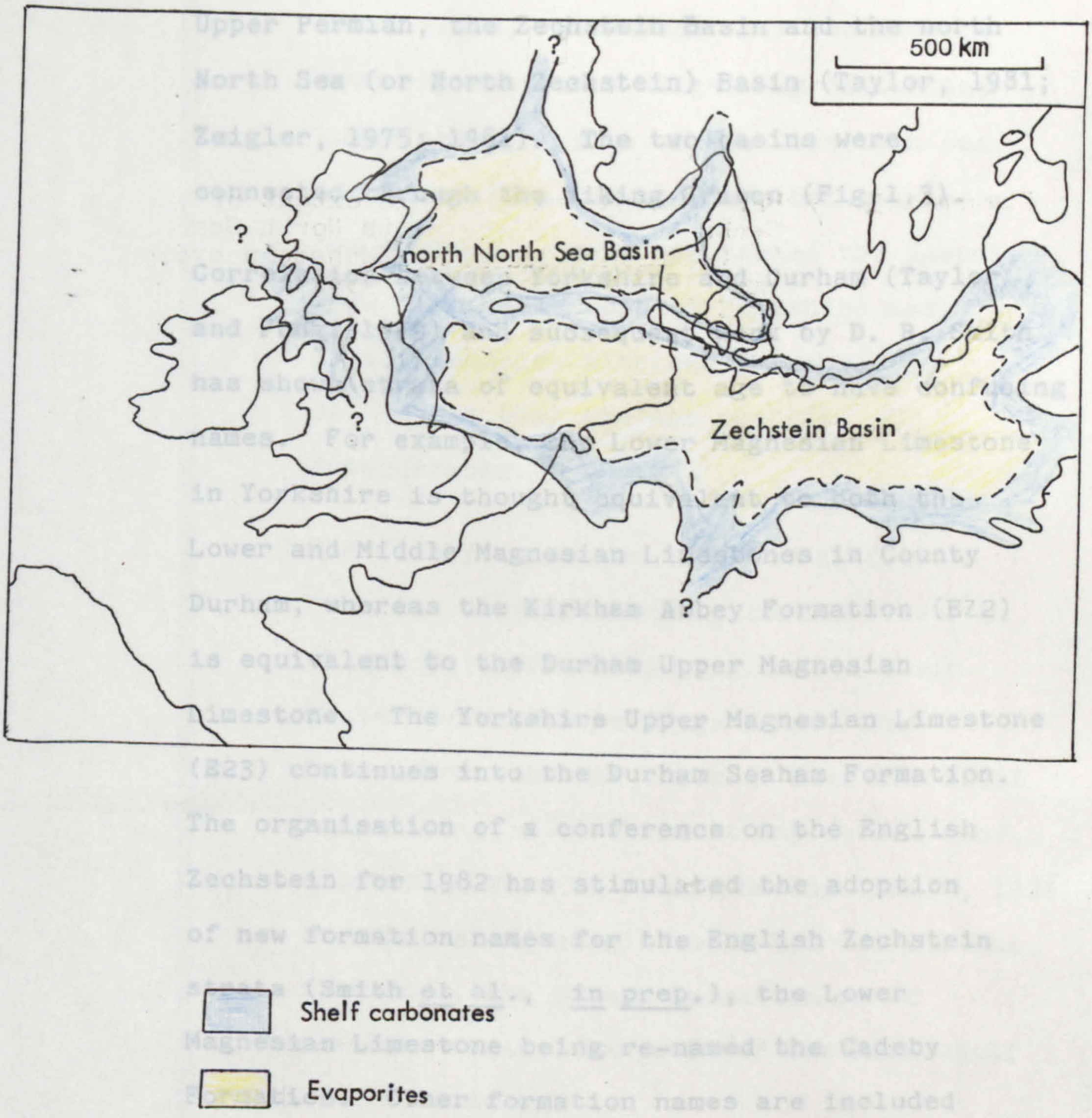
500 km
?
?
?
?
north North Sea Basin
Zechstein Basin
Shelf carbonates
Evaporites

evaporite basins in the North Sea area in the Upper Permian, the Zechstein Basin and the north North Sea (or North Zechstein) Basin (Taylor, 1981; Zeigler, 1975; 1981). The two basins were connected through the Viking Graben (Fig 1.3).

Correlation between Yorkshire and Durham (Taylor and Fong, 1969) and subsequent work by D. B. Smith has shown strata of equivalent age to have confusing names. For example, the Lower Magnesian Limestone in Yorkshire is thought equivalent to both the Lower and Middle Magnesian Limestones in County Durham, whereas the Kirkham Abbey Formation (EZ2) is equivalent to the Durham Upper Magnesian Limestone. The Yorkshire Upper Magnesian Limestone (E23) continues into the Durham Seaham Formation. The organisation of a conference on the English Zechstein for 1982 has stimulated the adoption of new formation names for the English Zechstein strata (Smith et al., in prep.), the Lower Magnesian Limestone being re-named the Cadeby Formation. Other formation names are included on Figure 1.2.

1.2.2 The Cadeby Formation - sedimentology

Much of the available information on the Cadeby Formation sedimentology results from the detailed field work of D. B. Smith throughout Yorkshire and County Durham. Mitchell (1947) first mapped the Upper

and Lower Members of the Cadeby Formation. Smith (1968) recognised that the Hampole Beds represented a slight regression and later transgression of the Zechstein sea, and hence form the boundary between the two Members. Smith has traced the Hampole Beds throughout most of Yorkshire and Nottinghamshire although in many core se- ctions they are not readily recognisable.

The Cadeby Formation thickens eastwards from its outcrop reaching some 100 metres (Fig 1.4a) before thinning into a basin facies further east (Figs 1.4a). The Cadeby Formation is thickest near the shelf margin (Fig 1.4a) where it may form a reef, similar to that in County Durham (Smith, 1981) or other shelf margin build up. At outcrop, therefore, the Cadeby Formation is of platform facies, landward of the main shelf margin build-up.

The lowest Zechstein formation, the Marl Slate (Fig 1.2) does not outcrop in Yorkshire and Nottinghamshire but is present in the subsurface further east. The Cadeby Formation therefore rests uncomformably on Carboniferous strata, or overlies pockets of Permian Basal

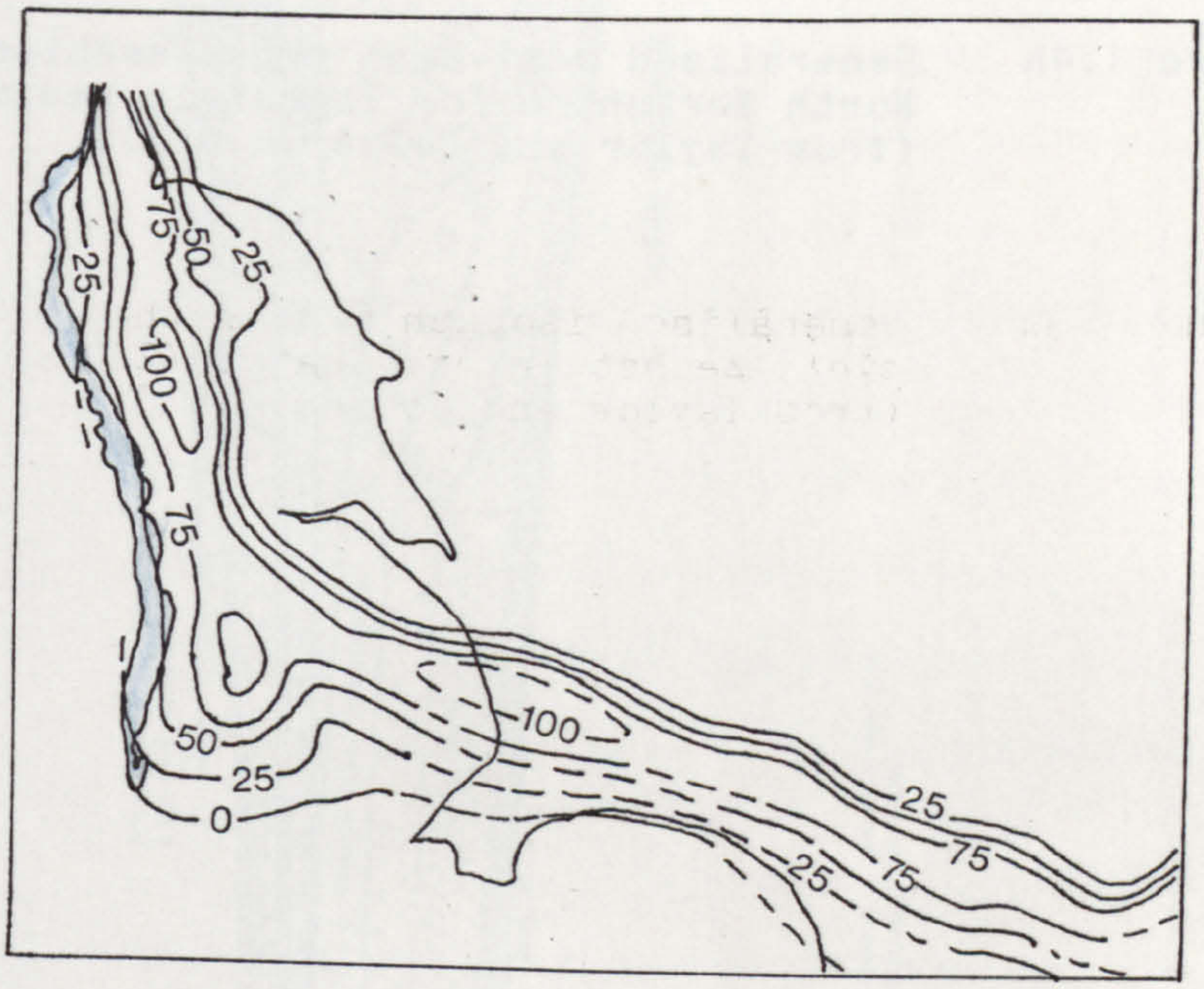
75
50
25
25
100
75
50
25
0
100
25
75
25
75

Figure 1.4b Generalised west-east cross-section North Yorkshire for Zechstein sediments (from Taylor and Colter, 1975).

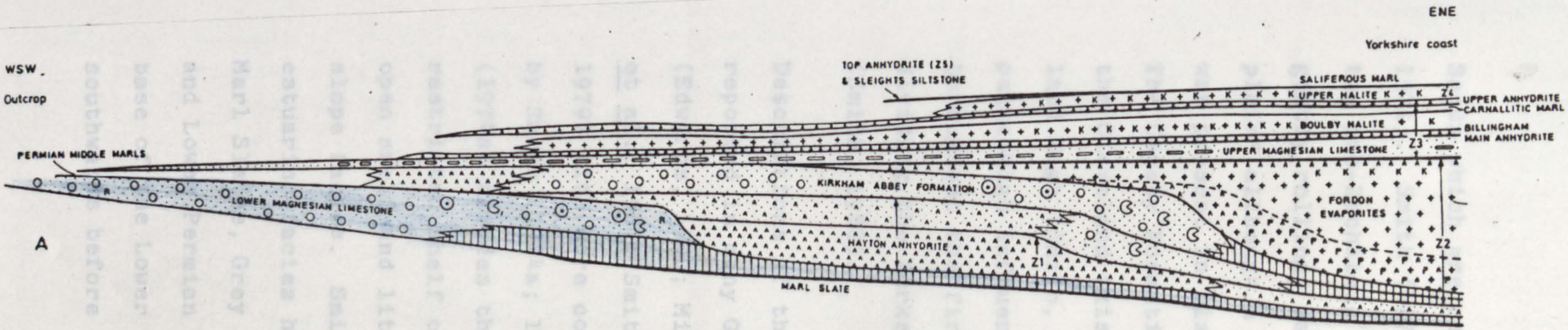
WSW
Outcrop
ENE
Yorkshire coast
TOP ANHYDRITE (Z5)
& SLEIGHTS SILTSTONE
SALIFEROUS MARL
UPPER HALITE
Z4
UPPER ANHYDRITE
CARNALLITIC MARL
BOULBY HALITE
BILLINGHAM
MAIN ANHYDRITE
Z3
UPPER MAGNESIAN LIMESTONE
PERMIAN MIDDLE MARLS
KIRKHAM ABBEY FORMATION
LOWER MAGNESIAN LIMESTONE
FORDON
EVAPORITES
Z2
HAYTON ANHYDRITE
Z1
MARL SLATE
A
NORTH YORKSHIRE
POTASH SALTS
POLYHALITE
HALITE
ANHYDRITE
DOLOMITE
LIMESTONE
REDBEDS
CALCINEMA
PISOLITHS
OOLITIC & PELLETOID SANDS
SKELETAL GRAINS
REEF
M
FT
300
1000
200
580
100
VERTICAL EXAGGERATION x 20
1 2 3 4 MILES
0 1 2 3 4 5 6 KM
NB THICKNESS OF IMPORTANT THIN UNITS
EXAGGERATED FOR CLARITY

Sands which are reworked in places (Pryor, 1971). Smith (1974a, p. 117) describes the pre-Zechstein surface as "a mature, gently rolling, eastward sloping pene-plain" although a considerable palaeo-relief was present in places (Chapter 3, 3.2). The Cadeby Formation thins northwards over the Cleveland axis (Rastall, 1963) or Cleveland High (Smith, 1974c) (Fig 1.5). This palaeohigh influenced sedimentation throughout the first two Zechstein cycles, dividing the Yorkshire and Durham Provinces (Smith, 1980).

Descriptions of the Cadeby Formation are reported in many Geological Survey Memoirs (Edwards, 1940; Mitchell, 1947; Edwards et al., 1967; Smith, 1973; Frost and Smart, 1979) with more comprehensive summaries by Smith (1974a; 1974c; 1980; 1981). Smith (1974a) divides the Lower Member into restricted shelf or estuarine facies open shelf and littoral facies, and basin slope facies. Smith's restricted shelf or estuarine facies have been variously termed Marl Slates, Grey Beds, Dolomite Silstones and Lower Permian Marls; they occur near the base of the Lower Member and thicken southwards before passing laterally into

Figure 1.5 Generalised north-south cross section through the Cadeby Formation.

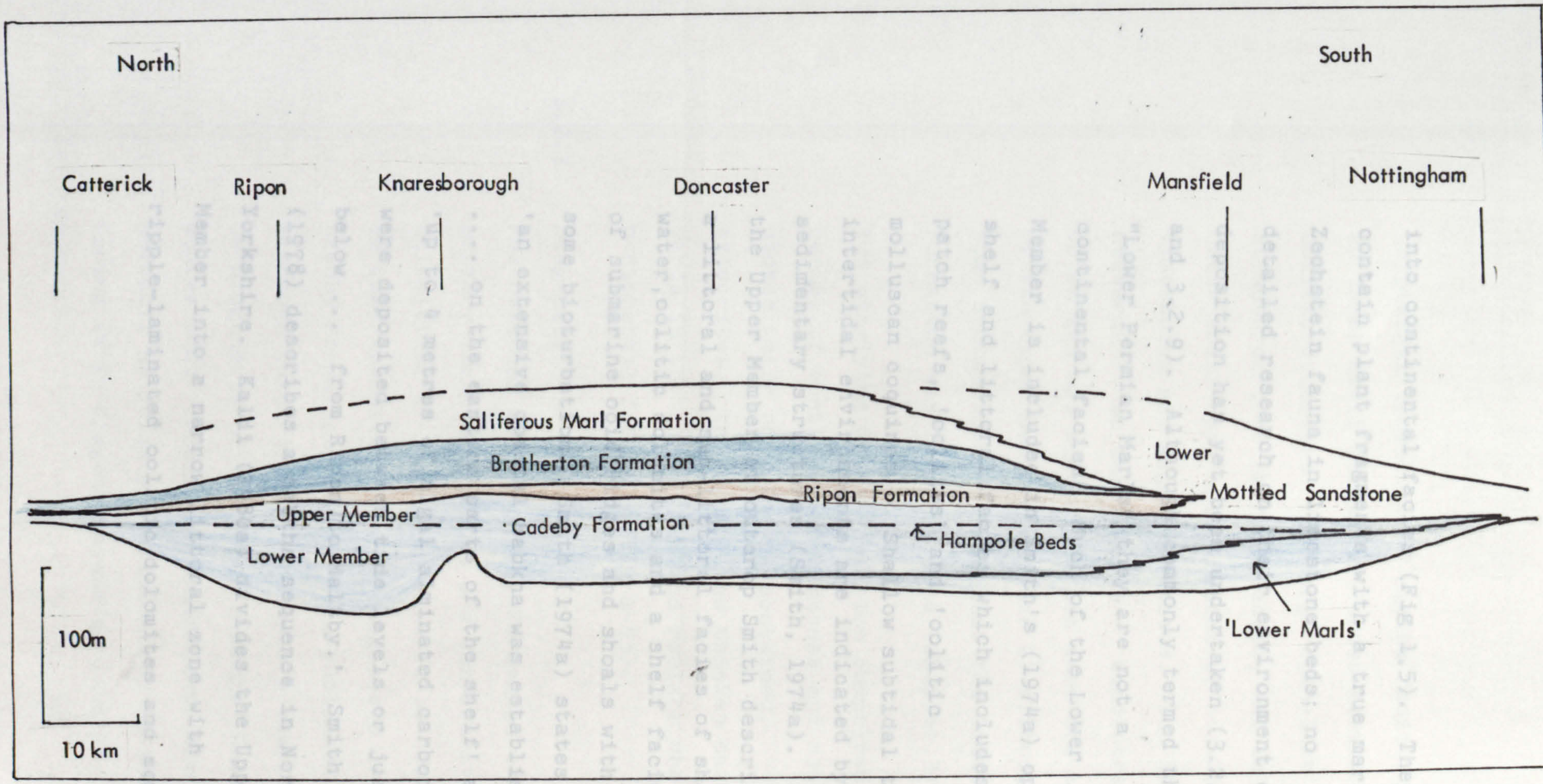
North
South
Catterick
Ripon
Knaresborough
Doncaster
Mansfield
Nottingham
Saliferous Marl Formation
Brotherton Formation
Ripon Formation
Upper Member
Cadeby Formation
Lower Member
Hampole Beds
Lower Mottled Sandstone
'Lower Marls'
100m
10 km

into continental facies (Fig 1.5). They contain plant fragments with a true marine Zechstein fauna in limestone beds; no detailed research on their environment of deposition has yet been undertaken (3.2.8 and 3.2.9). Although commonly termed the "Lower Permian Marls" they are not a continental facies. Much of the Lower Member is included in Smith's (1974a) open shelf and littoral facies which includes patch reefs, 'oolites' and 'oolitic molluscan coquinas'. Shallow subtidal to intertidal environments are indicated by the sedimentary structures (Smith, 1974a). In the Upper Member at outcrop Smith describes a littoral and sub-littoral facies of shallow water,oolitic dolomites and a shelf facies of submarine ooid ridges and shoals with some bioturbation. Smith (1974a) states 'an extensive coastal sabkha was established .... on the eastern parts of the shelf' and 'up to 4 metres of algal alminated carbonates were deposited between tide levels or just below ... from Ripon to Maltby.' Smith (1978) describes a sabkha sequence in North Yorkshire. Kaldi (1980a) divides the Upper Member into a narrow littoral zone with ripple-laminated oolitic dolomites and some

cryptalgal laminites of sabkha facies, an inner shelf facies of 'cross-stratified oolitic dolomites' on 'large dune-like structures', or barrier facies, and an outer shelf open water facies of nodular limestones and algal laminites. The initial research - in this thesis - concentrated on facies and mineralisation near the top of the Upper Member (Chapter 2) although some sedimentology throughout the Cadeby Formation was later studied (Chapter 3).

The overlying Ripon Formation comprises a series of continental mudstones and sandstones which contain, or contained, evaporites. The evaporites thicken eastwards in the subsurface and replace the continental facies. (Fig 1.4b).

1.2.3 Diagenesis

Few outcrops of the Cadeby Formation contain primary limestones; most are completely dolomitised or have been altered to dedolomites. No comprehensive study of diagenesis of the Cadeby Formation has yet been published although Kaldi (1980a) includes a chapter on diagenesis of the Upper Member. Kaldi states that 'dolomites formed penecontemporaneously, as primary precipitates, as cements during early diagenesis and as locally

controlled late diagenetic replacement.' He concludes that 'evaporites formed as early nodules within the supratidal zone or as a late diagenetic pore-fill.' He does not describe replacive evaporites, nor displacive gypsum crystals and does not detail evidence of displacive evaporite nodules.

1.2.4 Mineralisation

Although some of the earliest reports (Pilkington 1789; Sedgwick, 1829; Hunt, 1884) mention small mining ventures there has been no large scale extraction of mineralisation from the Cadeby Formation. Publications on Cadeby Formation mineralisation only cover restricted areas and most detailed studies of Permian mineralisation have been confined to the Marl Slate or its lateral equivalent, the Kupferschiefer (Deans, 1950; Hirst and Dunham, 1963; Brongersma Saunders, 1966; Turner et al., 1978; Vaughan and Turner, 1980).

The most comprehensive survey of mineralisation in the Cadeby Formation was by Deans (1961) who noted the occurence of galena and wulfenite at and near the top of the Upper Member; he concluded lead originated from (i) redeposition of syngenetic lead present in either the

carbonate of the Marl Slate or (ii) a similar origin to Derbyshire (Pennine) galenas. It was the combination of these occurences and Smith's sabkha hypothesis (1978) which led to the initiation of this research.

Many authors report small occurences of mineralisation. Aldred (1969) notes galena and baryte west of Mansfield within the "Lower Permian Marls" and near their boundary with the overlying carbonates. Other localities are mineralised near this boundary (Taylor and Elliot, 1971; Taylor, 1974). Aldred (1969) relates the localities to northwest-trending faults and suggests links with Pennine deposits. Ineson et al., (1972) found largescale baryte mineralisation at Whitwell, Derbyshire. Davies (1971) reported barium anomalies in stream sediments near Bramham, West Yorkshire, which were followed up by Barratt in an appendix to his thesis (1975). Baryte is also known from Aberford (P. R. Ineson, pers. comm., 1978) and at West Tanfield, North Yorkshire, baryte and galena occur on a fault plane (Lamming and Robertson, 1968).

Most references to Cadeby Formation mineralisation are to galena and/or baryte. Sphalerite is often overlooked due to its pale

honey (almost dolomite) colour. Barratt (pers. comm., 1979) found chalcopyrite at Bramham and Sedgwick (1829), Marshall (1856) and Hunt (1884) mention occurences of malachite at Newton Kyme, near Tadcaster and at Farnham, North Yorkshire. Copper mining at Farham around 1800 A.D. is mentioned in "The History of Farnham" (Prof. Versey, pers. comm., 1978). Other brief mentions of mineralisation appear in Geological Survey Memoirs. Reported mineralised localities and new localities discovered during this research are listed in Appendix 1.

1.3 Scope of this research

This thesis is divided into three parts; Introduction and Sedimentology, Diagenesis and Mineralisation. The early study of mineralisation near the top of the Cadeby Formation (Chapter 2) showed that mineralisation was controlled by sedimentology and diagenesis. Sedimentology is briefly covered in Chapter 3. Diagenesis studies showed a complex history of dolomitisation (Chapter 4), dolomite replacement (Chapter 5) as well as replacement by and of evaporites (Chapter 6). Whole rock geochemical analyses, done in conjunction with

the initial project, are discussed in relation to sedimentology and diagenetic history in Chapter 7.

Part III contains details of mineral assemblages (Chapter 8), the results of stable and lead isotope determinations (Chapter 9) and the relation of the structure of the pre-Permian basement to mineralisation and metal origins (Chapter 10). Thesis conclusions are in Chapter 11 with recommendations for future research.

The aims of this thesis are to delineate some of the controls of mineralisation within the Cadeby Formation and to use these to predict other areas of potential mineralisation which may possibly have some economic value. Research into diagenesis may also be important in the evaluation of hydrocarbon reserves in Zechstein carbonates both on-and off-shore.

CHAPTER 2

The top of the Cadeby Formation

2.1 The initial project

2.1.1 Outline and objectives

The initial project concerned investigation of occurrences of mineralisation at the top of the Upper Member of the Cadeby Formation and determination of trace element concentrations in the upper few metres in both mineralised and non-mineralised localities. The project was suggested by D.B. Smith, prompted by his interpretation of an exposure at Quarry Moor, south of Ripon (SE 308691) (Smith, 1976). Smith then considered the top of the Upper Member to be a fossil sabkha (i.e. an arid supratidal flat) extending over most of the outcrop area. The hypersaline brines produced by intense evaporation at the sabkha surface (2.2.2) may have also concentrated base metals. Research was warranted to determine if the mineralisation reported by Deans (1961) (1.2.4) was related to sabkha development and diagenesis.

2.1.2 Drawbacks

Lack of mineralisation at this level in the formation and the scarcity of localities where

controlled sampling was possible severely limited the project. Few exposures showed evidence of fossil sabkhas; they were, however, more common in cores (3.4.4; Fig 3.31). Leaching due to Pleistocene and Recent weathering combined with dedolomitisation (6.5.1, 5.3) meant that measured base metal concentrations were rarely representative of the original carbonates. Cores showed large scale replacement of carbonate by evaporites (6.3.2; Figs 6.3 a+b). No trace element concentrations measured could confidently be ascribed to sabkha diagenesis; most showed little concentration.

These drawbacks combined to provide insufficient substance for a thesis; a broader project surveying all the mineralisation in the Cadeby Formation was initiated, prompted by sphalerite occurrences at Wormald Green, N. Yorks. (SE 304650) (Harwood, 1980). This chapter describes the theory behind, and the results of the initial project.

2.2 Theory and methods

2.2.1 Sabkha morphology and sedimentology

Sabkhas are arid supratidal flats. Interest in them was stimulated by reports of Holocene

dolomite formation within Persian Gulf sabkha sediments (Curtis et al., 1963; Illing et al., 1965; Shearman, 1966; Evans et al., 1969). Research on sabkhas in other regions has followed (Butler, 1970; Levy, 1977; Sherif, 1978).

Sabkhas form in areas of shoreline progradation. An idealised vertical sediment profile is shown in Figure 2.1a and lateral profile in Figure 2.1b. Intertidal algal mats prograde over subtidal lagoon sediments. Continued progradation leads to the formation of supratidal sediments which contain windblown carbonate and quartz grains. Holocene sabkha surfaces may extend over several tens of kilometers (Fig 2.2) and are physiographically very flat; undulations are from upwarping caused by evaporite formation, aragonite precipitation and desiccation structures. Supratidal facies are characterised by nodular and/or enterolithic anhydrite and gypsum, penecontemporaneous dolomitisation of aragonite, tepee structures, contorted beds, desiccation polygons and sheet cracks. Fenestrae, rip-up clast breccias and local erosion surfaces show further evidence of exposure. Mineral and brine diagenesis within the sabkha is summarised by Figure 2.1c.

Figure 2.1a Vertical sediment profile through the Abu Dhabi sabkha, U.A.E. (from McKensie et al., 1980).

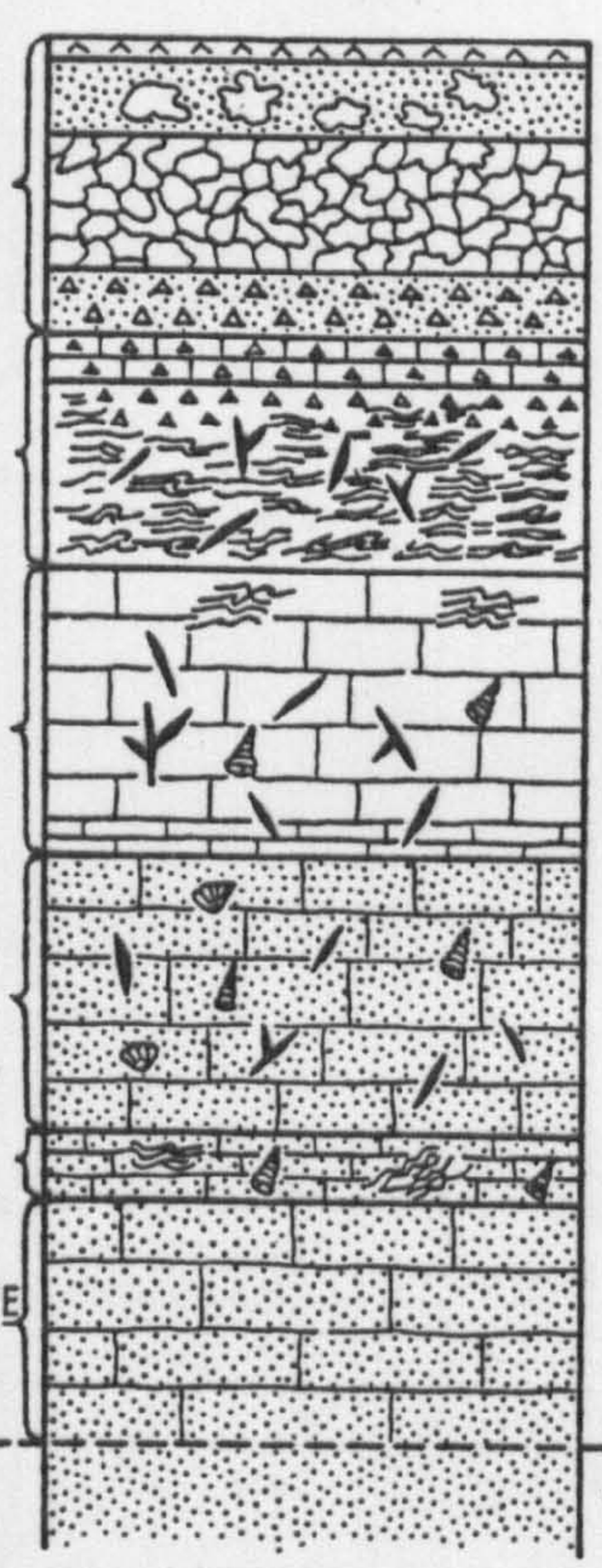

Unit	
7 SUPRATIDAL FACIES (0–100 cm)	– salt crust of halite crystals – eolian, brown, quartzose–carbonate sand with anhydrite nodules – massive, mosaic ("chickenwire") anhydrite – discoid gypsum mush in eolian sand
6 UPPER INTERTIDAL FACIES (60 cm)	– discoid gypsum mush in carbonate sand or mud – laminated algal mats with discoid gypsum mush and disks, intensely dolomitized
5 LOWER INTERTIDAL FACIES (60 cm)	– light, gray–green carbonate mud with scattered algal mats, cerithids and gypsum disks, intensely dolomitized, with base cemented to form a crust
4 SUBTIDAL FACIES (0–3000 cm)	– light, gray–green carbonate sand with varying carbonate mud composition, cerithids, bivalves and gypsum disks, dolomitized
3 LAGOON–INTERTIDAL FACIES	– algal mats and light, gray–green carbonate mud rich in cerithids and pellets
2 TRANSGRESSIVE FACIES	– dark, blue–gray quartzose–carbonate sand, cross–bedded, some gypsum, sometimes dolomitized
1 SUBAERIAL	– eolian, brown, quartzose–carbonate sand

Figure 2.1b Generalised lateral profile through the Abu Dhabi sabkha, U.A.E. (from Shearman, 1966 and Fuller and Porter, 1969)

Figure 2.1c Generalised lateral profile through a carbonate sabkha showing brine diagenesis (from Shearman, 1966).

a

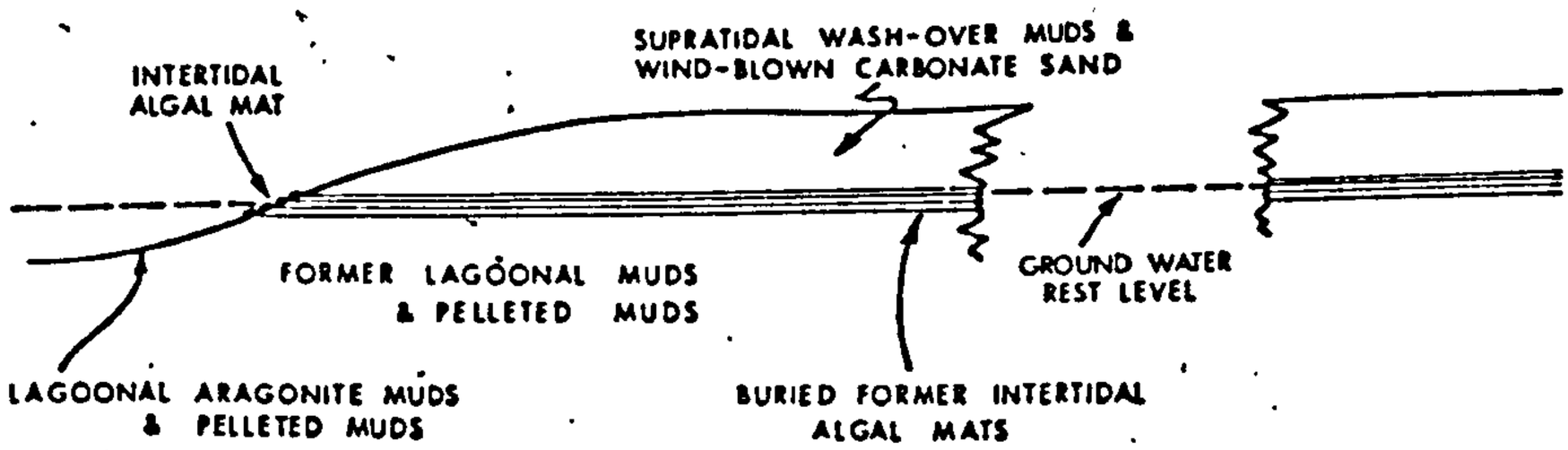
SUPRATIDAL WASH-OVER MUDS &
WIND-BLOWN CARBONATE SAND
INTERTIDAL
ALGAL MAT
FORMER LAGOONAL MUDS
& PELLETED MUDS
GROUND WATER
REST LEVEL
LAGOONAL ARAGONITE MUDS
& PELLETED MUDS
BURIED FORMER INTERTIDAL
ALGAL MATS

b

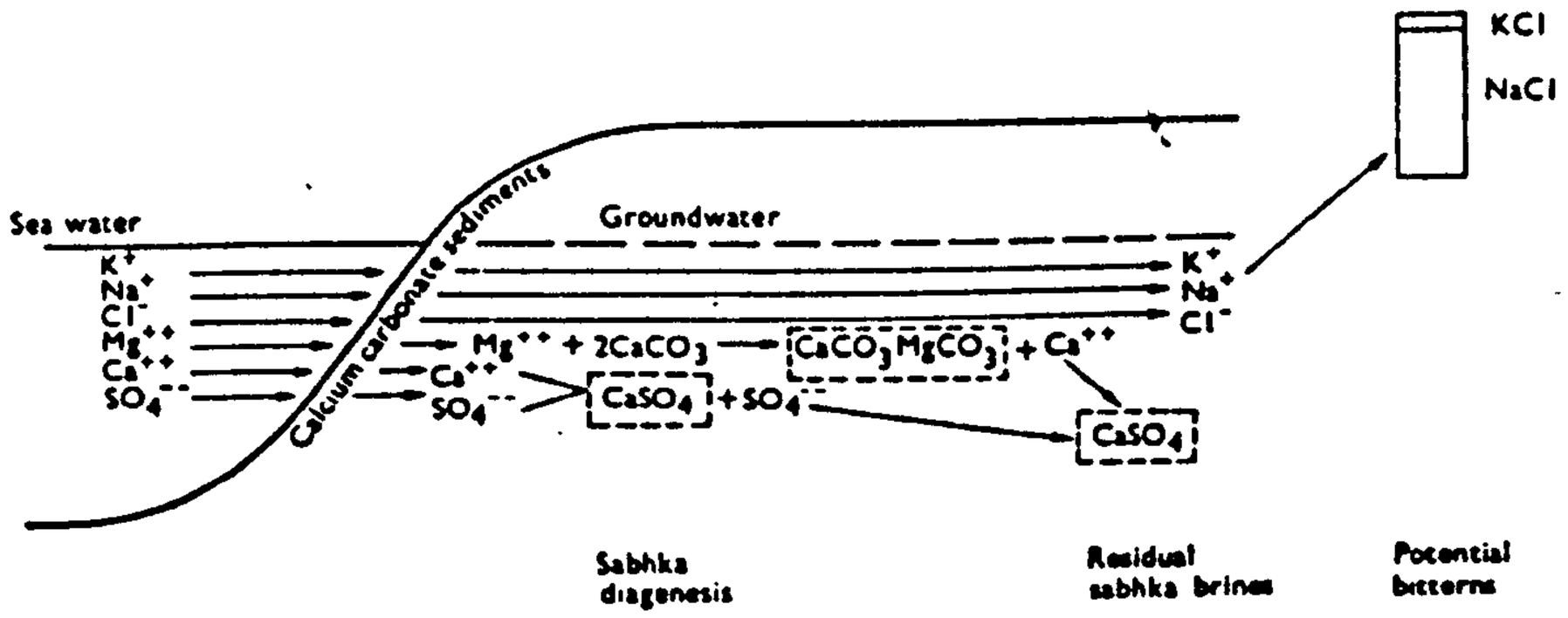
KCl
NaCl
Sea water
Groundwater
Calcium carbonate sediments
K^+
Na^+
Cl^-
Mg^{++}
Ca^{++}
SO_4^{--}
$Mg^{++} + 2CaCO_3 \rightarrow CaCO_3MgCO_3 + Ca^{++}$
$CaSO_4 + SO_4^{--}$
$CaSO_4$
Sabhka
diagenesis
Residual
sabhka brines
Potential
bitterns

Figure 2.2 Extent of sabkhas in the Trucial Coast region of the Persian Gulf. Note the sabkhas behind the lagoon barriers (red) and the more landward lagoon margin sabkhas (yellow). (from Purser and Evans, 1973).

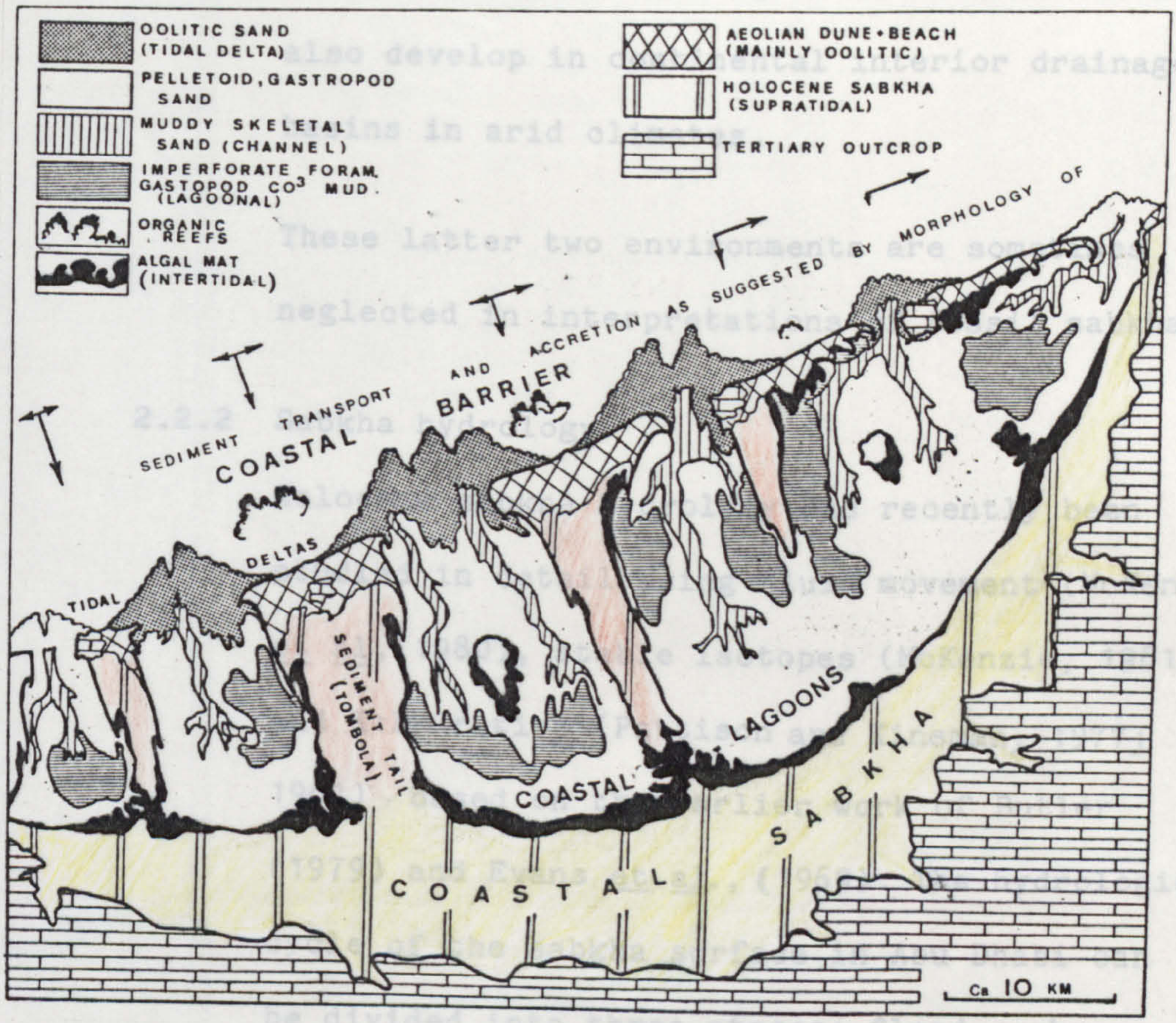
OOLITIC SAND (TIDAL DELTA)
PELLETOID, GASTROPOD SAND
MUDDY SKELETAL SAND (CHANNEL)
IMPERFORATE FORAM. GASTOPOD CO3 MUD. (LAGOONAL)
ORGANIC REEFS
ALGAL MAT (INTERTIDAL)
AEOLIAN DUNE+BEACH (MAINLY OOLITIC)
HOLOCENE SABKHA (SUPRATIDAL)
TERTIARY OUTCROP
SEDIMENT TRANSPORT AND ACCRETION AS SUGGESTED BY MORPHOLOGY OF
COASTAL BARRIER
TIDAL DELTAS
SEDIMENT TAIL (TOMBOLA)
COASTAL LAGOONS
SABKHA
COASTAL
Ca 10 KM

Sabkhas not only form on the prograding coastline; they also form in the lee of offshore islands and lagoon barriers (Fig 2.2). Inland sabkhas also develop in continental interior drainage basins in arid climates.

These latter two environments are sometimes neglected in interpretations of fossil sabkhas.

2.2.2 Sabkha hydrology

Holocene sabkha hydrology has recently been studied in detail using fluid movement (McKenzie et al, 1980), stable isotopes (McKenzie, 1981) and K:Br ratios (Pattison and Kinsman, 1977; 1981). based on the earlier work of Butler (1979) and Evans et al., (1969). The hydrologic cycle of the sabkha surface in Abu Dhabi can be divided into three stages; flood recharge, capillary evaporation and evaporative pumping (Schneider, 1975; McKenzie et al., 1980) (Fig 2.3a). Water movement over and within the sabkha is shown in Figures 2.3 b+c. The active area of pumping is in the intermediate sabkha where waters are of mixed origin (Fig 2.3c). Landwards of this area the water table is too deep and capillary forces too small for effective evaporite pumping.

Figure 2.3 a The three stages of water movement from the hydrologic model in the intermediate region of the Abu Dhabi sabkha. Note the constant seawards flow of groundwater in the lower beds. (from McKenzie et al., 1980).

Figure 2.3 b Diagram of the sabkha illustrating water movement during recharge on the sabkha. Recharge is mainly from shamal storms in winter or spring (from McKensie et al., 1980).

Figure 2.3 c Diagram of the sabkha, illustrating the origin of the water and circulation pattern during evaporation, the situation during most of the year. (from McKensie et al., 1980).

a

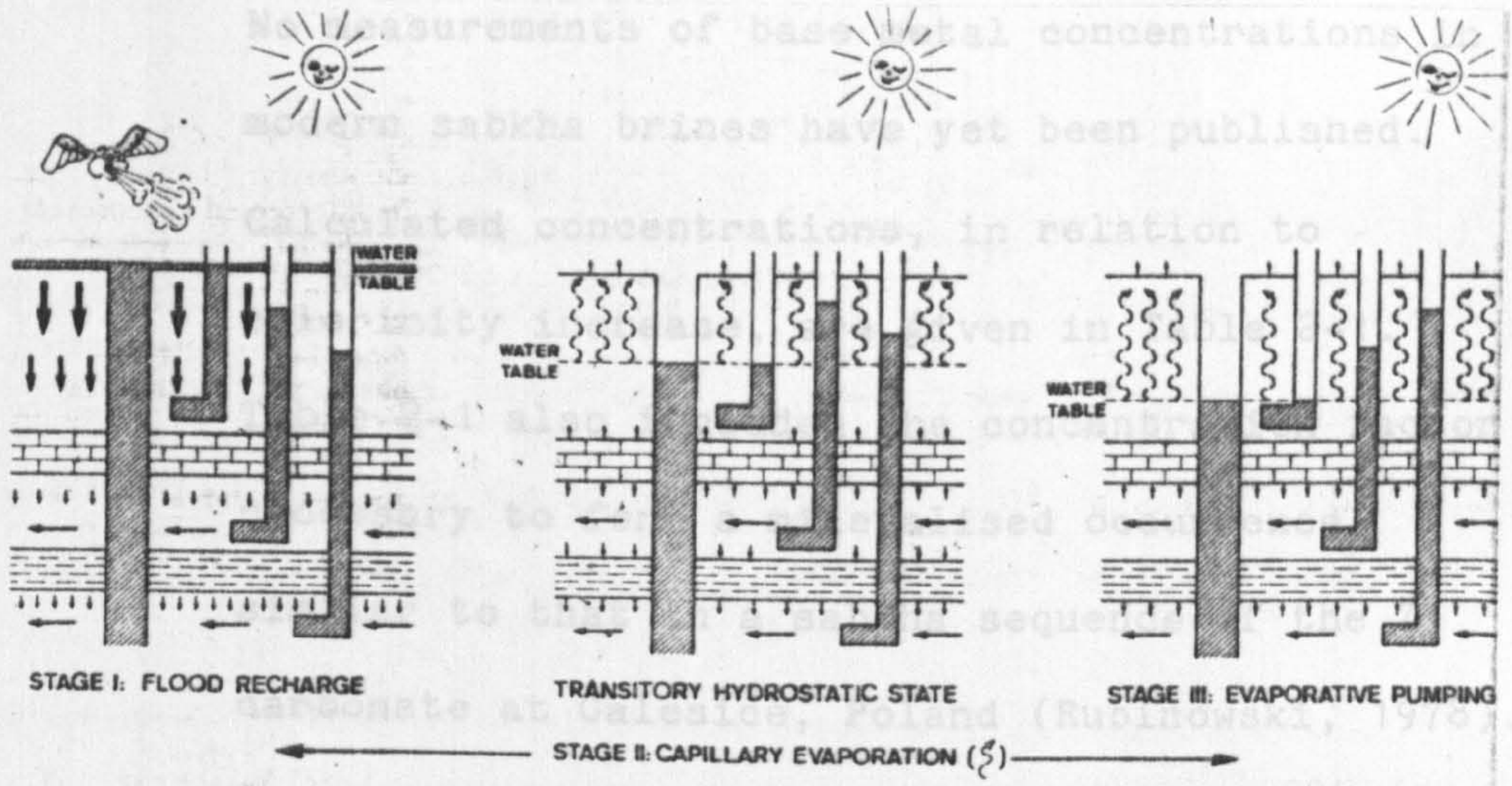
WATER TABLE
WATER TABLE
WATER TABLE
STAGE I: FLOOD RECHARGE
TRANSITORY HYDROSTATIC STATE
STAGE III: EVAPORATIVE PUMPING
STAGE II: CAPILLARY EVAPORATION (ξ)

b

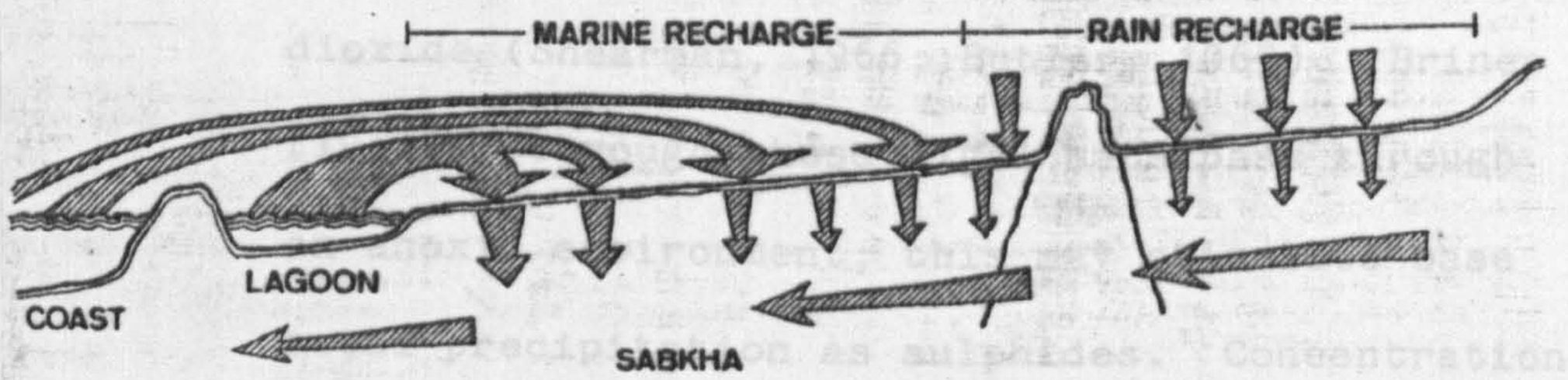
MARINE RECHARGE
RAIN RECHARGE
LAGOON
COAST
SABKHA

c

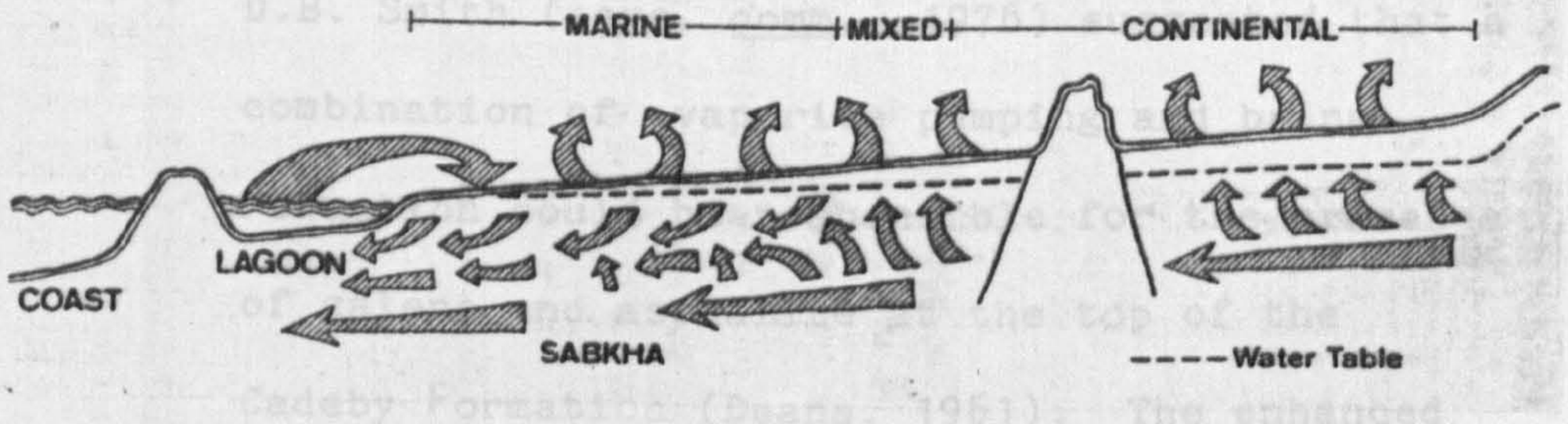
MARINE
MIXED
CONTINENTAL
LAGOON
COAST
SABKHA
Water Table

2.2.3 Metal concentrations in sabkha waters

No measurements of base metal concentrations in modern sabkha brines have yet been published. Calculated concentrations, in relation to - chlorinity increase, are given in Table 2-1. Table 2-1 also includes the concentration factor necessary to form a mineralised occurrence similar to that in a sabkha sequence of the Z1 carbonate at Galesice, Poland (Rubinowski, 1978). Concentrations of several orders of magnitude are necessary (Table 2-1).

Decaying algal mats in the sabkha subsurface generate hydrogen sulphide, methane and carbon dioxide (Shearman, 1966; Butler, 1969). Brines flushing through these algal mats pass through an anoxic environment; this may stimulate base metal precipitation as sulphides. Concentration of sulphides may result in continuous reduction of brines which move through the algal mats.

D.B. Smith (pers. comm., 1976) suggested that a combination of evaporite pumping and brine reduction could be responsible for the presence of galena and asphaltite at the top of the Cadeby Formation (Deans, 1961). The enhanced base metal concentrations should be detectable within the top metre or so of the sediments.

TABLE 2-1

	Sea Water	Persian Gulf lagoon water	Marine sabkha max. conc[n. 2]	Cont. sabkha max. conc[n. 3]	Fresh water	Salton Sea brine[6]	Bulwell conc[ns. 7]	Galesice conc[ns. 8]
s.g.	1.02	1.033[1]	1.20	1.14	1.00			
cl grm/l		24.7[1]	142	157	$7x10^{-3}$			
clorinity	19o/oo	25.5o/oo	170o/oo	179o/oo	7o/oo	184o/oo		
Ca grm/l	$2x10^{-6}$ [4]	$2.7x10^{-6}$ o/oo [11]	$2.1x10^{-5}$ o/oo [11]	$7.7x10^{-5}$ o/oo [12]	$3x10^{-6}$	0.02o/oo	0.1o/oo	1.2o/oo
Pb	$3x10^{-8}$ o/oo	$4.1x10^{-8}$ o/oo [11]	$3.2x10^{-7}$ o/oo [11]	$1.3x10^{-5}$ o/oo [12]	$0.5x10^{-6}$ [9]	0.5o/oo	6.5o/oo	5o/oo[10]
Zn	$4.9x19^{-6}$ o/oo	$6.7x10^{-6}$ o/oo [11]	$5.2x10^{-5}$ o/oo [11]	$3.8x10^{-4}$ o/oo [12]	$15x10^{-6}$	0.1o/oo	trace	1o/oo
Ba	$2x10^{-5}$ o/oo	$2.7x10^{-5}$ o/oo [11]	$2.1x10^{-4}$ o/oo [11]	$2.6x10^{-4}$ o/oo [12]	$10x10^{-6}$	0.2o/oo	trace	no info.

Concentration factors necessary to attain mineralization values of Gałesice for 33% porosity in dolomites

	Sea Water	P.G. lagoon	Marine Sabkha	Cont. Sabkha	Fresh Water	Salton Sea[13]
Cu	$6x10^5$	$4x10^5$	$6x10^4$	$2x10^4$	$4x10^5$	60
Pb	$2x10^8$	$2x10^8$	$2x10^7$	$4x10^5$	$1x10^7$	10
Zu	$2x10^5$	$1x10^5$	$2x10^4$	$3x10^3$	$7x10^4$	10

1 Average of 5 values from Butler, 1969

2 Values at about point A on Fig 19, from Butler, 1969

3 Inland sabkha, Sabkha al Daiyah, between Abu Dhabi and Al Ain, U.A.E. Values from P. Bush, pers. comm.

4 Values from Riley and Skirrow, 1975.

5 Values from Bowen, 1979.

6 Values of evaporated residue from Fyfe, Price and Thompson, 1978.

7 from Deans, 1961

8 from Rubinowski, 1978

9 Present day value $3x10^{-6}$ o/oo, but prehistoric values more like $0.5x10^{-6}$ o/oo, Bowen, 1979.

10 Galena was prominent later sulphide, Rubinowski, 1978.

11 Calculated values from sea water concentrations.

12 Calculated values from ground water concetrations.

13 Note how little concentration is necessary from such a brine.

2.3 Methods

2.3.1 Sampling

The overlying Ripon Formation comprises soft marls which have been eroded by glacial and fluvio-glacial agents. The top of the Cadeby Formation is thus exposed, or has only a thin soil covering, over large areas. Weathering subsequent to exposure may leach base metals from the carbonates (6.5.1); sampling was thus confined to exposures where the overlying marls were still preserved. Ground water circulation would still be responsible for some leaching. Cores provide ideal samples. Solid core sections are rarely taken through the Cadeby Formation; they are restricted to NCB colliery shaft sinkings and occasional I.G.S. holes.

2.3.2 Localities

Several exposures mentioned by Deans (1961) are no longer in existence (Fig 2.4). New mineralised exposures in the Doncaster area (Fig 2.4) were not in sabkha facies (3.4.5). Localities where the overlying marls were preserved were also limited (Fig 2.4).

2.3.3 Sample collection and preparation

Carbonate specimens were taken throughout the

Figure 2.4 Occurrences of mineralisation at the Cadeby Formation Ripon Formation boundary

○ Exposures with no mineralisation

● Mineralised localities

✦ Mineralised core sections

⌖ Localities recorded by Deans but no longer exposed

✸ Previously un-recorded mineralised localities

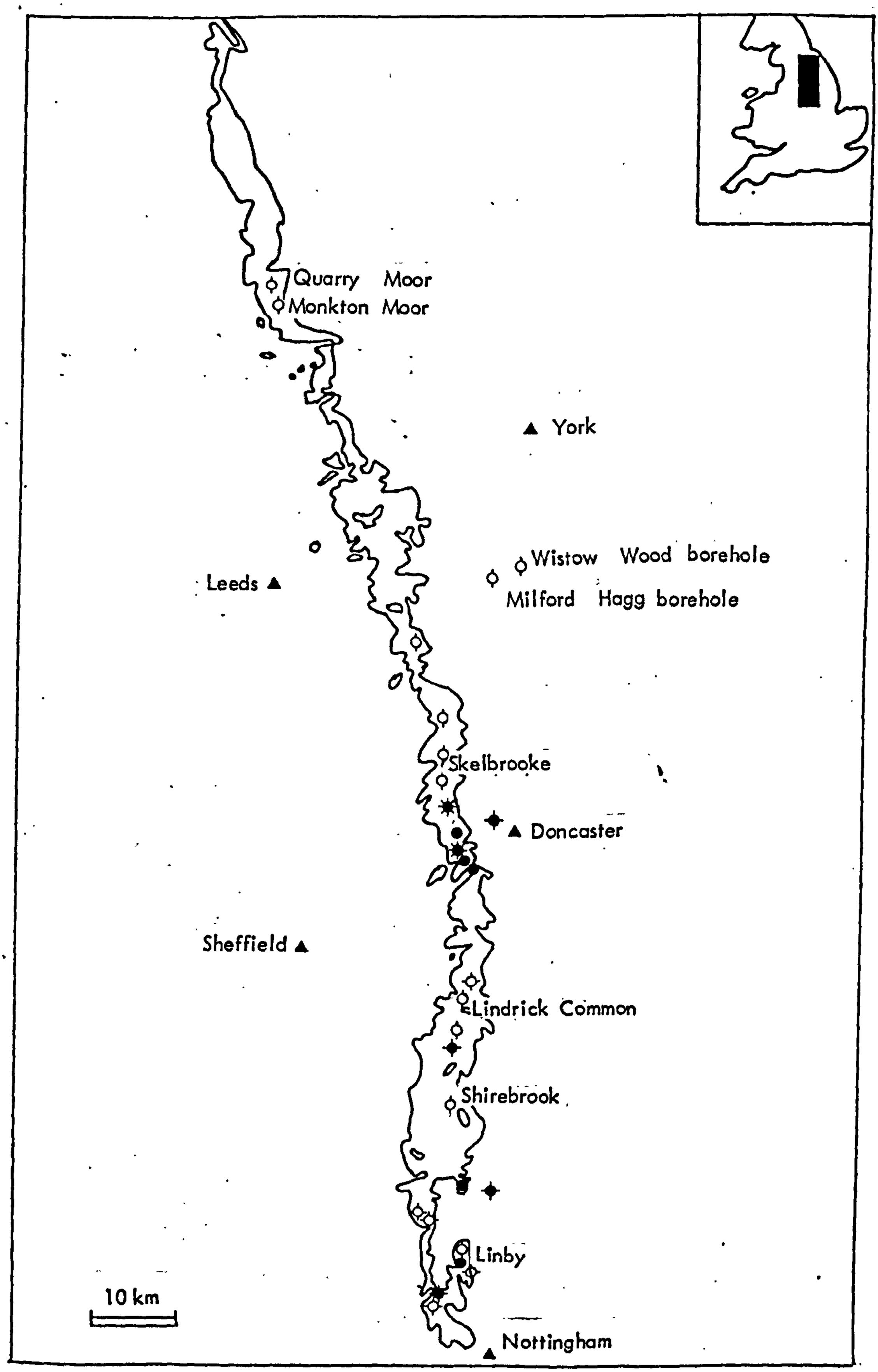
Quarry Moor
Monkton Moor
York
Wistow Wood borehole
Milford Hagg borehole
Leeds
Skelbrooke
Doncaster
Sheffield
Lindrick Common
Shirebrook
Linby
Nottingham
10 km

top two metres of exposures, with one further specimen from lower in the sequence. Weathered faces were trimmed and specimens powdered for X.R.F. analysis (Appendix 2). A range of specimens were analysed by wet chemical methods to provide standards (Appendix 3). X.R.F. results were calibrated (Appendix 4); whole rock X.R.F. analyses are given in Appendix 5.

2.4 Results

2.4.1 Sedimentology and diagenesis

Sequences interpreted as fossil sabkhas occur at three exposures at the top of the Upper Member: Quarry Moor (SE 308961) (Smith, 1976), Darrington (SE 494202) and Walling-wells (SE 570843) (3.4.4). None host mineralisation. Elsewhere ooid and peloid grainstones continue to the top of the formation (3.4.2) or siliciclastic grainstones and packstones are present (3.4.3). Sucrose dolomitisation in the latter facies (4.5.9) obscures sedimentary features; possible sabkha sequences may have developed in this facies but are, as yet, unrecognised.

Dolomitisation in sabkha aragonite-rich sediments is penecontemporaneous (Shearman, 1966; Bush,

1970). Cryptalgal laminites are preserved and there is evidence of the existence of former evaporites as displacive crystals at the top of the sequence at Quarry Moor. Several localities are dedolomitised; dedolomitisation at Quarry Moor was illustrated by Sedgwick (1829) (Fig 2.5). Calcite replaces dolomite in these localities (Figs 2.6 a+b) (5.3). Replacement on this scale will have radically altered original trace element concentrations.

In many cores, dolomites at the top of the Cadeby Formation are replaced by evaporites for several metres (e.g. Appendix 6, Log 11). Crypt-algal laminites are found at the top of the Upper Member in several cores; e.g. Milford Hagg (SE 533323), Bank End (SK 70639972), Whitecross (SK 569979) (Smith, 1976) and Camblesforth No. 1 (Fusezy, 1970; 1980). Crypt-algal laminites are interbedded with gypsum (Fig 2.7a). The presence of overlying gypsum/anhydrite nodules, marls and massive evaporites suggests these were sabkha sequences; it should be remembered, however, that palaeozoic crypt-algal laminites are not necessarily representative of intertidal environments (3.4.4).

Figure 2.5 Sketch of the section at Quarry Moor, Ripon (SE 308391), modified from Plate 7, Fig 3 of Sedgwick, 1829.

Grey dedolomite

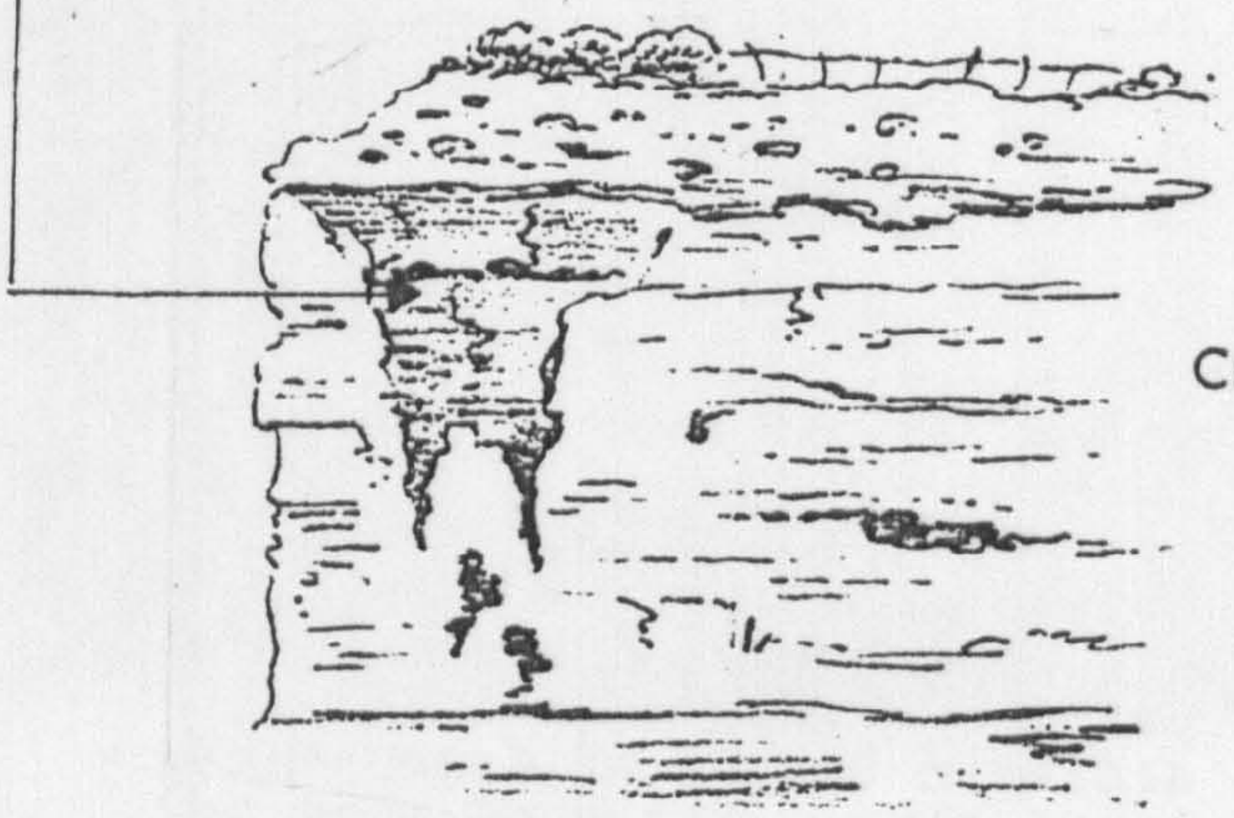

Crypt-algal laminites

Figure 2.6 a Dedolomitised peloid grainstone/ packstone. Corroded dolomicrospar crystals are enclosed in poikilitic calcites (stained with alizarin Red S). Rims of some peloids are shown more clearly by inclusions of ferric oxides. Field of view is 3.5mm. Specimen 101.

b Dedolomitised peloid grainstone/ packstone. Peloid rims are shown by inclusions within dolomite crystals. Dolomites are corroded and peloid rims transected by calcite crystals (stained with alizarin Red S) of approximately equal size. Field of view is 5.6mm. Specimen 111.

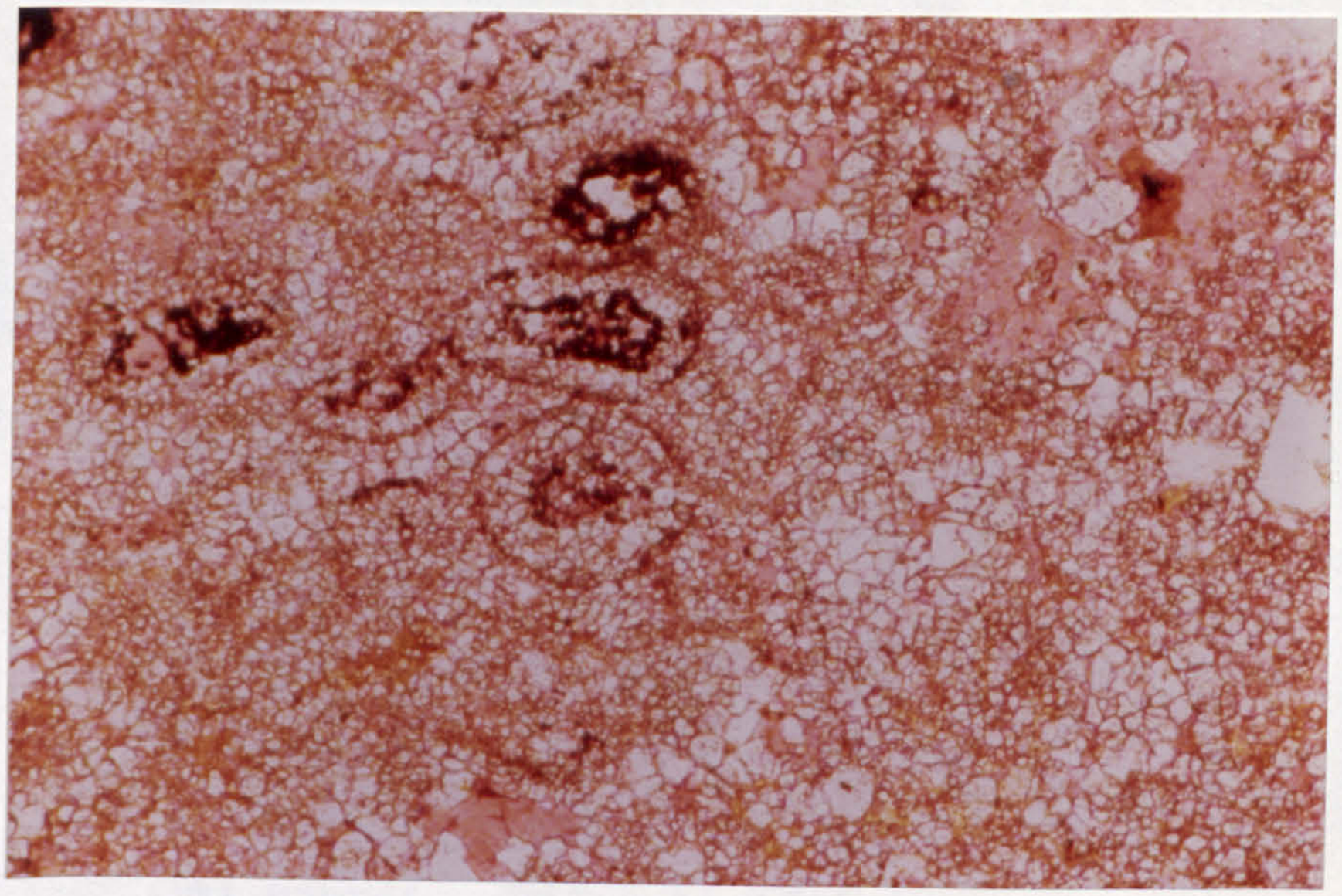

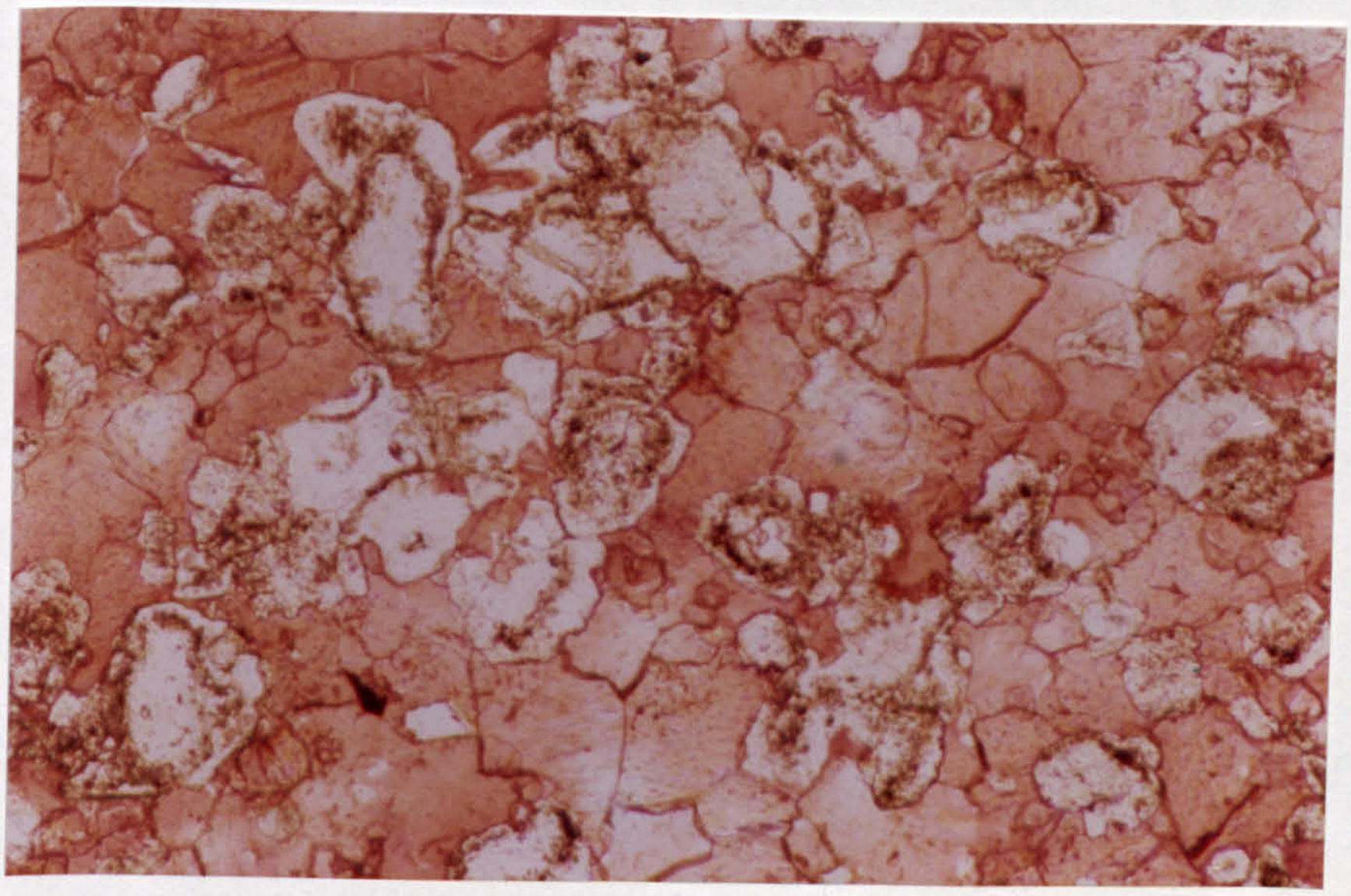

Figure 2.7

a Crypt-algal laminites with interbedded gypsum from near top of Upper Member in Bank End borehole (SK 706972). Crinkled algal mats comprise mainly peloids with some foraminifera. Some peloid-cores are replaced by evaporites.

b Cerussite (c) corroding galena (g) with caries texture in mineralised vug near top of Upper Member, New Edlington Brick Works Quarry. Field of view is 2.2mm. Viewed in reflected light.


2cm

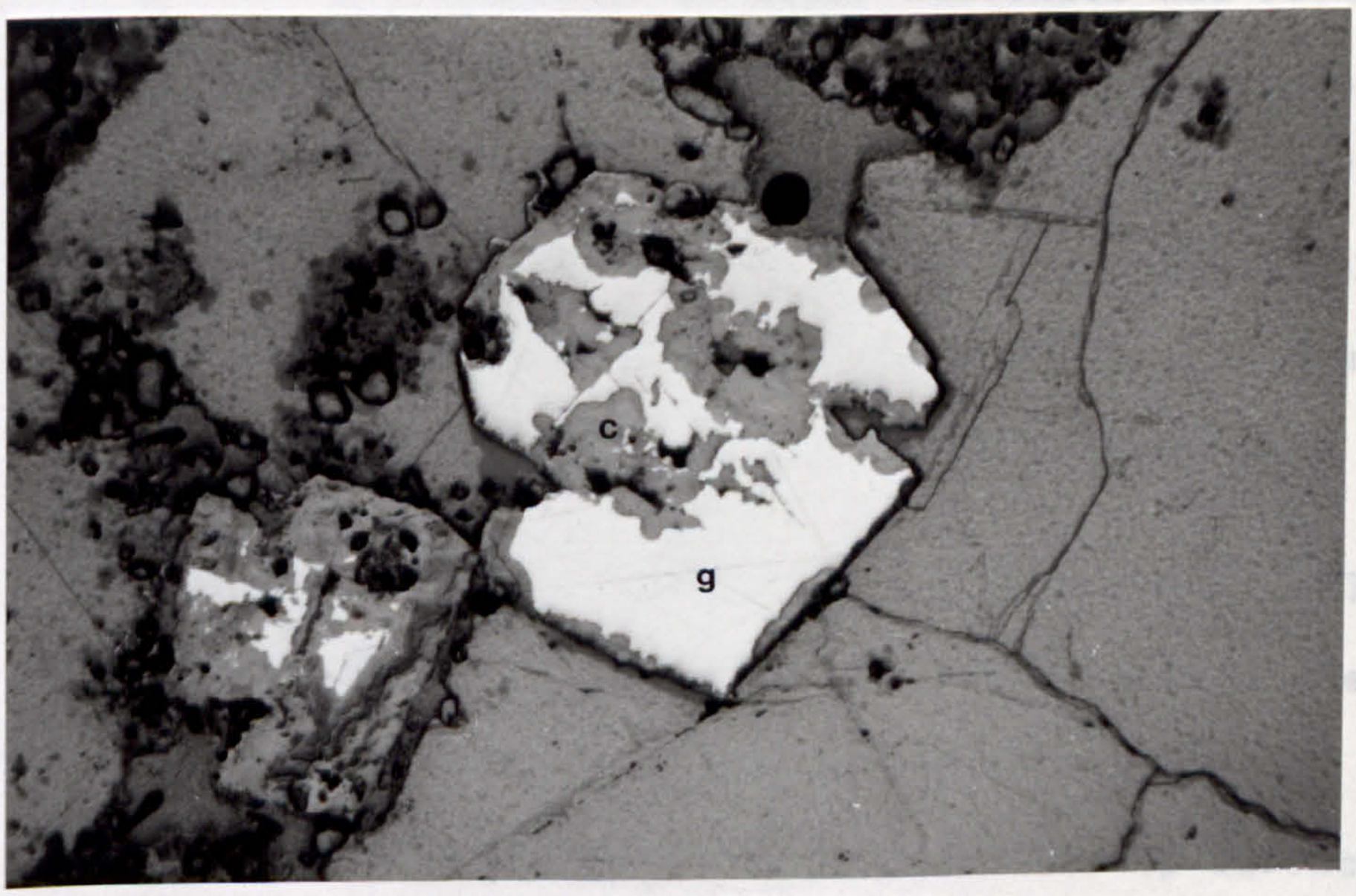
c
g

2.4.2 Mineralisation

Deans (1961) recorded galena with traces of cerussite, wulfenite, baryte, chalcopyrite, malachite and uraniferous asphaltite (Fig 2.4; Appendix 1). A black mineral, taken to be asphaltite, was hand separated from specimens from two localities (New Edlington Brick Works Quarry, SK 532986; Shirebrook new cutting, SK 530687). Electron microprobe scans showed no traces of uranium; feeble radioactivity was due to potassium, presumably from the overlying marls. Cerussite is secondary after galena (Fig 2.7b). Deans' wulfenite localities are no longer exposed; no other wulfenite was found. Deans (1961) states "wulfenite is the youngest mineral present ..... and ..... might be of very recent formation". It has therefore little relation to sabkha diagenesis although may form from remobilisation of pre-existing minerals.

At Quarry Banks, Linby, Nottinghamshire (SK 537523) (Appendix 1) galena and calcite in veinlets are found in the top few metres of the Cadeby Formation; there is no galena on the top surface of the dolomite. Galena, sphalerite and marcasite are present in a shell bed three metres below the

top of the formation; this bed can be traced over at least fifty square metres. The veinlets are derived from this bed. Deans' neighbouring localities (Papplewick, SK 545520; Newstead, SK 536531) are now inaccessible; descriptions do not specify the mode of mineralisation occurrence there.

No mineralisation found at or near the top of the Upper Member could be linked to concentration of base metals during sabkha development. It remained to determine whether trace element concentrations could be linked to exposure and subsequent evaporation during early diagenesis.

2.4.3 Trace element concentrations

Trace element concentrations with lithological logs are plotted in Figure 2.8; lithological symbols appear in Appendix 6. Whole rock X.R.F. analysis results are given in Appendix 5.

No sections show enrichment of all base metals at the top of the Upper Member; neither is macroscopic mineralisation evident. Slight concentrations (Figs. 2.8 a+b) can be explained as the overlying green marls imply a local anoxic environment. Dedolomitised sections (Figs. 2.8, f+g) show depletion of base metals.

Figure 2-8 a-g Logs of the upper few metres of the Cadeby Formation at different localities showing variation in trace element concentrations, calcium carbonate and insoluble residue. Vertical scale is 1m to 1cm throughout. Symbols are detailed at the start of Appendix 6.

a Old railway cutting, Shirebrook (SK 534681). Entire section is dolomite. Overlying Ripon Formation poorly exposed under soil.

b New railway cutting, Shirebrook (SK 532 686). Entire section is dolomite. Ripon Formation marls are green adjacent to main carbonates and near dolomite beds within marls. Remainder of marls are red.

Shirebrook

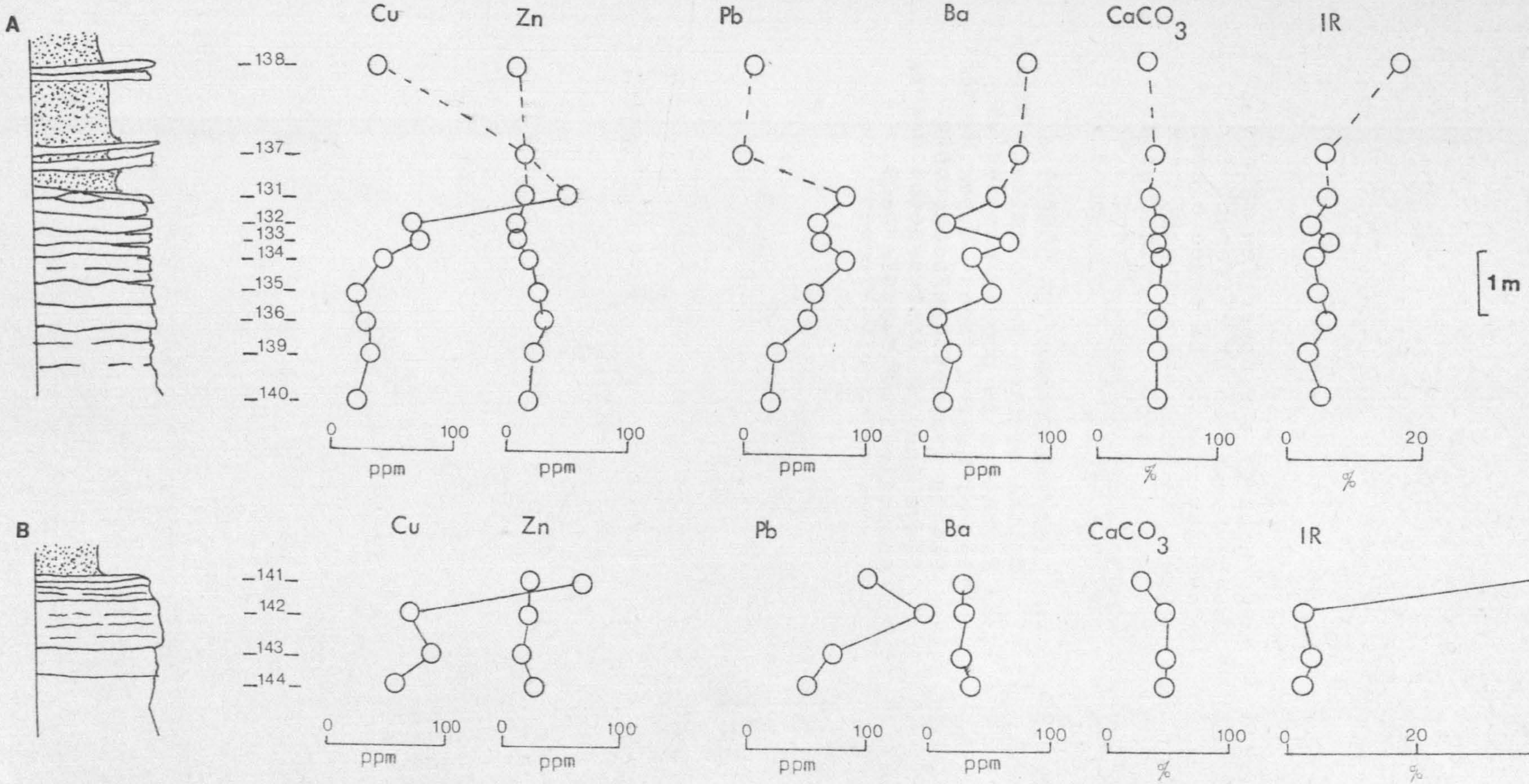
A
138
137
131
132
133
134
135
136
139
140
Cu
Zn
Pb
Ba
CaCO3
IR
0
100
ppm
%
20
1m
B
141
142
143
144
40

Figure 2.8 c Lindrick Common (SK 556826). Entire section is dolomite. Ripon Formation is poorly exposed at top of quarry face. Upper Member peloid grainstones/packstones. Clays near base of section may be equivalent of Hampole Beds.

Lindrick Common

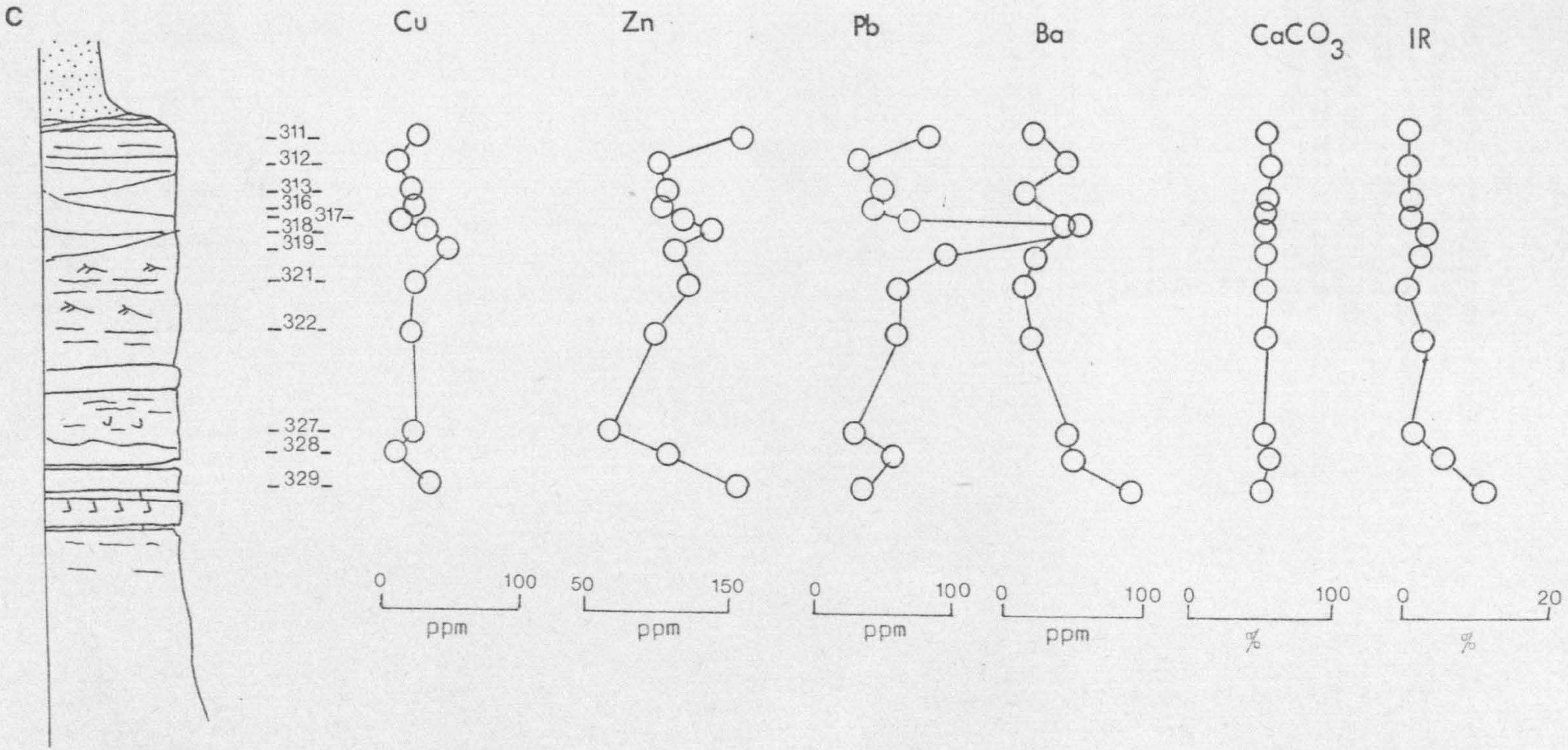

Figure 2.8 d Milford Hagg bore hole (SE 533323). Base of section is dolomite peloid grainstones/packstones with some replacive evaporites. Massive gypsum (after anhydrite) shows replaced dolomite peloids in places. Brown muds are at top of section.

Milford Hagg borehole

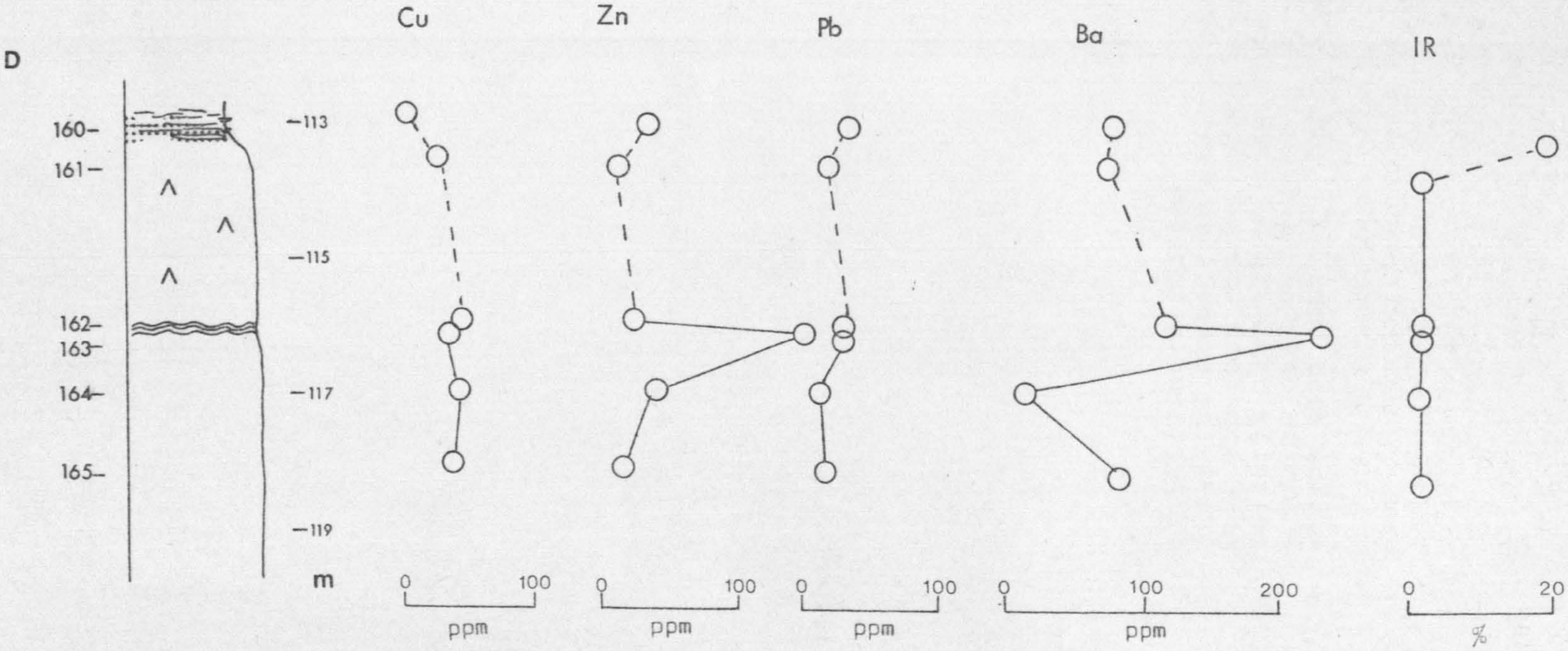

Figure 2.8 e Wistow Wood bore hole (SE 567356). Dolomitè crypt-algal laminites are patchily replaced by evaporites near apparent top of Cadeby Formation. Overlying evaporites contain traces of replaced dolomites.

E

Wistow Wood borehole

148–
149–
150–
260–
151–
262–
265–
266–
261–
152–
267–
268–

–192
–194
–196
–198
–200
–202
–204

m

Cu

Zn

Pb

Ba

IR

0 100 ppm

0 100 ppm

0 100 ppm

0 20 40 %

0 200 400 ppm

Figure 2.8 f Monkton Moor Quarry (SE 308653). Top of section is dedolomite (Fig 2.6 b). Originally peloid grainstones/packstones. Ripon Formation poorly exposed at top of section.

F

Monkton Moor

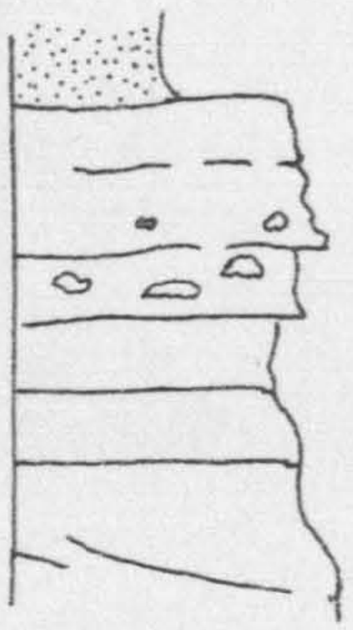

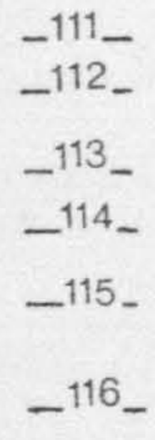

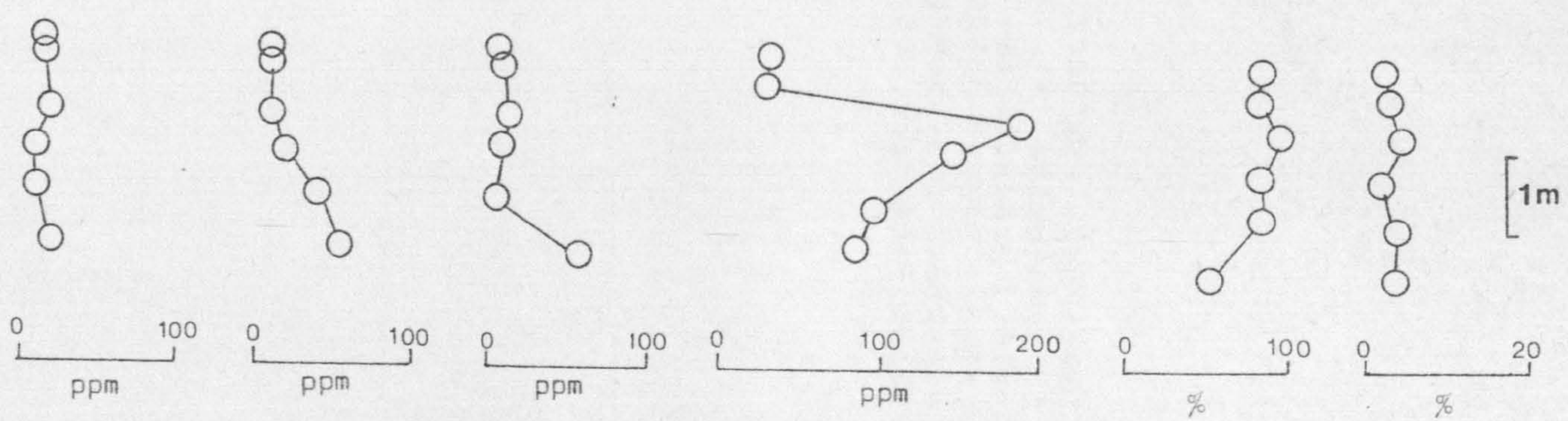

Figure 2.8

g Skelbrooke (SE 501124), Top of section is dedolomite (Fig 2.6 a). Originally peloid grainstones/packstones with some thinner bedder dolomites. Exposure in overgrown dis-used railway cutting with Ripon Formation not visible.

G

Skelbrooke

1m

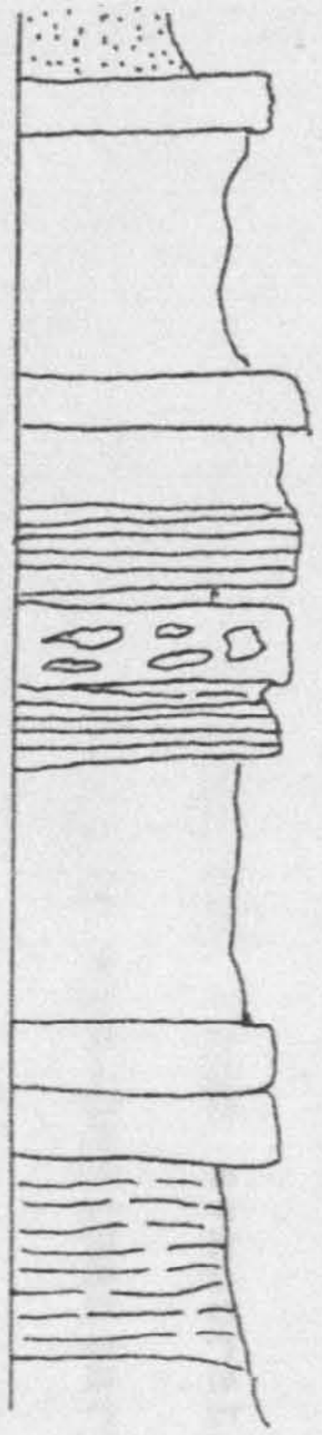

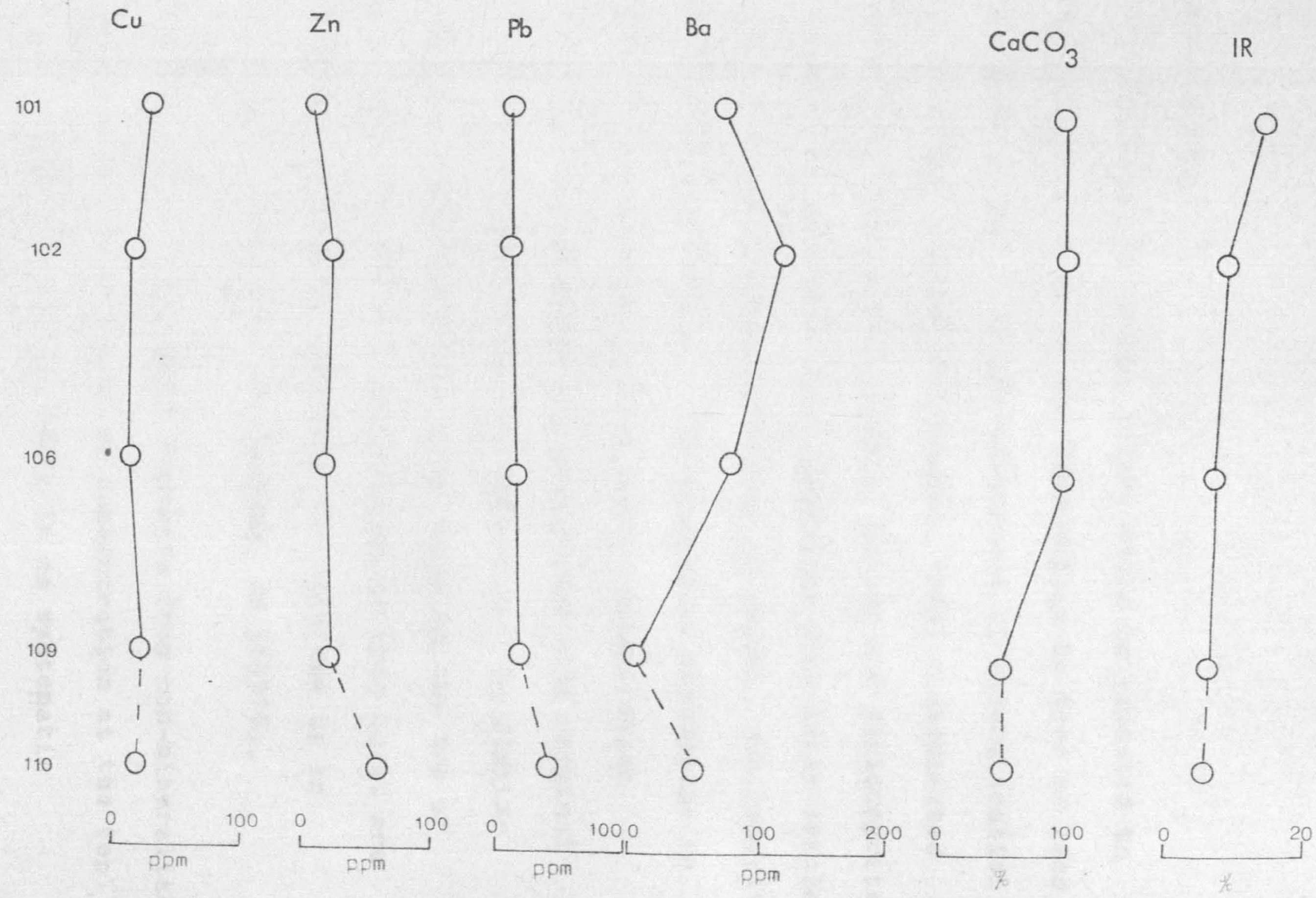

2.5 Conclusions

Concentration in sabkha brines would be expected to enrich the content of all base metals to more or less the same extent. In the occurrence of mineralisation at Galesice, Poland (Rubinowski, 1978) disseminated syngenetic sphalerite, pyrite, galena and chalcopyrite are present in crypt-algal laminites with later veinlets, vug fills and stylolite sutures of galena, chalcopyrite sphalerite and baryte. The syngenetic assemblage is what would be expected from brine concentration (Table 2-1); sulphides are associated with original organic material within the laminites. No similar sulphide assemblages have been found at the top of the Cadeby Formation. Occurrences at this level are dominated by galena (Appendix 1); only one is in crypt-algal laminites (Whitecross, SK 569979).

Measurements of base metal contents from non-mineralised localities show little or no concentration at the top of the Cadeby Formation; there is no systematic increase in all measured base metal contents as would be expected from brine formation from evaporation. Dolomitisation (4.5) may modify syn-sedimentary concentrations; dedolomitisation (5.3) considerably decreases concentrations.

It was therefore concluded that the mineralisation

described by Deans (1961) could not be attributed to concentration of brines and precipitation of sulphides within a sabkha environment. Neither was there any evidence of associated base metal enrichment at the top of the Cadeby Formation. The research into these occurrences formed the basis of a broader project on mineralisation within the Cadeby Formation. This research was important as it demonstrated the need to study both sedimentology and diagenesis of the formation when considering controls on mineralisation occurrences.

CHAPTER 3

Sedimentology of the Cadeby Formation

3.1 Introduction

Because the sedimentology of the Cadeby Formation is presented in a single chapter, facies description and interpretation are oversimplified; emphasis is on facies which host mineralisation. Full discussion of facies relevance to mineralisation is, however, dealt with after Part II, Diagenesis and Chapter 8, Mineral Occurrences.

Sedimentary features in many peels and thin sections have been obscured by dolomitisation (4.5.5 and 4.5.9); evidence for carbonate environments thus comes largely from logs of weathered sections and cut specimens. Late, post-dolomitisation, replacive evaporites (Harwood, 1980 and 6.3.2) occur throughout the Lower Magnesian Limestone and can also hinder interpretation.

The facies in the Cadeby Formation at outcrop formed on a shallow, carbonate platform (1.2.2) and include Wilson's (1975) major carbonate facies belts of open marine platform, restricted marine platform and platform evaporites (Fig. 3.1). The term 'platform evaporites' is used here in preference to supratidal evaporites as some beds host displacive evaporites without positive evidence of a supratidal environment.

Figure 3.1 Summary of generalised carbonate facies belts (from Wilson, 1975, p.351).

Scaled cross section									
Diagrammatic cross section	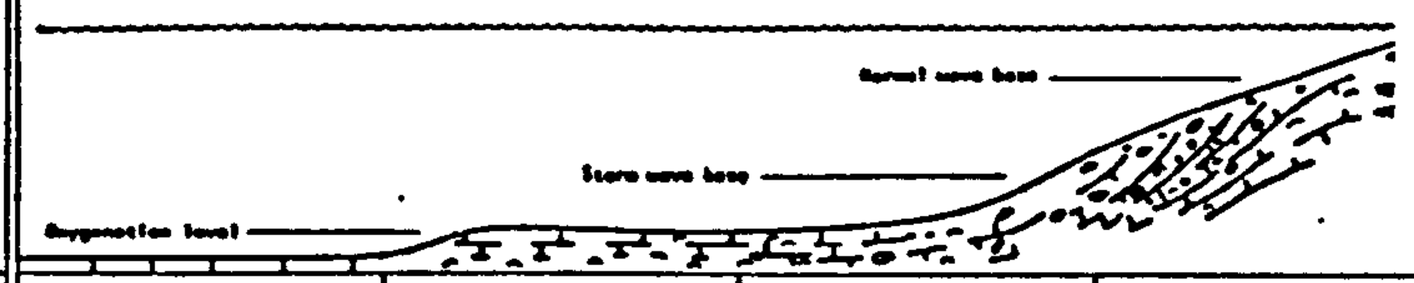				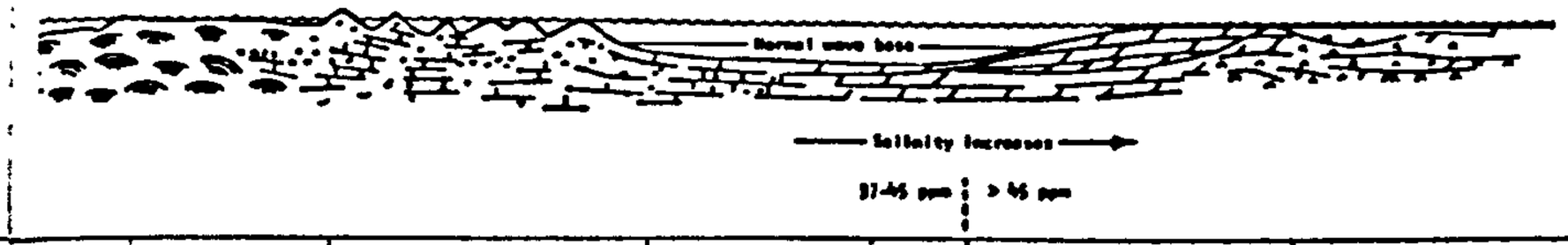				
Facies number	1	2	3	4	5	6	7	8	9
Facies	*Basin* (euxinic or evaporitic) a) Fine clastics b) Carbonates c) Evaporites	*Open shelf* (undaform) Open marine neritic a) Carbonates b) Shale	*Toe of slope carbonates*	*Foreslope* a) Bedded fine grain sediments with slumps b) Foreset debris and lime sands c) Lime mud masses	*Organic (ecologic) reef* a) Boundstone mass b) Crust on accumulation of organic debris and lime mud; bindstone c) Baffiestone	*Sands on edge of platform* a) Shoal lime sands b) Islands with dune sands	*Open platform* (normal marine, limited fauna) a) Lime sand bodies b) Wackestone-mudstone areas, bioherms c) Areas of clastics	*Restricted platforms* a) Bioclastic wackestone, lagoons and bays b) Litho-bioclastic sands in tidal channels c) Lime mud-tide flats d) Fine clastic units	*Platform evaporites* a) Nodular anhydrite and dolomite on salt flats b) Laminated evaporite in ponds
Lithology	Dark shale or silt, thin limestones (starved basin); evaporite fill with salt	Very fossiliferous limestone interbedded with marls, well segregated beds	Fine grain limestone, cherty in some cases	Variable, depending on water energy upslope; sedimentary breccias and lime sands	Massive limestone-dolomite	Calcarenitic-oolitic lime sand or dolomite	Variable carbonates and clastics	Generally dolomite and dolomitic limestone	Irregularly laminated dolomite and anhydrite, may grade to red beds
Color	Dark brown, black, red	Gray, green, red, brown	Dark to light	Dark to light	Light	Light	Dark to light	Light	Red, yellow, brown
Grain type and depositional texture	Lime mudstones; fine calcisiltites	Bioclastic and whole fossil wackestones; some calcisiltites	Mostly lime mudstone with some calcisiltites	Lime silt and bioclastic wackestone-packestone; lithoclasts of varying sizes	Boundstones and pockets of grainstone; packstone	Grainstones well sorted; rounded	Great variety of textures; grainstone to mudstone	Clotted, pelleted mudstone and grainstone; laminated mudstone; coarse lithoclastic wackestone in channels	
Bedding and sedimentary structures	Very even mm lamination; rhythmic bedding; ripple cross lamination	Thoroughly burrowed, thin to medium; wavy to nodular beds, bedding surfaces show diastems	Lamination may be minor, often massive beds; lenses of graded sediment; lithoclasts and exotic blocks. Rhythmic beds	Slump in soft sediments; foreset bedding; slope bioherms; exotic blocks	Massive organic structure or open framework with roofed cavities; Lamination contrary to gravity	Medium to large scale crossbedding; festoons common	Burrowing traces very prominent	Birdseye, stromatolites, mm lamination, graded bedding, dolomite crusts on flats. Cross-bedded sand in channels	Anhydrite after gypsum; nodular, rosettes, chickenwire, and blades; irregular lamination; carbonate caliche
Terrigenous clastics admixed or interbedded	Quartz silt and shale; fine grain siltstone, cherty	Quartz silt, siltstone, and shale, well segregated beds	Some shales, silt, and fine grained siltstone	Some shales, silt, and fine grained siltstone	None	Only some quartz sand admixed	Clastics and carbonates in well segregated beds	Clastics and carbonates in well segregated beds	Windblown, land derived admixtures, clastics may be important units
Biota	Exclusively nektonic-pelagic fauna preserved in local abundance on bedding planes	Very diverse shelly fauna preserving both infauna and epifauna	Bioclastic detritus derived principally from upslope	Colonies of whole fossil organisms and bioclastic debris	Major frame building colonies with ramose forms in pockets; in situ communities dwelling in certain niches	Worn and abraided coquinas of forms living at or on slope, few indigenous organisms	Open marine fauna lacking (e g echinoderms, cephalopods, brachiopods), mollusca, sponges, forams, algae abundant, patch reefs present	Very limited fauna, mainly gastropods, algae, certain foraminifera (e g miliolids) and ostracods	Almost no indigenous fauna, except for stromatolitic algae

WIDE BELTS → ← VERY NARROW BELTS → ← WIDE BELTS →

Carbonate texture descriptions used are from Dunham (1962) unless otherwise referenced.

Siliciclastic components within both members are generally low, implying little fluviatile input; some may be aeolian derived. Faunal diversity, at its maximum near the base of the Lower Member, is low, possibly due to salinity increase (Smith, 1974a) combined with the restricted connections between the Zechstein, the north North Sea Basin and the Boreal Ocean (Fig. 1.2). Many species are indeterminate because of dolomitisation.

Detailed logs of representative sections are in Appendix 6; Appendix 7 contains subsurface data from the Selby coalfield.

3.2 The Lower Member

3.2.1 Facies

Considerable local variations in thickness of the Lower Member result from the irregularity of the underlying Carboniferous palaeosurface (Fig.3.2). More regional thickness variations are from differential subsidence towards the basin and wedging towards limiting sea level (D.B. Smith, pers. comm., 1981). Lower Member facies are delineated in Table 3.1; localities mentioned in this chapter are on Figure 3.3

Table 3.1

Facies in the Lower Member of the Cadeby Formation

Major Facies Groups	Facies
Open marine platform facies	Carbonate mudstones and wackestones Patch reefs and flank grainstones and packstones Shallow water peloid grainstones and packstones Skeletal grainstones and packstones Shallow water carbonates and siliciclastics Grainstone barriers
Restricted marine platform facies	Non-bioturbated lagoon wackestones Bioturbated lagoon wackestones and mudstones Bioturbated lagoon wackestones and mudstones with evaporites Intertidal grainstones, packstones and boundstones Supratidal carbonates Patterned carbonates

Figure 3.2 Contours on the sub-Cadeby Formation unconformity in the Wetherby area, Yorkshire. Contour interval is 15 metres.

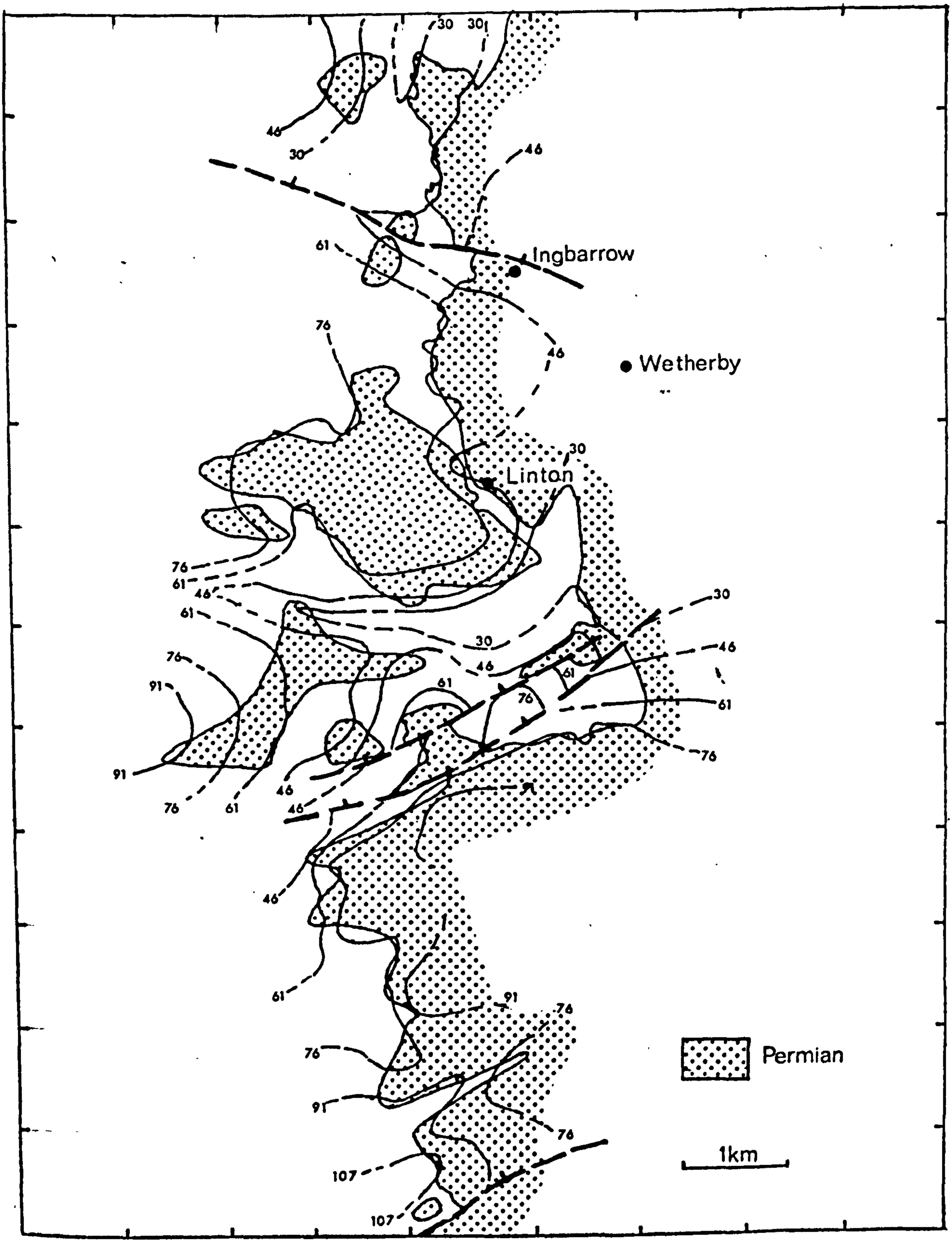
30
30
46
30
46
61
Ingbarrow
76
46
Wetherby
30
Linton
76
61
46
61
30
76
46
61
91
76
61
76
61
91
46
46
46
61
91
76
76
107
107
Permian
1km

Figure 3.3 Localities of exposures mentioned in Chapter 3. Localities of logged sections in Appendix 6 are underlined.

● Both members

◓ Upper Member

◒ Lower Member

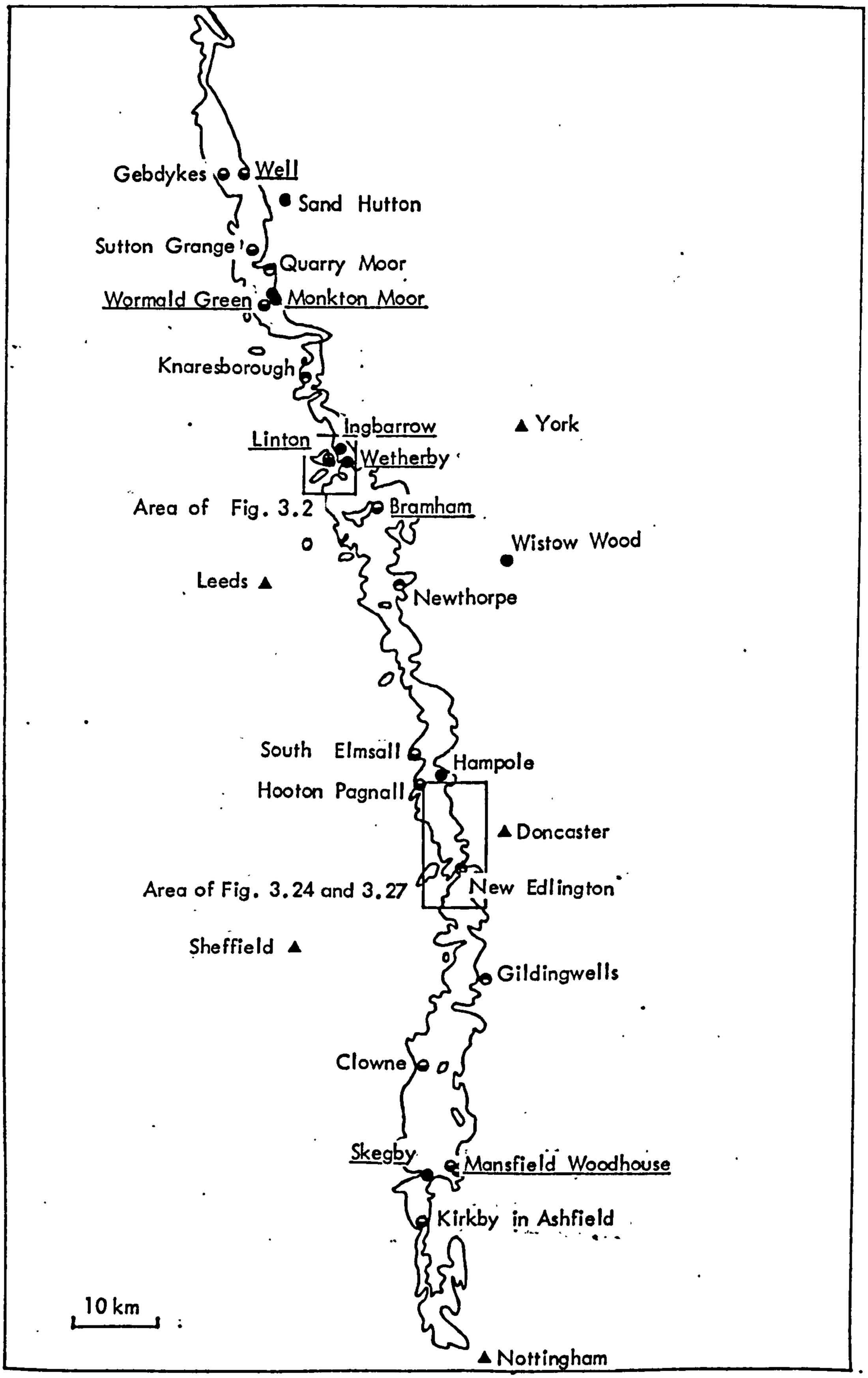
Gebdykes
Well
Sand Hutton
Sutton Grange
Quarry Moor
Wormald Green
Monkton Moor
Knaresborough
Ingbarrow
York
Linton
Wetherby
Area of Fig. 3.2
Bramham
Wistow Wood
Leeds
Newthorpe
South Elmsall
Hampole
Hooton Pagnall
Doncaster
Area of Fig. 3.24 and 3.27
New Edlington
Sheffield
Gildingwells
Clowne
Skegby
Mansfield Woodhouse
Kirkby in Ashfield
10 km
Nottingham

Because evaporites never constitute more than a small percentage of the strata within the formation, a separate evaporite facies belt is not defined; evaporite-rich strata are included adjacent to the lateral carbonate equivalents. Since the Zechstein was itself a restricted basin 'open marine' and 'restricted marine' are used as relative terms.

3.2.2 Open marine platform; carbonate mudstones and wackestones

Borehole sections in both members contain nodular carbonate mudstones and wackestones with varying amounts of clastic muds (Fuzesy, 1970, 1980; Kaldi, 1980b) deposited in relatively deep water behind the platform margin build-up (Fig. 3.18). No similar strata occur at outcrop. Smith (1974a) considers the carbonate mudstones and wackestones of Nottinghamshire (e.g. Clowne, SK 468757) and Yorkshire (e.g. Appendix 6, Logs 1, 9 and 10) were also formed on the open marine platform; however, sedimentary features suggest these carbonates are of shallower origin within the restricted marine platform facies belt (3.2.9).

3.2.3 Open marine platform; Patch reefs and flank grainstones and packstones

Patch reefs are circular or sub-circular in plan and in places are symmetrical in section (Smith, 1974a; 1981), individual reefs commonly reaching 3 to 8 metres in height by 10 to 25 metres diameter. A bryozoan bafflestone (Embry and Klovan, 1971) reef core (mainly Acanthocladia Thamniscus) forms large pillow structures to 2m across (Smith, 1981, Figs.2 + 8). Reefs are single or multiple bafflestone pillows, but higher in the member many possess a cryptalgal laminite boundstone covering (Smith, 1981, Fig.13). This upwards increase of algal boundstone indicates a progressive disappearance of browsing benthos, perhaps linked to salinity increases.

Reef cavities may remain voids or contain skeletal debris or flank sediments. Penecontemporaneous exposure, evident by cavity fills or red mudstone, affected at least one reef (Fig. 3,4) whilst other reefs formed positive fractures at the Hampole Discontinuity, near the top of the Lower Member (Smith, 1974a; 1981).

The flanking, grainstones and packstones

Figure 3.4 Patch reef, Gedbykes Quarry, N. Yorks. (SE 237823). Reef base is on flat-bedded packstones. The irregular reef top (dotted line) was blanketed by later packstones. Reef contains bryozoa and bivalves. Reef cavities (arrowed) are filled with red clays. Hammer is 0.35m long.

contain pisoliths, coated skeletal grains, ooids, rare oncoliths and some intraclasts. Few channel or scour features are present. Reefs and grainstones formed in an oxic agitated moderate to low energy environment. Water depths were shallow, less than 5 metres (Smith, 1974a); some larger reefs were periodically partially emergent (Smith, 1981).

3.2.4 Open marine platform; shallow water peloid grainstones

Peloid grainstones and possible packstones contain former ooids, pellets and uncoated skeletal debris. In places they comprise large thicknesses of the Lower Member (Appendix 6, Logs 2+3). Sedimentary structures include asymmetrical and oscillatory ripple cross laminations, scour and fill structures, sometimes with two stages of fill (Fig. 3.5), small channel sands with planar cross-stratification, rare thin sheet sands and isolated intraclasts of dolomite crusts (Appendix 6, Log 3). Skeletal debris includes single values of Bakevellia, Schizodus and Permorphus with some bryozoan fragments. Bioturbation is common but not prolific; vertical burrows ($\leqslant \frac{1}{2}$ centimetre diameter) seldom

Figure 3.5 Two stages of channel fill, Lower Member, Wetherby (SE 396484). Original channel profile (dotted) was partially filled (a) then later completely filled (b). Upper bed is continuous over the two stages of fill. Pen is 15cm long.

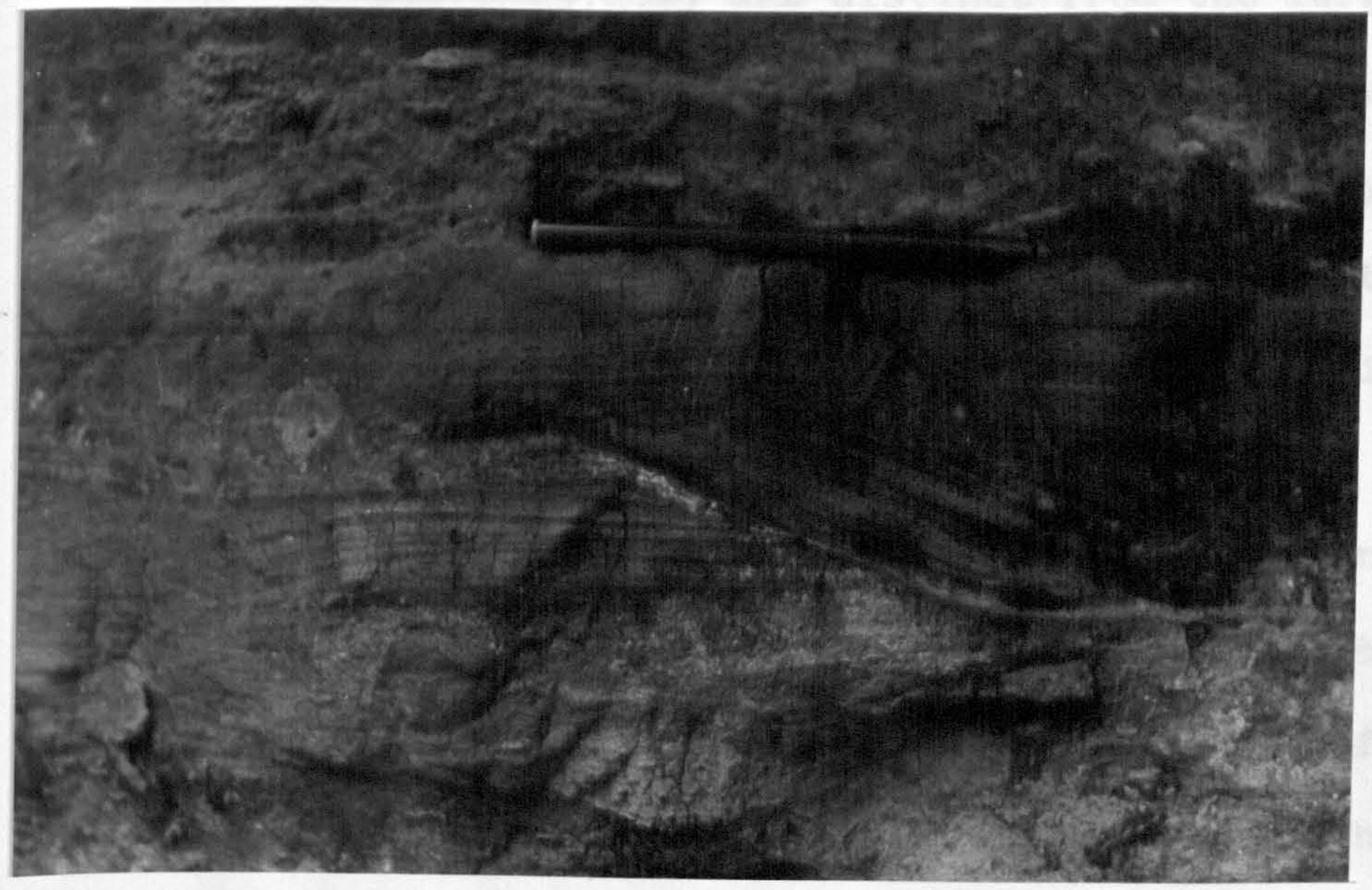

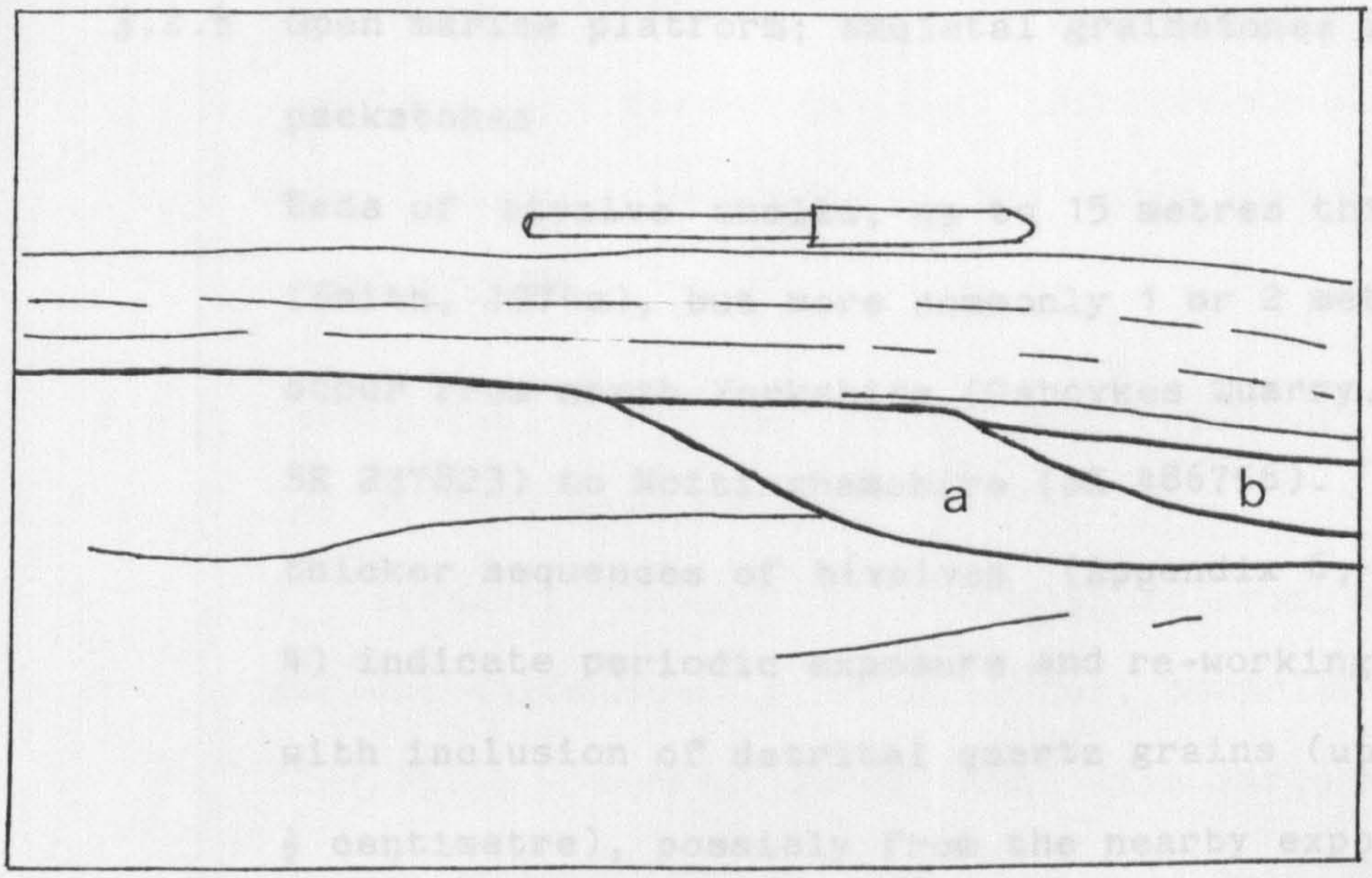
a
b

ramify, trails occur on bedding plane surfaces. Burrows and trails in both this and the grainstone barriers (3.2.7) are distinct from the larger and more ramifying bioturbation in the Upper Member (3.4.2). Sedimentary features imply these beds were deposited in a shallow subtidal to low intertidal environment with meandering small tidal channels and occasional storms producing sheet sands. Lack of algal laminites, found higher in the sequence (3.2.11) may be due to a continually shifting sediment surface and/or the presence of a grazing fauna. This facies in places passes laterally and vertically into intertidal carbonates (3.2.11).

3.2.5 Open marine platform; skeletal grainstones and packstones

Beds of bivalve shells, up to 15 metres thick (Smith, 1974a), but more commonly 1 or 2 metres, occur from north Yorkshire (Gebdykes Quarry, SE 237823) to Nottinghamshire (SK 486756). The thicker sequences of bivalves (Appendix 6, Log 4) indicate periodic exposure and re-working with inclusion of detrital quartz grains (up to ½ centimetre), possibly from the nearby exposed Namurian gritstones. Sedimentological evidence and the irregular nature of the base of the

Lower Member in this area (Fig 3.2) indicates deposition of thick skeletal grainstone shoals, temporarily exposed as beach rock, around emergent palaeohills.

The thinner, more planar bedded skeletal grainstones and packstones (Appendix 6, Log 2) are possibly the winnowed lateral equivalents of the thick shoals. Smith (1974a) considers the "Bakevellia Bed" to occur 1 to 3 metres above the base of the Lower Member; the diachronous nature of this base, the occurrence of a "Bakevellia Bed" higher in the sequence (Appendix 6, Log 2) and its inter-digitations with shallow water peloid grainstones argue against the "Bakevellia bed" being laterally continuous; it cannot, therefore, be used as a stratigraphic marker horizon. Bivalve accumulations are, however, restricted to the lower part of the Lower Member.

3.2.6 Open marine platform; shallow water carbonates and siliciclastics

Siliciclastic facies in the Mansfield area, the Red and White Mansfield Sandstones, comprise fluviatile - derived sands mixed with carbonates in two well-defined tongues (Fig. 3.6) with quartz contents in excess of fifty percent (Nutting,

Figure 3.6 Extent of the Red and White Mansfield Sandstones (compiled from Nutting, 1980).

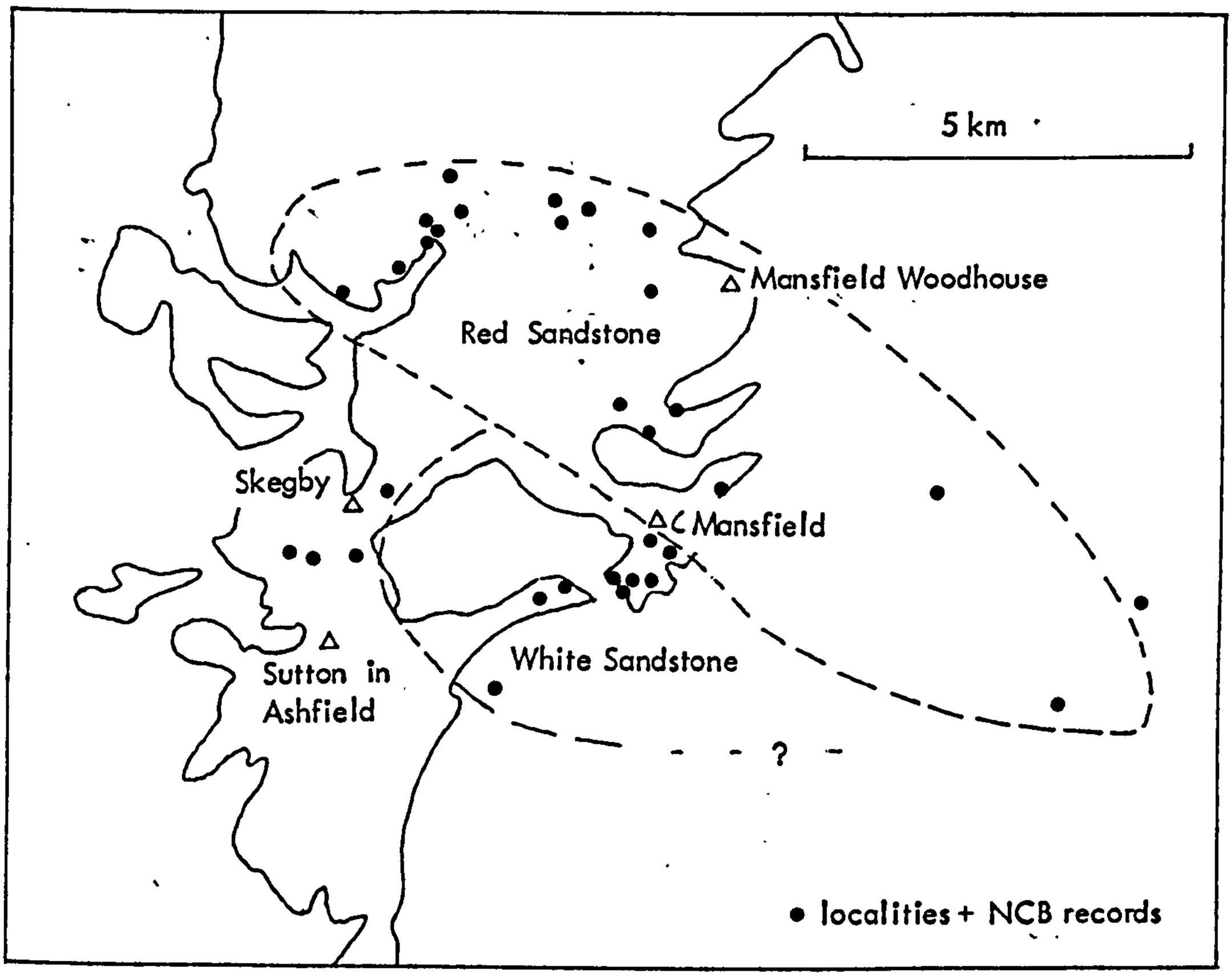
5 km
Mansfield Woodhouse
Red Sandstone
Skegby
Mansfield
Sutton in Ashfield
White Sandstone
?
• localities + NCB records

1980). These quartz sands are present at the top of the Lower Member and base of the Upper Member (Appendix 6, Log 5) and may have been generated during the regression marked by the Hampole Beds.

Course, sucrose, highly bioturbated dolomites with moderate percentages of silt and fine sand sized siliciclastics are problematical in origin due to their textural alteration (4.5.9); peloid ghosts are present in some crystal centres (Fig. 4.19c). Siliciclastics increase in proportion westwards and southwards (Nutting, 1980); some may be aeolian in origin. Bioturbation, visible in exposures and defined in thin section by lack of siliciclastics (Fig. 4.19b) is intense. Small channel cross-sets and ripple cross-laminations (Appendix 6, Log 6) are characteristic of shallow water environments. These beds are probably the more clastic equivalents of the shallow water peloid grainstones. Input of siliciclastics promoted high organic productivity and hence a high level of bioturbation.

3.2.7 Open marine platform; grainstone barriers

Large bed forms with non-planar reactivation surfaces, uni-directional cross stratification

and some erosive bases characterise these grainstones (Appendix 6, Log 7). Laterally equivalent beds in places may show these features to a lesser extent (Appendix 6, Logs 8+9). Bioturbation is generally slight although some intensely bioturbated massive beds (Appendix 6, Log 1) may also belong to this facies. These ooid grainstones are not extensive in the Lower Member; they represent tidal barriers, or sections of barriers, protecting restricted, quiet water lagoons (3.2.14, Fig. 3.18).

3.2.8 Restricted marine platform; non-bioturbated lagoon wackestones

Thin skeletal wackestones with irregular surfaces and mud drapes are present near the base of the Lower Member in Nottinghamshire (Appendix 6, Log 5); they contain bivalves including pectenoids. Many individual valves have a coating of green algae, some rolled (Fig. 3.7a), some preferentially developed on one side (Fig. 3.7b) and, where valves are not dislocated, on top of geopetally filled shells (Fig. 3.7c).

These carbonates have hitherto been placed within the Lower Permian Marls; their sedimentary features, characteristic of a quiet, clear water

Figure 3.7 a Bivalve shells with algal coating in Lower Member non-bioturbated carbonate wackestone, Vale Road Quarry, Mansfield Woodhouse (SK 532648). Shells have coating surround.

b Bivalve shell with algal coating preferentially developed on upper side. Vale Road Quarry Mansfield Woodhouse (SK 532648). Field of view is 3.45mm.

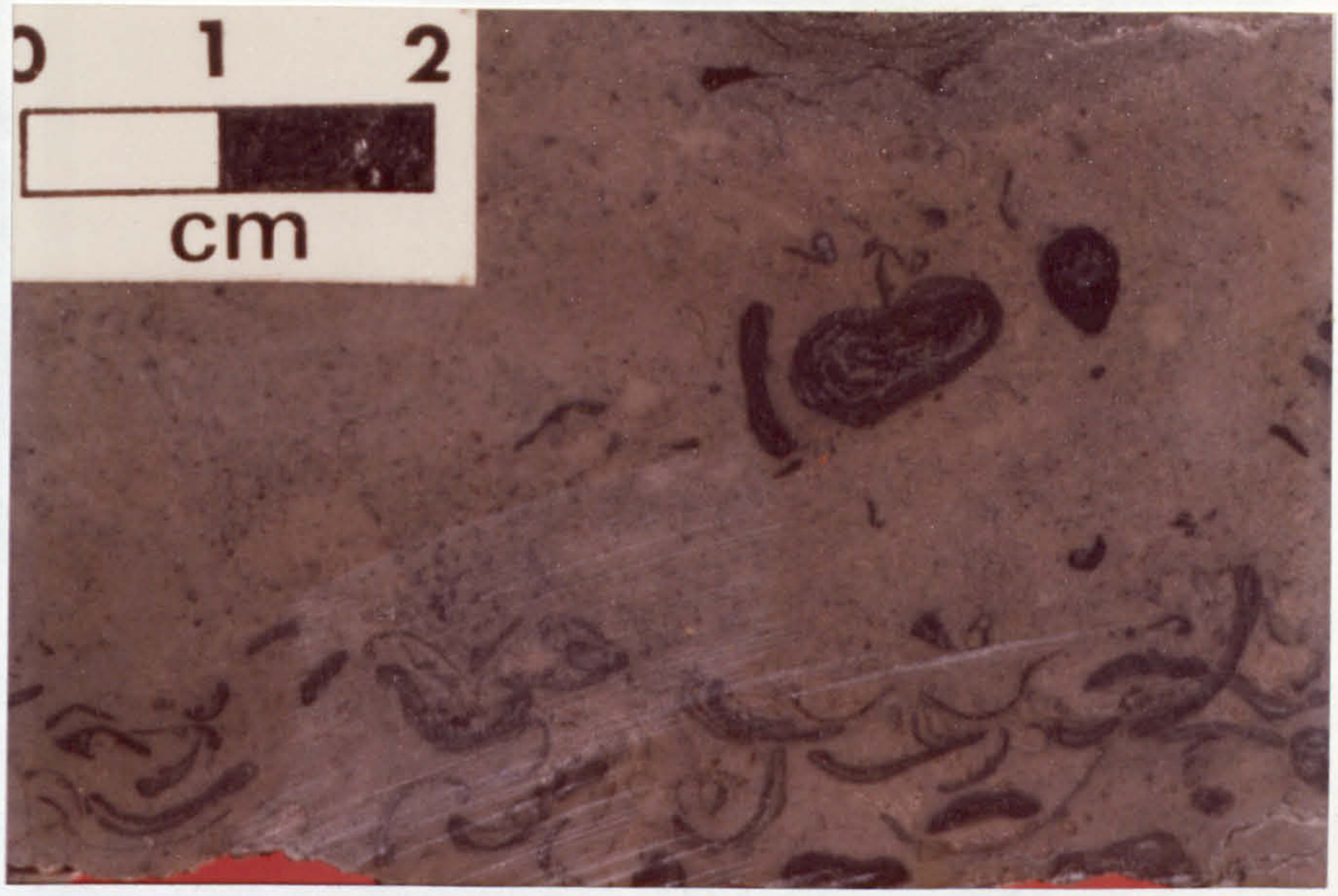
0 1 2
cm

Figure 3.7 c Geopetally filled ?ostracod shell with algal coating on outside, Vale Road Quarry, Mansfield Woodhouse (SK 532648). Shell is still right way up. Shell wall was replaced after spar fill as crystal sizes increase in shell away from outside. Shell is approximately 5mm long.

lagoon with periodic clastic incursions, are of true marine Zechstein strata and demonstrate the necessity for a re-appraisal of the Lower Permian Marls. Discrete clastic incursions, the distal evidence of pluvial periods, decline in number upwards into the more homogenised bioturbated lagoonal mud facies of the Cadeby Formation (Appendix 6, Log 5).

Black, recrystallised limestones belonging to this facies occur at one locality (Appendix 6, Log 10) and contain a varied fauna of foraminifera, ostracods, blue green algae, brachiopods and spores (Fig. 3.8; Table 3.2). Good preservation of the delicate organisms in micrite and neomorphic spar indicates these were originally skeletal wackestones. The limestone may owe its preservation to the former presence of gypsum acting as a seal to the dolomitising fluids. Nearby limestones are secondary with gypsum pseudomorphs (3.2.10) and several are partially dolomitised (4.5.3). Blue green algae with foraminifera indicate clear marine conditions. Surrounding carbonaceous muds and bioturbated mottled dolomites (Appendix 6, Log 10) show evidence of periodic exposure; they are thought to be lagoonal (3.2.9). A lagoonal environment

Figure 3.8 Primary limestone, Lower Member, Bedale Quarry, Well (SE 257812). Limestone is fossiliferous wackestone with much neomorphic calcite spar with sutural boundaries. Foraminferal tests show partial neomorphism (arrowed). Carbonaceous fragments are opaque. Field of view is 2.2mm.

Table 3.2

Fauna at Bedale Quarry, Well

Agathammina pusilla

Agathamming (sp.)

Cyclogyra kinkelini

Ammodiscus (sp.)

Horridonia horrida

Orthothrix (sp.)

Fenestella (sp.)

Bakevellia (sp.)

J. Pattison helped with faunal identification

with good marine connections and episodic clastic incursions is thus envisaged for lime-stone formation. The variety of fauna in these lagoons contrasts with the sparse fauna of the back-reef lagoons of the Durham Ford Formation (J. Pattison, pers. comm., 1980).

3.2.9 Restricted marine platform; bioturbated lagoon wackestones and mudstones

This facies incorporates both mottled and homogenised carbonate wackestones and mudstones with varying proportions of clastic muds. Mottling is due to preferential cementation of sub-horizontal burrow margins (Fig. 3.9, a+b) whereas burrow centres remain as voids or have later evaporite (Fig. 3.9a) or calcite fills(Fig. 3.9b) The cemented margin of the burrows, up to 2 centimetres in diameter, in places grades into the surrounding matrix but elsewhere partially cemented burrow tubules have been winnowed and later compacted, fracturing the earlier tubule cement (Fig. 3.9c). Hardgrounds occur on some surfaces; synerhesis cracks, small scale load casts, oscillation ripples and possible desiccation cracks are also found. Beds of "zebra dolomite" (Fig. 3.10a), similar to strata from the Devonian of Western Canada (C. Jowitt,

Figure 3.9 a Preferential burrow margin cementation, Lower Member Sand Hutton borehole (SE 392830). Burrow margins are lighter coloured dolomite which lithified before the matrix dolomite, forming small fractures (arrowed). Burrows now occluded by evaporite (gypsum after anhydrite) cement.

b Preferential burrow margin cementation, Lower Member, Bedale Quarry, Well (SE 257812). Burrows now occluded by calcite.

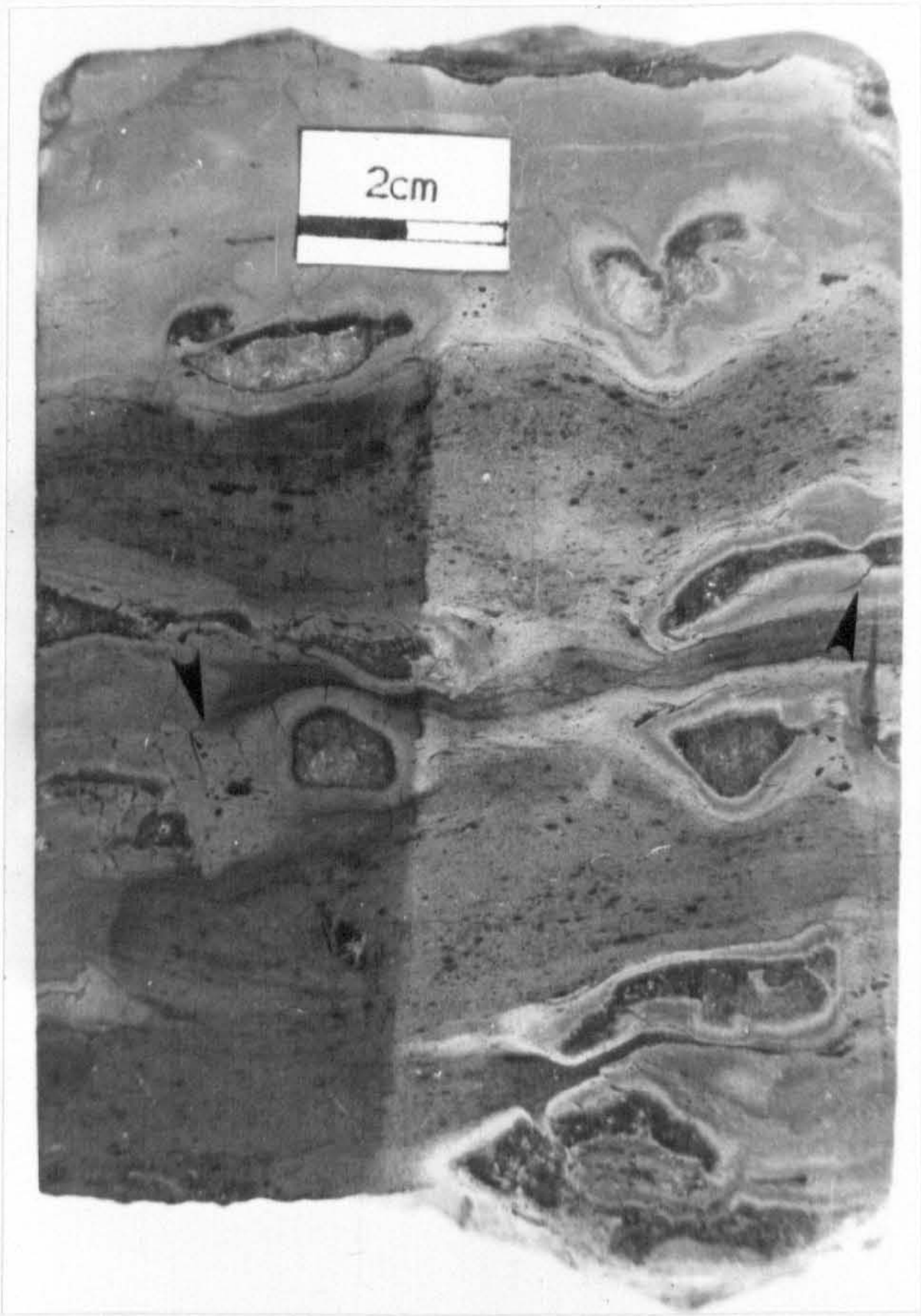
2cm

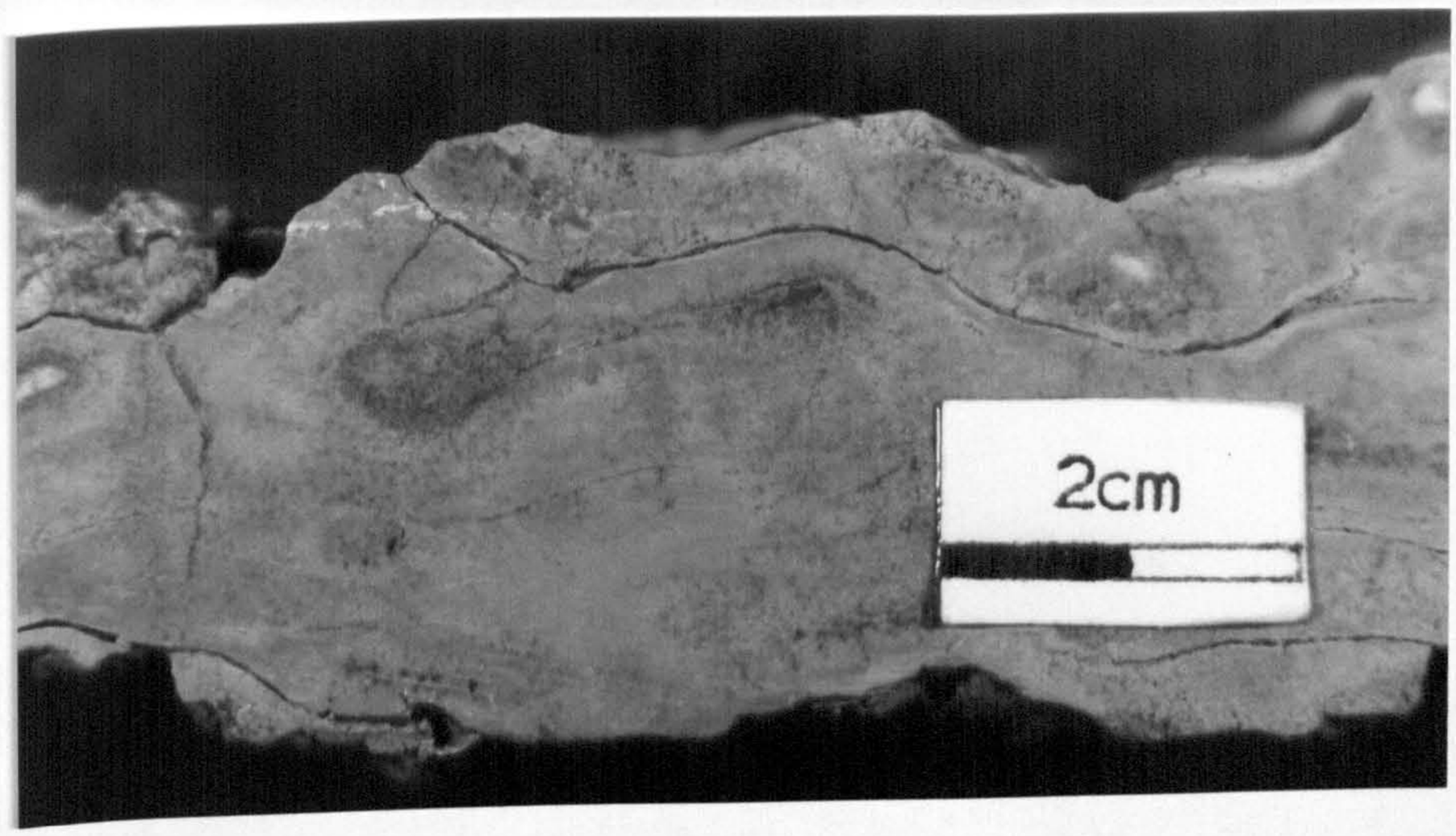
2cm

Figure 3.9 c Preferential burrow margin cementation which has been fractured (arrowed) by compaction after winnowing. Bedale Quarry, Well (SE 257812).


2cm

pers. comm., 1979), form persistent beds (Appendix 6, Log 10); the domal nature of their cracks (Fig. 3.10a) suggest stromatolitic heads, but, as no algal structures are preserved, these may be sheet cracks due to exposure and desiccation. Contortion into tepee-like structures and disrupted bedding (Fig. 3.10b; Appendix 6, Log 10) also indicate period exposure; intervening quiet water conditions are indicated by bryozoans (fenestelled fans and stems) on some bedding surfaces.

Carbonaceous muds drape many bedding surfaces and in places pass laterally into bioturbated mottled dolomites (Fig. 3,11), where they formed synsedimentary depressions. Other lateral transition of carbonates to clastic muds is due to secondary causes including gypsum dissolution (Harwood, in press).

A lagoonal environment with periods of still-stand (forming hardgrounds), influxes of carbonaceous muds during wet spells and periodic desiccation resulting in exposure and some evaporite formation (3.2.10) is envisaged for formation of the mottled dolomites. The sedimentary structures do not accord with

Figure 3.10 a "Zebra" dolomite, Bedale Quarry, Well (SE 257812) voids now have calcite fill. Undulating upper surface of bed is primary feature as is covered by later planar-laminated clayey dolomite (arrowed).

b Contorted bedding, Gebdykes Quarry (SE 237823). Contortions may be due to dewatering, or may be formed during exposure. Planar overlying bed is evidence of penecontemporaneous erosion. Lens cap is 4cm diameter.


2cm

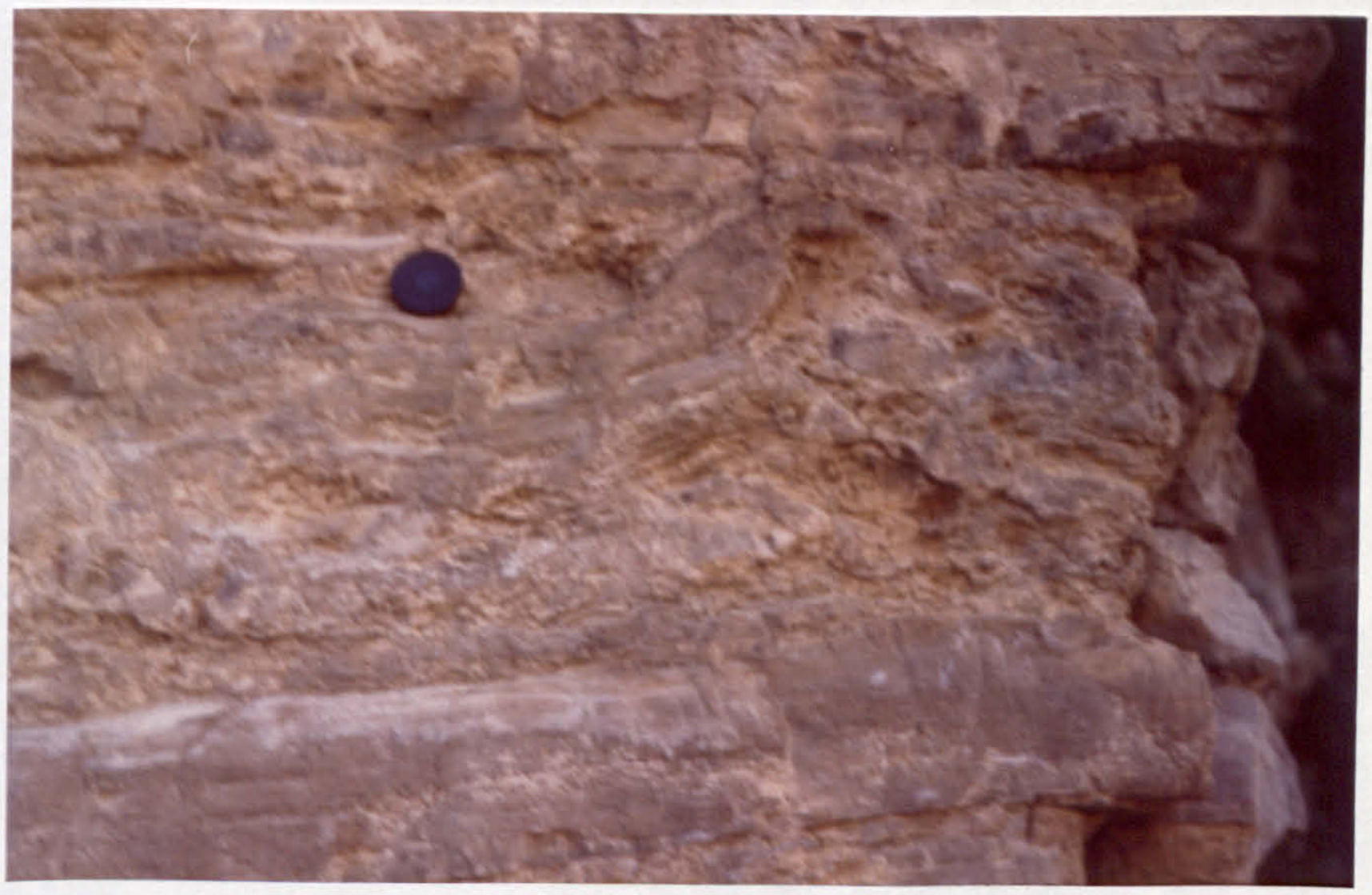

Figure 3.11 Field sketch of lateral transition of bedded carbonates into carbonaceous muds, Bedale Quarry, Well (SE 257812). Individual beds thin towards centre of sketch and these have a higher siliciclastic and carbonaceous content. Syn-sedimentary hollow was preferentially filled by overlying dolomites

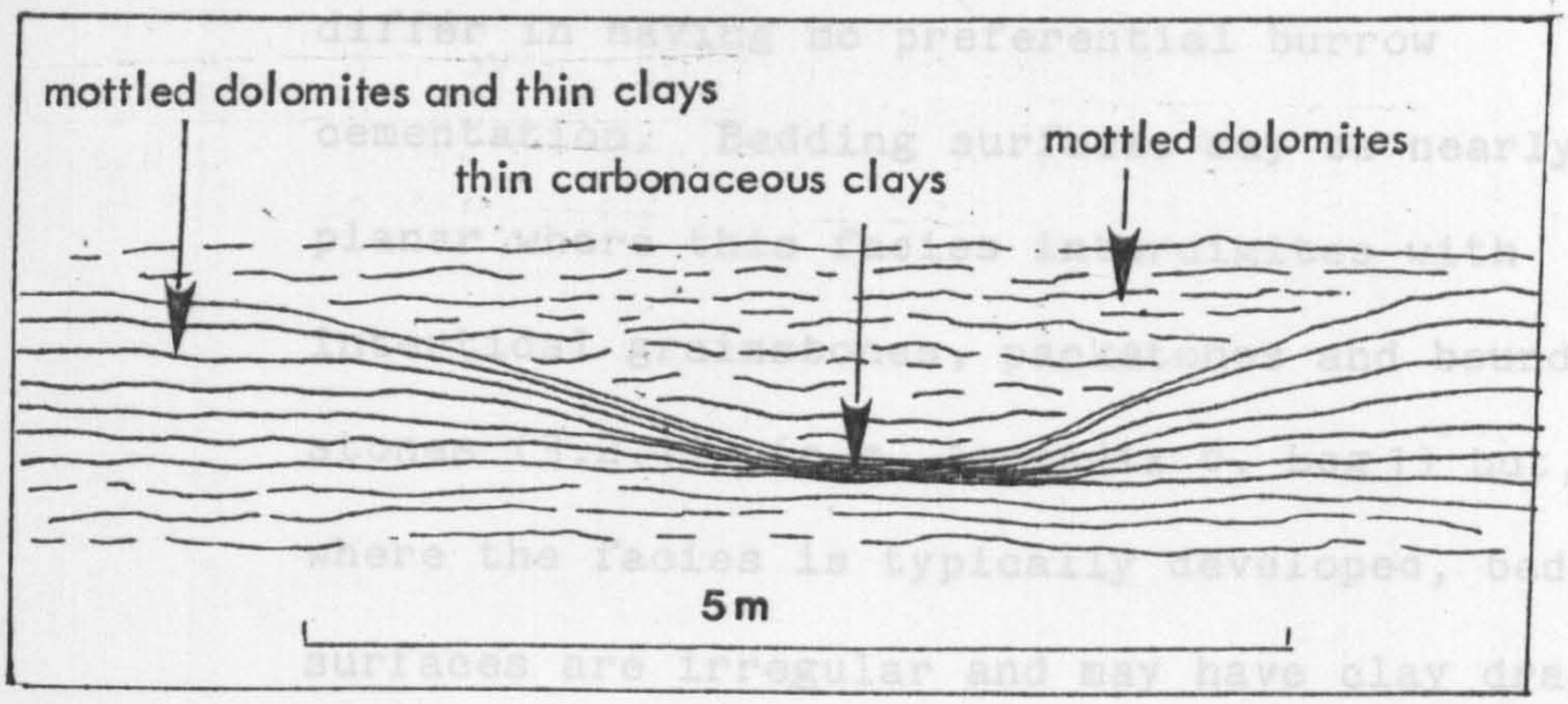
mottled dolomites and thin clays
thin carbonaceous clays
mottled dolomites
5m

Smith's (1970) proposal of a deeper water Ripon Gulf (Fig. 3.12).

The homogenised mudstones and wackestones differ in having no preferential burrow cementation. Bedding surfaces may be nearly planar where this facies interdigites with intertidal grainstones, packstones and bound-stones (3.2.11) (e.g. Appendix 6, Log 1) but, where the facies is typically developed, bedding surfaces are irregular and may have clay drapes which are often carbonaceous (Appendix 6, Logs 5+9), Apart from indistinct bioturbation traces, no internal sedimentary structures are visible. Former gypsum/anhydrite nodules are present in nearby beds (3.2.10) (Harwood, 1980). Early cementation of parts of these beds may have caused some of the bedding surface irregularities; others have been emphasised during diagenesis. These carbonate mudstones were also deposited within the lagoon. Carbonate deposition was possibly more rapid with organic productivity higher than in the areas where mottled dolomites formed. Homogenisation by bioturbation and subsequent burial resulted in more fetid carbonate mudstones, separated by carbonaceous clastic mud laminae introduced during pluvial periods.

Figure 3.12 Sketch map of the 'Ripon Gulf' as envisaged by D.B. Smith.

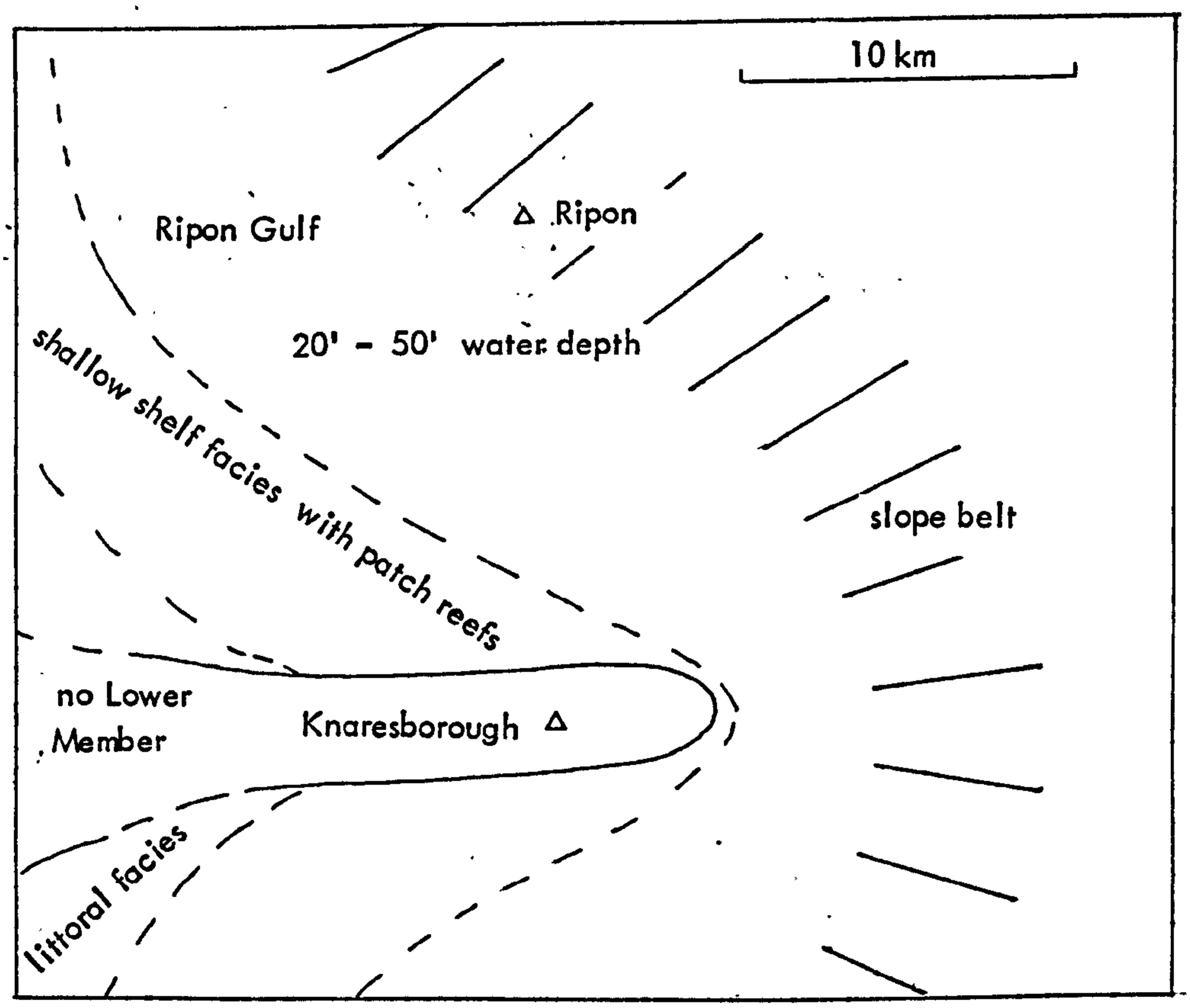
10 km
Ripon Gulf
Ripon
20' - 50' water depth
shallow shelf facies with patch reefs
slope belt
no Lower Member
Knaresborough
littoral facies

3.2.10 Restricted marine platform; bioturbated lagoon wackestones and mudstones with evaporites

The evaporite-rich equivalent of the black limestones (3.2.8) at Well (SE 257812) are secondary limestones with a vertical fabric of gypsum crystals now pseudomorphed by calcite (4.5.3) (Fig. 4.7 b-d) and partially dolomitised limestones with gypsum rosette casts on some surfaces (Fig. 4.8a). Both gypsum and dolomite replace original calcium carbonate (4.5.3).

Gypsum rosettes on dolomite sediment surfaces occur today in the supratidal zone of sabkhas (Kinsman, 1969); they also form as "desert roses". The thin dolomite crusts (Fig. 4.8a) are also typical of exposed sediments; they probably developed on the exposed floor of the desiccating lagoon. Vertical gypsum crystals within the sediment are more characteristic of intertidal zones (Shearman, 1966; Kinsman, 1969; Sherif, 1978); where individual crystals are usually discoid or lenticular in form and rarely coalesce (e.g. Schreiber, 1978). Gypsum crystals also sometimes contain inclusions of the host sediment (Kinsman, 1969). The coalesced vertical gypsum crystals probably

grew within the sediments at the lagoon margins. I can find no detailed descriptions of comparable modern analogues.

Former evaporites also are present within slightly mottled carbonate mudstones at Sutton Grange Quarry (SE 285744), concentrated at certain levels (Fig. 3.13). Their discoid and lenticular form suggests these, too, were former gypsum, rather than anhydrite, crystals, now replaced by calcite (5.4.1). The crystals show no preferential orientation (Fig. 3.13) and contain small dolomite inclusions. No evaporite nodules, either gypsum or anhydrite, are present; lateral correlation is difficult because of extensive calcitisation (5.4.1). Gypsum crystal form again suggests an intertidal or lagoon margin environment; the radial orientation may imply a high fluid pressure of the interstitial brines within the carbonate muds, perhaps due to a less permeable sediment surface.

The mode of formation of anhydrite nodules in the homogenised carbonate muds is more debatable. Bioturbation, which would destroy algal laminites, is usually not prolific in supratidal

Figure 3.13 Calcite pseudomorphing displacive gypsum crystals in lagoon mudstones and wackestones, Sutton Grange Quarry (SE 285744). Crystals have random orientation.


0 1 2
cm

sediments. Apart from the evaporites (Harwood, 1980) and interbedded horizons of "zebra dolomite" (Clowne, SK 486757; Appendix 6, Log 10), there is commonly none of the evidence usually associated with intertidal or supra-tidal conditions in these beds; such evidence occurs in the intertidal grainstones, packstones and boundstones (3.2.11). The presence of large, (30 centimetres plus long at Rock Cottage Quarry, SE 304650) vertical, replacive halite or gypsum crystals (Fig. 3.14a) similar to those in modern sabkhas (Kinsman, 1969; Sherif, 1978), halite hopper casts between nodules (Fig. 3.14b) and possible halite crystals within the nodules (Fig. 3.14 c+d) with evidence of calcitised anhydrite within the nodules (Harwood, 1980) does, however, indicate hypersaline and possibly supratidal conditions. The high organic and the contained sulphide content of the sediments (Harwood, 1980) is evidence of an anoxic sequence impoverished in sulphate (Kendall, 1979). Bacterial reduction of sulphate prevented anhydrite growth beyond nodule formation. This explains both the lack of enterolithic and ptygmatic anhydrite and the presence of pyrite framboids within the carbonates. It is thus

Figure 3.14 a. Vertical cast after ?halite crystal in lagoon wackestones and mudstones, Rock Cottage Quarry, Wormald Green (SE 304650).

b Cast of hopper cube after ?halite in margin of dissolved former displacive evaporite nodule, Rock Cottage Quarry, Wormald Green (SE 30465). Field of view is 0.8mm.

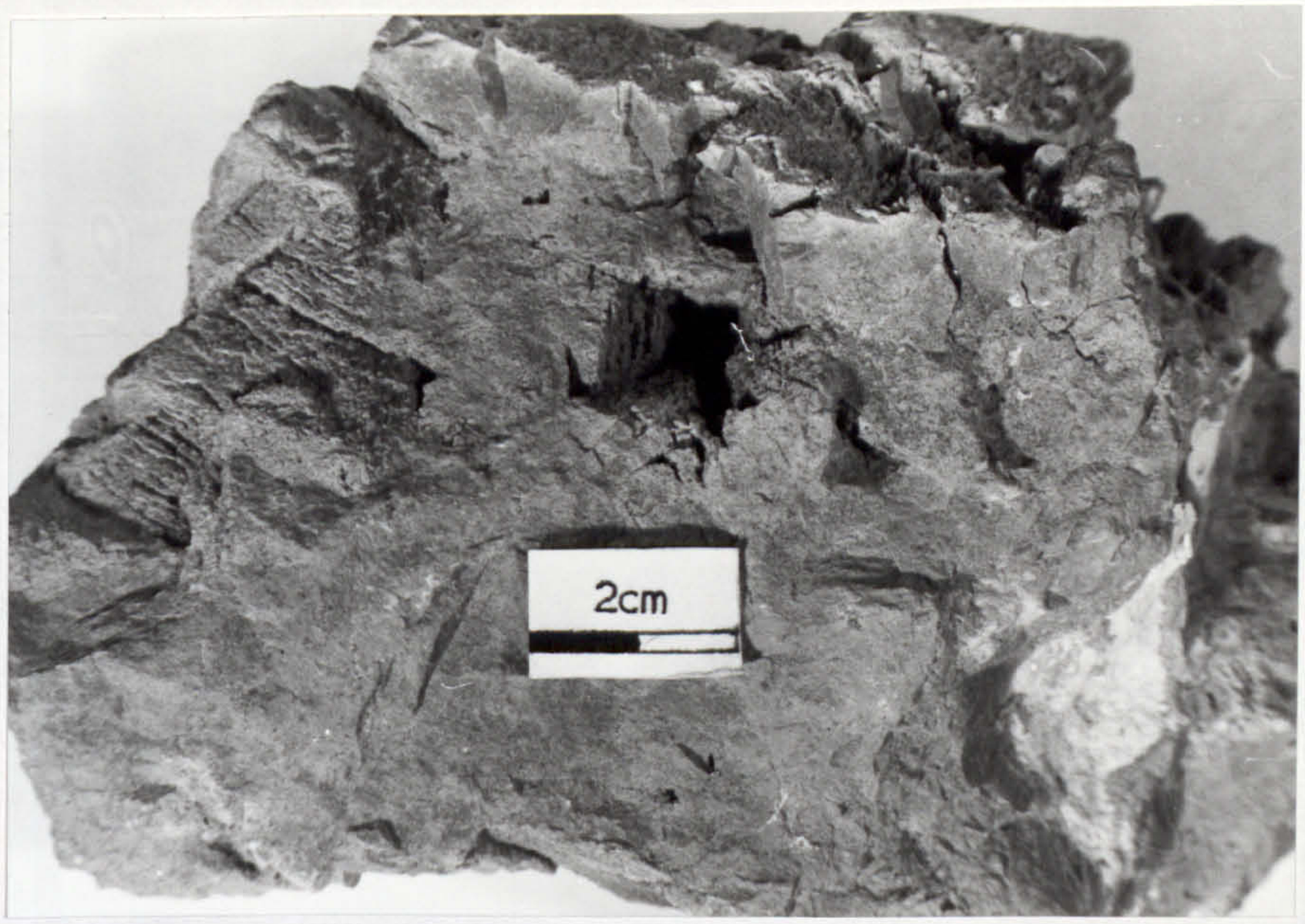
2cm

Figure 3.14 c "Firtree" crystals, now of calcite, replacing ?halite within displacive evaporite nodule, Rock Cottage Quarry, Wormald Green (SE 304650). Field of view is 2.2cm.

d "Fir tree" crystals of displacive halite from sabkha sequence (from James, 1980).

12 cm

tentatively concluded that these anhydrite nodules did form in a supratidal environment during periodic lagoon desiccation or a possible minor re-gression (3.2.14).

3.2.11 Restricted marine platform; intertidal grainstones, packstones and boundstones

Grainstones, packstones and boundstones with cryptalgal laminae, fenestrae, (Fig. 3.15a) laterally continuous millimetre-centimetre bedding, rip-up clast breccias, contorted bedding (Fig. 3.15 b+c) and dewatering structures, many with syn-sedimentary erosion (Fig. 3.15d) characterise intertidal environments with periodic exposure. Original sediments were ooids, pellet and skeletal debris; no carbonate muds have been recognised with these sedimentary structures. Smith (1968, 1974a + c) recognises this facies in the Lower Dolomite of the Hampole Beds. Present research shows it to be more widespread (Appendix 6, Logs 1, 2 + 3); fenestral ooid-rich laminites are found below the Hampole Disconformity at Hampole Quarry (SE 515097) and New Micklefield (SE 446325) and are present for several metres below the Hample Beds near Wetherby (Appendix 6, Logs 2+3). These

Figure 3.15 a Fenestral ooid grainstone, Lower Member, Hampole Quarry (SE 516097). Note elongated fenestrae following small channel (arrowed).

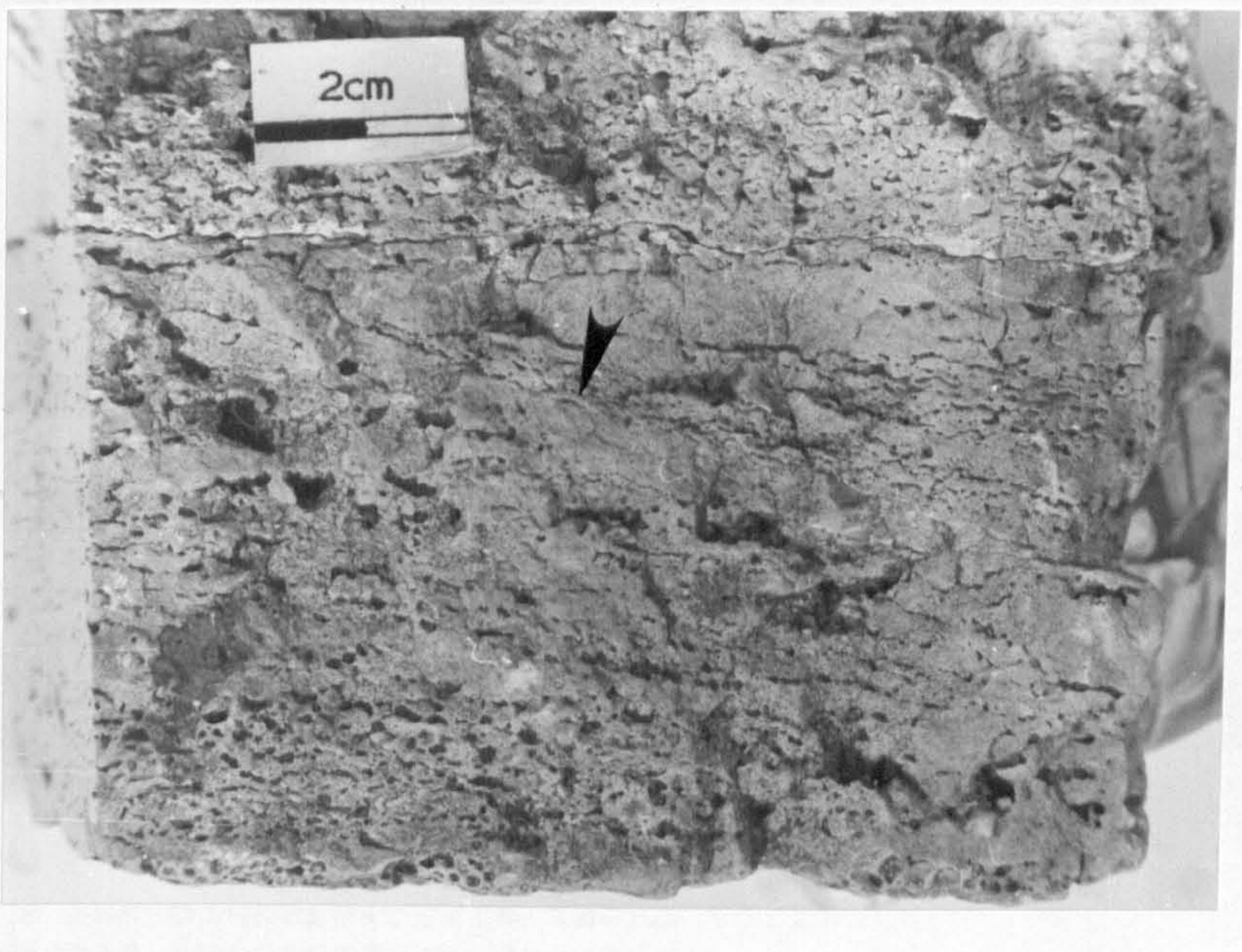
2cm

Figure 3.15 b Contorted bedding at top of Lower Member, Wetherby (SE 400486). Contorted bed contains cross laminations (see Fig 3.15 c . Hammer is 0.35m long.

c Mode of origin of contorted bedding in Fig 3.15 .b .

(i) Ooid grainstone with sigmoidal cross lamination.

(ii) Contortion of semi-lithified sediment preserving cross laminations.

(iii) Later siliciclastic mud infill between contortions before deposition of later flat bedded dolomites.

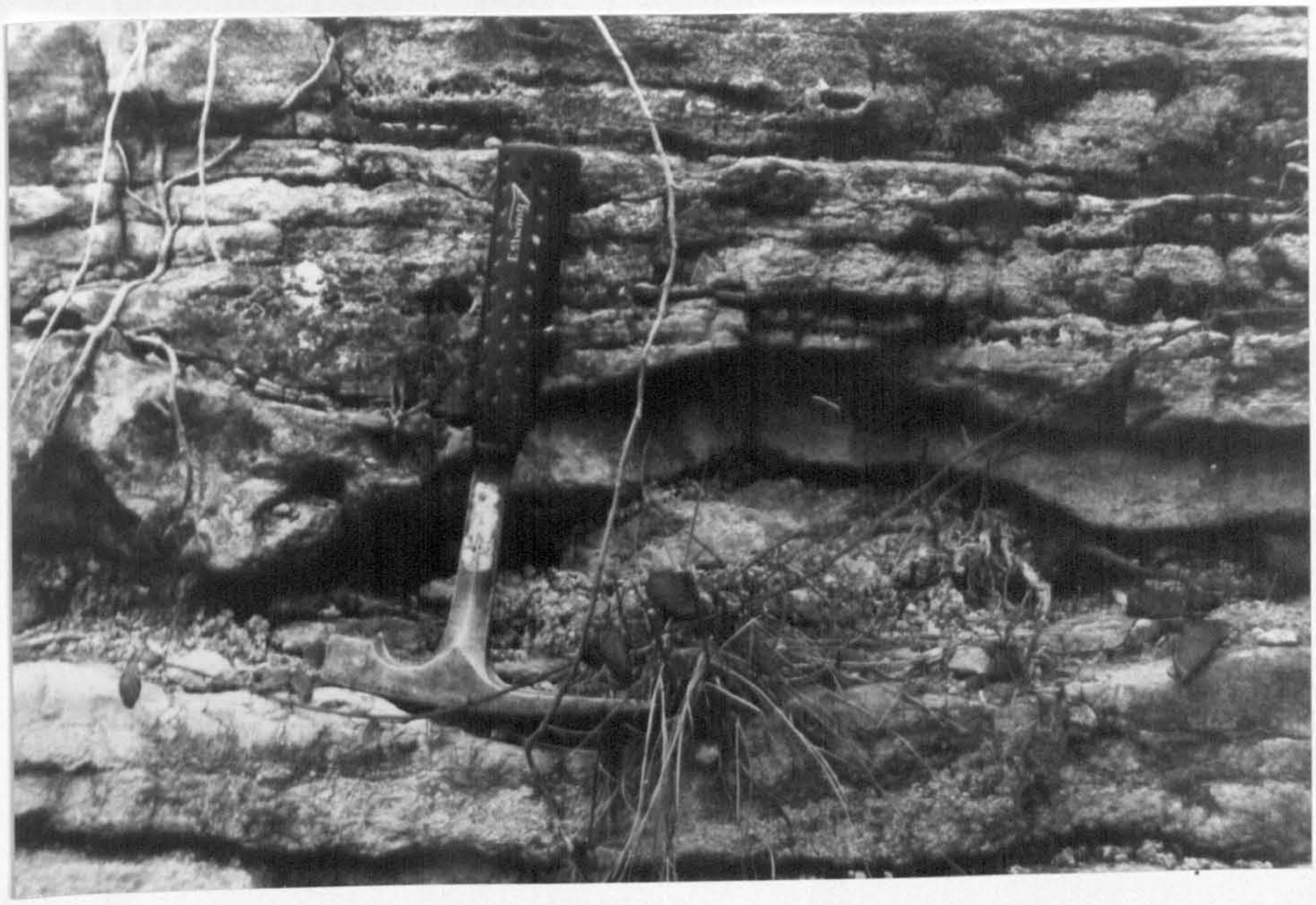

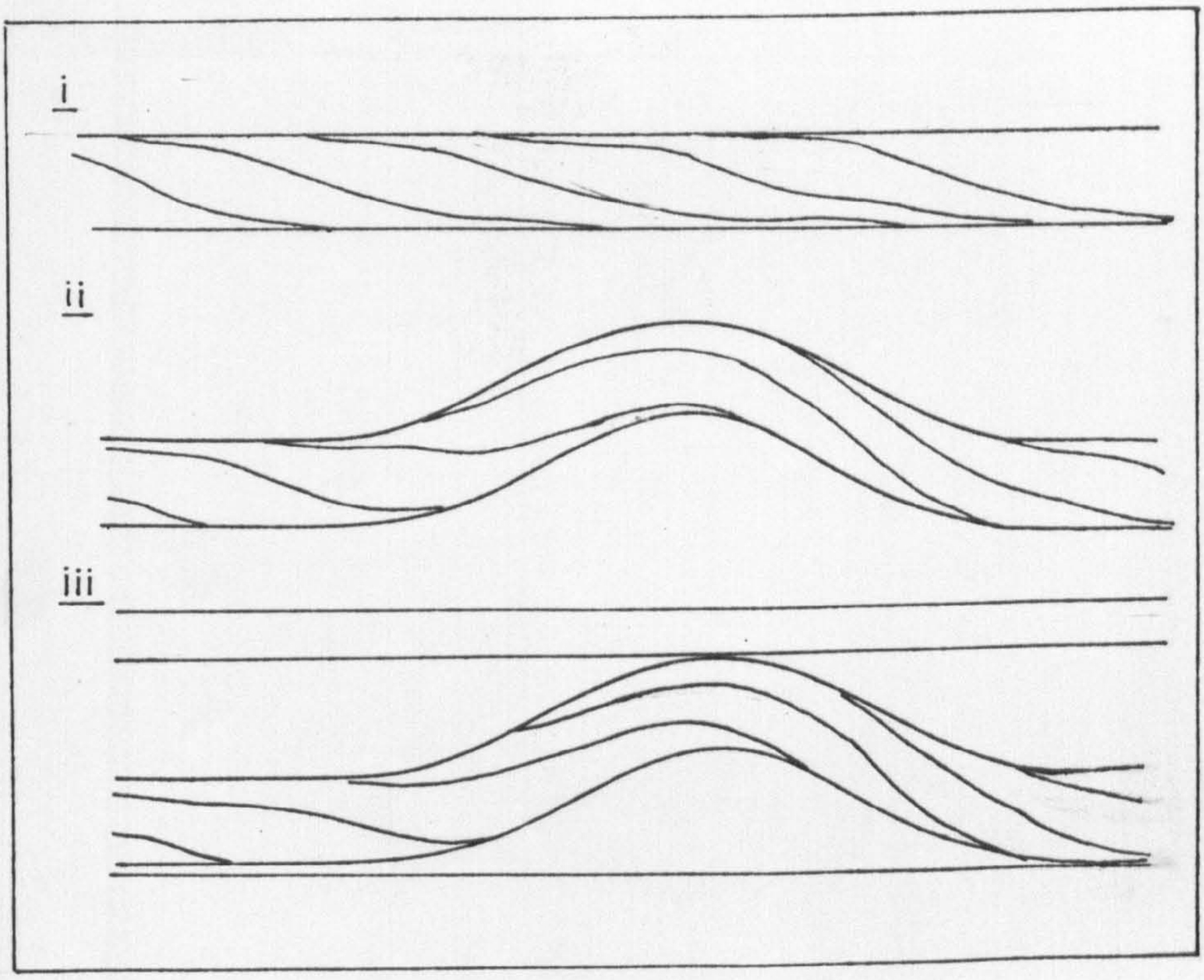
i
ii
iii

Figure 3.15 d Synsedimentary erosion of blisters in crypt algal laminites, Bramham (SE 422429). Upper laminite bed (arrowed) cuts across blisters caused by dewatering or desiccation during exposure.

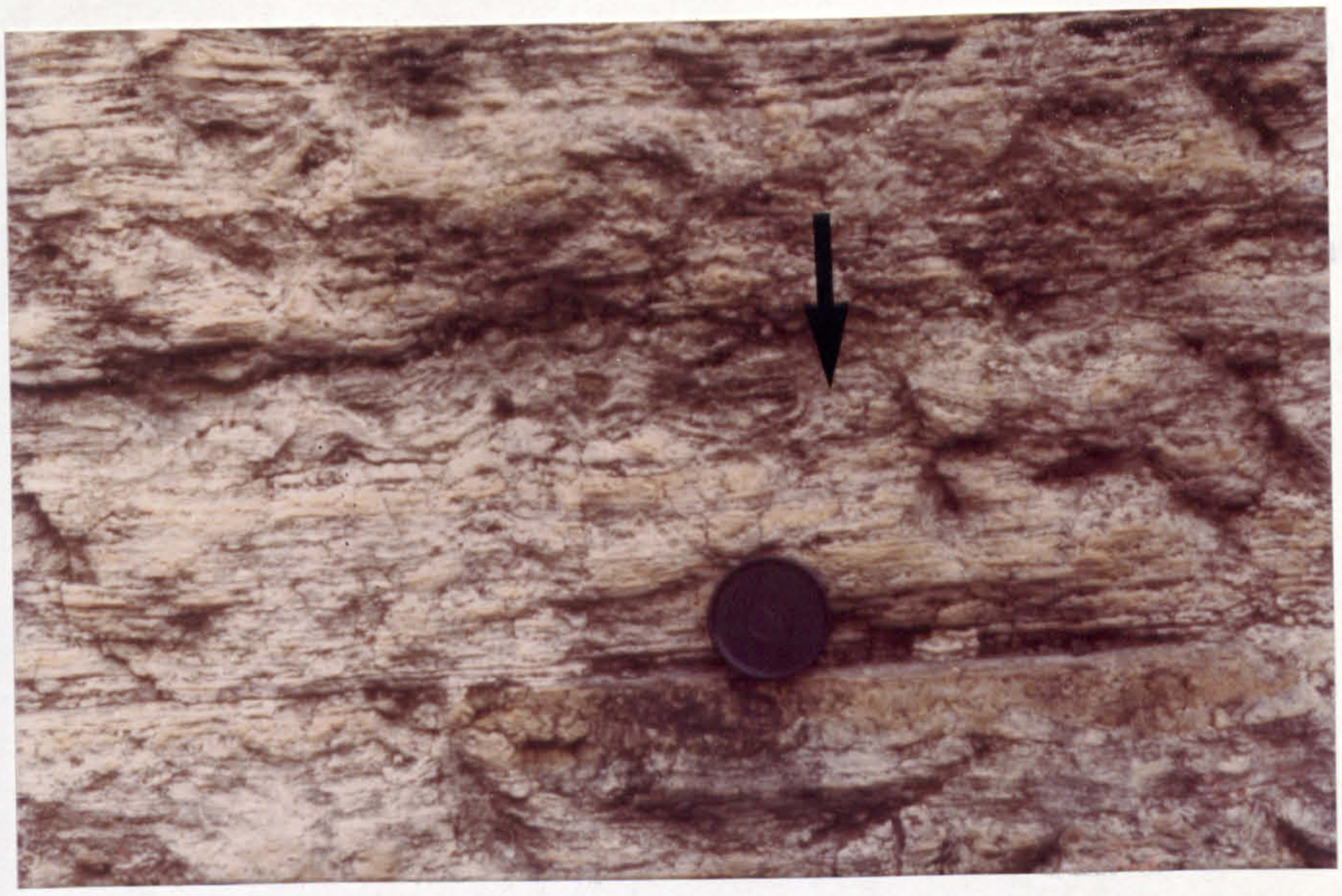

sedimentary structures are typical of the broad intertidal margins of carbonate platforms of shallowing upwards sequences (James, 1979) in protected locations; laterally equivalent tidal channel areas may be partially represented by the shallow water peloid grainstones (3.2.4). A prograding coastline would need some degree of protection from wave action, either with a wide shallow platform which would dissipate wave force, or with an offshore barrier; this barrier could comprise ooid shoals, reefs or pre-Permian palaeohighs. Grain size and composition suggest a higher energy environment than the lagoon facies, with better open marine connections.

3.2.12 Restricted marine platform; supratidal carbonates

The presence of displacive evaporite nodules (Fig. 3.16 a+b) in cryptalgal laminites (Appendix 6, Log 1) indicates supratidal conditions, the lateral equivalent of the intertidal facies (3.2.11). Although the nodules shown (Fig. 3.16 a+b) are now baryte, or baryte, calcite and goethite, sulphur isotope analyses (Coleman and Harwood, 1980) (9.2.2) indicate replaced evaporites. Preservation of original dimensions

is shown by analogues with modern gypsum/ anhydrite nodules (Fig. 3.16 c+d). Evaporites in displacive nodules are dissolved in near surface environments creating voids (6.5.1) (Harwood, 1980). Penecontemporaneous dissolution also occurred in places; one result is a bed containing disorientated carbonate blocks, some distorted by soft sediment deformation, in a soft dedolomite matrix at Wetherby (Appendix 6, Log 3).

Despite the extensive nature of the intertidal facies (3.2.11), few localities contain the supratidal equivalent. This may be partly due to penecontemporaneous evaporite dissolution or, more likely, to penecontemporaneous erosion.

3.2.13 ?Restricted marine platform; patterned carbonates

Patterned carbonates (Dixon, 1976) have variegated light and dark coloured areas of rock, varying in shape, complexity and intensity of development. The colour difference is also, in part, caused by concentrations of small pyrite crystals in the dark areas (Dixon, 1976) and, in part, by differences in crystal size and inclusion density within the carbonates.

Figure 3.16 (a) + (b) Replaced displacive evaporite nodules in crypt algal laminites, Bramham (SE 428429), Nodules now comprise calcite and baryte. Note "cauliflower"-like outline characteristic of displacive evaporite nodules. Lens cap is 4cm diameter.

(a) side view

(b) top view

Figure 3.16 (c) and (d). Recent displacive gypsum nodules from an inland sabkha, Sabkha al Daiyah, U.A.E. Note similarity of shape to those of Figs 3.16 (a) and (b). Gypsum nodules kindly loaned by Dr. P.R. Bush.

(c) side view

(d) top view


1 CM


1 CM

Figure 3.17 a Patterned carbonates. Wistow Wood borehole (SE 567356). Note light and dark colouration and similarity of rounded forms to evaporite nodules.

Adjacent sediments contain pyrite framboids. The patterns are a diagenetic feature (Dixon, 1976; Kendall, 1977), indicators of evaporitic environments where sulphate reduction has occurred. In the Lower Member, patterned carbonates have not been recognised at outcrop but occur in the shallow subcrop (Appendix 6, Log 11) when, in places, they have considerable porosity (Appendix 7). In the Wiston Wood core (Appendix 6, Log 11) the patterned carbonates (Fig. 3.17a) include possible algal mats; modern analogues (Fig. 3.17 b+c) suggest a high intertidal-supratidal environment although Permian algal mats may have extended into sub-tidal environments (Smith, 1981). Kendall (1977) argues some patterned carbonates may be of subaqueous origin. Because patterned carbonates are a "diagenetic facies" they are not included in the environmental reconstruction of the Lower Member.

3.2.14 Environmental reconstruction of the Lower Member

Inter-relationships of the facies developed in the Lower Member are given in the environmental reconstruction of Figure 3.18 with a synopsis of the facies and their environments in Table

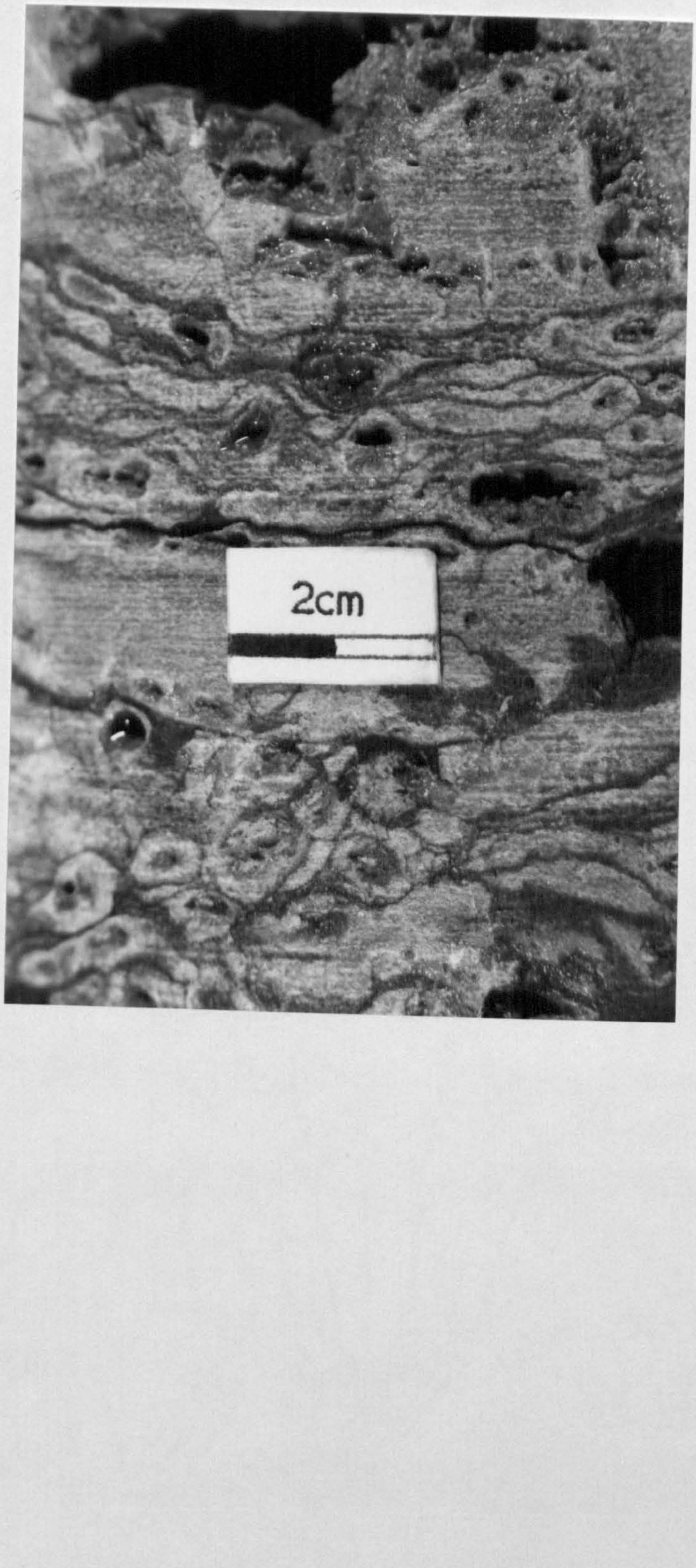
2cm

Figure 3.17

b Possible algal mats in patterned carbonates, Wistow Wood borehole (SE 567356). Laminated dolomicrite is broken across centre of picture. Zoned limpid dolomite overgrowths grew before break, but pore-filling calcite is after the break. Cathodoluminescence. Field of view is 2.25mm.

c; Algal mat punctured by displacive gypsum crystal in sabkha intertidal zone, Gulf of Sirte, Libya. (from Sherif, 1978).

2.5 mm

Figure 3.18 Distribution of facies in the Lower Member, Cadeby Formation.

Carbonate mudstones and wackestones

Patch reefs and flank grainstones

Shallow water peloid grainstones and skeletal grainstones and packstones

Shallow water carbonates and siliciclastics

Grainstone barriers

Lagoon wackestones and mudstones

?
York
platform
margin
Leeds
?
?
Doncaster
Sheffield
10 km
Nottingham

3-3. Not all facies existed in the outcrop area at any one time; supratidal facies, for example, are more widespread towards the top of the Lower Member, whereas patch reefs are more common lower in the succession. Contrary to former reports, there is evidence for contemporaneous evaporite formation throughout the Lower Member; algal mats with disruptive gypsum crystals (3.2.13), anhydrite nodules (3.2.10) (Appendix 6, Logs 5+9; Clowne SK 486756) and vertical replacive gypsum crystals (3.2.10) (Appendix 6, Log 10) occur well below the Hampole Beds. A compilation of sections across North Yorkshire (Fig.3.19), correlating evidence of supratidal conditions and subaerial exposure, suggests a possible earlier minor regression of the Zechstein sea about 8 metres below the level of the Hampole Beds. At about the same level, a bed of crusts and breccias can be recognised at Wistow Wood (Appendix 6, Log 11) and open vugs after dissolved, displacive evaporites occur at Mansfield Woodhouse (Appendix 6, Log 5) (Fig.6.8b). Further detailed field work is necessary to determine the full extent of this regression.

TABLE 3-3

Synopsis of facies and environments of deposition in the Lower Member

Open Marine Facies	Characteristics and environments of deposition
Carbonate mudstones and wackestones	Nodular carbonates with varied amounts of siliciclastic muds. Some winnowing of nodules. Low energy environment. Relatively deep water near platform margin.
Patch reefs and flank grainstones and packstones	Sub-circular bryozoan patch reefs of baffleStone 'pillows'. Crypt-algal laminite covering near top of Lower Member. Flank beds indicate moderate energy oxic environment. Shallow water marine platform.
Shallow water peloid grainstones and packstones	Small cross laminations and channel and fill structures with some bioturbation. Shall subtidal-low intertidal moderate energy environment with meandering small tidal channels.
Skeletal grainstones and packstones	Shoals and beach assumulations around emergent palaeohills and winnowed lateral equivalents. High-moderate energy shallow sub-tidal exposed environments.
Shallow water carbonates and siliciclastics	Highly bioturbated coarsely crystalline dolomites with varied amounts of fine sand-silt sized siliciclastics. Shallow subtidal moderate-low energy oxic environments.
Grainstone barriers	Large bedforms with uni-directional cross-stratification. Moderal-high energy tidal barriers

TABLE 3-3 (Cont'd)

Restricted Marine Facies	Characteristics and environments of deposition
Non-bioturbated lagoon wackestones	Varied fauna in limestones with interbedded siliciclastic and carbonaceous muds. Low energy shallow lagoon environment.
Bioturbated lagoon wackestones and mudstones	Mottled and homogenised dolomicrites with hardgrounds and exposed surfaces. Some clastic mud drapes. Low energy lagoon environment and periodic desiccation.
Bioturbated lagoon wackestones and mudstones with evaporites	Pseudomorphs or casts of displacive anhydrite nodules and gypsum crystals. Some bioturbation and clastic mud drapes. Anoxic dolomicrites. Low energy lagoon with periodic desiccation and evaporite growth. Landward equivalent of bioturbated lagoon wackestones and mudstones.
Intertidal grainstones, packstones and boundstones	Crypt-algal laminites, fenestrae, dewatering structures and syn-sedimentary erosion in peloid-rich sediments. Moderate energy intertidal oxic environment.
Supratidal carbonates	Displacive evaporite nodules in crypt-algal laminites - lateral equivalent of intertidal packstones and boundstones. Rare supratidal environment.
Patterned carbonates	Light and dark anoxic dolomicrites with high proportion of void space. Diagenetic facies. Possibly algal laminites which were evaporite-rich.

Figure 3.19 a Compilation of sections across North Yorkshire showing the Hampole Beds and relative position of the possible earlier regression. Logged sections are shown in line outline; known thicknesses from borehole data are in dashed outline (most from D.B. Smith, pers. comm.)

b Localities and line of section for Figure 3.19 a.

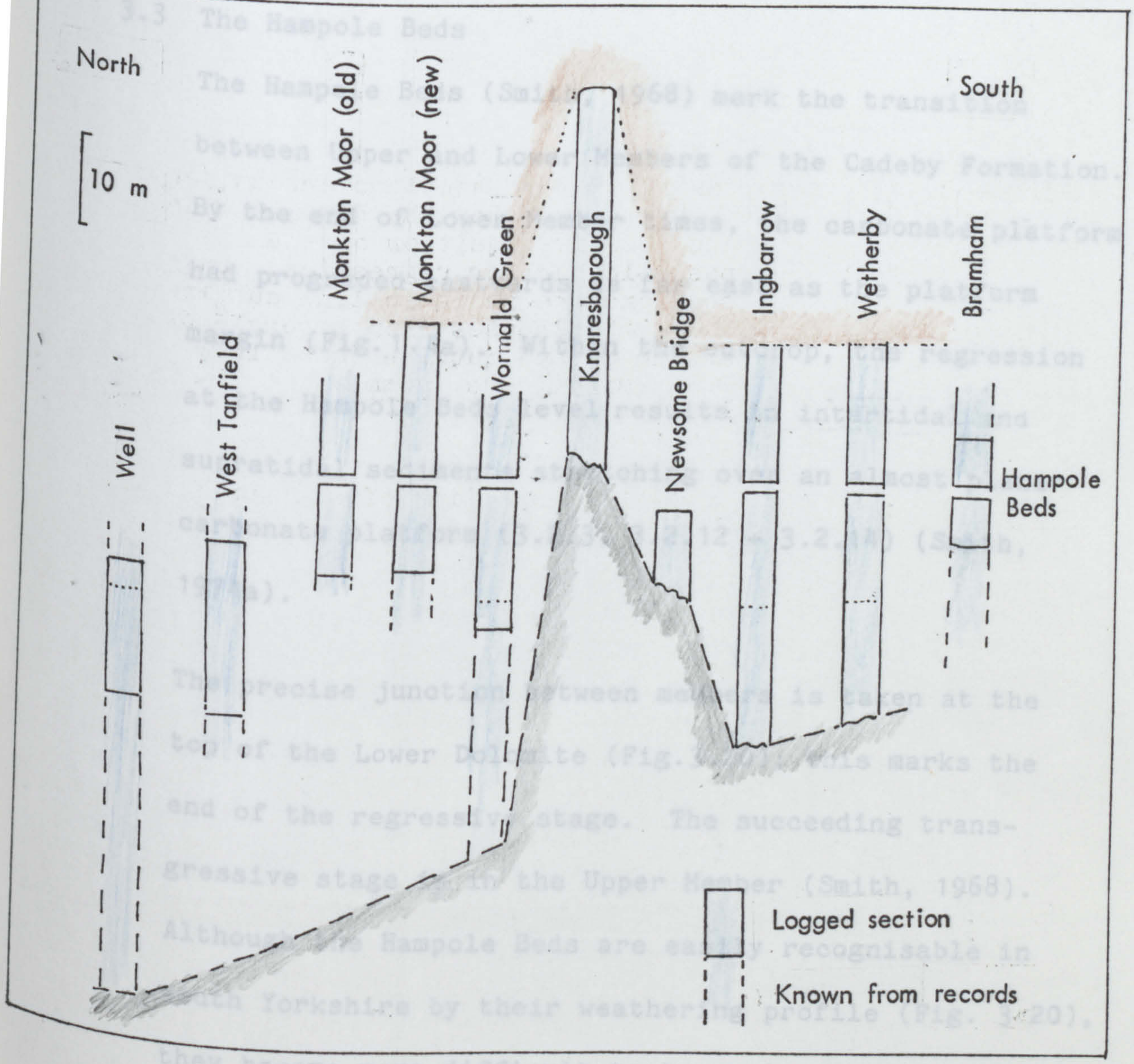
North
South
10 m
Well
West Tanfield
Monkton Moor (old)
Monkton Moor (new)
Wormald Green
Knaresborough
Newsome Bridge
Ingbarrow
Wetherby
Bramham
Hampole Beds
Logged section
Known from records

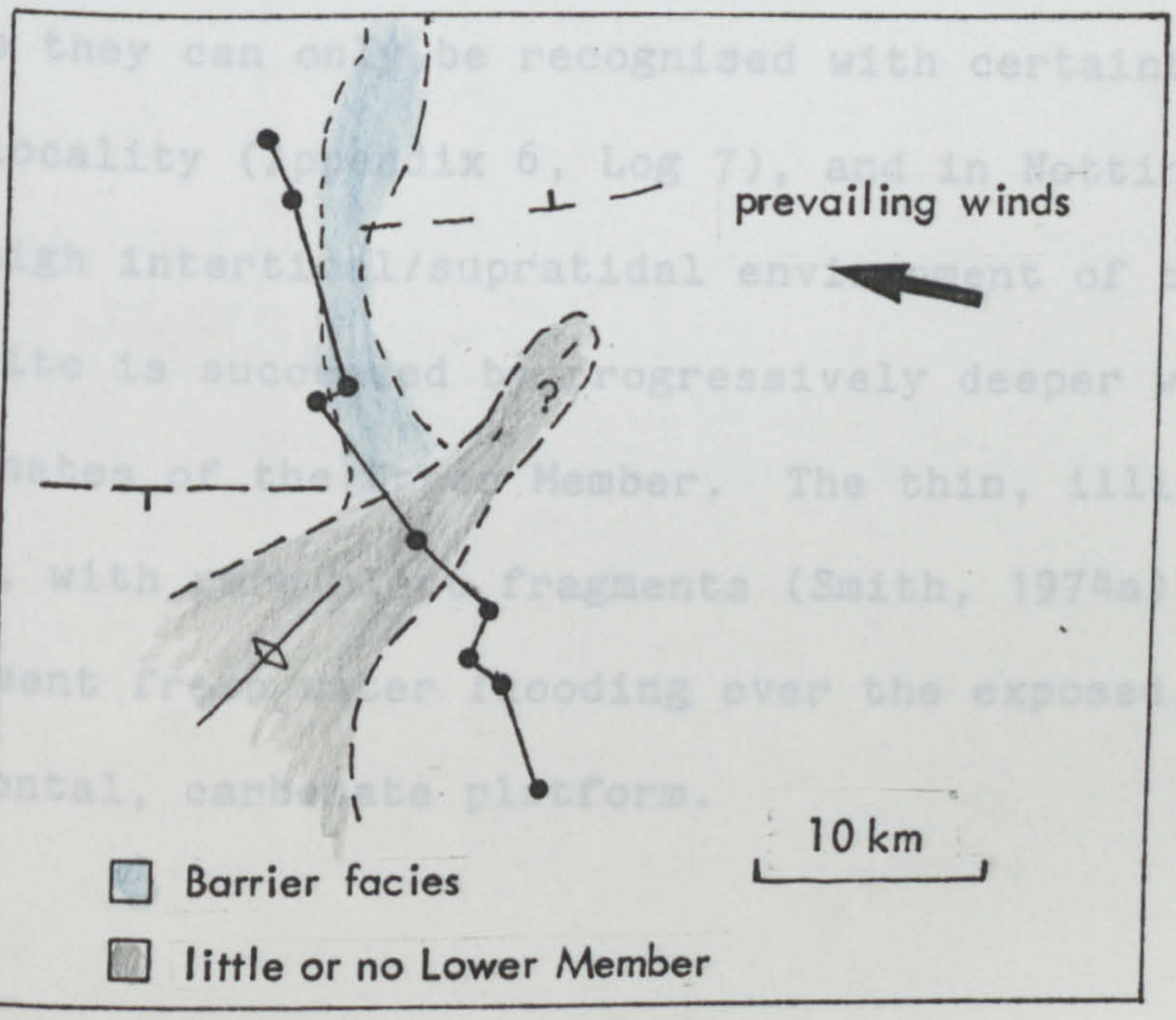
prevailing winds
?
10 km
Barrier facies
little or no Lower Member

3.3 The Hampole Beds

The Hampole Beds (Smith, 1968) mark the transition between Upper and Lower Members of the Cadeby Formation. By the end of Lower Member times, the carbonate platform had prograded eastwards as far east as the platform margin (Fig.1.4a). Within the outcrop, the regression at the Hampole Beds level results in intertidal and supratidal sediments stretching over an almost planar carbonate platform (3.2.3, 3.2.12 + 3.2.14) (Smith, 1974a).

The precise junction between members is taken at the top of the Lower Dolomite (Fig.3.20); this marks the end of the regressive stage. The succeeding transgressive stage is in the Upper Member (Smith, 1968). Although the Hampole Beds are easily recognisable in south Yorkshire by their weathering profile (Fig. 3 20), they become more difficult to trace in north Yorkshire, where they can only be recognised with certainty at one locality (Appendix 6, Log 7), and in Nottinghamshire. The high intertidal/supratidal environment of the Lower Dolomite is succeeded by progressively deeper water carbonates of the Upper Member. The thin, illitic clays, with rare plant fragments (Smith, 1974a) may represent fresh water flooding over the exposed, near-horizontal, carbonate platform.

Figure 3.20 The Hampole Beds (from Smith, 1968).

HAMPOLE BEDS

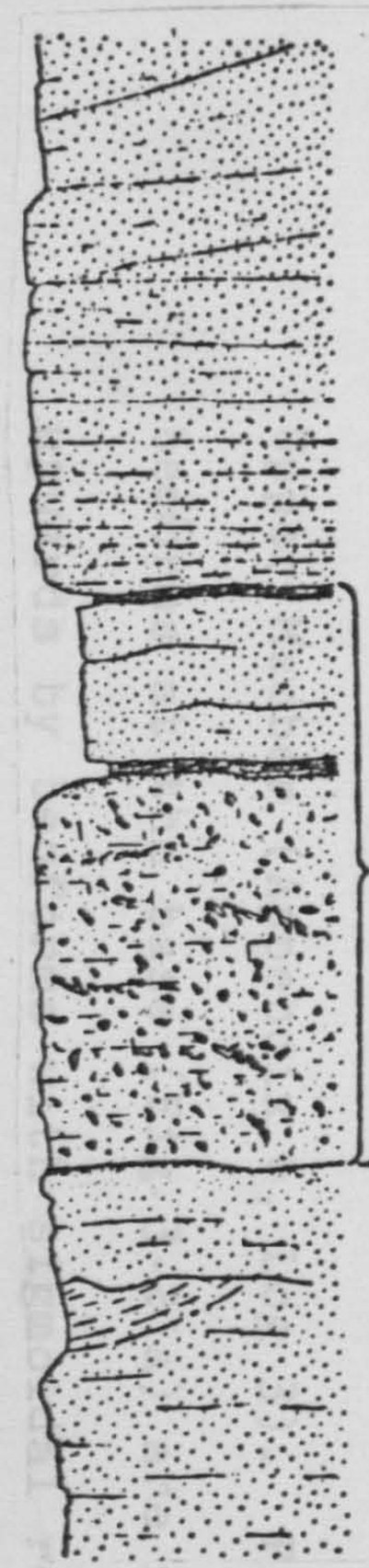

		CMS	
	Dolomite, pale cream, finely oolitic, soft, coarsely wedge-bedded except near base where more evenly bedded	1050+	planar laminated→ripple laminated→cross laminated oolites; increasing current energy and increasing water depth
	Dolomite, as above but weakly laminated	30to40	
Hampole Beds	Mudstone, green, shaly	1to3	pluvial or ?blown in continental dust
	Dolomite, calcitic, pale cream, finely oolitic, partly laminated	10to15	?storm deposit - reworked in shallow water?
	Mudstone, green, shaly	1to4	continental, pluvial some plants
	Dolomite, calcitic, pale cream, finely oolitic, soft, irregularly laminated (partly cross-laminated), highly porous due to the presence of many small irregular and elongate cavities, with thin laminae of denser dolomite and green clay and scattered shell fragments and dolomite intraclasts	30to40	supratidal/high intertidal fenestral dolomite with cryptalgal laminites. Some small channels
	Mudstone green shaly	0to05	?pluvial - continental
	Disconformity (The Hampole Discontinuity)	-	subaerial exposure forms crust stillstand and some tectonic tilt
	Dolomite, calcitic, cream-buff, oolitic, in upper part, pisolitic and shelly below, regularly thick-bedded The top half-inch is denser and harder than underlying beds	450+	shallow water/intertidal/ supratidal pisolitic, oolitic, rare fenestral and some cryptalgal laminites

3.4 The Upper Member

3.4.1 Facies

As the Upper Member was deposited on the sub-horizontal intertidal/supratidal carbonates at the top of the Lower Member (3.2.14, 3.3) any thickness variations within the Upper Member are due to build-ups within the member itself and to differential subsidence. Facies, delineated in Tale 3-4, are much less varied than in the Lower Member, the grainstone barriers covering much of the outcrop area; supratidal facies are limited in lateral extent (2.4.1) and are restricted to the upper parts of the member. Kaldi (1980a) details the sedimentology of the grainstone barriers using certain representative sections.

3.4.2 Open marine platform; grainstone barriers

Bedforms in the grainstone barriers show evidence of deepening water at the base of the Upper Member (Appendix 6, Log 3). Planar bedforms at the base (Fig. 3.21a) are replaced upwards by bedforms with sigmoidal reactivation surfaces (Fig.3.21a) characteristic of shallow pulsating currents. Higher in the succession, and laterally eastwards, bedforms become larger with more than 2 metres between reactivation

TABLE 3-4

FACIES IN THE UPPER MEMBER OF THE CADEBY FORMATION

Major Facies Groups	Facies
Open marine platform	Carbonate mudstones and wackestones Grainstone barriers
Restricted marine platform	Siliciclastic carbonates Crypt-algal laminite boundstones
Restricted/exposed marine platform	Breccias

Figure 3.21 a Planar bedforms passing upwards into more sigmoidal bedforms, base of Upper Member, Wetherby (SE 398487). Clay bed at base of section is in Hampole Beds. Hammer is 0.35 m long.

b Abrupt contact of large convex-upwards bed forms in peloid grainstone barrier facies, Knaresborough (SE 346573). Lower shoal form must have been partially cemented to withstand erosion; peloids may have been agglutinated by organic muc us to form convex-upwards structures.

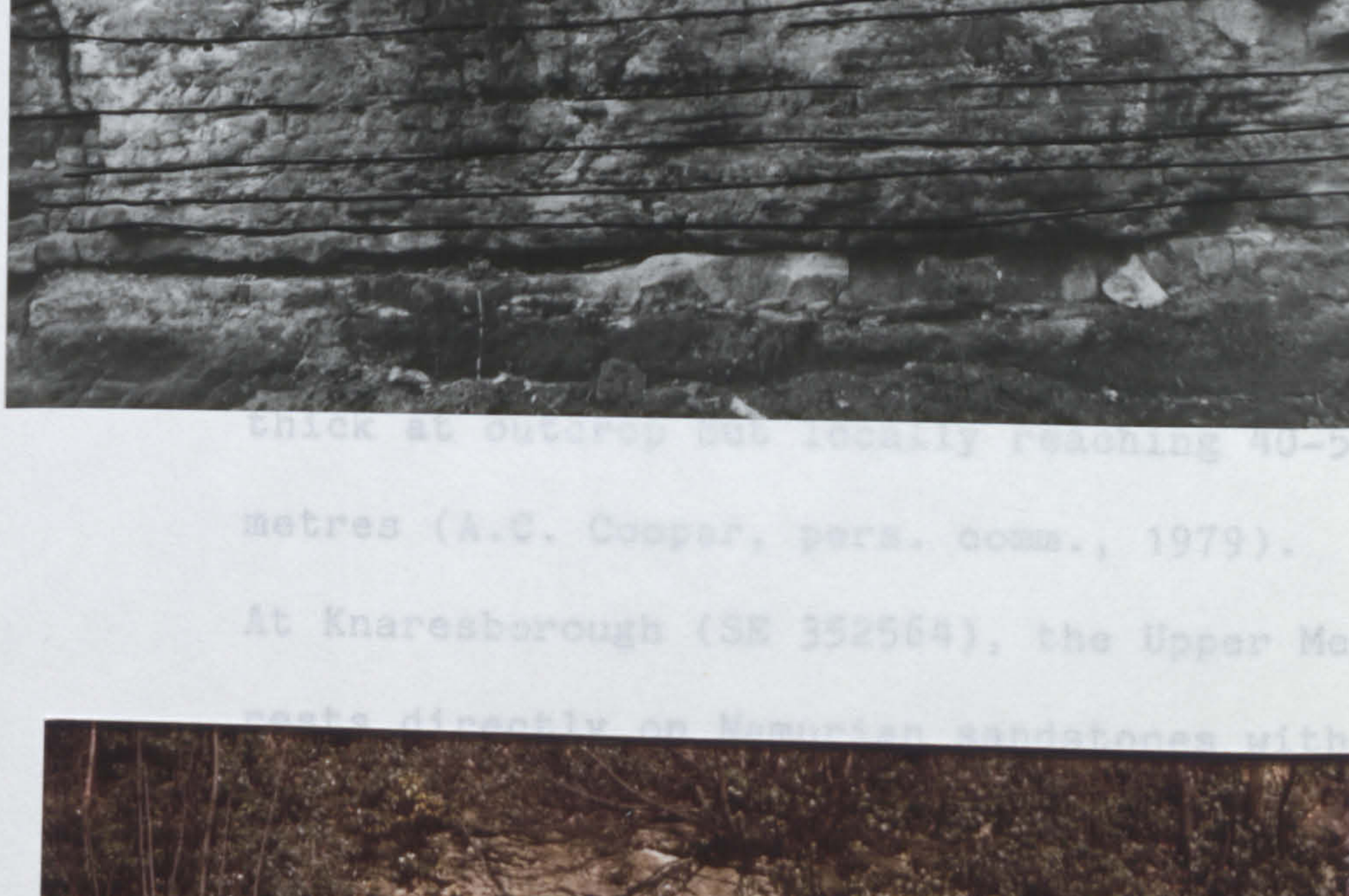

surfaces. Internal cross laminae may be convex upwards and terminate abruptly against earlier reactivation surfaces (Fig.3.21b); a high sediment load, possibly spillover deposits, with some degree of stabilisation of earlier sediments is indicated. Grains were ooids and pellets, well sorted in many places, with few pisoids and intraclasts.

Grainstone barriers may constitute the whole of the Upper Member, normally about 15 metres thick at outcrop but locally reaching 40-50 metres (A.C. Cooper, pers. comm., 1979). At Knaresborough (SE 352564), the Upper Member rests directly on Namurian sandstones with a palaeorelief of more than 5 metres; resistant palaeohills form the core of individual shoals (Fig.3.22). Grainstone barriers thicken from 3 to 50 metres in about one kilometre (Fig.3.23 a+b) and form a linear shoal.

Not all shoals are linear; "domes" of limestone, upstanding through the base of the Ripon Formation have been recognised from Gildingwells, south Yorkshire (SK 563858) (Eden et al., 1957). A survey of the top of the Upper Member in the Doncaster area (Smith and Harwood, 1980) proved

Figure 3.22 Base of Upper Member, Knaresborough (SE 563353). Resistant palaeohill of Namurian sandstones (N) with overlying unconformable peloid grainstones. Palaeohill has total relief (not all shown) of over 15m (exposed palaeohill is approx. 2m high). Grainstone bedforms are continuous (dotted) over palaeohill.


N

Figure 3.23 a Map of Knaresborough area showing the Cadeby Formation (re-drawn from a map by A.C. Cooper).

b Generalised cross section NW-SE across Fig 3.23 (a), showing change in thickness of Cadeby Formation.

Brotherton Formation

Ripon Formation

Cadeby Formation

Carboniferous strata

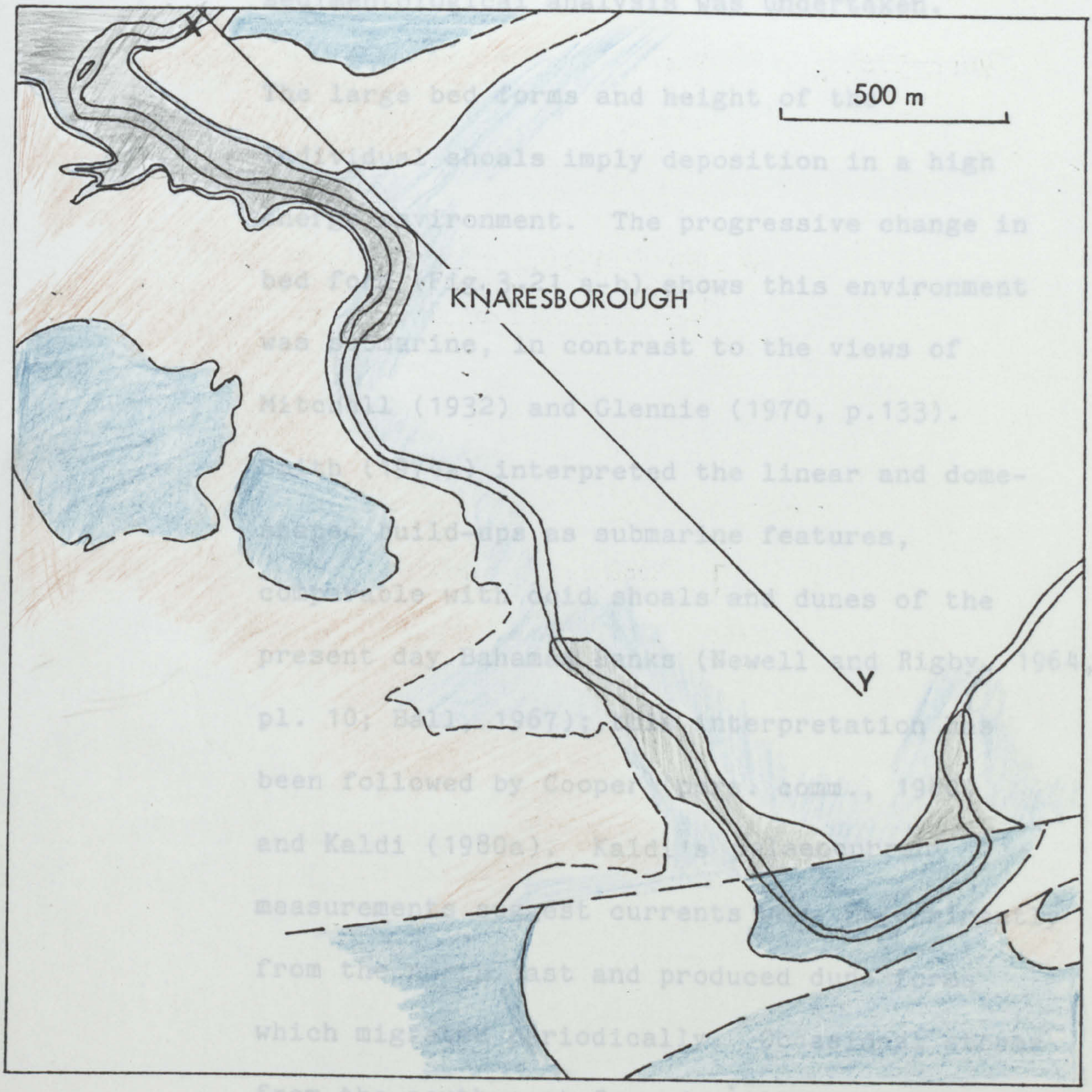
500 m
KNARESBOROUGH
X
Y

many more of these features (Fig. 3.24); no sedimentological analysis was undertaken.

The large bed forms and height of the individual shoals imply deposition in a high energy environment. The progressive change in bed form (Fig. 3.21 a-b) shows this environment was submarine, in contrast to the views of Mitchell (1932) and Glennie (1970, p.133). Smith (1974a) interpreted the linear and dome-shaped build-ups as submarine features, comparable with ooid shoals and dunes of the present day Bahamas Banks (Newell and Rigby. 1964, pl. 10; Ball, 1967); this interpretation has been followed by Cooper (pers. comm., 1980) and Kaldi (1980a). Kaldi's palaeocurrent measurements suggest currents were predominantly from the north east and produced dune forms which migrated periodically. Occasional storms from the south east formed spillover lobes orientated towards the north west (Kaldi, 1980a).

The build-ups in places contain large (> 1 centimetre diameter) individual ramifying burrows (Fig. 3.25a). Elsewhere burrows are concentrated in pockets (Fig. 3.25b) where sediments are homogenised; these were zones of high nutrition.

Figure 3.24 Map showing peloid grainstone build-ups (or 'domes') at the top of the Cadeby Formation in the Doncaster area.

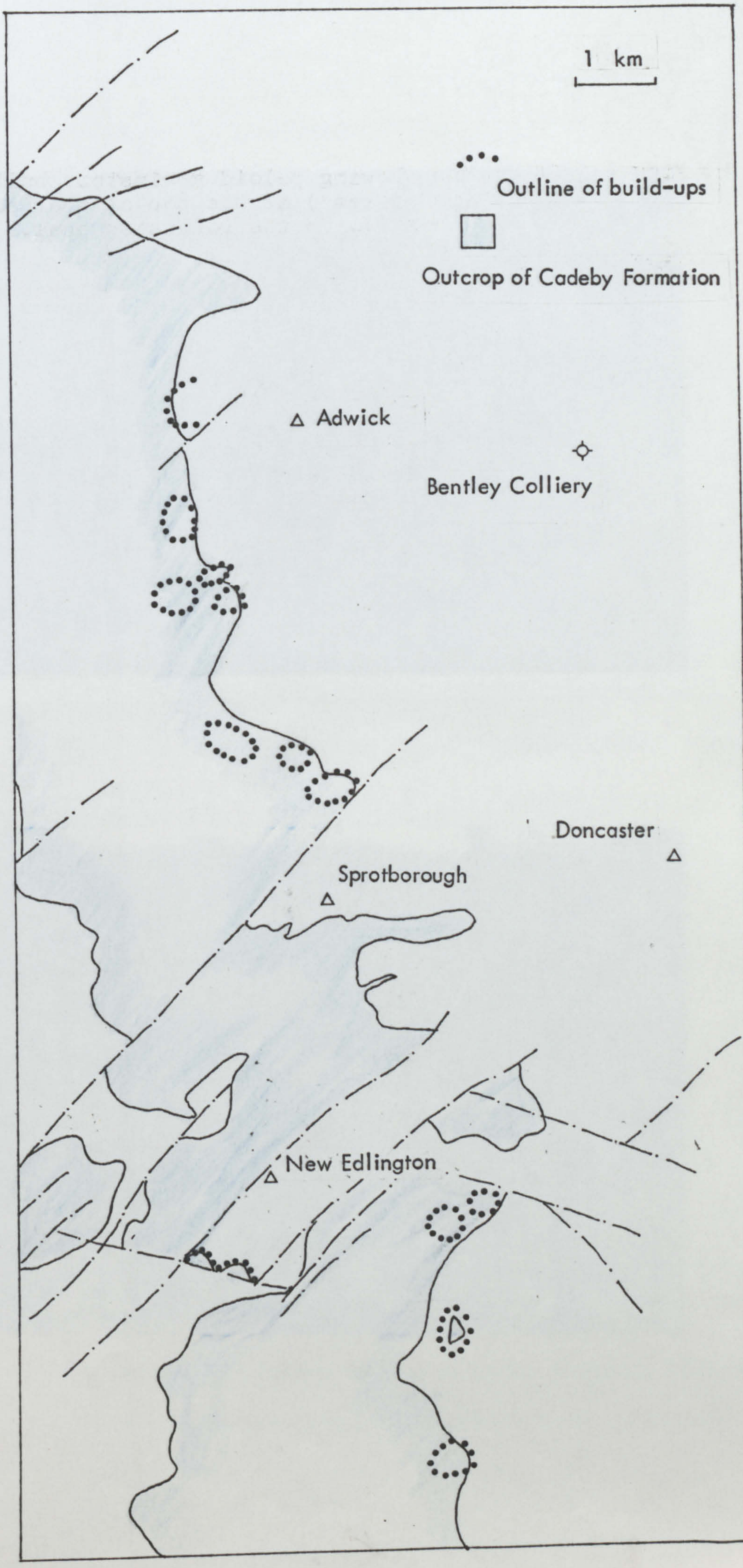
1 km
Outline of build-ups
Outcrop of Cadeby Formation
Adwick
Bentley Colliery
Doncaster
Sprotborough
New Edlington

Figure 3.25 a Individual burrows in Upper Member peloid grainstones, New Micklefield (SE 446325). Note better cemented burrow margins and some hollows in burrow centres. Lens cap is 4cm diameter.

b 'Pocket' of intense bioturbation in Upper Member peloid grainstones, New Micklefield (SE 446325). Surrounding grainstones have little or no bioturbation.


ASAHI
PENTAX

Burrow margins are better cemented than surrounding grainstones (Fig. 3.25a) and centres may remain as voids. There is little recognisable skeletal debris within build-ups.

Between build-ups, planar bedforms with low angle internal cross-sets and some ripple cross-laminations are found. Sedimentary structures are superficially similar to the higher energy bedforms of the shallow water peloid grainstones of the Lower Member. They can be distinguished on burrow forms; Upper Member burrows are large and ramifying whereas Lower Member burrows are smaller, near vertical and seldom bifurcate more than once or twice (3.2.4). Grainstones in intershoal areas were sheltered from the main current and wave action; pellets are more abundant in these areas and may constitute the major allochem.

3.4.3 ?Restricted marine platform; siliciclastic carbonates

Siliciclastic carbonates in the Upper Member were deposited shorewards of the grainstone barriers (Fig. 3.31). The carbonates are now sucrose dolomites; sedimentary structures visible include low angle, cross-laminated dune forms (Appendix

6, Log 6) which are interbedded with carbonates containing scour and fill structures, channels with steep margins and lip fills and some ripple cross-laminations. In places skeletal debris is concentrated into beds. Siliciclastic contents are variable and are of silt or fine sand grain size; some may be aeolian in derivation.

Sedimentary structures indicate shallow, perhaps intertidal environments, protected by the barrier shoals. Enigmatic structures are continuous at some levels (Fig. 3.26a); concentric cementation in these structures reflects a primary fabric as it has been disrupted by dewatering (Fig. 3.26b). The origin of the structures remains in doubt.

3.4.4 Restricted marine platform; crypt-algal laminite boundstones

Crypt-algal laminites bind sediments at some localities (2.4.1; Fig. 3.31). Peloids, washed onto the mucilagenous algal mats, were trapped there; most laminites are peloid dominated. Kaldi (1980a) explained peloid abundance by postulating drawdown and laminite formation within pre-existing grainstones. This development of algal mats throughout 4 metres of existing

Figure 3.26 a Concentric structures along several beds in siliciclastic carbonates, Linby (SK 537523).

b Close up of concentric structure, with evidence of syn-sedimentary dewatering.

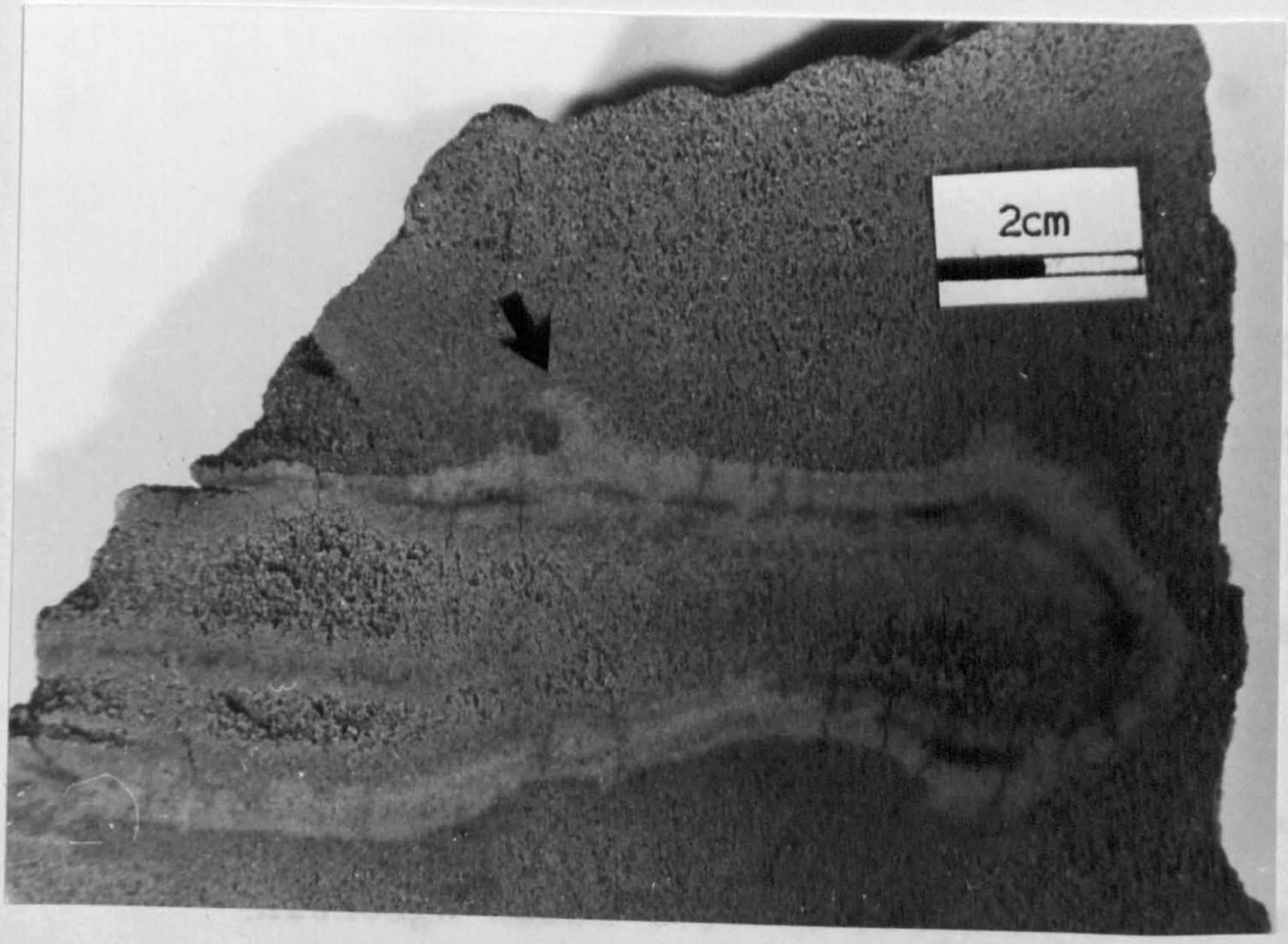
2cm

sediment (e.g. Quarry Moor; Smith, 1976) seems improbable, particularly where modern algal mats are known to trap both ooids and foraminifera tests (P. Bush, pers. comm., 1979).

This facies is present only at the top of the Upper Member; in the outcrop area it apparently developed in the lee of some grainstone barriers (Fig. 3.31). In the subsurface the facies is more widespread (Fig. 3.31) although sometimes replaced by evaporites (6.3.2).

Crypt-algal laminites characterise Holocene sabkha intertidal zones; in the Mesozoic and Palaeozoic laminites probably extended into sub-tidal environments (Gebelein, 1969; Monty, 1971; Smith, 1981; James, 1981, in press). Permian crypt-algal laminites cannot therefore be interpreted as intertidal sediments without further evidence of exposure. Exposure is indicated by contorted beds occurring in the top levels at Quarry Moor (Smith, 1976) and displacive discoid gypsum crystals have recently been recognised within these laminites. Although Kaldi (1980a, p.20) defines his sabkha facies by the presence of crypt-algal laminites some of these, however, may represent subtidal environments.

3.4.5 Restricted/exposed marine platform: breccias

Two types of breccia are present near the top of the Upper Member. The first comprises breccia lenses within grainstone barriers within the top few metres of the Upper Member at several localities (e.g. Jackdaw Crag Quarry, near Tadcaster, SE 465415 and Vale Road Quarry, Mansfield Woodhouse, SK 532648). The breccias are composed of angular grainstone clasts intermixed with continental red silts and clays. Grainstone clasts indicate early cementation of the barriers and penecontemporaneous reworking of the sediments. This could be by storm action on exposed barrier crests; storms would also wash in continental clastics.

In the Doncaster area a distinct breccia is present at the immediate top of the Upper Member (Fig.3.27); it is of intermittant occurrence over 25 square kilometres and hosts gelena mineralisation. No occurrences of similar breccias outside the area of Figure 3.27 were found. The breccia occurs between the crests of the dome-shaped grainstone build-ups and ranges from a few centimetres to one metre in thickness. It contains angular clasts, from a few millimetres to several centimetres across, of green

Figure 3.27 Map showing distribution of breccia at the top of the Upper Member in the Doncaster area.

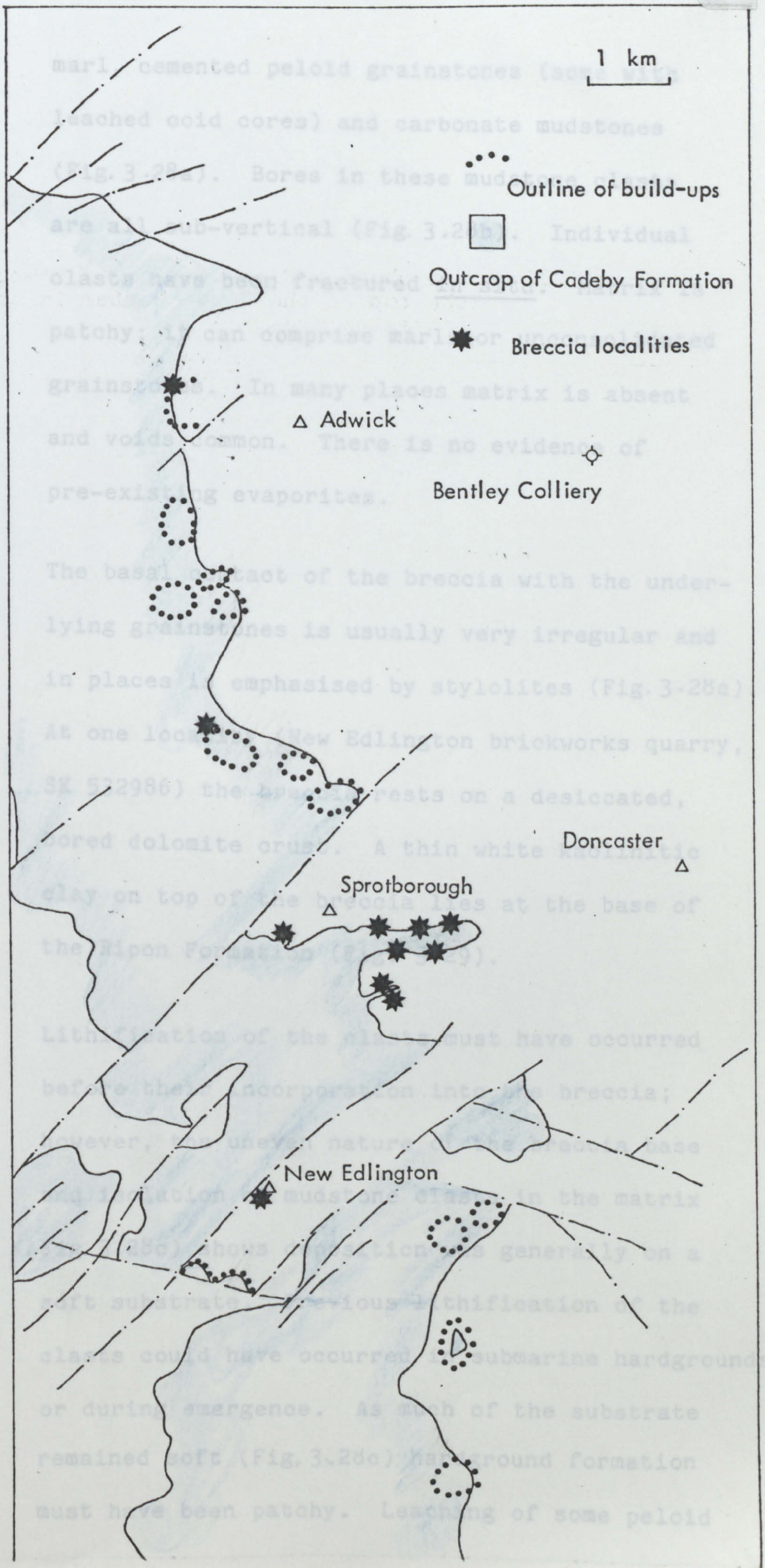
1 km
Outline of build-ups
Outcrop of Cadeby Formation
Breccia localities
Adwick
Bentley Colliery
Doncaster
Sprotborough
New Edlington

marl, cemented peloid grainstones (some with leached ooid cores) and carbonate mudstones (Fig. 3.28a). Bores in these mudstone clasts are all sub-vertical (Fig. 3.28b). Individual clasts have been fractured in situ. Matrix is patchy; it can comprise marls or unconsolidated grainstones. In many places matrix is absent and voids common. There is no evidence of pre-existing evaporites.

The basal contact of the breccia with the underlying grainstones is usually very irregular and in places is emphasised by stylolites (Fig. 3.28c). At one locality (New Edlington brickworks quarry, SK 532986) the breccia rests on a desiccated, bored dolomite crust. A thin white kaolinitic clay on top of the breccia lies at the base of the Ripon Formation (Fig. 3.29).

Lithification of the clasts must have occurred before their incorporation into the breccia; however, the uneven nature of the breccia base and isolation of mudstone clasts in the matrix (Fig. 3.28c) shows deposition was generally on a soft substrate. Previous lithification of the clasts could have occurred in submarine hardgrounds or during emergence. As much of the substrate remained soft (Fig. 3.28c) hardground formation must have been patchy. Leaching of some peloid

Figure 3.28 a Breccia, New Edlington Brick Works Quarry (SK 532986). Note clasts of different carbonate composition, green 'marl' and galena (arrowed).

b, Bores in clast in breccia, filled by surrounding matrix. Field of view is 2.2mm.


2cm

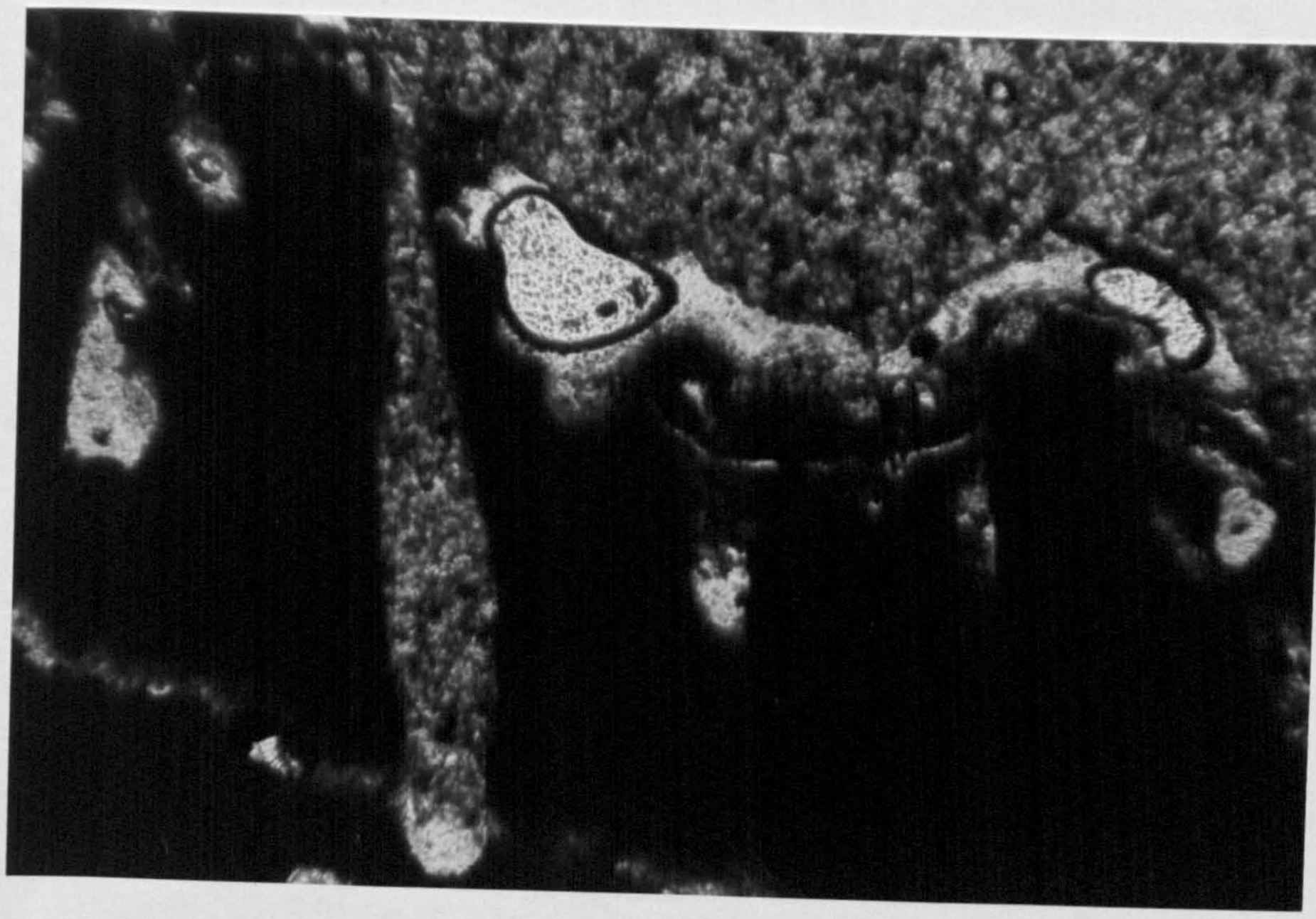

Figure 3.28 c Irregular boundary at base of breccia on peloid grainstones, Lovers Leap, Sprotborough (SE 546 018). Boundary is followed by stylolites in places. Clasts appear to have been deposited on soft substrate.

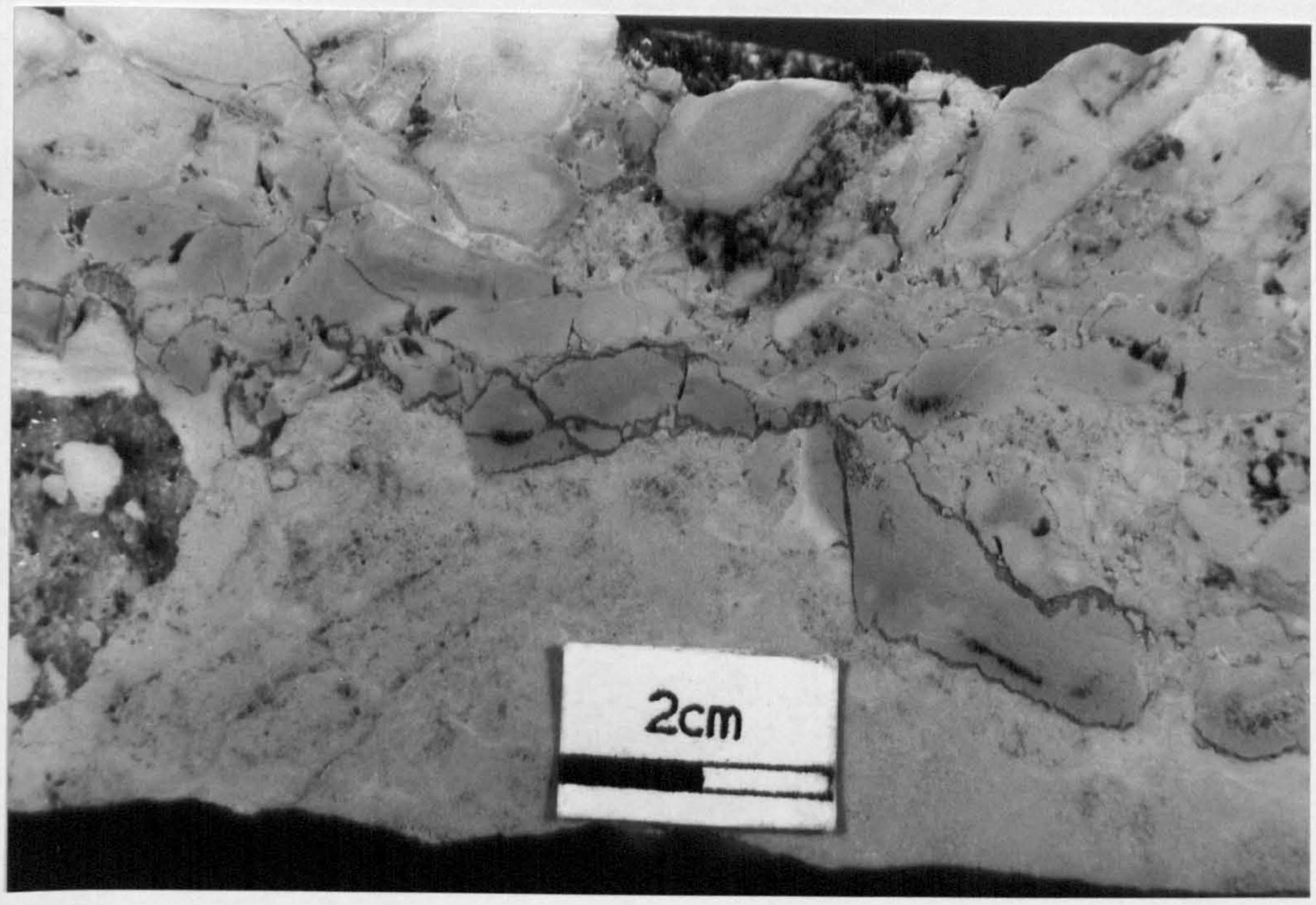
2cm

Figure 3.29 Log through section through top of Cadeby Formation, Doncaster area.

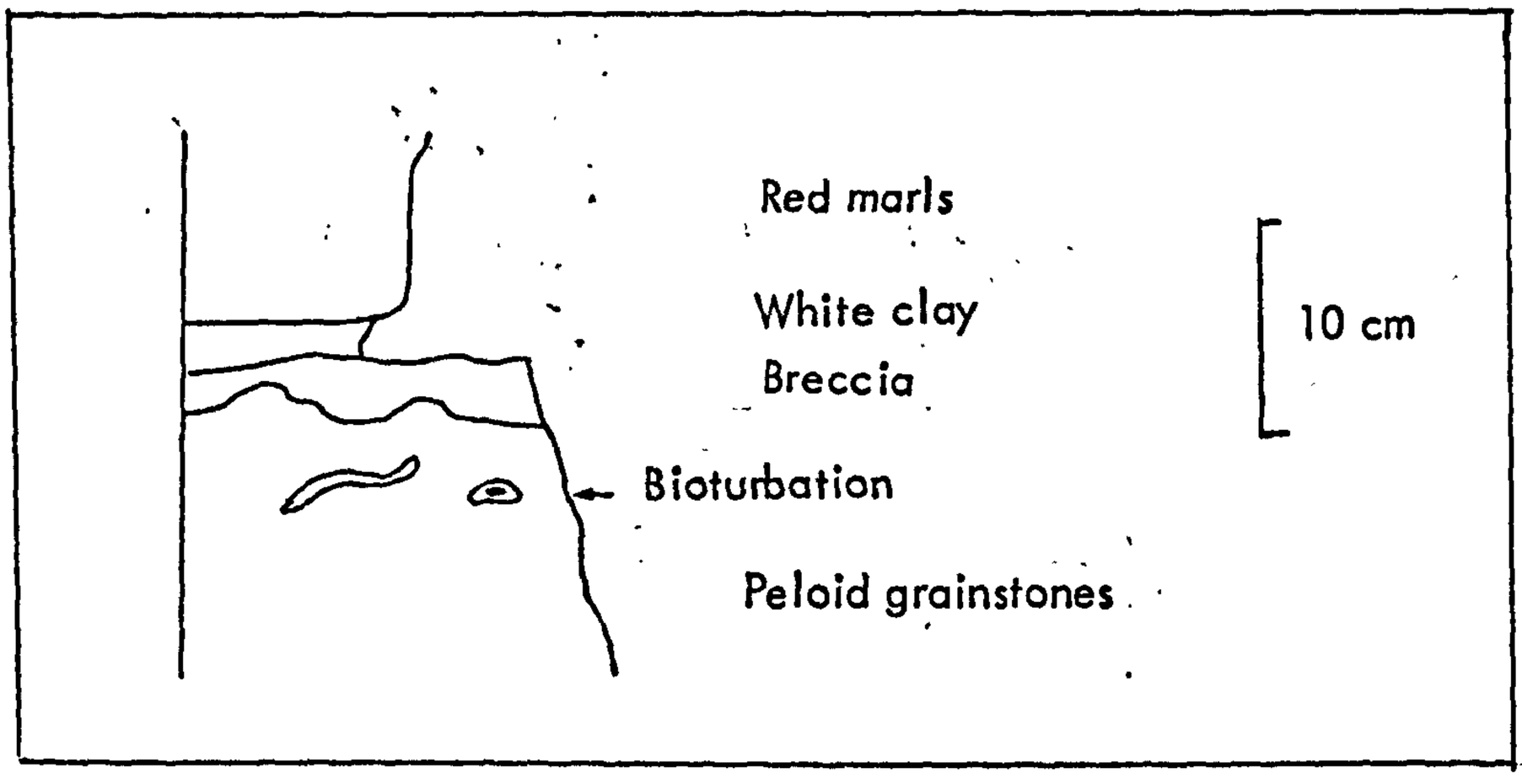
Red marls
White clay
Breccia
Bioturbation
Peloid grainstones
10 cm

centres in these clasts suggests meteoric pore fluids (Carozzi, 1963; Conley, 1977); spalling of clast margins and dolomite geochemistry support this hypothesis (4.5.8). Therefore, lithification and leaching occurred before the breccia was formed; they took place in an environment exposed to meteoric pore fluids, probably the build-up crests. The crests were then eroded during storms and clasts redeposited on the build-up flanks. Clast cements show some meteoric influence (4.5.8); breccias may have been periodically exposed during their formation. Boring occurred after breccia formation. Late pore-filling dolomite cements have little or no meteoric influence (4.5.8); they suggest later inundation of the breccias during formation of the overlying evaporites of the Ripon Formation, below the continental sediments. This interpretation of the breccia formation is summarised in Figure 3.30.

3.4.6 Environmental reconstruction of the Upper Member

Lateral variations in facies in the Upper Member are shown on Figure 3.31 and a synopsis of facies characteristics in Table 3-5. Crypt-algal

Figure 3.30 Diagramatic summary of formation of breccia.

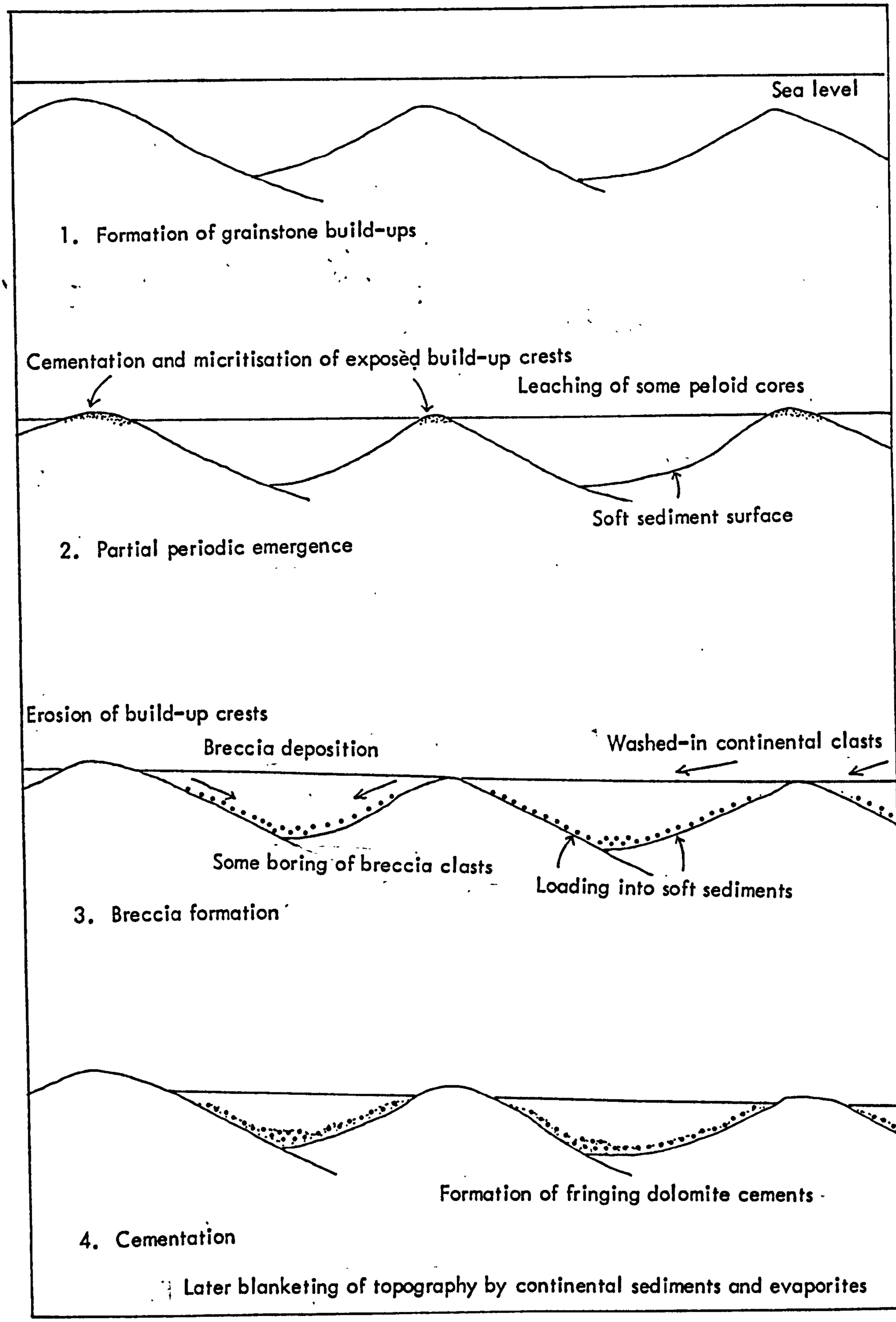
Sea level
1. Formation of grainstone build-ups
Cementation and micritisation of exposed build-up crests
Leaching of some peloid cores
Soft sediment surface
2. Partial periodic emergence
Erosion of build-up crests
Breccia deposition
Washed-in continental clasts
Some boring of breccia clasts
Loading into soft sediments
3. Breccia formation
Formation of fringing dolomite cements
4. Cementation
Later blanketing of topography by continental sediments and evaporites

Figure 3.31 Facies distribution near the top of the Upper Member, Cadeby Formation.

Grainstone barriers

Siliciclastic carbonates

Crypt-algal laminite boundstones

Breccias

York ▲

Leeds ▲

platform margin

?

?

▲ Doncaster

Sheffield ▲

10 km

▲ Nottingham

TABLE 3-5

SYNOPSIS OF FACIES AND ENVIRONMENTS OF DEPOSITION IN THE UPPER MEMBER

Open marine facies	Characteristics and environments of deposition
Carbonate mudstones and wackestones	Nodular carbonates with varied amounts of siliciclastic muds. Low energy environment in relatively deep water
Grainstone barriers	Large bedforms in peloid grainstones forming dunes and ridges. Spill-over lobes. Some bioturbation but little skeletal debris. High energy shoals and barriers.
Restricted marine facies	
Siliciclastic carbonates	Small scale dune and channel bedforms with some skeletal debris. Coarsely crystalline dolomites with varied amounts of siliciclastics Moderate-low energy shallow water environment.
Crypt-algal laminite boundstones	Crypt-algal laminites with dewatering structures and some gypsum crystal pseudomorphs. Shallow water-intertidal environments with no grazing fauna.
Restricted/exposed facies	
Breccias	Breccia lenses within grainstone barriers and breccia at top of Upper Member. Nearby lithification and reworking of grainstones. High energy environment with nearby possible exposure.

laminite boundstones and breccias are present only at the top of the Upper Member; during the remainder of the time the outcrop area was covered by grainstone barriers and siliciclastic carbonates. Deposition was generally in a moderate to high energy environment. No anoxic sediments have been recognised within the Upper Member in the outcrop area; there is no evidence of sulphate reduction within the sediments. Potential for syngenetic mineralisation is therefore low.

3.4.7 Post-depositional history of the Upper Member

Smith (1974a) and Kaldi (1980a) postulate regression with considerable drawdown after deposition of the Upper Member. Mitchell (1932) reported sink holes near Wadworth (SK 5797) which Smith (1974a) relates to underlying karstic fissures produced during drawdown. Many "sink holes" are shown on the 1:10000 scale maps at the Ripon Formation/Cadeby Formation boundary and within the Ripon Formation (sheets SK 59NE, SK59NW, SE 50SW). Disused plaster pits are also marked (e.g. SE 549036). A survey of the area showed the Ripon Formation/Cadeby Formation boundary had been mapped on the basis of these

"sink holes"; augering showed the boundary to be inaccurate in many instances and that "sink holes" were within the Ripon Formation outcrop. "Sink holes" were also between some grainstone build-ups (Fig. 3.27); collapse was caused by gypsum dissolution within the Ripon Formation, similar to the collapse funnels near Ripon. These "sink holes" are not, therefore, necessarily indications of karstic weathering.

There is, however, evidence of near surface environments during, or shortly after, carbonate deposition in some localities: contorted bedding (Smith, 1976) (3.4.4), breccia formation (Smith, 1974a) (3.4.5) and leached peloid cores (Kaldi, 1980a, Chap. 7) (4.5.8). These features are not ubiquitous; they indicate exposure, or near exposure, of restricted areas.

Evidence from diagenesis and geochemistry shows little support for large scale drawdown after deposition of the Cadeby Formation (4.5.6). Aplin (1981) also questions whether substantial drawdown took place after deposition of the Durham upper Z1 carbonate, the Ford Formation.

It is thus concluded that drawdown at the top of the Upper Member was probably in the order

of a few metres and that exposed areas were limited. Most of the area now cropping out was submerged at the end of Cadeby Formation times. High evaporation with increased clastic input, from the west led to cessation of carbonate deposition; gypsum intercalated with continental derived sediments in the Ripon Formation.

3.5 Cadeby Formation Sedimentology; relevance to mineralisation

A summary of inferred sea level changes and related facies variations within the Cadeby Formation is shown in Figures 3.32 and 3.33. The Lower Member is characterised by a variety of facies of different depositional energy. After a brief regression, marked by the Hampole Beds, both water depth and depositional energy increased in the Upper Member; much of the area was covered by grainstone barriers. Near the top of the Upper Member sea level fell by a few metres but there is little evidence of large scale drawdown; increased evaporation with little or no replacement of less saline water led to evaporite formation and incursion of continental clastics in the Ripon Formation.

Syngenetic mineralisation occurs in anoxic environments. In the Lower Member anoxic facies are present in lagoon environments (3.2.8, 3.2.9 + 3.2.10) and, in the present subsurface, on the outer areas of the carbonate platform

Figure 3.32 Facies change with time through the Cadeby Formation.

EAST WEST

Lower Member

(i) Open shelf

(ii) Open shelf and lagoon

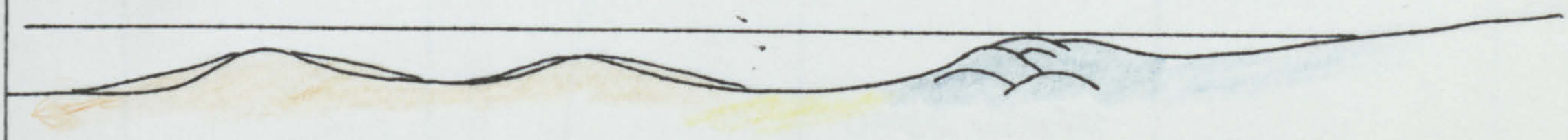

(iii) Top of Lower Member

Upper Member

(i) within Upper Member

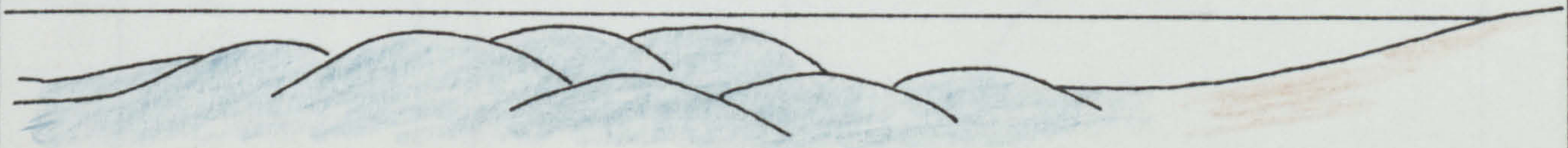

(ii) Top of Upper Member

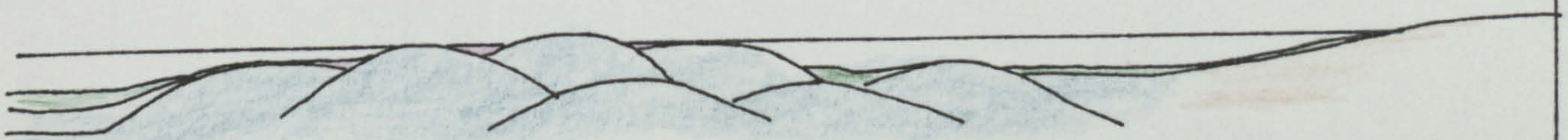

symbols as for Fig. 3.18 and 3.31

Figure 3.33 Relative change of sea level curve compared with general section through Cadeby Formation.

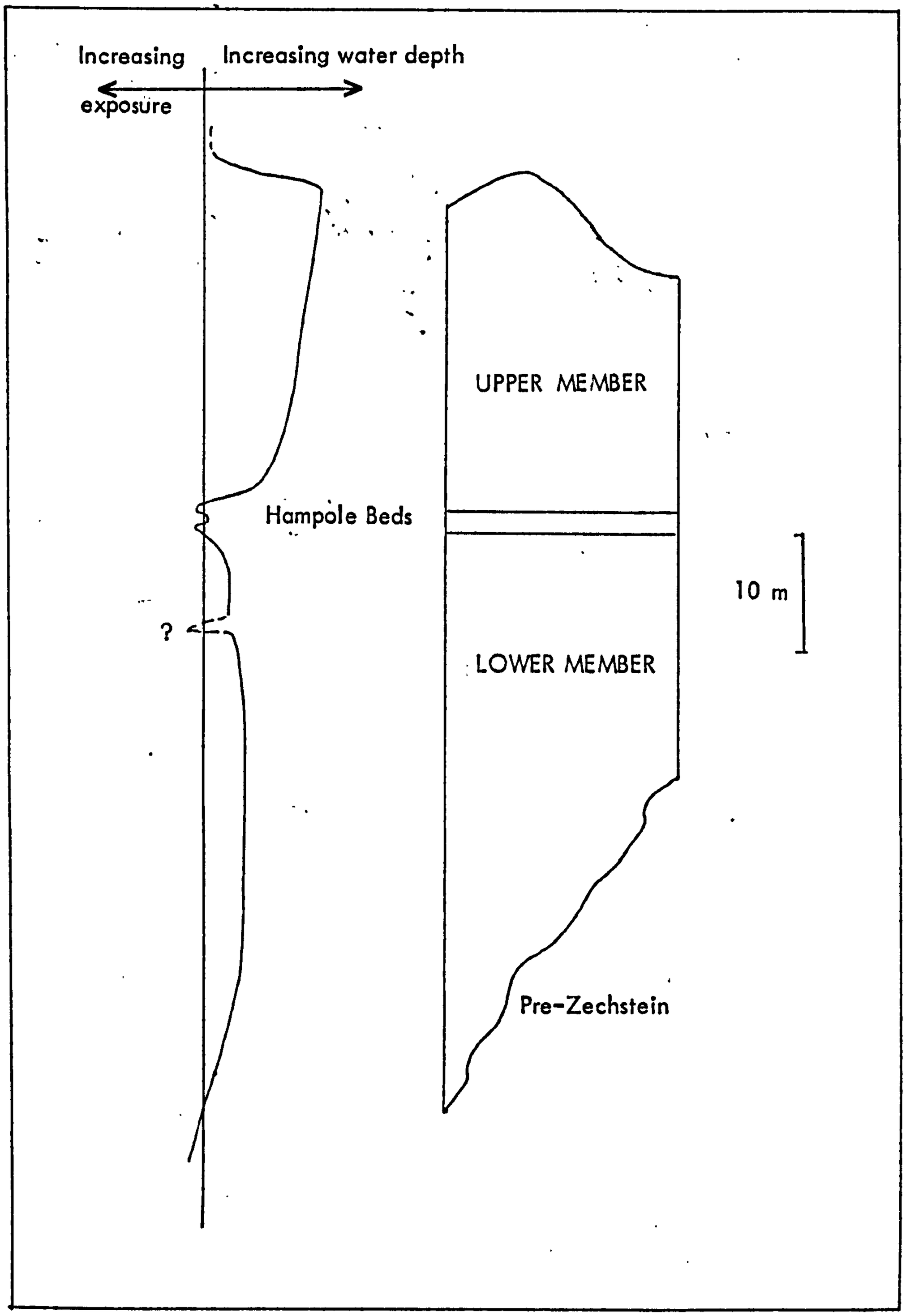
Increasing
Increasing water depth
exposure
UPPER MEMBER
Hampole Beds
?
LOWER MEMBER
10 m
Pre-Zechstein

(3.2.13). Anoxic facies are rare in the Upper Member.

Later mineralising fluids can be trapped by sedimentary structures in originally oxic facies; examples, in both members, include patch reefs with algal boundstone cappings (3.2.8) and the grainstone dome- and linear-shaped build-ups (3.4.2) which were sealed by overlying the evaporites and clastics. These structures also form potential hydrocarbon reservoirs.

PART II

DIAGENESIS

PART II DIAGENESIS

IIa Introduction

This section on diagenesis is divided into three major chapters; dolomitisation, alteration of dolomites - "dedolomitisation" and diagenetic history of the Cadeby Formation. A further chapter details information on whole rock XRF analyses.

Diagenetic events control both cementation and leaching in carbonates. Hence porosity, permeability and subsequent migration of mineralising fluids (or hydrocarbons) are dependent on diagenetic history. In any interpretation of diagenetic history diagenetic models are important. In carbonates initial sedimentary diagenetic characterisatics may be overprinted by different diagenetic regimes, the diagenetic environments of Choquette and Pray (1970) and Longman (1980).

IIb Methods

Diagenesis in the Cadeby Formation was investigated using 130 thin sections for petrographic studies plus 65 polished thin sections for cathodoluminscence and electron microprobe analysis. Conventional thin sections were partially stained using the technique initiated and developed by Dickson (1966; Appendix 8). Cathodoluminescence was principally done at Nottingham University.but also at Manchester; electron microprobe analyses were made at the Open University and microprobe scans at Leeds. Operating conditions for cathodoluminescence and electron microprobe analyses are

detailed in Appendices 9 and 10 respectively. Carbon, oxygen and sulphur isotope determinations were made at I.G.S., Grays Inn Road by Dr. M. Coleman (Coleman and Harwood, 1980; in prep.).

IIc Limitations on study

A comprehensive survey of diagenesis in these carbonates would involve more petrographic and cathodoluminescence (CL) work, scanning electron microscope (SEM) studies and many more isotope determinations. These were not feasible within the scope of the present project; research has concentrated on diagenetic sequences associated with mineralisation to assess the relations between diagenetic history and the diverse times of mineral deposition.

CHAPTER 4

Dolomitisation

4.1 Terminology

Descriptive terms proliferate in carbonate petrology. The petrological terms used in this thesis follow those of the AAPG Carbonate Guide (Scholle, 1978); diagenetic recrystallisation fabrics are from Folk (1965), cement fabrics from Bathurst (1975) and porosity from Choquette and Pray (1970). Descriptive terms relating to dolomites bear the prefix dolo- e.g. dolomicrite.

Where original textures are preserved a distinction can be made between grain size and crystal size; size descriptions follow the international clastic grain size scales (Table 4.1) with addition of actual crystal sizes. Additional petrological terms are referenced; where existing terms are non-specific further discussion is included in the text.

4.2 General carbonate diagenesis

The major diagenetic environments described in this thesis are shown in Figure 4.1.

In carbonate sediments early diagenesis commences with deposition. Choquette and Pray (1970) apply the term eogenetic to 'the time interval between final deposition and burial of the sediment or rock below the depth of significant influence by processes that either operate from the surface or depend for their effectiveness on proximity to the surface'. However, in carbonate

sediments a distinction can often be made between processes acting at or near the sediment surface immediately after deposition, penecontemporaneous processes and processes that occur later in the sediment history but before considerable compaction and burial. The term eogenetic is restricted to these later processes in this thesis; early diagenesis can thus be subdivided into penecontemporaneous and eogenetic events (Fig. 4.1).

Penecontemporaneous diagenesis commences with deposition; where carbonate sediments are reworked clasts may show some diagenetic alteration. In biogenic carbonates alteration may commence immediately after life; for example, a coral colony may be bored by sponges and partially micritised in one area but maintain living polyps elsewhere (N.P. James, pers. comm., 1981).

When deposited on shallow platforms, biogenetic and chemical carbonate sediments are a mixture of aragonite, high magnesian calcite (HMC) and some low magnesian calcite (LMC) with varying siliciclastic components; rare primary dolomite may also occur (Alderman and Skinner, 1957; Behrens and Land, 1972). Both aragonite and HMC are metastable in most pore waters; during diagenesis they are rapidly leached and reprecipitated as LMC [although aragonite may persist in some environments since Mississippian aragonite has been found (J.A. Dickson, pers. comm., 1981)] and/or dolomite. Although near surface diagenetic environments are well defined (Choquette and Pray, 1970; Longman, 1980) investigation

TABLE 4.1

Grain and crystal sizes in carbonate sediments from Wentworth, (1922) + Folk (1959, 1962, 1965).

GRAIN SIZE	mm	um	CRYSTAL DESCRIPTION
gravel	>2.00		very coarse
sand	2.00	2000	coarse
	0.0625	62.5	
silt	0.0625	62.5	medium
	0.030	30	
	0.030	30	microspar/fine
	0.005	5	
	0.005	5	micrite
	0.0039	3.9	
mud	<0.0039	<3.9	

Figure 4.1 Major diagenetic environments (modified from Choquette and Pray, 1970).

EVENT	DIAGENETIC ENVIROMENT
Sediment Deposition	
↓	Early Diagenesis (near surface) ..... Penecontemporaneous / Eogenetic
Burial and Compaction	..... Mesogenetic
↓	
Uplift to within Weathering Zone	..... Telogenetic

of cementation and leaching in the deeper subsurface is only now commencing (Moore, 1981; Mazullo, 1981). Diagenetic environments are susceptible to change throughout time and may be independent of depositional environments (Longman, 1980). Table 4.2 and Figure 4.2 summarise the major near surface diagenetic environments and their characteristics.

4.3 Dolomitisation

4.3.1 History

In 1791 the French naturalist Déodat de Dolomieu recognised that carbonates of mountains in the Austrial Tyrol were different from other limestones. Chemical analysis showed a new calcium magnesian carbonate, $CaMg(CO_3)_2$, named 'dolomite' after the Count. Literature on dolomites is now voluminous; they possess economic importance as hosts for lead-zinc sulphide mineralisation and as hydrocarbon reservoirs, often having a higher porosity than neighbouring limestones (e.g. Murray, 1960).

4.3.2 Models of dolomitisation

No single dolomitisation process explains all dolomite occurrences. Similarly, one dolomite formation may result from a combination of dolomitisation processes throughout its history (e.g. Fisher and Rodda, 1969; Sears and Lucia, 1980). Early reviews of dolomitisation are given by Steidtman (1911), Van Tuyl (1916), Fairbridge

TABLE 4.2

MAJOR NEAR SURFACE DIAGENETIC ENVIRONMENTS AND THEIR CHARACTERISTICS (based on Longman, 1980)

ZONE	ENVIRONMENT	CEMENTS	LEACHING	ASSOCIATED FEATURES
MARINE PHREATIC ZONE	Active water circulation	Active aragonite + HML	No	CO_2 degassing, micritisation, bacterial action.
	Stagnant Water	Little HMC and aragonite	No	Micritisation preservation of porosity.
FRESH WATER VADOSE	Near surface (under-saturated in $CaCO_3$)	----	Extensive solution, preferential aragonite solution	Vugs in limestone soil CO_2 aids solution
	Deeper zone (saturated in $CaCO_3$)	Minor meniscus, pendant + equant LMC cements	No	Patchy cementation concentrated in fine grained sediments. Some porosity preservation
FRESH WATER PHREATIC	Upper zone active circulation (under-saturated in $CaCO_3$)	----	Extensive. Aragonite only leached lower in zone	Vuggy texture Moldic porosity
	Moderate circulation	Heomorphism; aragonite LMC common cements bladed LMC equant + mosiac LMC	Aragonite solution but calcite reprecipit-ation	Syntaxial overgrowths on echinoderms
	Stagnant zone	Little aragonite LMC slowly isopachous rim	No	Preservation of primary structures and porosity
MIXING ZONE	Active circulation	Dolomit-isation aragonite LMC HMC LMC little micritic bladed cements	Aragonite + HMC leaching but LMC replacement	see 4.4

Figure 4.2 Near surface diagenetic environments (modified from Choquette and Pray, 1970 and Longman, 1980).

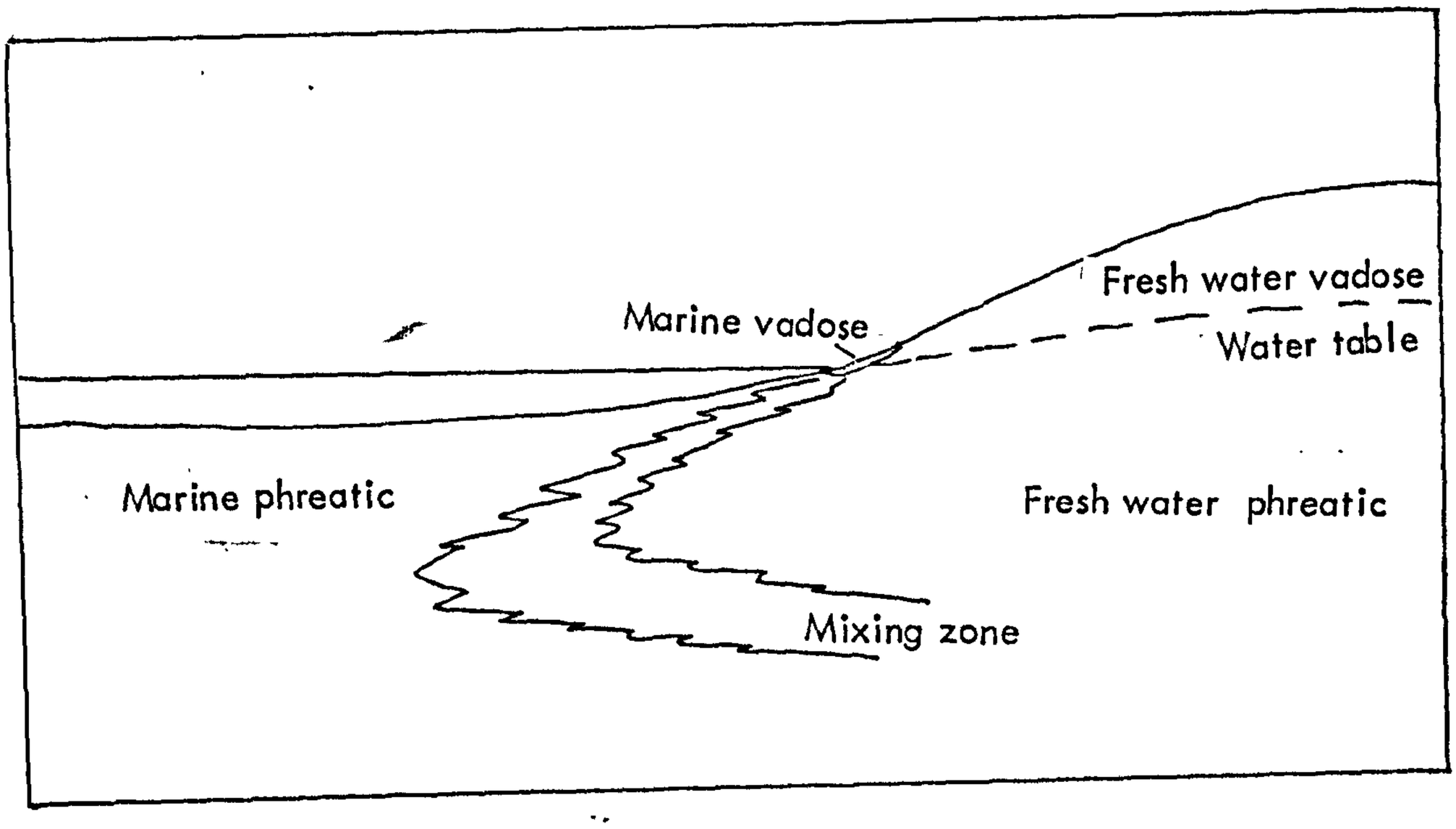
Fresh water vadose
Marine vadose
Water table
Marine phreatic
Fresh water phreatic
Mixing zone

(1957), Ingerson (1962) and Sonnenfeld (1964). The discovery of penecontemporaneous Holocene dolomites in the 1950s and 1960s (Alderman and Skinner, 1957; Curtis et al., 1965; Deffeyes et al., 1965; Illing et al., 1965; Shinn et al., 1965) stimulated renewed interest in 'the dolomite problem' (Fairbridge, 1957) and prompted numerous descriptions of ancient analogues. These Holocene dolomites have a small volume and restricted areal extent; they are all of marginal marine, mostly supratidal, origin. The greater volume of fossil dolomites, however, does not include supratidal, or near supratidal, sediments. Even where these do exist, dolomitisation may have occurred much later in the sediment history (Zenger, 1972).

These early Holocene dolomitisation models were all associated with hypersaline solutions with high Mg^{2+}/Ca^{2+} ratios. Several authors still maintain that nearly all dolomites have an evaporite association (Friedman, 1980; Beales and Hardy, 1980). Later hypotheses involved dolomitisation by mixing marine and meteoric waters (principally Hanshaw et al., 1971); the resultant low salinity waters had Mg^{2+}/Ca^{2+} ratios approaching unity. Subsequent work (Badiozamani, 1973; Land, 1973; Folk and Land, 1975; Folk and Siedlecka, 1974) developed this concept with references to ancient analogues.

Recent work on DSDP cores has shown growth of concretionary dolomites during the Holocene (Pisciotto, in press; Kelts, pers. comm., 1981) associated with methane generation in shale sequences. Results show similarities to the concretionary carbonates of Irwin (1980).

Little emphasis has yet been placed on late dolomitisation, caused either during deep burial or by migrating hydrothermal solutions. Burial dolomitisation may be more important than previously recognised (Jodry, 1969; Mattes and Mountjoy, 1980) and may be genetically associated with hydrocarbon generation (Moore, 1981).

In any discussion on dolomitisation modern analogues are inadequate when large evaporite basins such as the Zechstein or Messinian (Hsu, 1972; Hsu et al., 1977) are considered. Modern analogues should perhaps be taken "with a pinch of salt".

4.3.3 Dolomite classification

Dolomites may either form as primary precipitates or, more commonly, as secondary replacements of an earlier carbonate phase. It is generally agreed that Phanerozoic primary dolomites constitute an insignificant proportion of ancient dolomites and that secondary dolomites result from a dissolution-reprecipitation reaction in which original textures may or may not be preserved

(Zenger and Dunham, 1980). Genetic classification is hampered by obliteration of earlier textures during dolomitisation; factors controlling dolomitisation include original porosity, climate, organic and clastic contents as well as fluid chemistry and thermodynamics and diagenetic processes (Zenger and Dunham, 1980). Rates of dolomitisation are also important although few estimates have yet been made (Choquette and Steinen, 1980; Sears and Lucia, 1980). Timing of dolomitisation is various; secondary dolomites may be penecontemporaneous, eogenetic or meso-genetic. Hydrothermal and metamorphic dolomites also occur. The classification shown below (Fig 4.3) is based on that of Wilson (1975, p. 311) with additions from more recent literature.

4.3.4 Experimental synthesis of dolomite

Although many attempts have been made there has been no successful experimental synthesis of dolomite at temperatures, pressures and P_{co2}'s near that of the earth's surface (Chillingar et al., 1979). Only metastable phases or assemblages have been obtained under these conditions. Reports of synthesis of dolomite at higher temperatures (>120°C) are numerous; dolomite formation is rapid and relatively uncomplicated (Land, 1980). Protodolomite (as defined in Gaines, 1977) has been synthesised

Figure 4.3 Genetic classification of dolomites (modified from Wilson, 1975 p.311).

- DOLOMITE
  - PRIMARY — precipitate from standing body of water in hypersaline lakes
    Alderman and Skinner, 1957
    Clayton et al., 1968
    Behrens and Land, 1972
  - SECONDARY (replacement dolomite)
    - Penecontemporaneous
      - arid / hypersaline supratidal — sabkha evaporation
        Curtis et al., 1963
        evaporative pumping and flood recharge
        Hsu and Siegenthaler, 1968
        McKensie et al., 1980
      - humid supratidal — hammock - mixed water
        Shinn et al., 1978
    - Eogenetic
      - arid / hypersaline — seepage reflux
        Adams and Rhodes, 1960
        Deffeyes et al., 1965
      - arid / lacustrine — seasonal water table movement
        von der Borsch, 1965
        Muir et al., 1980
      - mixed water / subsurface — Hanshaw et al,, 1961
        'dorag" Badiozamami, 1973
        'schizohaline' Folk and Land, 1973
        Folk and Siedlecka, 1974
      - subsurface HMC dissolution — 'cannibalisation'
        Goodall and Garman, 1969
        Bathurst, 1975
      - concretionary dolomites — Kelts, Pisariotto, in press
    - Mesogenetic
      - shale de-watering — Jodry, 1969
        Mattes and Mountjoy, 1980
      - remobilised dolomites
      - hydrothermal
      - metamorphic

at 100°C and atmospheric pressure (Gaines, 1974; 1980).

In high ionic strength solutions the magnesite-dolomite-calcite phase boundaries between 120°C and 420°C were defined by Rosenburg and Holland (1964) and Usdowski (1967). Baker and Kastner (1981) documented dolomite formation in solutions of lower ionic strength. Gaines (1980) states dolomite preferentially replaces aragonite, then HMC and then original LMC; recrystallised LMC is more resistant. Baker and Kastner (1981) show dolomitisation of aragonite proceeds at a much faster rate than LMC at 200°C. They also demonstrate inhibition of LMC dolomitisation by minor amounts of dissolved SO_4^{2-} at both 100°C and 200°C, although the rate of aragonite dolomitisation is only slightly lowered. This may have important implications in studies of fossil dolomites.

4.4 Dolomitisation models and processes applicable to the Cadeby Formation

4.4.1 Holocene analogues

Three major analogues are applicable to the Cadeby Formation:

(a) seepage reflux

(b) mixing of saline and meteoric fluids

(c) sabkha models

(a) Seepage reflux was proposed by Adams and Rhodes (1960) and applied to the Permian Basin of West Texas. The model involves formation of dense, hypersaline brines from gypsum precipitation in restricted lagoons. These brines sink and flow seawards through the underlying carbonates (Fig. 4.4 a) dolomitising the sediments and displacing original, less saline pore waters. Sea water flooding or seepage through the permeable lagoon barrier recharges lagoon waters. This model was applied to Holocene dolomitisation at Bonaire, Netherlands Antilles (Deffeyes et al., 1965) although later drilling through the lagoon base showed pore waters of normal marine salinity (Lucia, 1972). Consequent modification of the model (Fig. 4.4 b) involved seasonal reversal of flow. Drawbacks of the revised model are the necessity for rapid dolomitisation during reflux (Bathurst, 1975) and the fact that, although brines are denser, lower pressure would be needed in the subsurface before the brines could descend (Bjorlykke, 1981), a rare occurrence.

(b) Mixed water models (Hanshaw et al., 1971), the 'dorag' model (Badiozamani, 1973) or 'schizohaline' dolomites (Folk and Land, 1973; Folk and Siedlecka, 1974) involve the interaction of low salinity, meteoric lenses with marine pore waters (Fig. 4.2). Dolomitisation occurs only in the mixing zone between fluids, a zone perhaps half the size of the meteoric lens (K. Bjorlykke,

Figure 4.4 a Seepage reflux (from Adams and Rhodes, 1960)

b Modified seepage reflux (from Deffeyes et al., 1965 and Lucia, 1972)

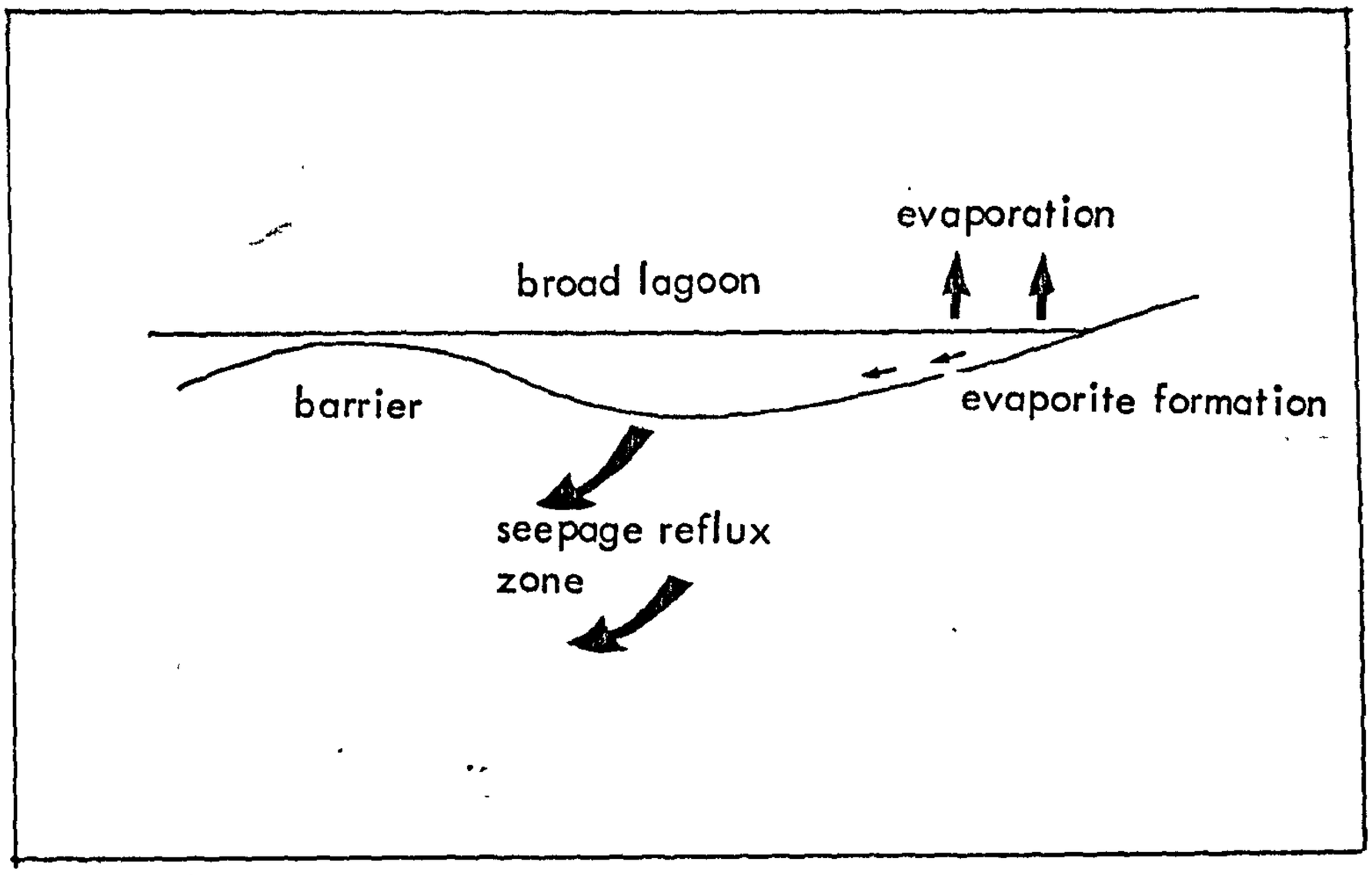
evaporation
broad lagoon
barrier
evaporite formation
seepage reflux
zone

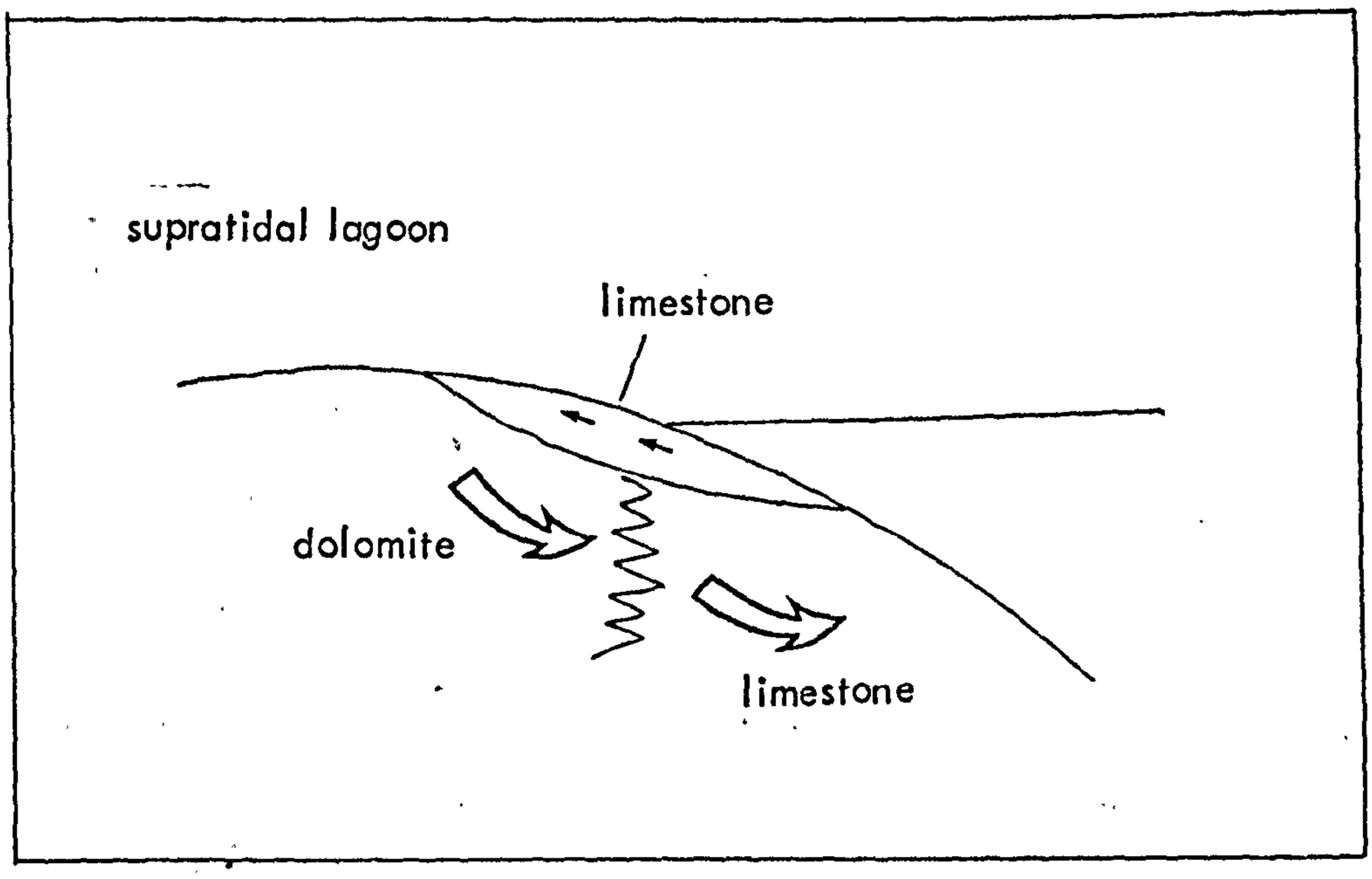
supratidal lagoon
limestone
dolomite
limestone

pers. comm., 1981). Migration of the fresh water lens is controlled by evaporation/precipitation onshore and hydraulic head as well as major tectonic/eustatic sea level variations (Dunham and Olsen, 1978). The model does not necessitate hypersaline fluids and has broad applications to dolomitised formations where evidence of former evaporites is absent. Rates of dolomitisation may be slow as meteoric influence would rapidly convert less stable carbonate phases to LMC within the fresh water lens.

(c) Sabkha models are dominated by flood recharge with dolomitisation occurring in the mixing zone between marine and continental barriers (McKensie, 1981; Pattison and Kinsman, 1981). Sabkhas are a restricted facies; dolomitisation occurs within one or two metres of the surface. A sabkha model cannot be invoked for large scale dolomitisation of varied facies.

Other dolomitisation models (Fig. 4.3) are also of restricted areal extent, largely inapplicable to dolomitisation of a large carbonate shelf sequence.

4.4.2 Pore water migration during dolomitisation

The models discussed above all invoke sea water as the major source of Mg^{2+} ions. The relative proportion of the Mg^{2+} and Ca^{2+} ions in some waters is given in Table 4.3. Constant flushing

TABLE 4.3

Relative proportions of Mg^{2+} and Ca^{2+} in different fluids

	Groundwater[1]	Continental[2] brines	Persian Gulf Sea Water[2]	Persian Gulf lagoon Water[2]	Persian Gulf Sabkha Brines	Bonaire brines[3]	Mixed Water (1)[4]	Mixed Water (2)[5]
Ca^{2+} ppm	8	1740	410	560	5910	400	98	146*
Mg^{2+} ppm	9	3750	1290	1910	14180	6000	74	267
Mg^{2+}/Ca^{2+}	1.9	3.5	5.2	5.6	3.9	24.7	1.2	3.0
SO_4^{2-} ppm	17	4420	2710	3940	850	---	149	544

1 Back + Hanshaw, 1970

2 Butler, 1969 (Samples: 3/1, L5 + 1/15 A+B)

3 Sears + Lucia, 1980 (recalculated from Deffayes et al, 1965)

4 Badiozamani, 1973 (5:95 sea:meteoric mixture)

5 Sears + Lucia, 1980 (1:4 sea:meteoric mixture)

* Sears + Lucia, 1980 obtained 87ppm Ca^{2+} using same mixture

by pore fluids is necessary for dolomitisation in all models; where models invoke low salinity fluids flushing has to be increased to supply the same amount of Mg^{2+} as hypersaline fluids (see below).

Efficiency of dolomitisation is low; it averages 10% in sabkhas where Mg^{2+}/Ca^{2+} ratios approach 10 (Kinsman, pers. comm., 1981) and nucleation occurs only during rare, extremely high temperatures (McKensie, 1981). Where Mg^{2+}/Ca^{2+} ratios approach unity, efficiency may be considerably lower.

Efficiency of dolomitisation is dependent on pore volumes and flow rate, or flushing as well as compositions. Estimates of pore volumes in unconsolidated carbonate sediments vary. Modern, uncompacted packstones-wackestones have an original porosity approaching 70% (Bathurst, 1975). Experimental compaction, with little mechanical fracturing, reduces this porosity to 40-50% (Shinn et al., 1977). A porosity of 45% may thus be typical of an uncemented but compacted carbonate sediment (Fig. 4.5 a). Early cementation in a phreatic environment may reduce this to 35% (Fig. 4.5 b).

Although the total porosity, this is not effective porosity. Some pores may be isolated. Also, each grain is covered by a static, or near-static,

Figure 4.5 Porosity in carbonates

a allochems with surrounding porosity (blue).

b allochems with rim cement (yellow). Porosity (blue) reduced from (a).

c allochems with rim cement and grain boundary fluid rim (colourless). Effective porosity is substantially reduced from (a).

a

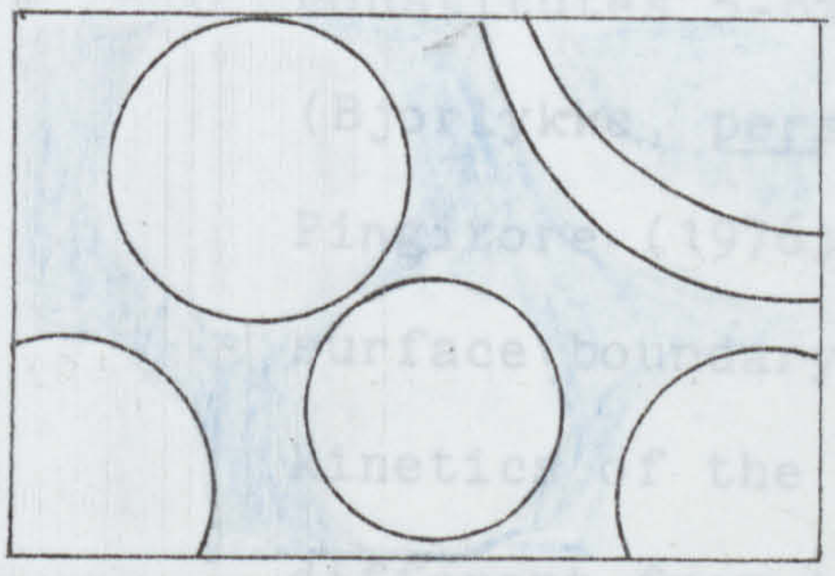

b

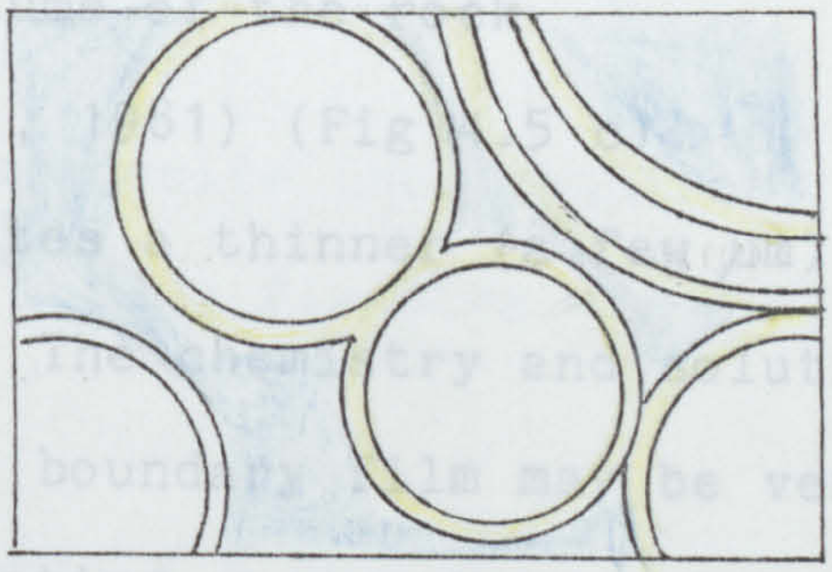

c

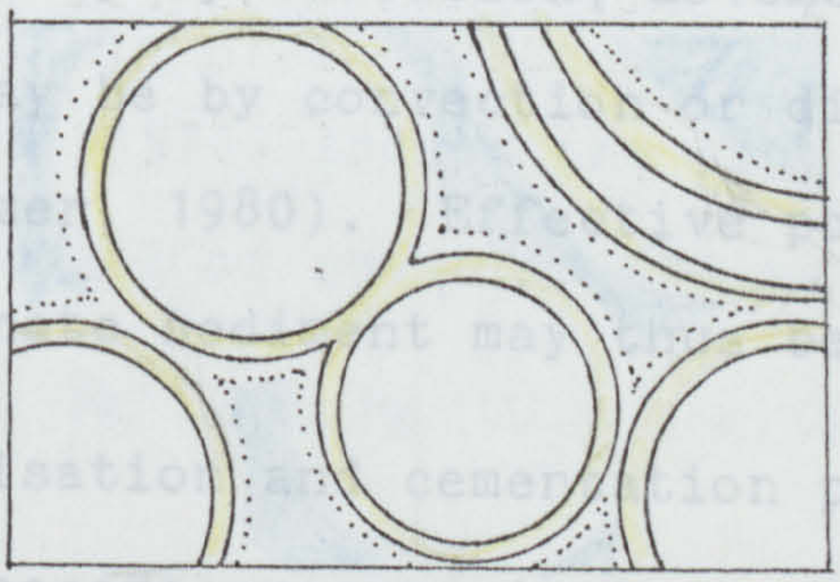

surface boundary film which may, by analogy with experments on transistor growth, be up to 20 μm thick (B. Velde, pers. comm., 1981) and constitutes 5-8% by volume of the rock (Bjorlykke, pers. comm., 1981) (Fig 4.5 c). Pingitore (1976) estimates a thinner (a few μm) surface boundary film. The chemistry and solution kinetics of the surface boundary film may be very different from the migrating pore waters. Ion movement between pore fluid and boundary layer is probably by diffusion; movement within the layer may be by convection or diffusion (Brand and Veizer, 1980). Effective porosity within a carbonate sediment may thus be only 30%. As dolomitisation and cementation proceed, pore spaces become progressively smaller; flushing mechanisms need to be consequently more efficient.

A simple calculation demonstrates flushing required. Petrographic evidence (4.5) shows no volume reduction or expansion during dolomitisation. I assume a volume for volume replacement of aragonite by dolomite (N.B. 4.2.4) and an initial effective porosity of 30% with boundary films comprising 5% of total volume. Carbonate volume is therefore 65% for $1cm^3$ carbonate sediment.

For aragonite, total Ca^{2+} = 0.767g [aragonite density 2.95g cm^{-3} (Deer, Howie and Zussman, 1962)]

For dolomite, total Ca^{2+} = 0.403g

total Mg^{2+} = 0.245g

[dolomite density 2.86g cm^{-3} , (Deer, Howie and Zussman, 1962)].

Dolomitisation of the aragonite thus requires addition of 0.245g Mg^{2+}, plus flushing of 0.364g Ca^{2+}.

Two pore waters from Table 4.2 are considered, a mixed water (4:1 meteoric:sea water) fluid and a hypersaline brine from Bonaire.

Langmuir (1971) showed the equilibrium contstant (K eq) molal of reaction (1) to be near unity:

$$2CaCO_3 + Mg^{2+} \rightarrow Ca\,Mg\,(CO_3)_2 + Ca^{2+} \quad (1)$$

$$Keq = \frac{Ca^{2+}}{Mg^{2+}} \quad (2)$$

(later research by Johnson and Pyktowicz (1978) indicates approximately 50% of Ca^{2+} and Mg^{2+} are complexed as chlorides, a much large extent than previously realised (Carpenter, 1980). This may affect this equilibrium constant).

Magensium available for dolomitisation in the fluids is the amount of Mg^{2+} in solution in excess of that in equilibrium with equal (molal) Ca^{2+}. This amounts to 180ppm Mg^{2+} for the mixed water fluid and 5670ppm for the hypersaline brine, supplied in the 30% effective porosity. If

efficiency of dolomitisation were 100%, complete dolomitisation of the aragonite would require pore volume flushing of 2950 and 93 times respectively to supply sufficient magnesium. Efficiency of 5% would incease these to 59000 and 1860 pore volumes, not taking into account the excess Ca^{2+} removed in solution in equation (1). This might necessarily increase flushing by a further order of magnitude; i.e. 600000 and 20000 pore volumes. An efficient method of pore fluid transfer is therefore necessary for both these models of dolomitisation, although the hypersaline fluid, with high Mg^{2+}/Ca^{2+} ratio, is more effective by over one order of magnitude.

4.4.3 Flow mechanisms

Flow type is dependent on dolomitisation model.

Effective flushing is demonstrable from a fresh water lens (Fig. 4.2). Flow is perpendicular to equipotentional lines (Galloway, 1977) and dependent on basin pore water pressure and hydrostatic pressure. With average sea water (e.g. 1.025g cm^{-3}), theoretical penetration of the fresh water lens is 1:40; for every 1000m relief fresh water may extend 4km laterally into the basin margin. High basin pore pressures and relatively restricted circulation generally reduce this (Bjorlykke, 1981 in press) although Mannheim (1967) has shown meteoric water in sediments 12km off the Florida coast. Increase

of basin salinity would theoretically increase fresh water penetration; for the same relief 16km is possible with the salinity of 1.1g cm^{-3}. Climatic variations and regression would produce effective movement of the meteoric lens, promoting dolomitisation within the mixing zone.

Modern reflux analogues are on a much smaller scale than the Zechstein basin margins. Flow during reflux would again be perpendicular to equipotentional lines; flow may be promoted by diffusion gradients towards less saline fluids, and by the dense nature of the hypersaline brines. Brines would be constantly replenished by evaporite formation (4.5.7).

4.5 Dolomitisation in the Cadeby Formation

4.5.1 Fabric retention and destruction

Dolomitisation in the Cadeby Formation has destroyed much of the original sediment texture, although ghost fabrics persist in places. This contrasts with the texture preserving dolomitisation of Clark (1980) in Dutch and Danish Zechstein carbonates. . Even where early textures are discernable in the Cadeby Formation there is no preservation of early porosity; most dolomitisation results in porosity occlusion. Evidence presented below indicates most dolomitisation to be been penecontemporaneous or eogenetic. This early

texture-destroying dolomitisation largely prevents recognition of calcium carbonate cement fabrics which characterise near-surface diagenetic environments if, indeed, these fabrics ever had time to develop.

4.5.2 Dolomitisation associated with displacive evaporite nodules

Lagoon wackestones and packstones (3.2.9 and 3.2.10) are now dolomicrites and dolomicrospars with low porosities (Fig. 4.6 a). Calcitisation of displacive evaporite nodules took place after dolomitisation (Harwood, 1980) (Fig. 4.6 b). Calcitisation was caused by bacterial reduction of the sulphate, with possible influence of meteoric pore fluids (Coleman and Harwood, 1980) (9.2). Sulphate reduction often occurs near the sediment surface, within 0.5m of the sediment/sea water interface (Berner, 1980) and within 1m of sabkha surfaces (P. Bush, pers. comm., 1980). Electron microprobe analysis of these dolomites was hampered by their small crystal size (<8um), (Fig. 4.6 a). Both microprobe and whole rock XRF analyses (Appendix 5, 462 and 470) show non-stochiometric calcian dolomites.

The small crystal size, close association with anhydrite nodules and evidence of dolomitisation

TABLE 4.4

ELECTRON MICROPROBE ANALYSES OF CARBONATES, WORMALD GREEN N. YORKS. (NE 304650)

mole %		$MgCO_3$	$CaCO_3$	$FeCO_3$	$MgCO_3/CaCO_3$
Dolomite	1	41.01	49.92	0.30	0.82
	2	41.16	57.73	0.23	0.71
	3	43.05	53.51	0.55	0.80
	4	44.26	54.39	0.55	0.82
	5	43.20	54.10	0.17	0.78
	6	37.12	50.84	0.21	0.73
	7	44.61	58.58	0.12	0.76
	8	48.48	49.3	0.05	0.98
	9	47.67	49.11	0.11	0.97
Calcite replaced anhydrite	a	0.42	98.26	0.16	
	b	0.60	96.30	0.25	
	c	0.42	96.73	0.11	
	d	0.97	96.78	0.23	

Dolomites 3,4 8+9 from dedolomite area

Calcites a + b from dedolomite area

Calcites c + d from centre replaced anhydrite

Figure 4.6 Penecontemporaneous dolomites

a dolomicrospar/dolomicrite, Rock Cottage Quarry, Wormald Green (SE 30465). Faint foraminifera ghosts are present in some dolomicrites. Field of view is 2.2mm.

b calcitised displacive anhydrite nodule, Rock Cottage Quarry, Wormald Green (SE 304650). Cathodoluminescence. Field of view is 2.25mm.

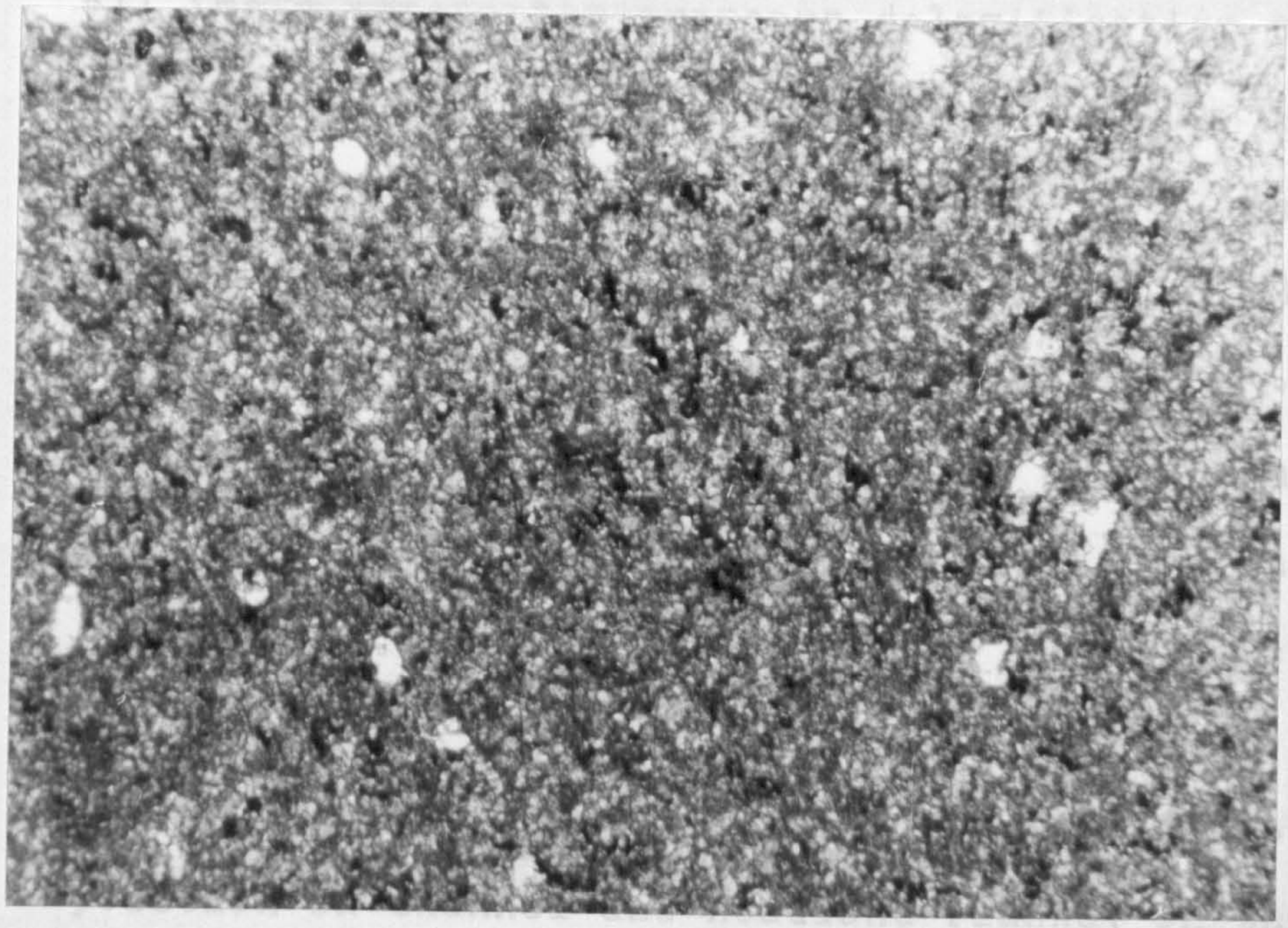

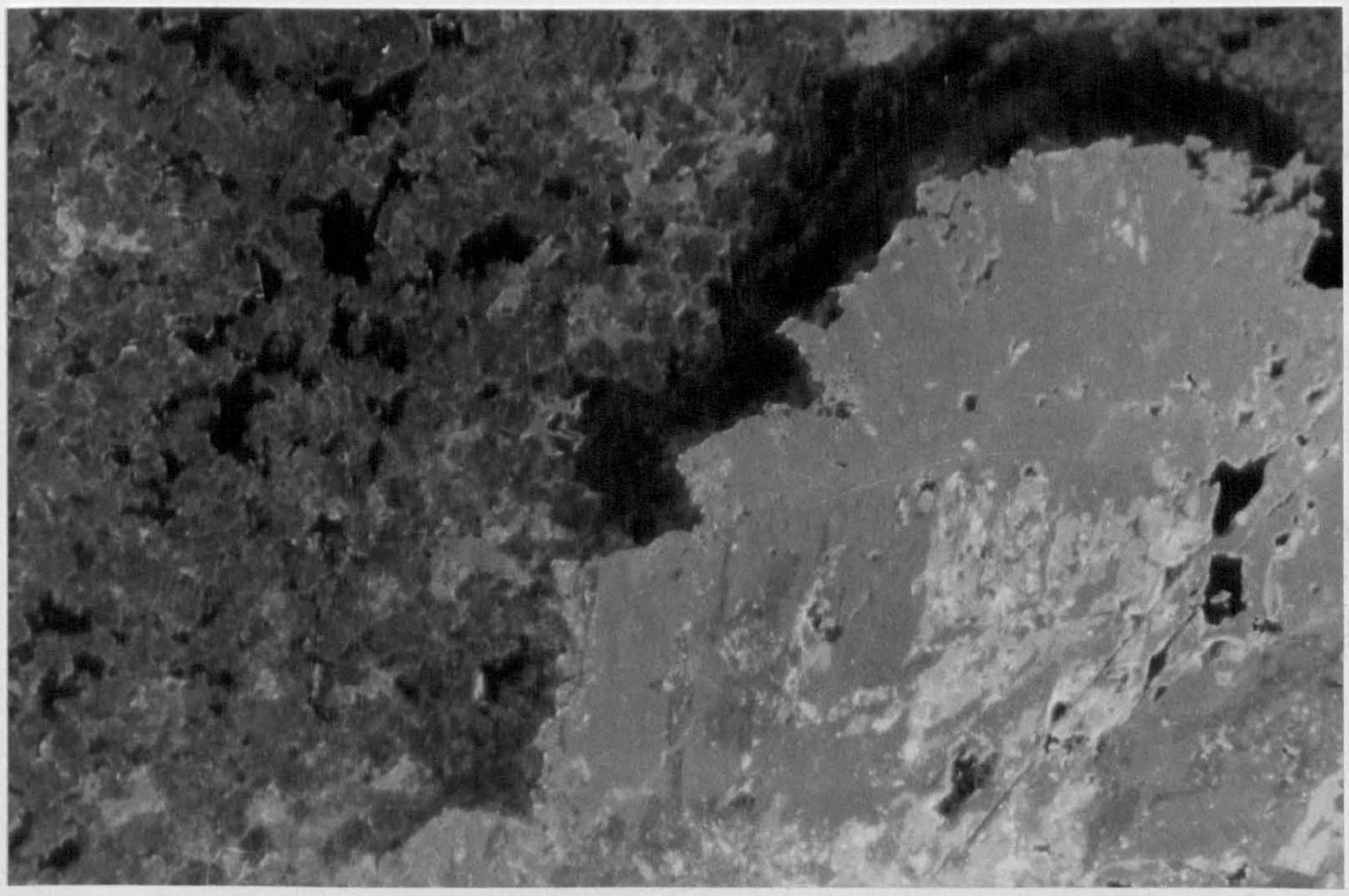

prior to anhydrite and dolomite calcitisation* all imply penecontemporaneous dolomitisation of an aragonite precursor. Although stochiometric dolomites are often associated with evaporites (Fuchtbauer, 1974; Lumsden and Chimakusky, 1980), the calcian dolomites here may be indicative of (i) instability of local conditions or (ii) the small amount of evaporite formation. Pattison and Kinsman (1981) demonstrate more complete dolomitisation of sediments when the marine-continental brine mixing zone maintains a constant position on channel and headland flanks; on the open sabkha progradation causes more rapid movement of the mixing zone and less complete dolomitisation. Also, evaporite formation is limited to anhydrite nodules and some displacive halite (3.2.10). Both these factors may account for the calcian nature of the dolomite.

Penecontemporaneous dolomitisation occurred in these restricted lagoons of the Lower Member (3.2.8-3.2.10), probably in the mixing zone between continental and marine brines, promoted by evaporative pumping and flood recharge. The

* The term 'calcitisation' of dolomite is used where occurrences are synchronous with calcite replacement of calcium sulphate minerals. Where not associated with evaporite replacement the term 'dedolomitisation' is preferred (see 5.3).

paucity of evidence of exposure associated with the formation of anhydrite nodules (Appendix 6, Log 9) suggests this was not a sabkha environment but remained mostly subaqueous throughout dolomitisation (see Fig. 4.11).

4.5.3 Dolomitisation and calcitised gypsum crystals

A sequence of cementation, gypsum formation, dolomitisation and gypsum calcitisation can be traced in some lagoon wackestones (Appendix 6, Log 10). Patchy early cementation by neomorphic calcite (Fig. 4.7 a) preceded replacement of some cemented zones by gypsum (Fig. 4.7 b) producing a vertical fabric (Fig. 4.7 c+d). Dolomitisation formed surface crusts with casts of gypsum rosettes (Fig. 4.8 a) and also cut across beds. Large evaporite casts within the dolomite (Fig. 4.8 b) may represent former selenite. Gypsum within the limestones was calcitised.

Preservation of the calcitised gypsum crystals and inclusion of small (<10μm) corroded dolomite crystals within the secondary calcites (Fig. 4.7 c) show calcitisation to again have post-dated dolomitisation. Vertical gypsum crystals with pyramidal terminations (Fig. 4.9 a) apparently pre-dated dolomitisation. Schreiber (1980) ascribed similar gypsum crystals to subaqueous precipitation. Here, however, replaced foraminiferal tests (Fig. 4.8 c) and included

Figure 4.7 Primary and secondary limestones and gypsum replacement, Bedale Quarry, Well (SE 257812).

a Patchy early cementation in primary limestone. Limestone is compacted, shown by increase in carbonaceous clasts (arrowed), around cemented areas. Field of view is 3.45mm.

b Calcite replacement of gypsum crystals. Note pseudomorphed crystal outlines (arrowed) and near vertical fabric. Gypsum replaced and/or displaced primary limestone and was later calcitised. Ostracod (o) has calcite spar centripetal fill and was not replaced by gypsum. Crossed nicols. Field of view is 3.45mm.

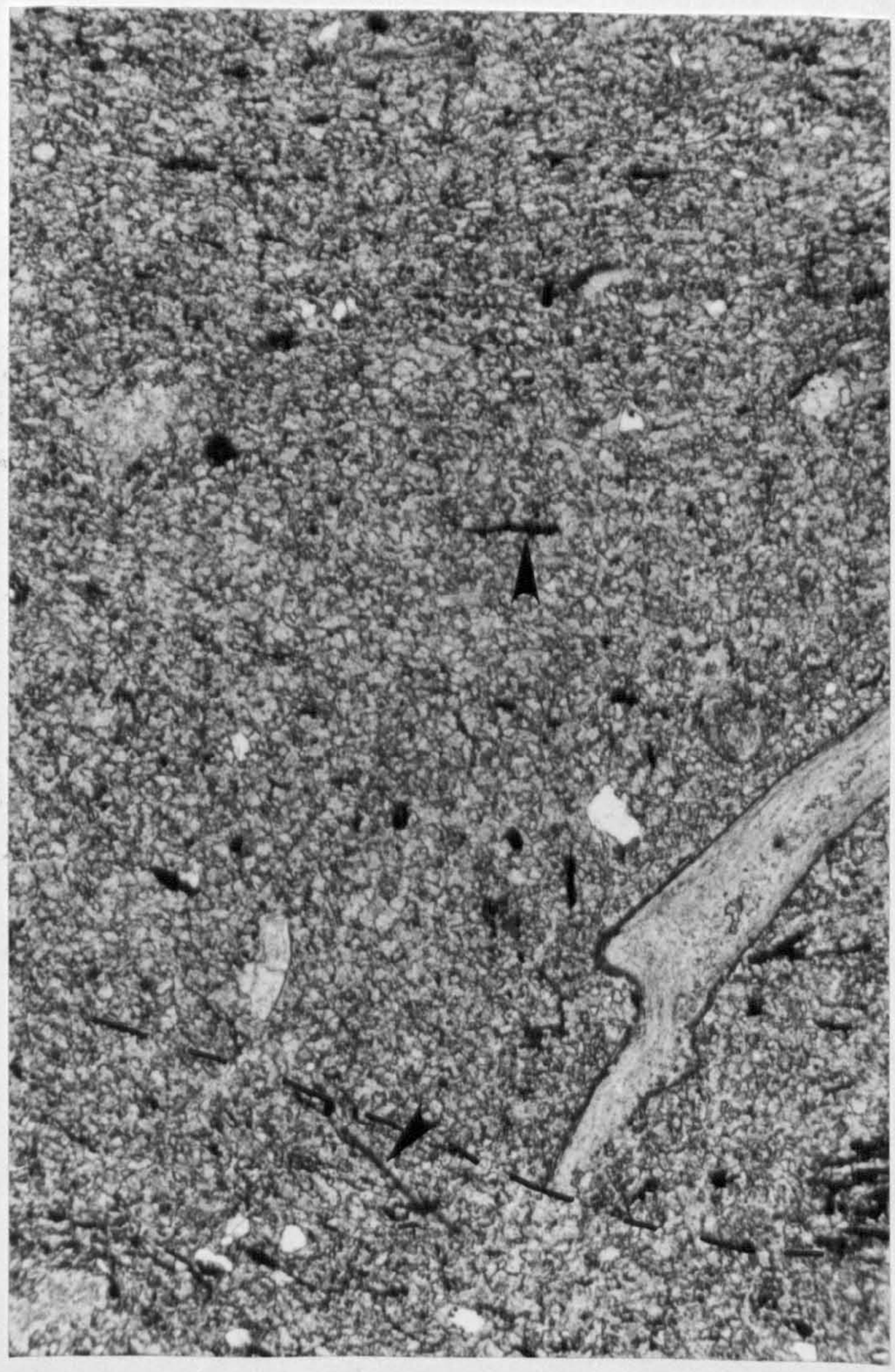

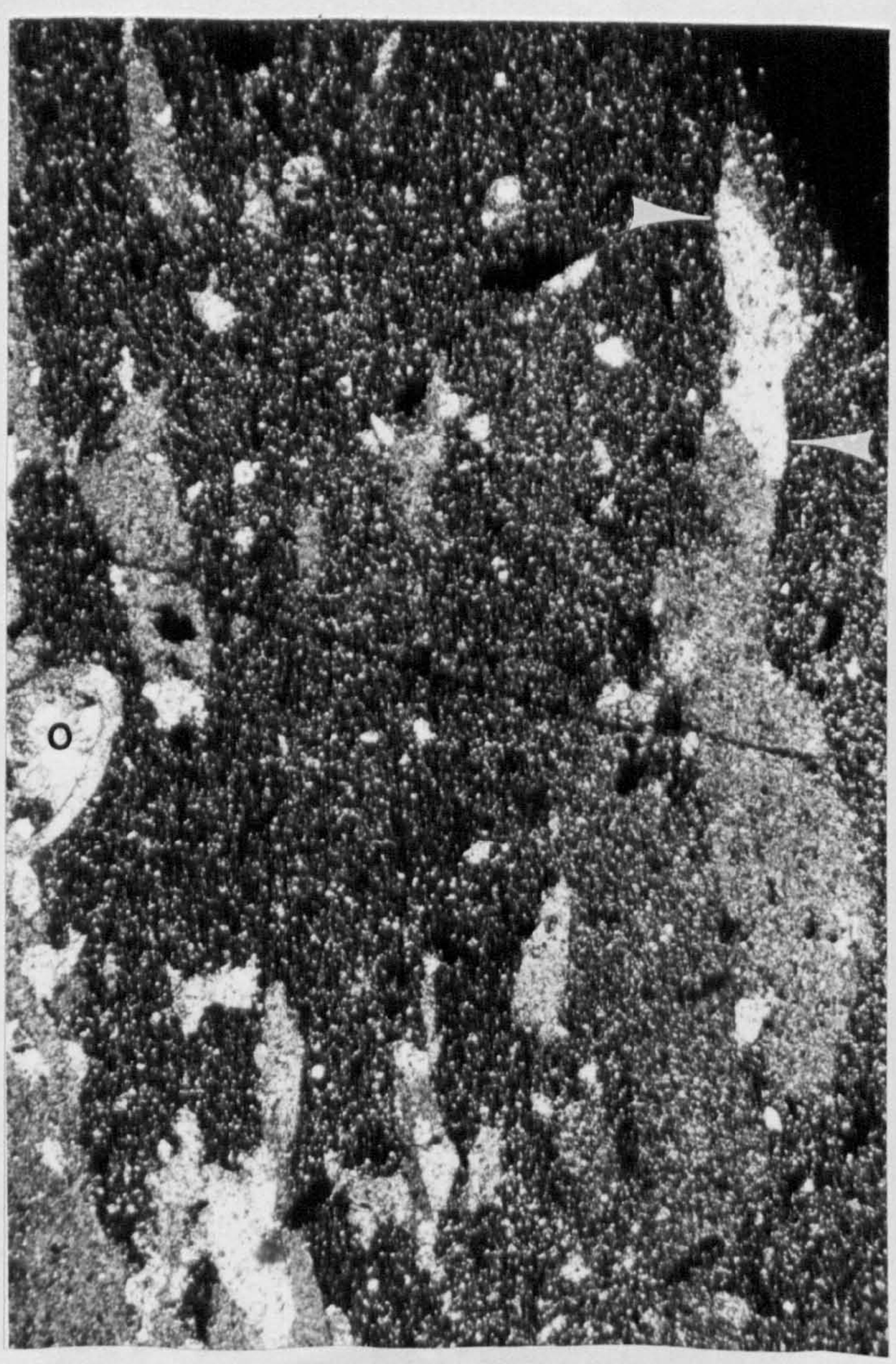
O

Figure 4.7 c Secondary limestones with ostracod (o) and carbonaceous clasts (arrowed). Field of view is 2.2mm.

d Crossed nicols view of same area showing near vertical fabric on calcitised gypsum. Gypsum had replaced primary limestone as carbonaceous clasts are still retained in fabric. Field of view is 2.2mm.

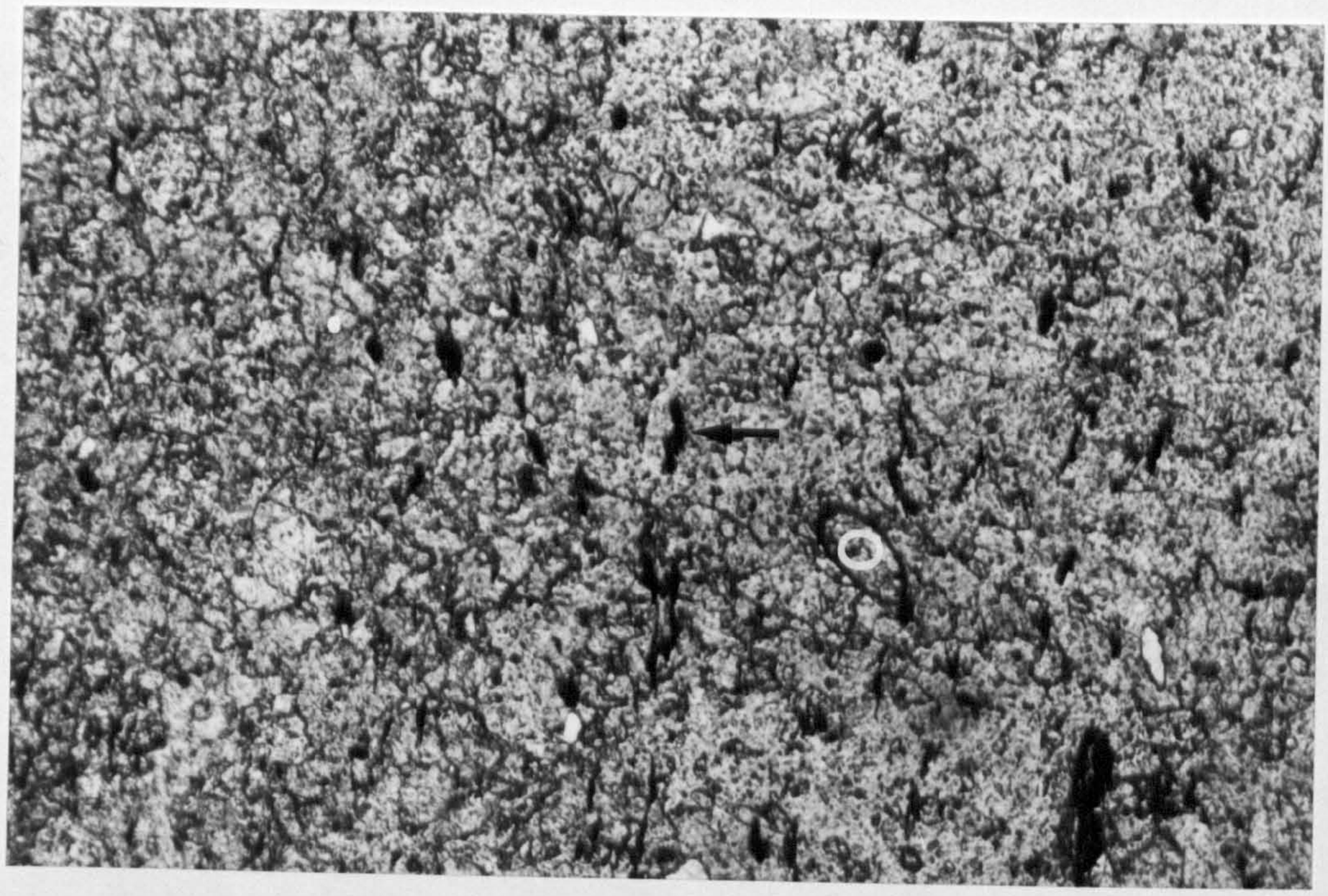

Figure 4.8 Limestones and evaporites, Bedale Quarry, Well (SE 257812)

a Black limestone with thin irregular brown dolomite upper layer. Dolomite has clasts (arrowed) after ?gypsum rosettes. Dolomite may have formed as crust on periodically exposed surface.

b Casts of evaporite (?selenite) in irregular-shaped dolomitised (D) area of primary limestone. Casts have concentrically zoned single crystal calcite fill. Field of view is 2.2mm.


2cm

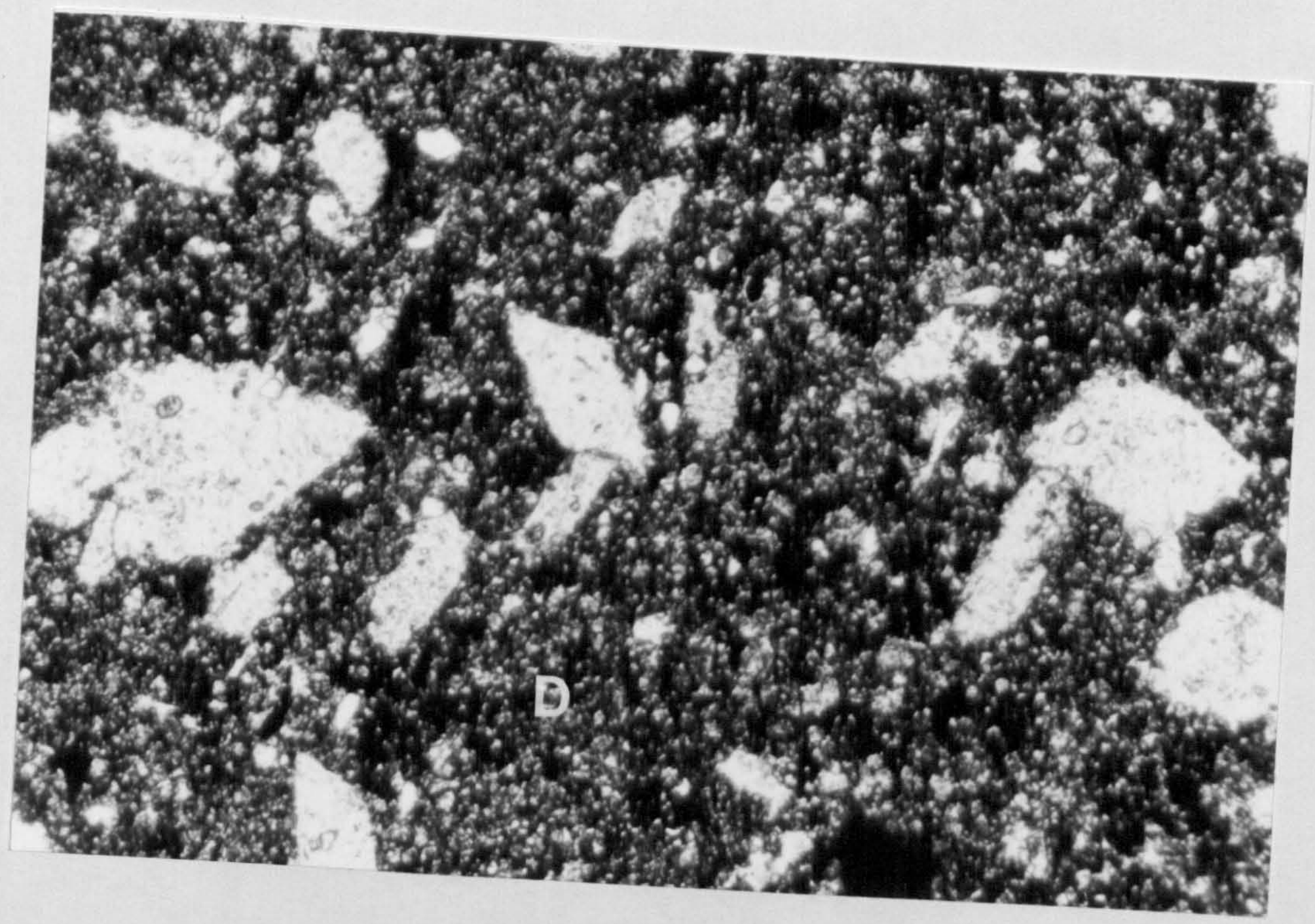
D

Figure 4.8 c Foraminifera in primary limestone. No fossils are visible in transmitted light but with cathodoluminescence foraminifera are obvious. Neomorphism has therefore retained vestiges of original fabric. Cathodoluminescence. Field of view is 2.2mm.

ostracods (Fig. 4.7 b+d) demonstrate replacive gypsum. Replacement of original carbonate by gypsum and subsequent replacement of gypsum by calcite must have been by dissolution/reprecipitation along an aqueous film (Bathurst, 1975; Pingitore, 1976) with some degree of textural preservation and not by dissolution and later void fill. No record of gypsum in the uncemented areas has been noticed although this does not preclude its former existence. Overpressuring with liquification of clastic sediments producing flame structures and hydraulic brecciation of overlying carbonates may have been caused by, or promoted, gypsum dissolution (Harwood, in press).

XRF analyses of the limestones (Appendix 5, specimens 512 and 527) shows high strontium, perhaps due to replaced evaporites (see Chapter 7.2.3) with $MgCO_3$ from probable dolomite inclusions. Calcite microprobe analyses have similar $MgCO_3$ contents and low total iron (Table 4.5). Dolomites of the surface crusts have a high iron content and Mg^{2+}/Ca^{2+} approaching unity. Iron is concentrated along the dolomite margin with calcitised gypsum (Figs. 4.9 a+b; Table 4.5).

Some wackestones were neither replaced by gypsum nor dolomitised (Appendix 6, Log 10 and Fig. 3.8). Gypsum or early calcite cements apparently protected these beds from dolomitisation.

TABLE 4.5

ELECTRON MICROPROBE ANALYSES OF CARBONATES, WELL, N. YORKS, (SE 257812)

		$MgCO_3$	$CaCO_3$	$FeCO_3$	$MgCO_3/CaCO_3$	$\frac{(MgFe)CO_3}{CaCO_3}$
Dolomite	1	48.99	52.33	7.63	0.94	1.08
	2	46.50	48.58	2.34	0.96	1.01
	3	50.27	49.62	1.93	1.01	1.05
	4	49.70	51.09	1.55	0.97	1.00
	5	43.51	52.70	2.34	0.83	0.87
	6	52.11	54.52	1.22	0.96	0.98
	7	49.71	50.52	1.22	0.98	1.01
	8	48.03	53.39	1.49	0.90	0.93
Calcite	a	0.68	102.17	0.29		
	b	1.49	97.39	0.14		
	c	1.22	93.86	0.23		
	d	1.02	99.19	0.97		

For position of dolomites 1-4 + calcites a-d see Fig 4-9b.

Figure 4.9 Dolomite-calcite boundary, Bedale Quarry, Well (SE 257812).

a Dolomite is darker near boundary with calcite. Calcite shows pyramidal projections into dolomite (arrowed) which are probably calcitised gypsum crystal terminations. Inclusions of corroded microdolomites in calcite (small arrows). Field of view is 2.2mm.

b Plot of analyses from Table 4-5 across dolomite-calcite boundary. Note that iron peak is within dolomites and that secondary limestones have low iron contents.

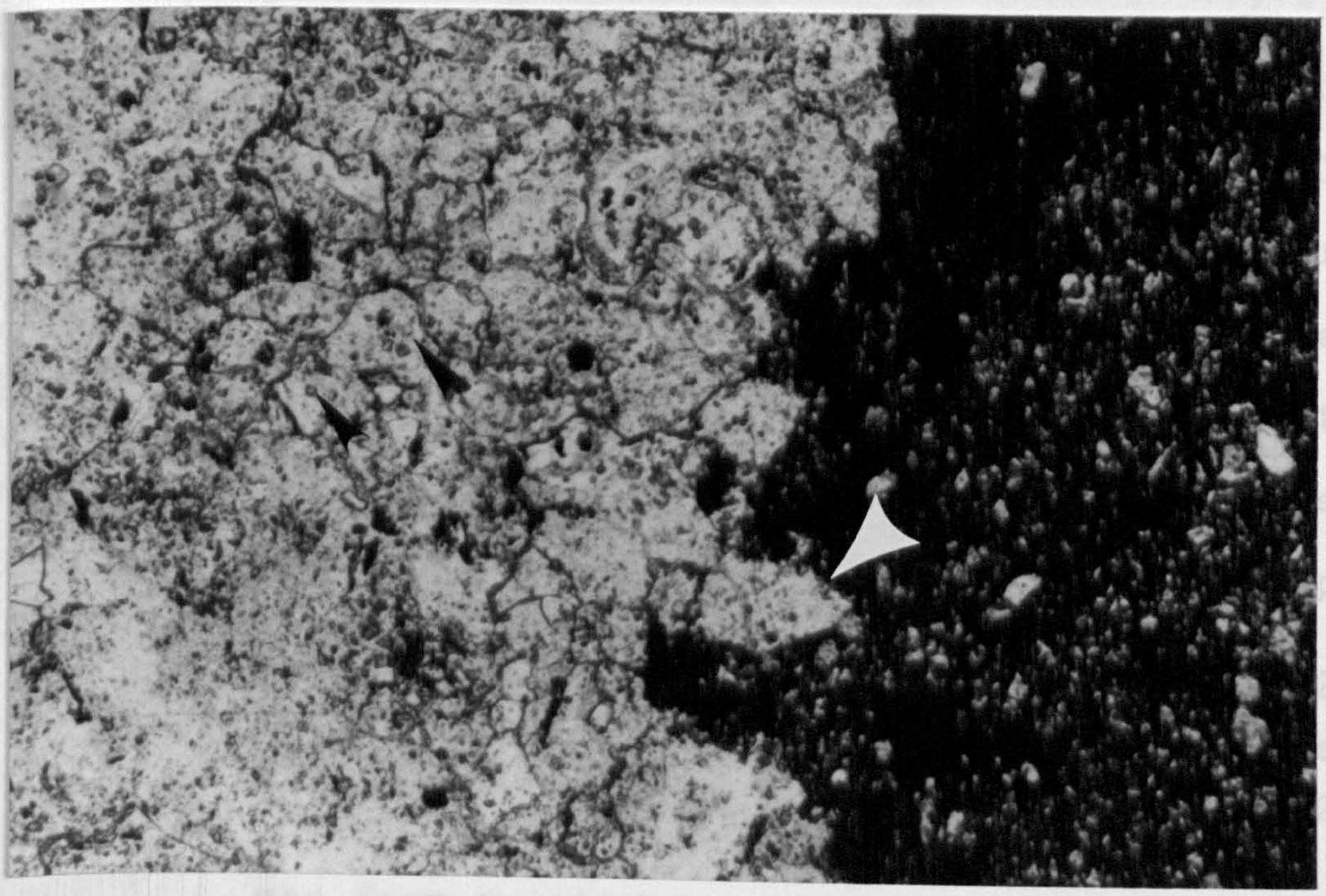

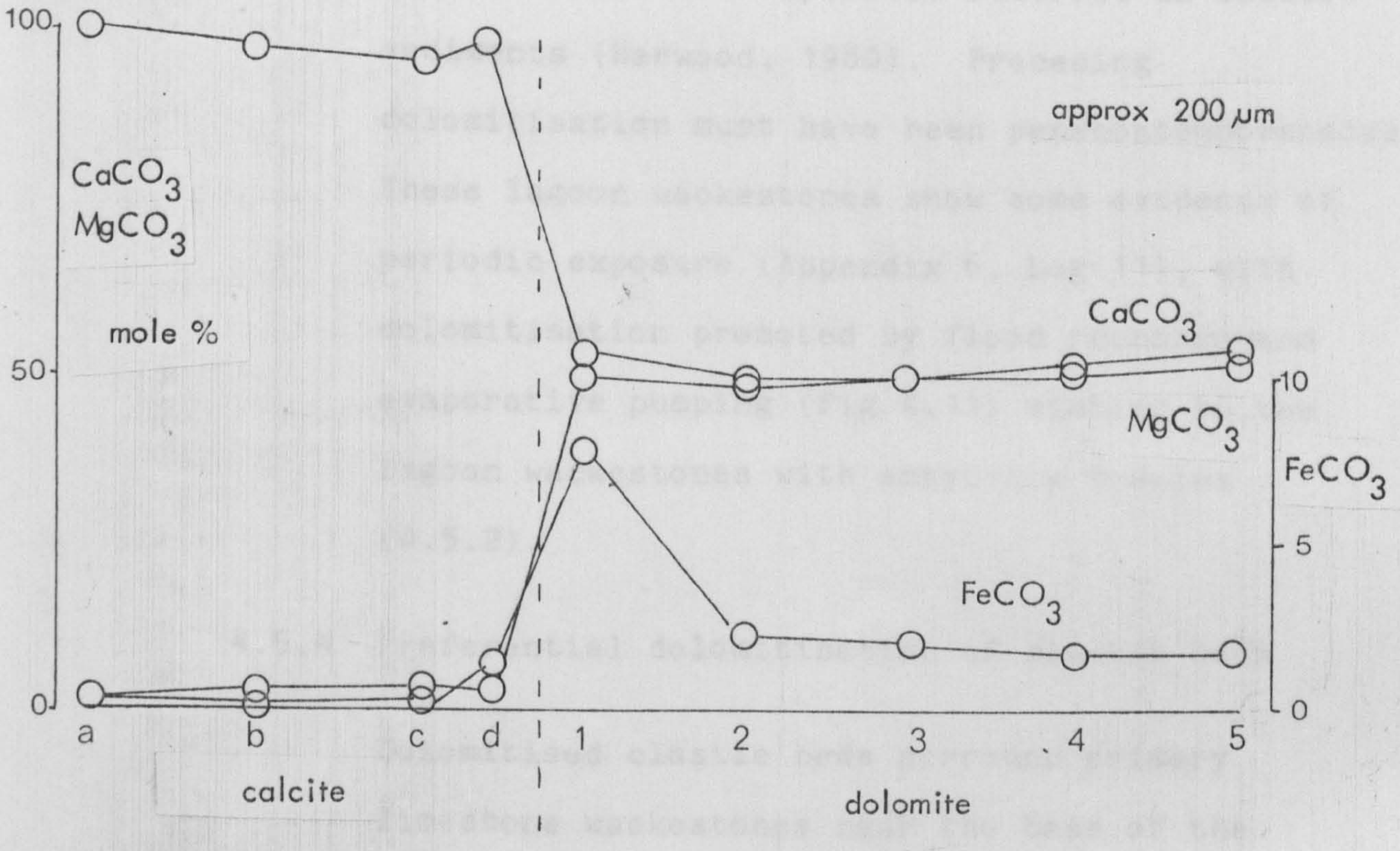
100
50
0
mole %
$CaCO_3$
$MgCO_3$
$FeCO_3$
10
5
0
a
b
c
d
1
2
3
4
5
calcite
dolomite
approx 200 µm

Calcitisation of evaporites is characterised by non-ferroan calcite (Tables 4.4 and 4.5) although surrounding dolomites may be ferroan (Fig. 4.6 b, 4.9 b). No calcitisation of sulphates is likely to occur in marine pore waters with high sulphur activities (Fig. 4.1 b) and large reserves of SO_4^{2-}. Continental waters and, more especially, continental brines have much lower SO_4^{2-} activities (Fig. 4.10, Table 4.3) which could be depleted by bacterial reduction. High Ca^{2+} activities plus CO_2 in pore waters buffers any bacterial CO_2 generated (Harwood, 1980) and causes calcite replacement of the evaporites. Iron, as Fe^{2+}, may form sulphides or become incorporated in the lattice of surrounding dolomites, partially replacing magnesium (Fig. 4.9 b).

Calcitisation of evaporites occurred in shallow sediments (Harwood, 1980). Preceding dolomitisation must have been penecontemporaneous. These lagoon wackestones show some evidence of periodic exposure (Appendix 6, Log 11), with dolomitisation promoted by flood recharge and evaporative pumping (Fig. 4.11) similar to the lagoon wackestones with anhydrite nodules (4.5.2).

4.5.4 Preferential dolomitisation of clastic beds

Dolomitised clastic beds surround primary limestone wackestones near the base of the Lower Member (Appendix 6, Log 5; 3.2.8).

Figure 4.10 Plot of effective sulphur concentrations against increasing chlorinity for marine and continental waters.

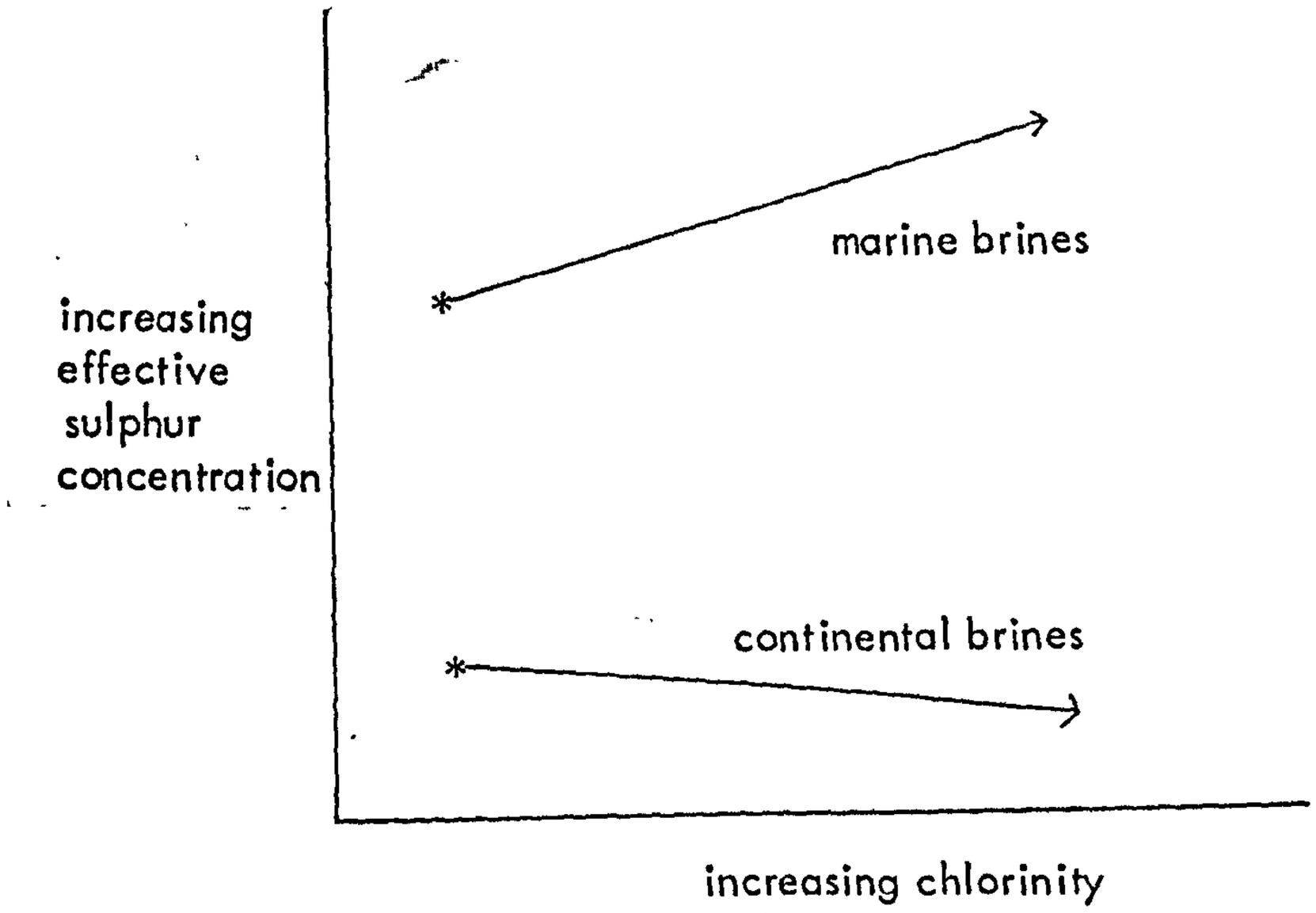
marine brines
increasing
effective
sulphur
concentration
continental brines
increasing chlorinity

Figure 4.11 Modified sabkha model for penecontemporaneous dolomitisation.

a Storm recharge of lagoon

b Evaporation and dolomitisation

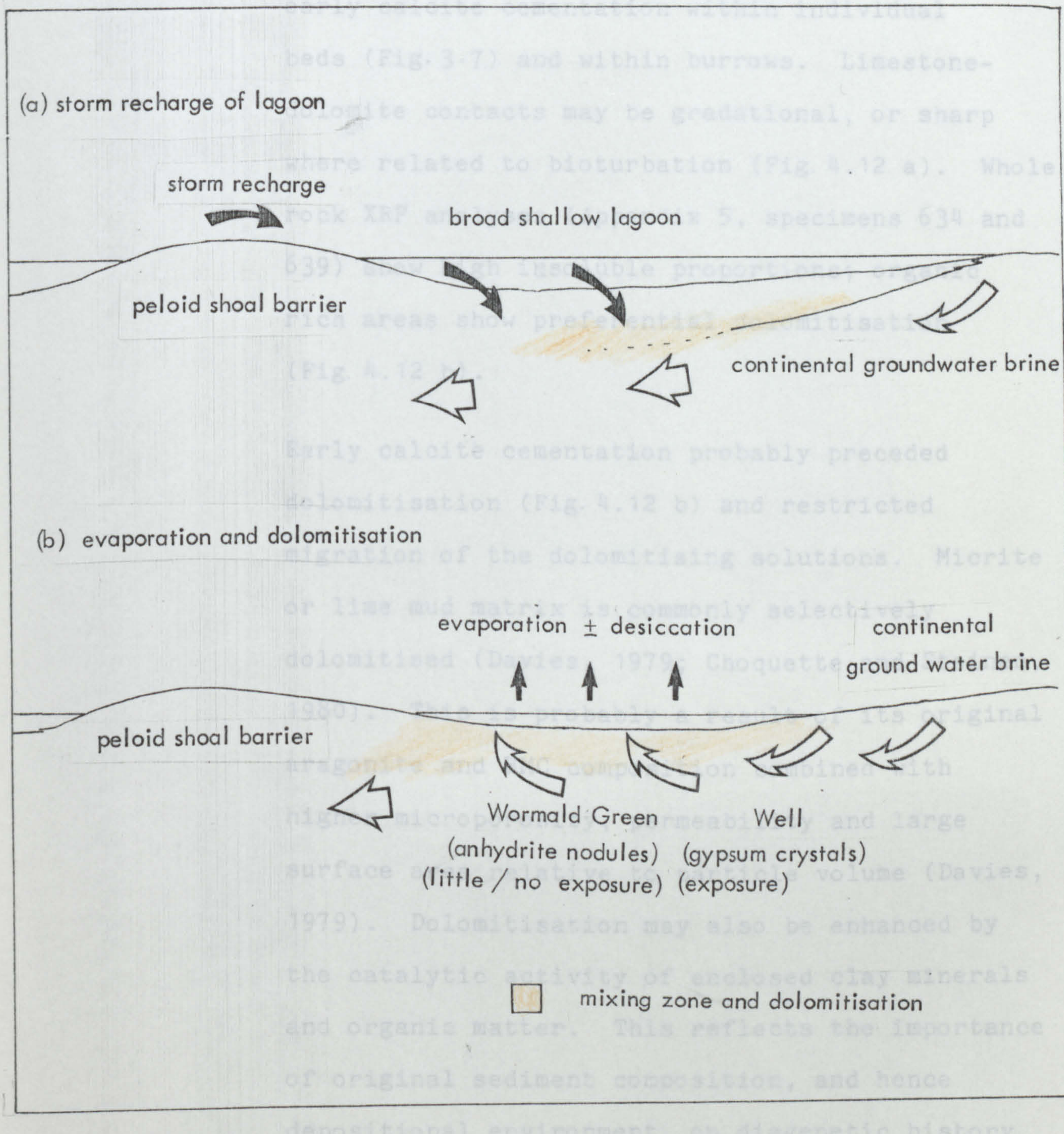
(a) storm recharge of lagoon
storm recharge
broad shallow lagoon
peloid shoal barrier
continental groundwater brine
(b) evaporation and dolomitisation
evaporation ± desiccation
continental
ground water brine
peloid shoal barrier
Wormald Green
(anhydrite nodules)
(little / no exposure)
Well
(gypsum crystals)
(exposure)
mixing zone and dolomitisation

Limestone preservation is apparently due to early calcite cementation within individual beds (Fig. 3.7) and within burrows. Limestone-dolomite contacts may be gradational, or sharp where related to bioturbation (Fig. 4.12 a). Whole rock XRF analyses (Appendix 5, specimens 634 and 639) show high insoluble proportions; organic rich areas show preferential dolomitisation (Fig. 4.12 b).

Early calcite cementation probably preceded dolomitisation (Fig. 4.12 b) and restricted migration of the dolomitising solutions. Micrite or lime mud matrix is commonly selectively dolomitised (Davies, 1979; Choquette and Steinen, 1980). This is probably a result of its original aragonite and HMC composition combined with higher microporosity, permeability and large surface area relative to particle volume (Davies, 1979). Dolomitisation may also be enhanced by the catalytic activity of enclosed clay minerals and organic matter. This reflects the importance of original sediment composition, and hence depositional environment, on diagenetic history (Davies, 1979). No exact time limits other than post-dating calcite cementation and slight compaction and pre-dating formation of micro-stylolites (see 6.4.3) can be given for this dolomitisation.

Figure 4.12 a Limestone-dolomite contact at burrow margin, Vale Road Quarry, Mansfield Woodhouse (SK 532648). Burrow is of limestone; surrounding carbonate with siliciclastic muds is dolomite. Burrow margin is arrowed. ▲Field of view is 2.2mm.

b Large dolomite crystal within ostracod shell, Vale Road Quarry, Mansfield Woodhouse (SK 532648). Dolomite crystal has grown preferentially with shell; dolomite crystals surrounding shell are microspar size. Shell wall is calcite. (Stained with Alizarin Red S). Field of view is 0.55mm.

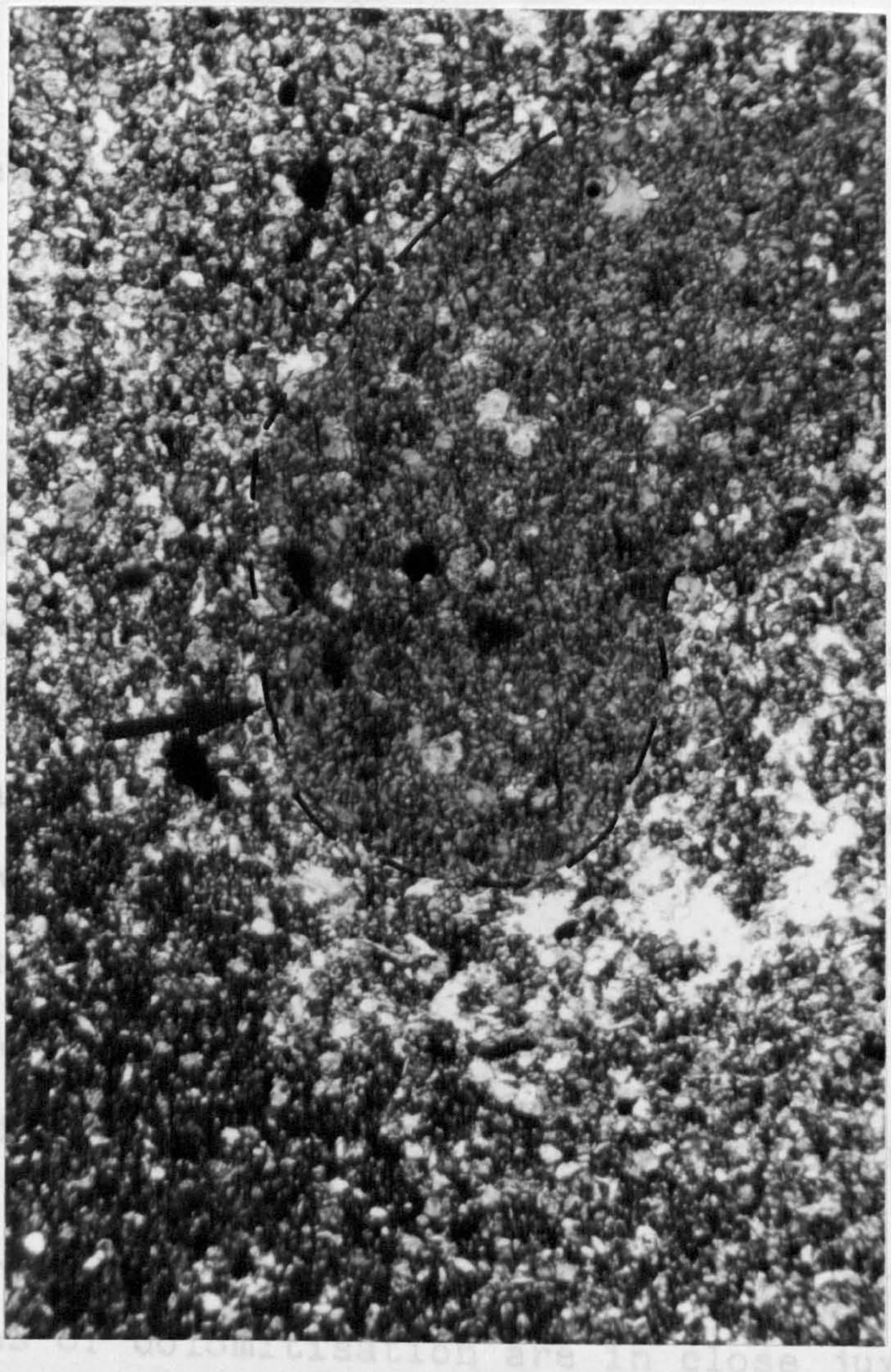

4.5.5 Eogenetic dolomitisation

Dolomitisation of most of the Cadeby Formation was eogenetic, occurring in the shallow subsurface beforé substantial compaction and burial. This eogenetic dolomitisation commonly produces medium to coarsely crystalline carbonates (50 μm - 1500 μm) and may completely destroy original textures. Texture preservation is common, however, within patch reefs (Smith, 1981) which may retain a high intergranular porosity. Flanking ooid and pisoid grainstones and the algal boundstone cappings are relatively impermeable.

Within the ooid grainstone barriers contrasting styles of dolomitisation are in close juxta-position and may be independent of depositional environment; lack of outcrop does not permit definition of diagenetic dolomite environments.

Dolomite crystal sizes are unrelated to original grain size. Comparable ooid grainstones on a shoal flank may have different crystal sizes (Fig. 4.13 a+b) but similar chemical compositions (Appendix 5, specimens 131 and 134). Original trace element concentration variations are retained within the dolomites in some instances (Fig. 4.14 a+b). Whole rock XRF analyses and strontium contents (Appendix 5, specimens 131-144, 311-329). The low strontium contents preclude

correlation of Sr^{2+} ppm and crystal size (e.g. Mattes and Mountjoy, 1980; M'Rabet, 1981).

Dolomitisation is texture destroying throughout most ooid grainstones although ghosts remain (Fig. 4.13 a). Texture is better preserved in burrow margins (Fig. 4.13 c). This may be due to the high organic content of the original mucus-rich burrow wall promoting more rapid dolomitisation. Burrows also were open voids allowing rapid flow of dolomitising fluids. Where visible relict ooids have point contacts with no planar or sutural grain boundaries (Fig. 4.13 c); dolomitisation of ooids plus formation of dolomite intergranular cement must thus have occurred before compaction and grain to grain dissolution. There is no evidence of volume reduction during dolomitisation.

Grain to grain dissolution is influenced by pore solutions and composition of the intergranular pore fluids. With undersaturated pore fluids (and boundary films), pressure solution may develop before significant overburdening. With saturated pore fluids, pressure solution may be retarded until deep burial (Bathurst, 1975). Any degree of overpressuring will also retard pressure solution. Lack of pressure solution between grain contacts can thus only be taken as a general guide to timing of dolomitisation.

In intershoal areas both fabric destruction and

Figure 4.13 a + b anhedral dolomites from peloid grainstones, Shirebrook (SK 530687).

a Top bed of Upper Member. Note ooid ghost with quartz core (arrowed). Dolomite crystals average 120μm. Field of view is 2.2mm. Specimen No. 131.

b Bed within Upper Member, 1 metre below Fig. 4.13 (b). Ghosts are faint (arrowed) and are cut by dolomite crystal boundaries. Dolomite crystals up to 400μm. Good later leached secondary porosity. Field of view is 2.2mm. Specimen No. 134.

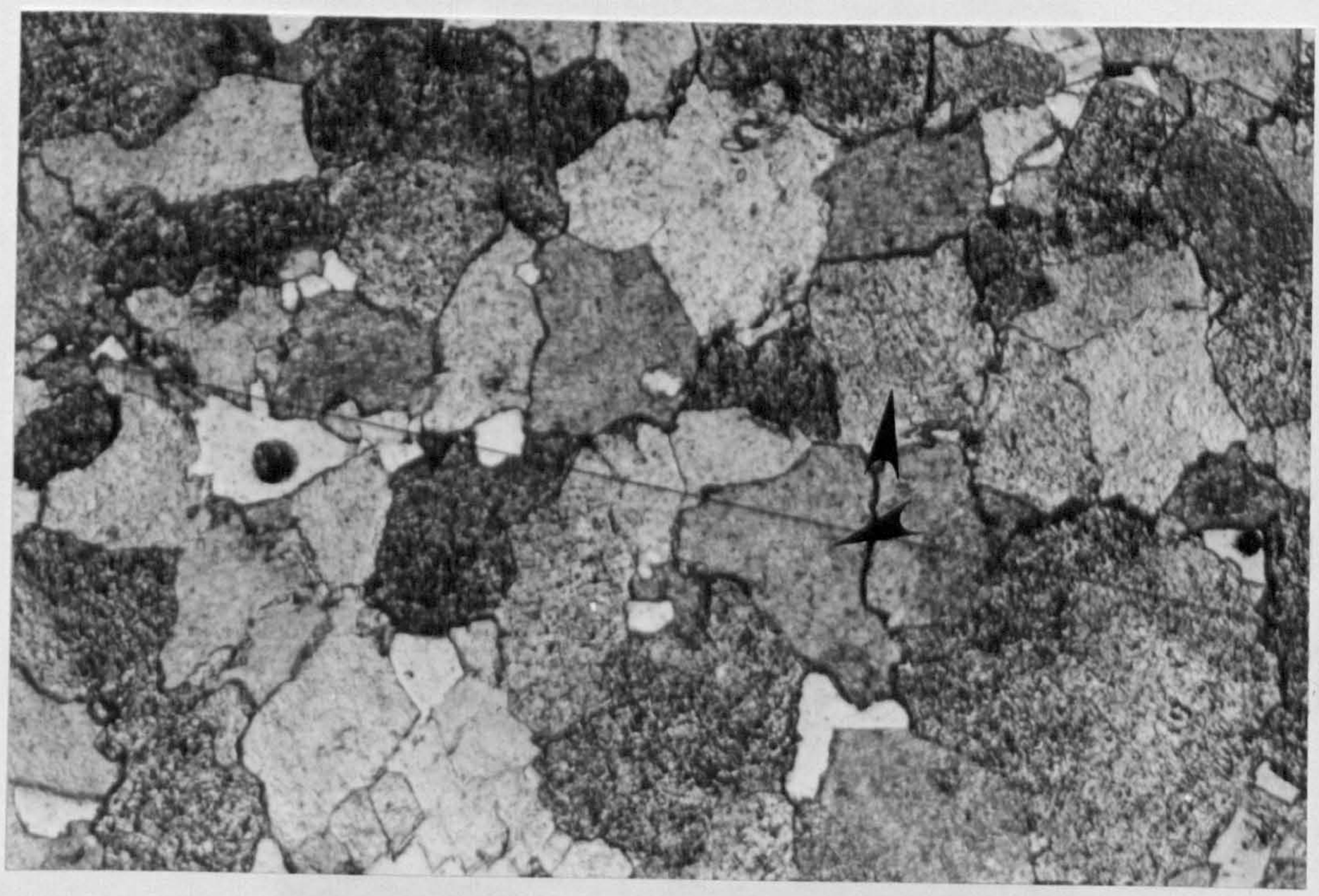

Figure 4.13 c Preferential texture preservation in burrow margins, Lovers Leap, Sprotborough (SE546018). Peloid forms are more distinct near burrow margin than in surrounding dolomite. Burrow wall has a 'psuedofibrous' dolomite cement. Field of view is 2.75mm.

d Zones of preferential cementation in peloid grainstone, Upper Member, Wistow Wood Core (SE 567356). Where early cementation took, peloids maintain their original shape, but in uncemented areas peloids are considerably compacted (arrowed). Field of view is 9.0mm.

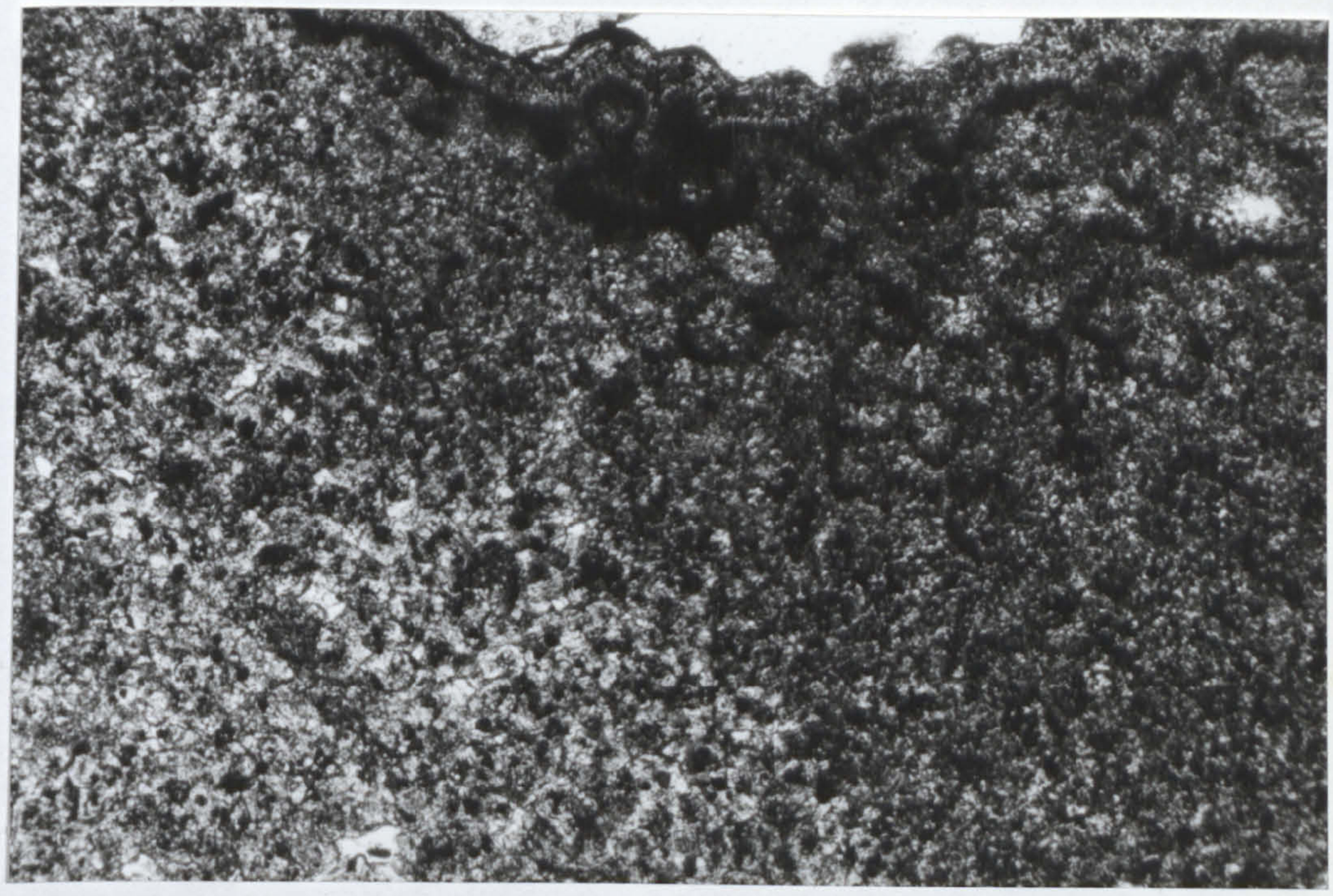

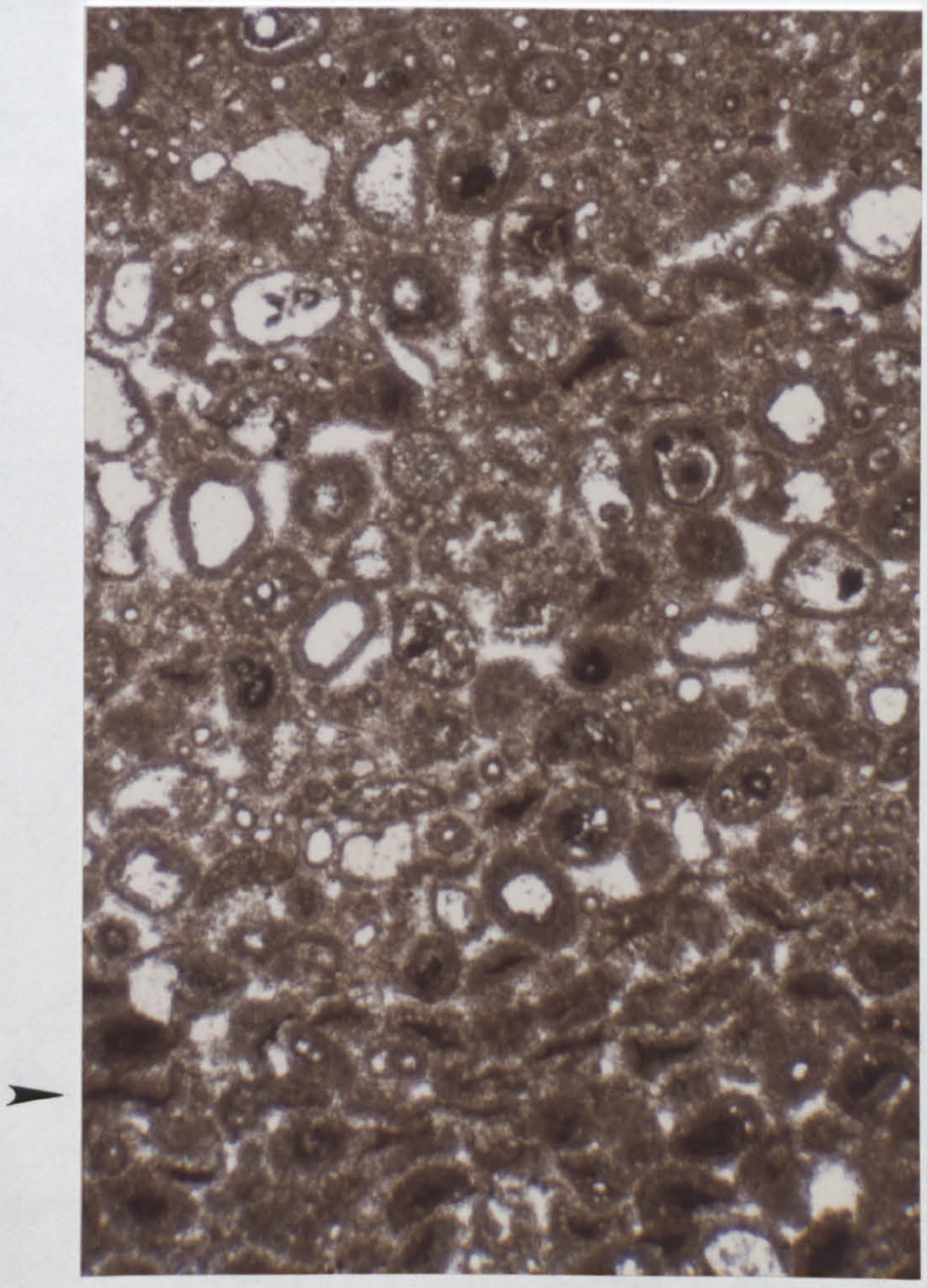

Figure 4.14 a Peloid in peloid grainstone, Upper Member, New Edlington Brick Works Quarry (SK 532986). Field of view is 0.9mm.

b Semiquantitative scan aross similar peloid showing variations in $MgCO_3$, $FeCO_3$ and $MaCO_3$.

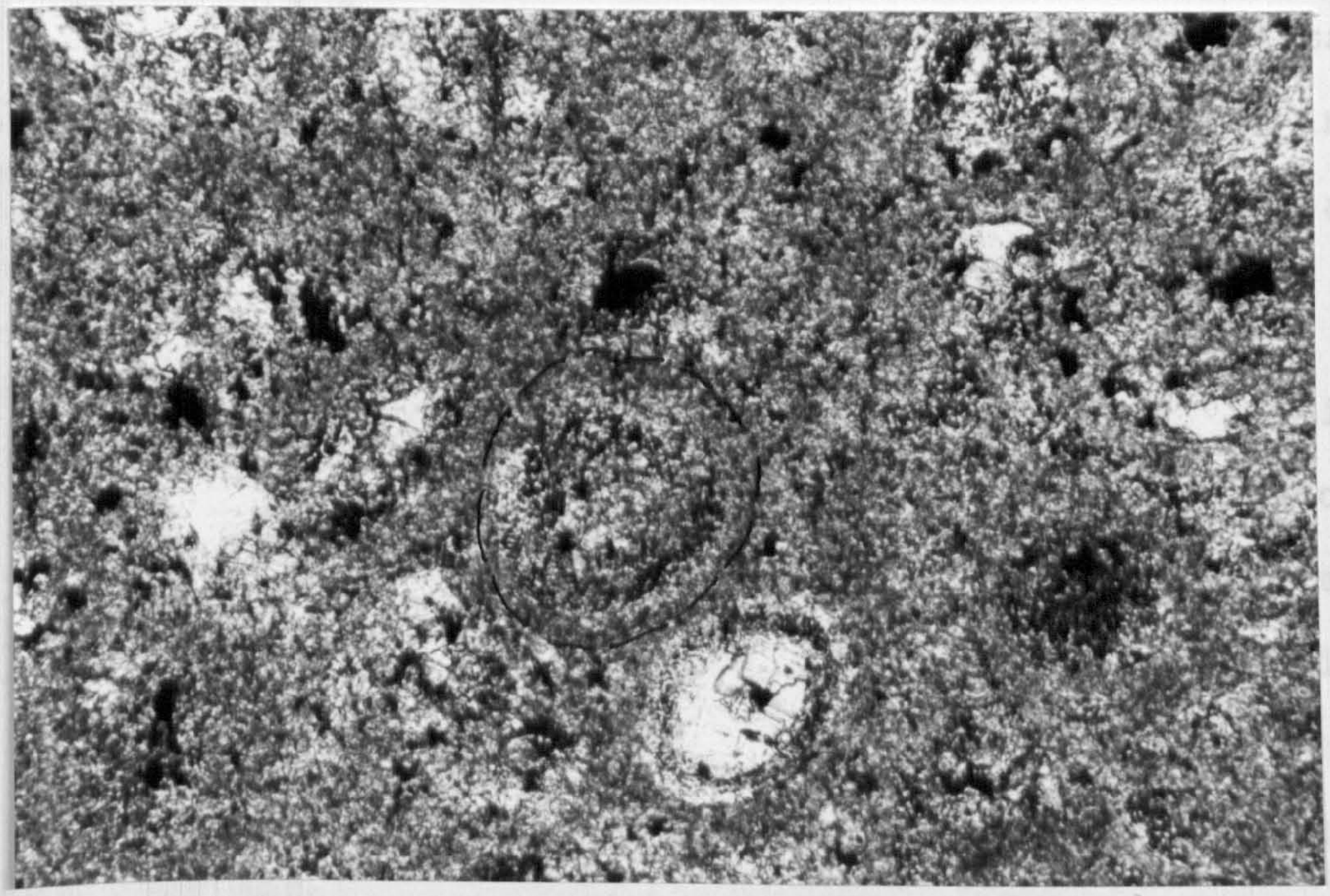

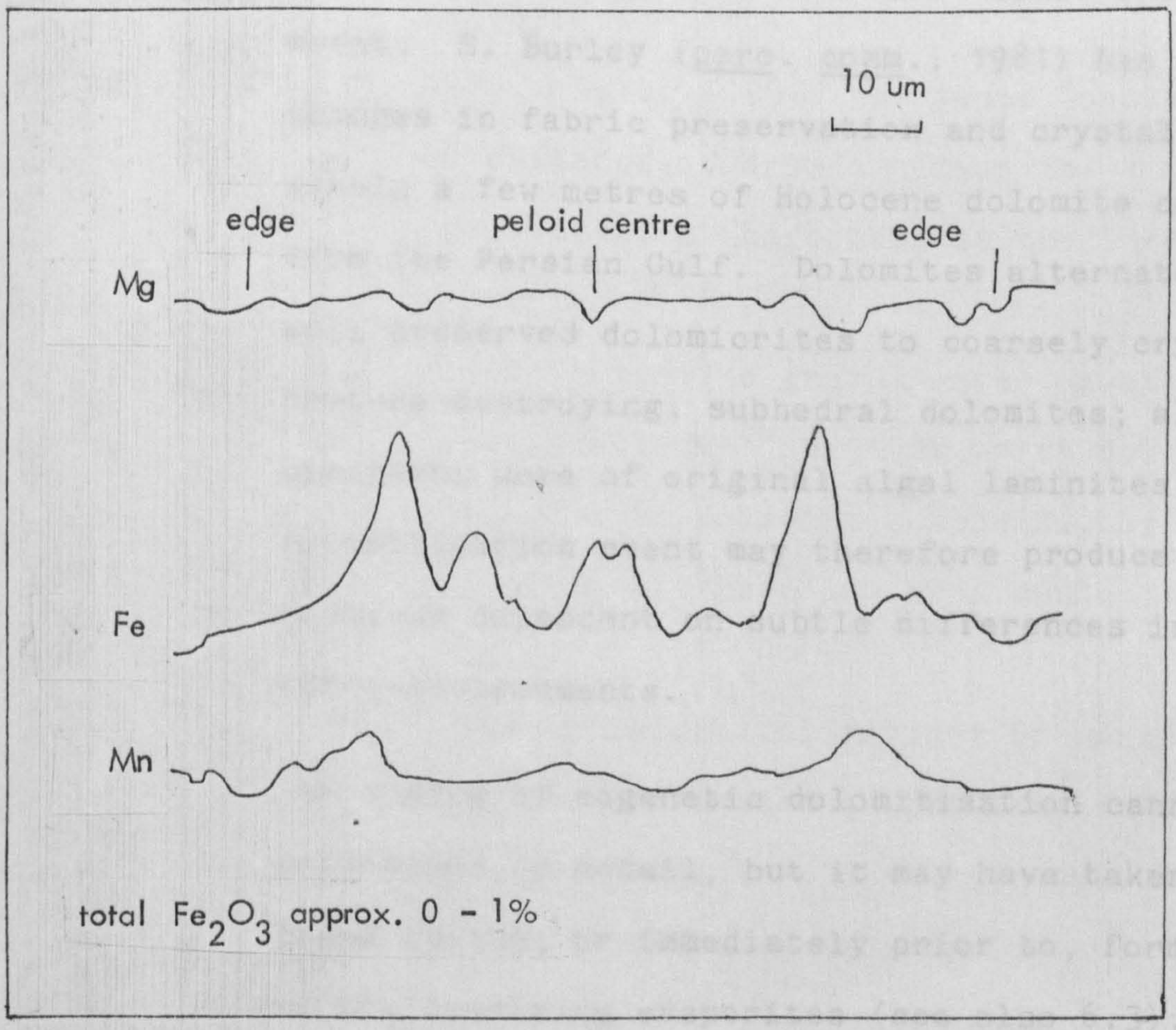
10 um
edge
peloid centre
edge
Mg
Fe
Mn
total Fe_2O_3 approx. 0 - 1%

retention occur during dolomitisation. Porosity is destroyed in both. Soft pellets are often deformed by compression prior to dolomitisation although early cementation prevents this in some zones (Fig. 4.13 d). Pisoids, grapestones and washed-in ooids were rigid.

No evidence has been found of different episodes of eogenetic dolomitisation between the two Members. The clays of the Hampole Beds are not aquicludes (Aldrick, 1978); their absence in much of the subsurface reinforces the hypothesis of one major event of eogenetic dolomitisation.

Differences in crystal size, texture retention or destruction (Figs. 4.13 a-d) all result from this event. S. Burley (pers. comm., 1981) has noticed changes in fabric preservation and crystal size within a few metres of Holocene dolomite cores from the Persian Gulf. Dolomites alternated from well preserved dolomicrites to coarsely crystalline, texture destroying, subhedral dolomites; all specimens were of original algal laminites; One dolomitisation event may therefore produce various textures dependent on subtle differences in micro-environments.

The timing of eogenetic dolomitisation cannot be determined in detail, but it may have taken place during, or immediately prior to, formation of the overlying evaporites (see also 6.3).

4.5.6 Application of Holocene analogues to eogenetic dolomitisation in the Cadeby Formation

Direct application of Holocene analogues is tenuous due to lack of modern comparative evaporite basins (4.4). Kaldi (1980a) proposed mixed water dolomitisation for the ooid grainstone barriers with migration of the meteoric lens caused by draw-down of up to 100m of the Zechstein sea after deposition of the Cadeby Formation. Several points argue against this hypothesis:

(i) Drawdown and subsequent meteoric influx would develop vadose leached fabrics throughout much of the Upper Member; evidence for this is rare (3.4.7 and 4.4). Aplin (1981) has found little or no evidence of drawdown near the top of the equivalent carbonate in the Durham Province.

(ii) Meteoric derived ground water usually has a measurable Fe^{2+} content which would be reflected in dolomite compositions; these dolomites all have low iron contents (4.5.5).

(iii) Drawdown before dolomitisation would convert original carbonates to LMC within the meteoric lens (4.4.1). This would retard the dolomitisation rate and produce fabric

differences between meteoric/non meteoric influenced areas. No such differences have been noticed.

(iv) As dolomitisation only occurs within the mixing zone, dolomitisation of the entire formation is difficult to visualise with one major drawdown period.

(v) Pore fluids were saturated in $CaSO_4$ after dolomitisation but before final burial (6.3.2). This would involve large flow through minute pore spaces (e.g. Figs. 4.13 a+b) displacing meteoric fluids (compare with higher porosity in 4.4.2).

These factors argue against both considerable drawdown and dolomitisation due to the mixed water model.

Sabkha models apply to restricted environments (4.4.1). Predominant groundwater flow beneath the sabkha surface is seawards (McKensie et al., 1980); dolomitisation occurs in surface sediments above the groundwater flow zone. Permian climates are unlikely to have been considerably more arid than the Trucial Coast today; a similar ground water flow is envisaged. Sabkha models, or modified sabkha models (4.5.2 and 4.5.3), can only have been responsible for local, penecontemporaneous dolomitisation in the Cadeby Formation.

Modern analogues of the seepage reflux model are

small and cannot be compared to Zechstein dolomitisation. Seepage reflux on a large scale, as originally proposed by Adams and Rhodes (1960), does, however, present a possible hypothesis.

4.5.7 Large scale seepage reflux

Large scale seepage reflux is suggested by post-dolomitisation pore fluid saturation in Ca SO_4 (4.5.6) and replacive anhydrite 6.3.2) (Harwood, 1980), probably developed during deposition of the overlying evaporites. Little or no drawdown but high evaporation rates over the shallow carbonate shelf would produce evaporite-rich brines. This relatively high sea level stand is implied by the evaporites overlying the EZ1 carbonate in the subsurface (Appendix 6, Log 11; Appendix 7; unpublished oil company and NCB data) and by the shape of the EZ1 and EZ2 evaporite lenses (Taylor and Colter, 1975; Reed and Colter, 1980) (Fig. 1.4 b). The marine brine would have high ionic strength and high Mg^{2+}/Ca^{2+} ratios, aiding rapid dolomitisation (4.4.2). Sediments would not have altered from their original compositions or probable aragonite and HMC; a further 'aid' to dolomitisation (4.3.4).

Evidence of later hypersaline pore waters is shown by the replac-ive evaporites (6.3.2; Harwood, 1980). Original limestones are preserved at the base of the Lower Member (3.2.8; Appendix 6, Log 5); this is in accord with downwards

penetration of dolomitising fluids which may have lost some strength by this level, dolomitisation being confined to the more permeable, clastic beds (4.5.4).

The main argument against the reflux hypothesis is the lack of an adequate flow mechanism. Flow rates based on differences in salinity and hence high diffusion gradients would be very slow. Existing pore water pressures would act against downwards flow of these denser brines (4.4.1, 4.4.3). However, the presence of replacive evaporites demonstrates that such pore water flow of hypersaline brines did occur; future research may elucidate a mechanism of flow.

It is therefore proposed that eogenetic dolomitisation in the Cadeby Formation is due to a large scale seepage reflux model (Fig. 4.15), similar to that originally proposed by Adams and Rhodes (1960). Modern analogues do not exist.

4.5.8 Dolomite fringing cements

Isopachous euhedral dolomite fringing cements have been described by Kaldi (1980a) from the crusts of some ooid barrier shoals. Similar cements line fenestrae and ooids in the Lower Dolomite of the Hampole Beds (Fig. 4.16 a) and surround clasts in the breccia facies at the top of the Upper Member (Fig. 4.16 b). Rare spalling of clast cements occurs (Fig. 4.16 c).

Figure 4.15 Eogenetic dolomitisation by large scale seepage reflux

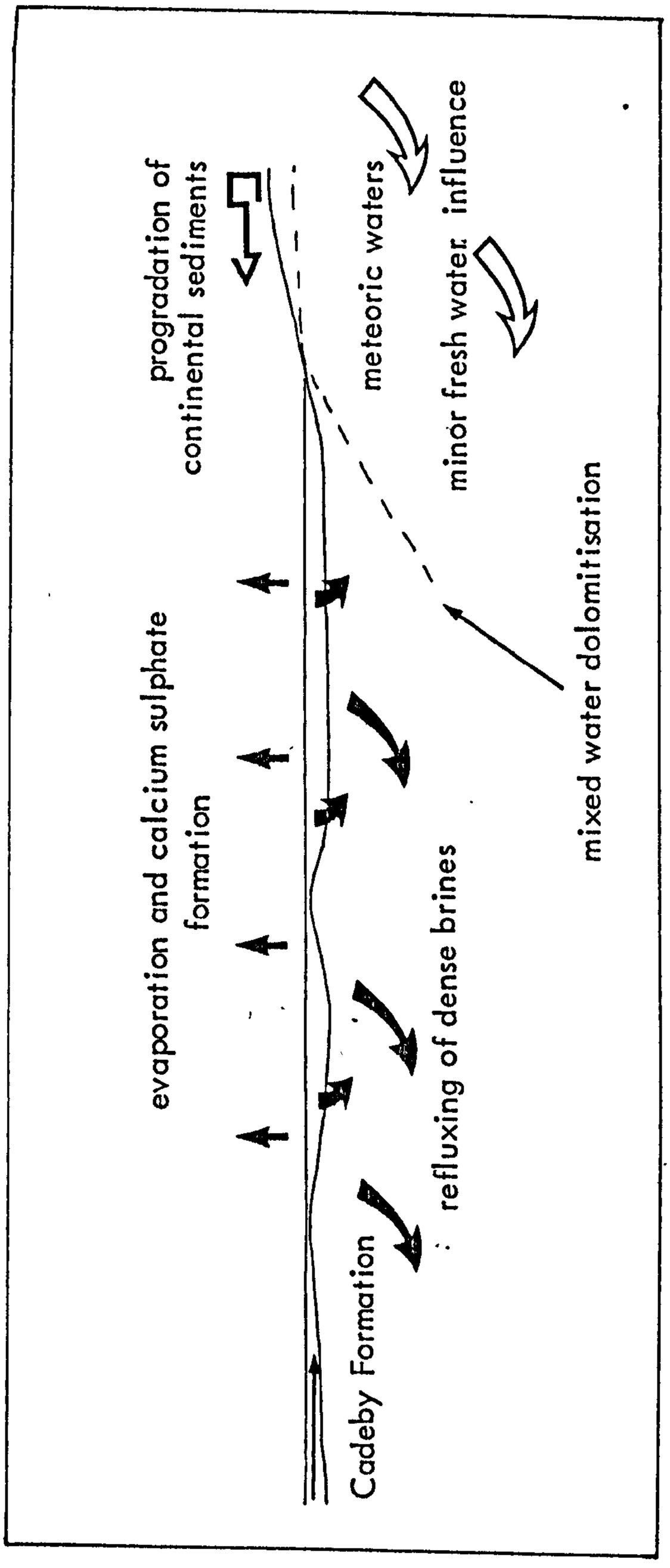
progradation of continental sediments
meteoric waters
minor fresh water influence
evaporation and calcium sulphate formation
mixed water dolomitisation
refluxing of dense brines
Cadeby Formation

Figure 4.16 Dolomite fringing cements

a Dolomite fringing cements on peloid micrite envelopes, Lower Dolomite, Hampole Quarry (SE 516097). Large open pores are fenestrae (f); peloid centres are open (p) or partially occluded by later calcite (c). Micrite envelopes are arrowed. Field of view is 0.9mm.

b Dolomite fringing cements on clasts in breccia, New Edlington Brick Works Quarry (SK 532986). Clasts were lithified before inclusion in breccia as peloids are fractured (arrowed). Dolomite fringing cement surrounds clasts. Porosity partially occluded by later void-filling calcite (c). Field of view is 2.2mm.

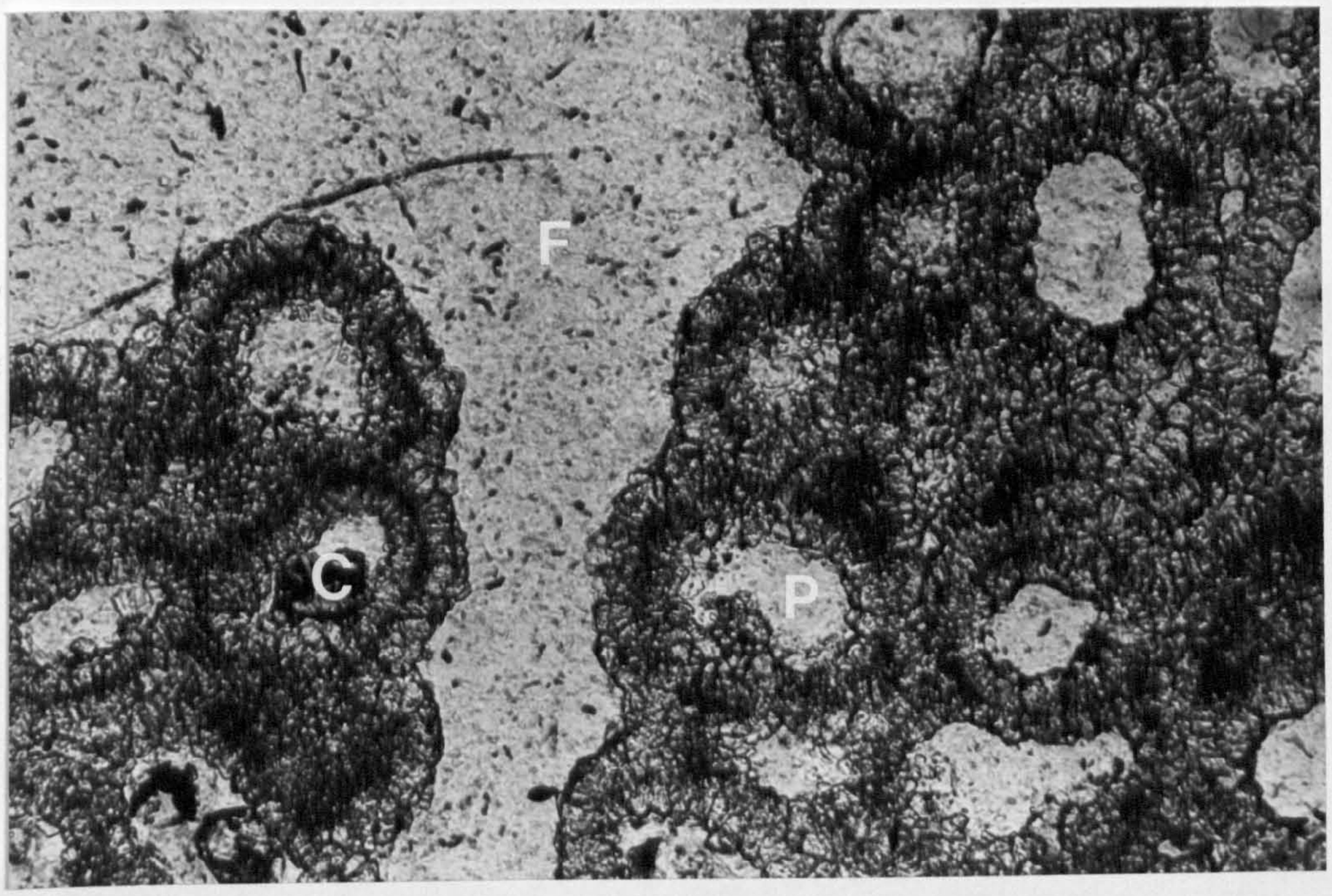
F
C
P

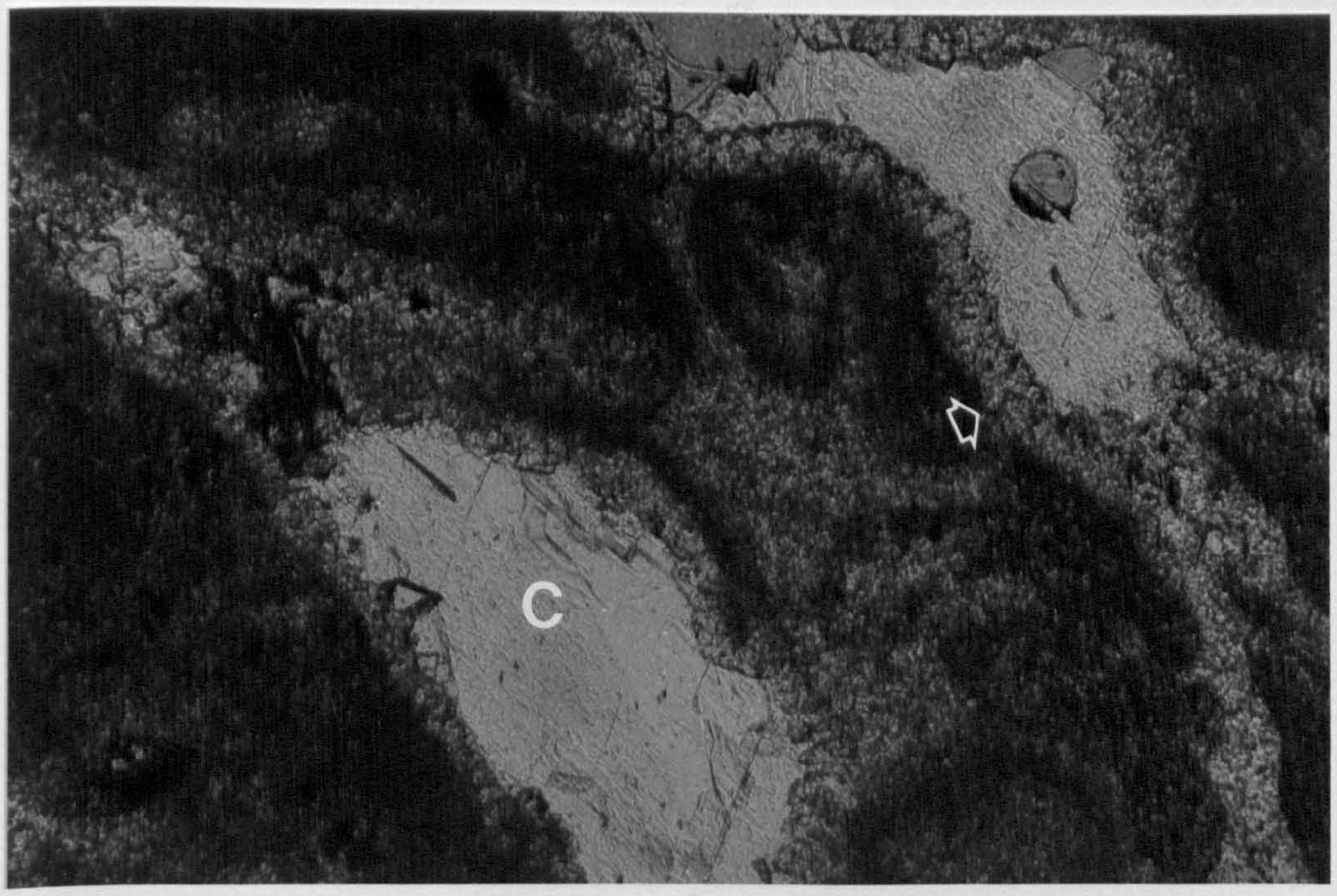
C

Figure 4.16 c Spalling of clast margin with dolomite fringing cement (arrowed). Fringing cement must have grown shortly after or during spalling. Peloids in clast have leached centres (p) and are transected by clast boundary (b) showing cementation and lithification before clast formation. Pore fill of later dolomite (d). Field of view is 0.9mm.

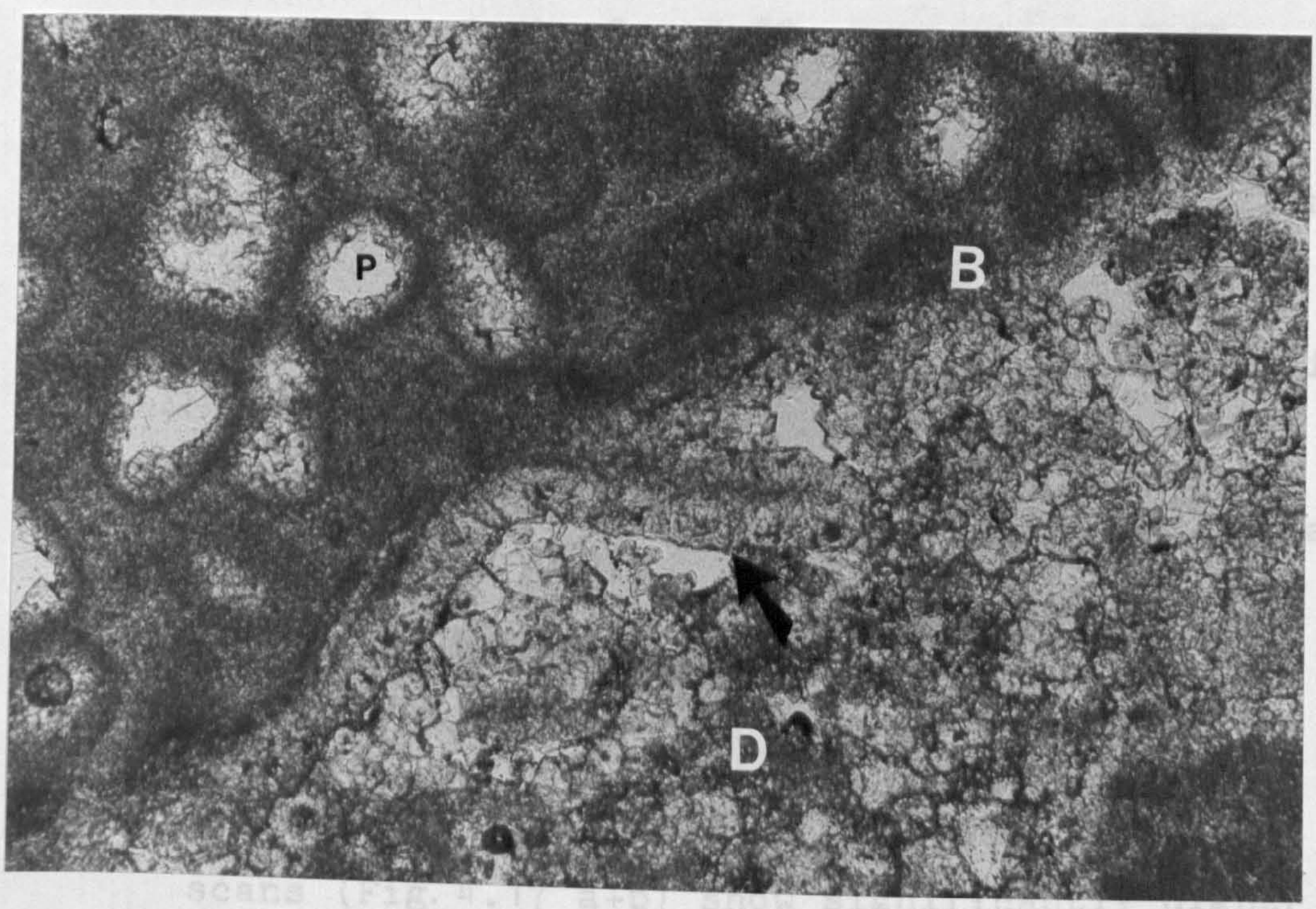
P
B
D

Euhedral terminations indicate cement growth into voids. The crystals contain few inclusions. The absence of inclusions together with the crystal form implies this is a dolomite cement and not replacement of a $CaCO_3$ precursor. Both clasts and micrite envelopes (Figs. 4.16 a+b) were dolomitised prior to cement growth. Cement growth precedes some degree of mechanical compaction (Kaldi, 1980a) and tectonic fracturing. A later dolomite partially fills pores after formation of the fringing cements (Kaldi, 1980a). There is no evidence of concurrent evaporite formation.

Analyses (Table 4.6) and electron microprobe scans (Fig. 4.17 a+b) show significantly higher iron contents in the cements than in the enclosed clasts. Iron exists in carbonate lattices as Fe^{2+}. Fe^{2+} (soluble) is rapidly oxidised to Fe^{3+} (insoluble) in normal marine waters (Fig. 4.21). The cement crystals must thus have grown in anoxic marine pore waters, or pore waters with a meteoric influence. Both these waters are capable of leaching less stable carbonate phases; ooid centres are often selectively leached by meteoric-derived fluids early in the sediment history (Conley, 1977; Moore, 1981). Experiments have shown similar leaching by non-marine fluids in conditions comparable to burial depths up to 300m (Donath et al., 1980). Euhedral cement

TABLE 4.6

Electron microprobe analyses of dolomite fringing cements and associated dolomites, New Edlington, S. Yorkshire, (SK 532986).

Mole%		$MgCO_3$	$CaCO_3$	$FeCO_3$	$MaCo_3$	$CaCO_3/MgCO_3$
dolomite micrite envelope	1	47.89	49.88	0.09	0.17	0.96
dolomite between ooids	2	46.35	50.10	0.11	0.07	0.93
original dolomite	3	42.34	48.95	0.09	0.10	0.86
	4	46.40	48.86	0.00	0.10	0.95
	5	47.05	48.31	0.19	0.10	0.97
fringing cement	6	48.03	48.72	0.14	0.04	0.99
	7	43.03	43.64	0.58	0.17	0.99
	8	47.21	49.26	0.70	0.13	0.96
later dolomite	9	48.03	48.98	0.20	0.15	0.98
calcite in ooid centres	a	1.56	89.84	0.00	0.16	
	b	1.42	89.58	0.13	0.00	

Figure 4.17 a Diagram of points analysed in Table 4-6.

b Semiquantitative scan across peloid and fringing cement.

a

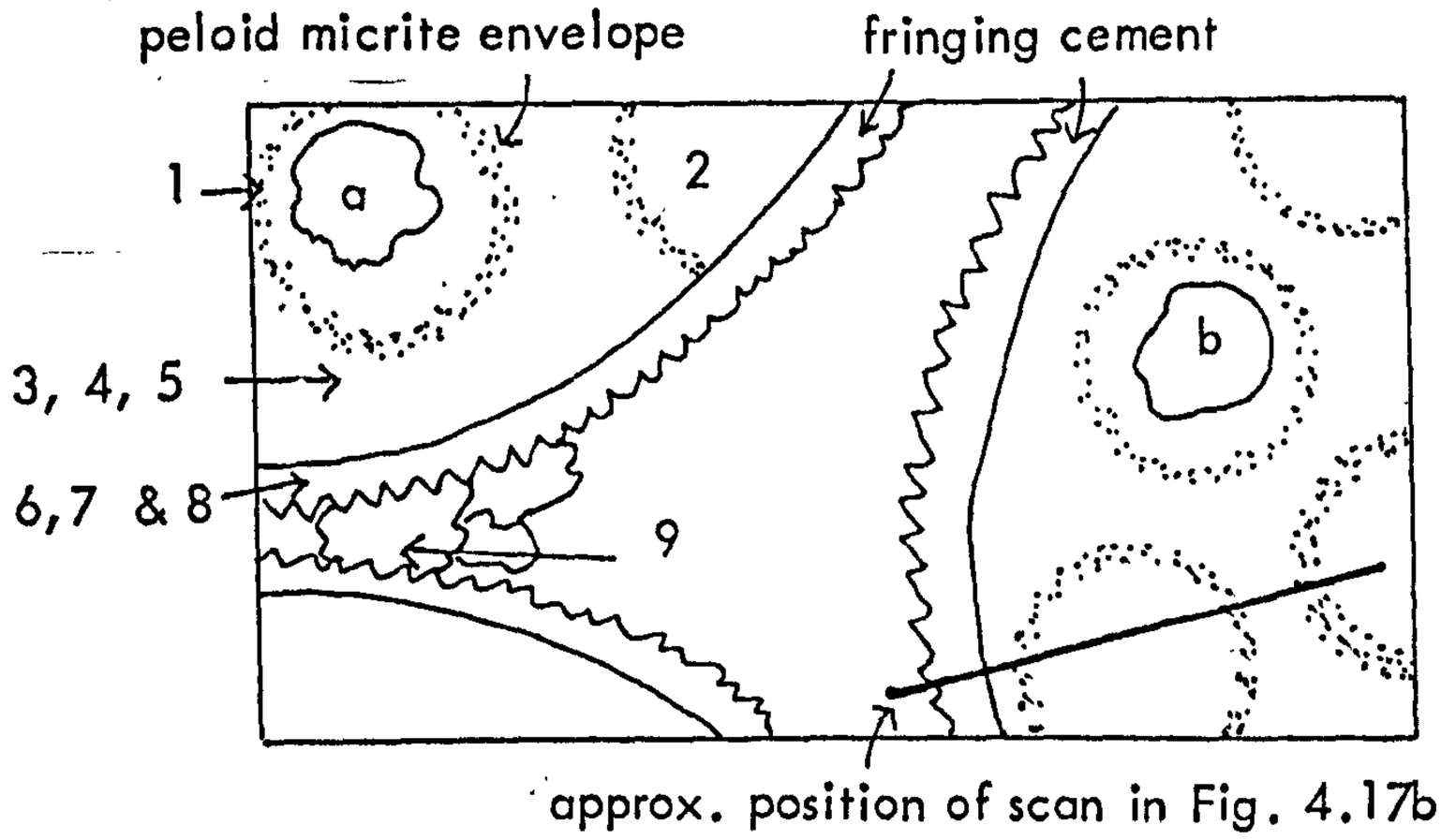

approx. position of scan in Fig. 4.17b

b

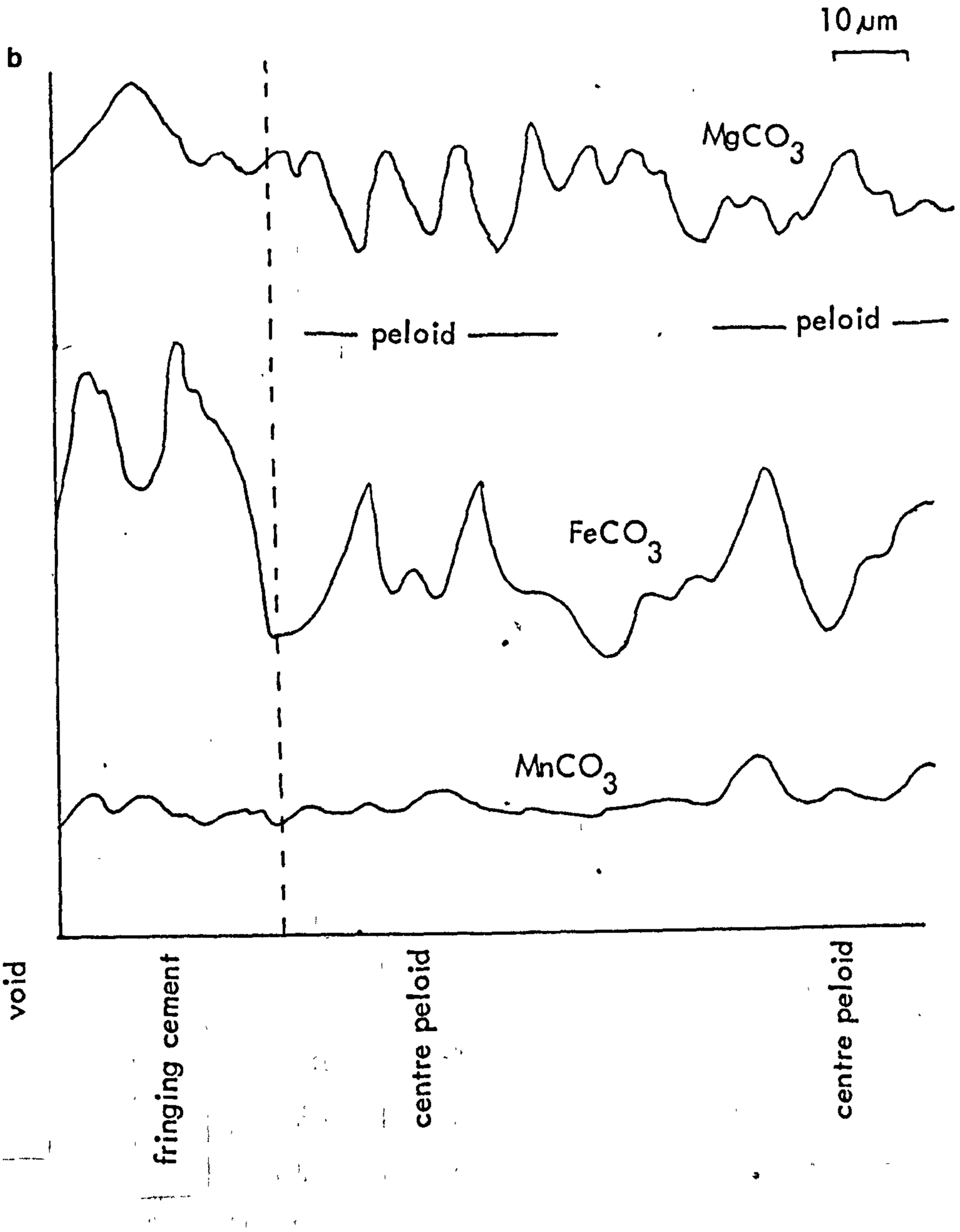

crystals and Mg^{2+}/Ca^{2+} ratios approaching unity (Table 4.6) imply growth under stable conditions. As the containing beds are supratidal fenestral grainstones, ooid shoal crusts and breccias, fluids forming these cements may have had some meteoric influx. Later, more anhedral pore filling dolomites may have formed when meteoric input declined.

Similar, although more widespread, dolomite fringing cements were described by Schmidt (1965); fringes ranged between 4μm and 250μm and also predated compaction and tectonic fractures. Schmidt surmised that these cements formed during, or immediately after, his early dolomitisation event, equivalent to the eogenetic dolomitisation here. Fringing cements in the Cadeby Formation probably formed during eogenetic dolomitisation; the sequence of cement development is shown in Figure 4.18.

4.2.9 Coarse sucrose dolomites

The siliciclastic packstones and grainstones in the south of the area (3.2.6 and 3.4.3) are now coarse sucrose dolomites (Figs. 4-19 a+b). Individual dolomite crystals contain silt-sized siliciclastic clasts, some of which may have originated as wind-blown continental dust (Smith, pers. comm., 1981) and later formed ooid cores. Rounded peloid ghosts (Fig 4.19c) occur in crystal centres but not in the outer rims.

Figure 4.18 Sequence of development of fringing cements.

Breccia	Peloid Grainstones
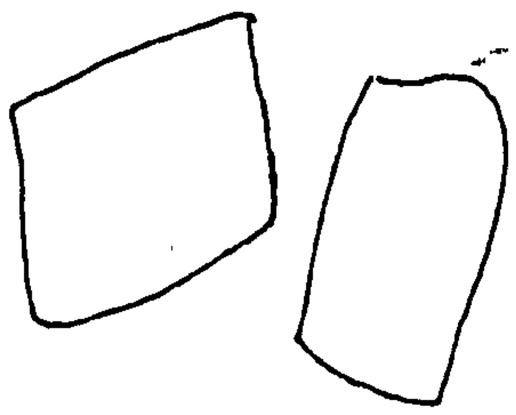	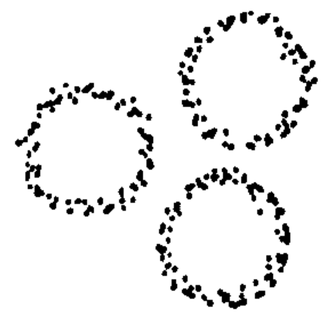
1. Eogenetic dolomitisation of clasts	1. Eogenetic dolomitisation of peloid micrite envelopes
2. zLeaching of un-dolomitised carbonate phases in clasts and peloid centres. Associated spalling of some clast margins.	
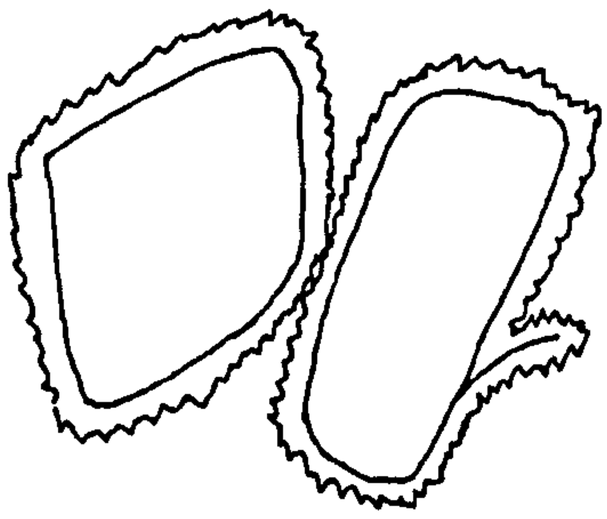	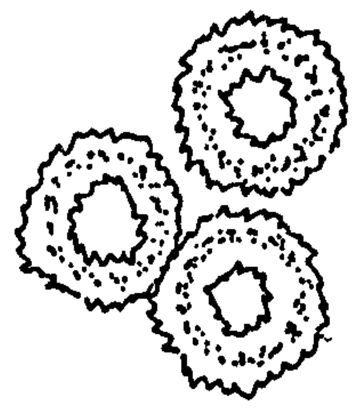
3. Growth of dolomite fringing cements	
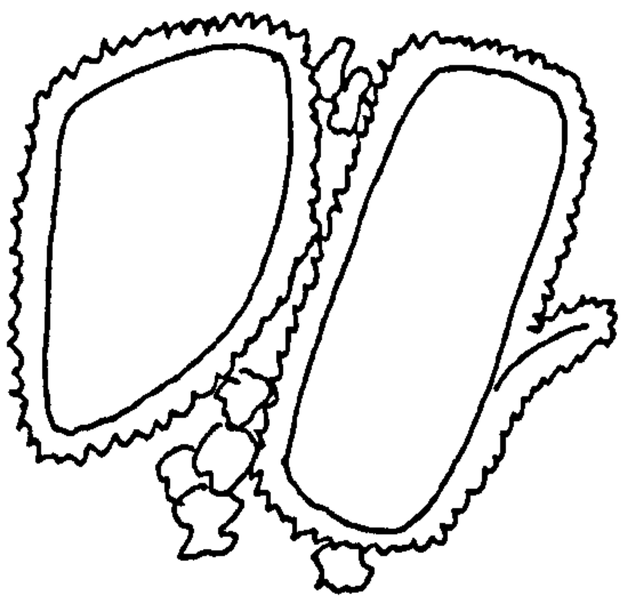	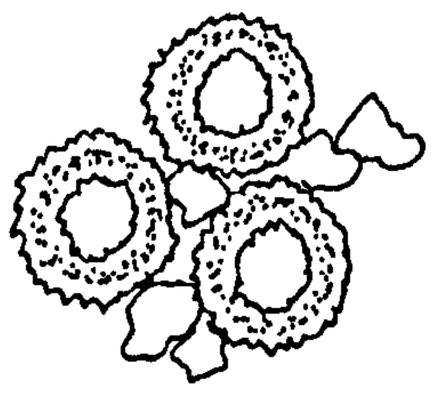
4, Later patchy dolomite growth in voids.	
Porosity may or may not be later occluded by calcite	

Figure 4.19 Sucrose dolomites, Kirby-in-Ashfield (SK 570561).

a Zoned dolomite crystals in calcite cement. Crystals contain silt to fine sand sized siliciclastics, also present in cement. Outer zones now comprise opaque-iron oxides as inclusions in cement. A few dolomite crystals are ferroan (arrowed) and have no iron oxide surround. Quartz siliciclastics are corroded by calcite but not by dolomite. Calcite stained with Alizarin Reds. Field of view is 2.75mm.

b Area of ferroan dolomites from same stained thin section. Ferroan dolomites have no iron oxide rims or inclusion; areas of ferroan dolomites are poor in siliciclastics and may contain large areas of calcite cement (c). Peloid ghosts (arrowed) in centre of large crystal. No zones visible with cathodoluminescence. Field of view is 2.75mm.

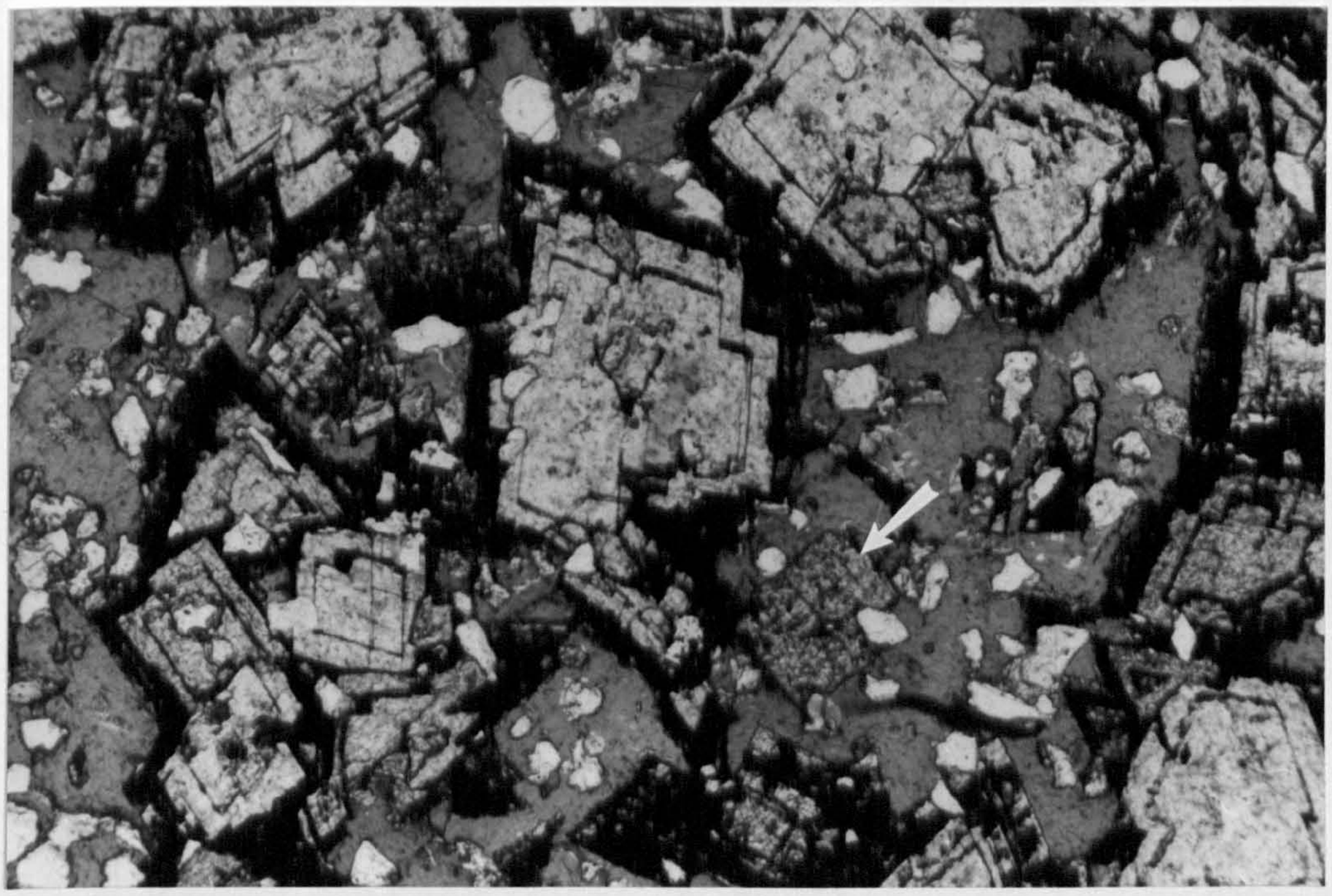


C

Figure 4.19 c Close up of ferroan dolomite crystal. Peloid ghosts (arrowed) in crystal centre are indistinct. Centres of some peloids are now calcite (c) replacing dolomite. Opaque mineral is galena. Field of view is 0.7mm.

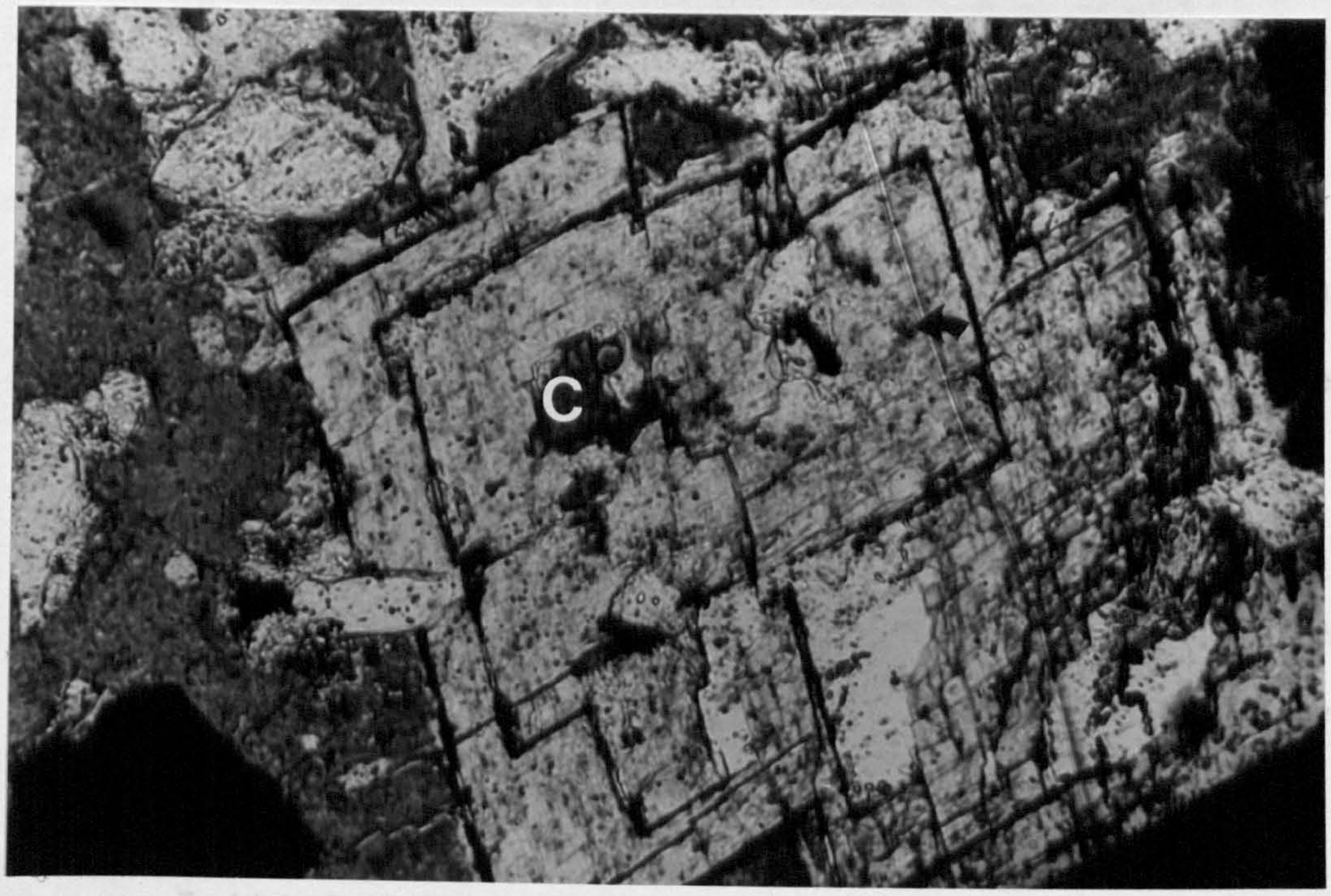
C

Opaque iron oxide zones occur in some crystal rims or extend outside the remnant crystals.

Element contents of the crystals differ considerably. Where there is no iron oxide formation (e.g. Fig.4.19b) iron concentrations show small variation (Fig. 4.20 a) with crystal size 250-300μm. Where iron oxides occur (e.g. Fig.4.19a) crystals are usually larger (~500μm+) and elements show more variation (Fig. 4.20 b; Table 4.7). Whole rock XRF analyses confirm the high siliciclastic content (Appendix 5, specimens 168, 172 and 177) with higher total iron and manganese than the ooid grainstones.

Initial dolomitisation with preservation of peloid ghosts probably took place during eogenetic dolomitisation; continued dolomite diagenesis took place within a different diagenetic environment. There is no evidence to support a separate development of the zoned/unzoned crystals. Later alteration (Chapter 5) produced the opaque/non opaque zones. The crystal centres may typify the original dolomite composition (Table 4.7); these are more ferroan than eogenetic dolomites (e.g. Table 4.5, analyses 1-5). The high iron and manganese contents reflect the influence of restricted meteoric fluids (Fig. 4.21). Sucrose dolomites occur near the contemporary shoreline where there is a high siliciclastic content, no overlying evaporites (Edwards, 1951) and little

TABLE 4.7

Electron microprobe analysis of zoned dolomite, Kirby in Ashfield, Nottinghamshire (SK 570561)

		$MgCO_3$	$CaCO_3$	$FeCO_3$	$MnCO_3$
1	edge of rhomb	6.58	88.60	3.35	0.82
2	near opaque zone	35.33	56.70	3.60	0.63
3	inside opaque zone	40.88	53.17	2.95	0.61
4	near ghost ooid margin	41.40	52.66	2.94	0.70
5	ghost ooid margin	41.74	52.64	2.85	0.65
6	centre ghost ooid	41.55	53.35	2.70	0.65
7	outside semi-opaque near centre	21.94	76.55	0.69	0.16
8	semi-opaque near centre	33.61	60.83	0.96	--
9	centre of remnant rhomb	35.39	54.76	2.12	0.85

Figure 4.20 a Semi-quantitative scan showing variations in iron and magnesium sucrose dolomite with no ferric oxides (as in Fig 4-19 b).

b Semi-quantitative scan showing variations in iron and magnesium across larger zoned dolomite crystal with opaque zone.

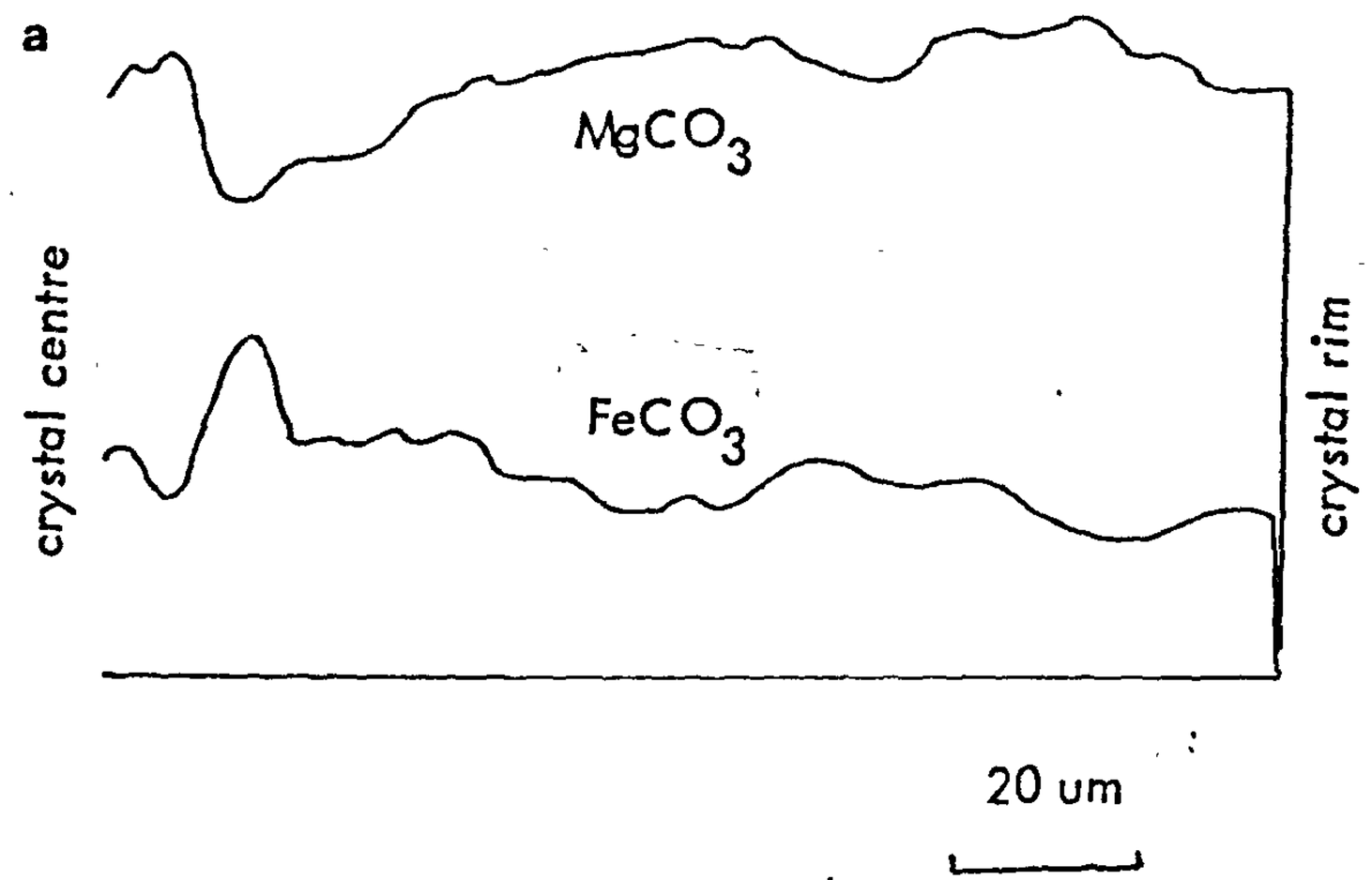
a
$MgCO_3$
$FeCO_3$
crystal centre
crystal rim
20 um

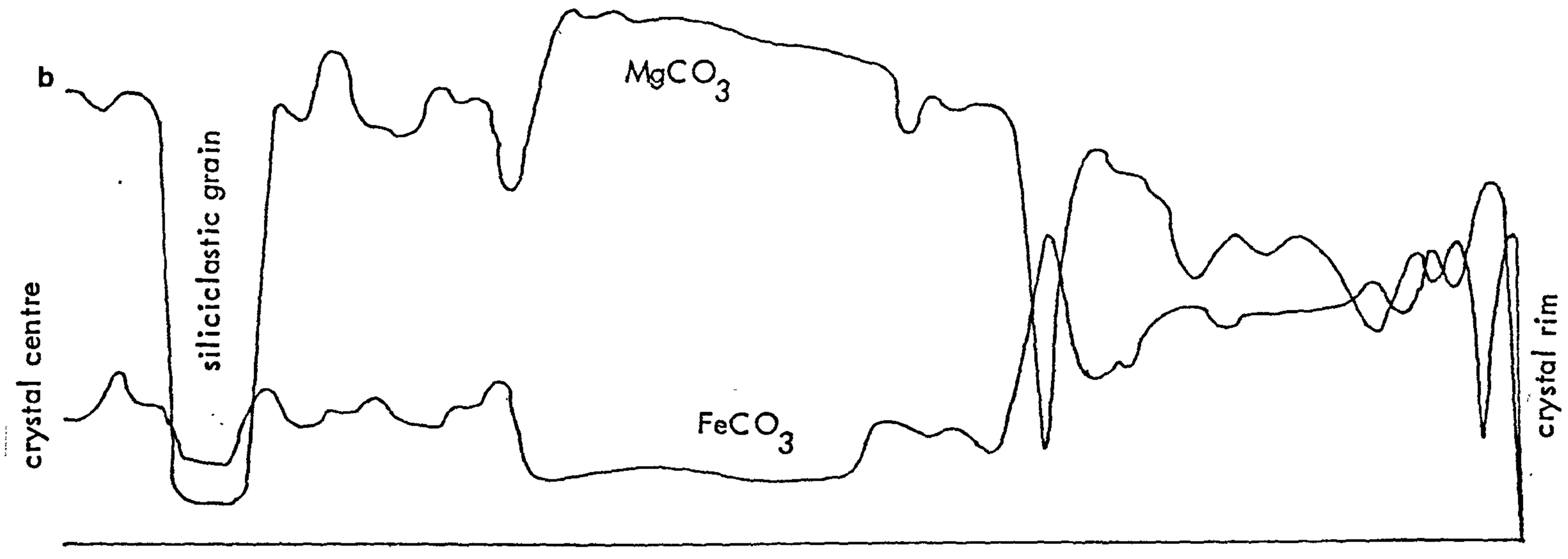
b
$MgCO_3$
$FeCO_3$
siliciclastic grain
crystal centre
crystal rim

c Plot of point analyses across large zoned dolomite crystal (from Table 4.7).

c

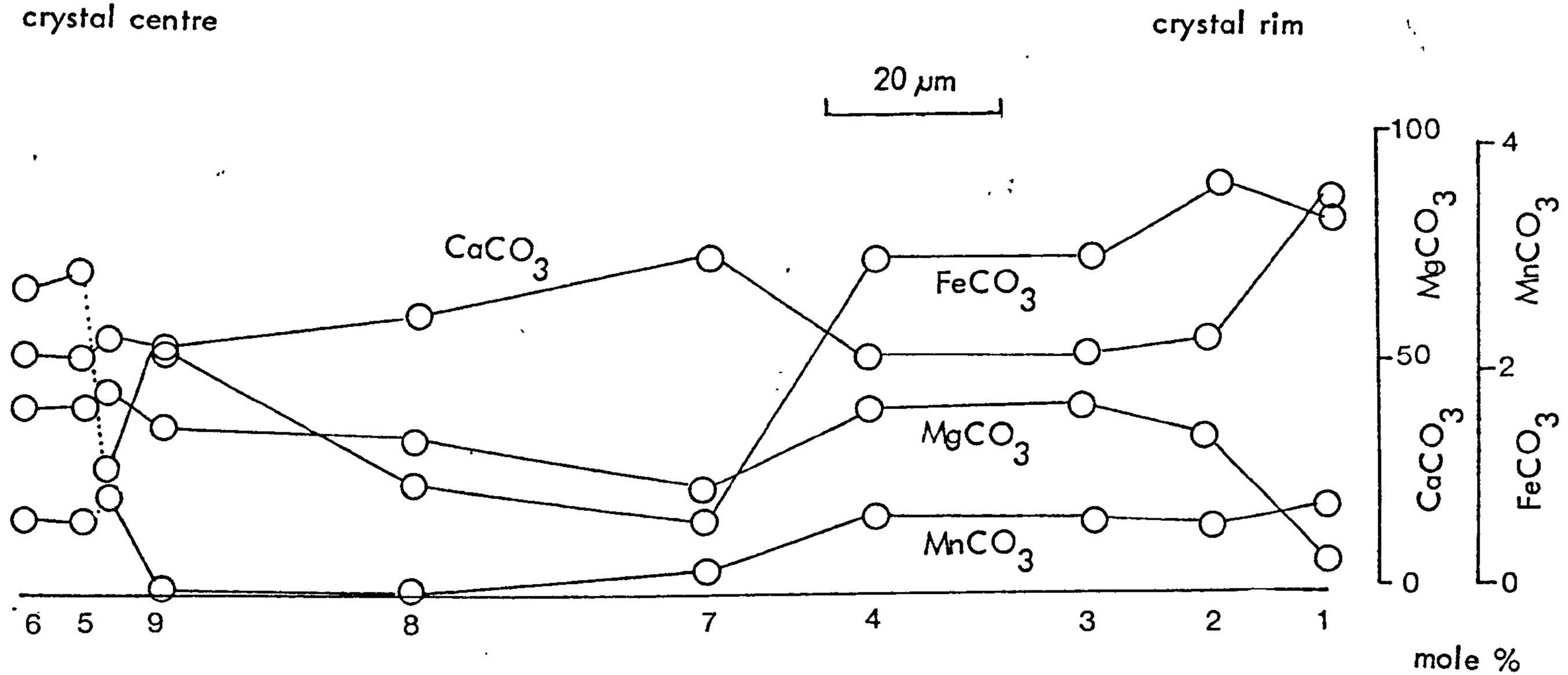
crystal centre
crystal rim
20 μm
CaCO3
FeCO3
MgCO3
MnCO3
100
50
0
4
2
0
6 5 9 8 7 4 3 2 1
mole %

Figure 4.21 Eh/pH diagram of natural waters carbonate stability fields and field of Fe^{2+} (aq).

..... $FeCO_3$ field

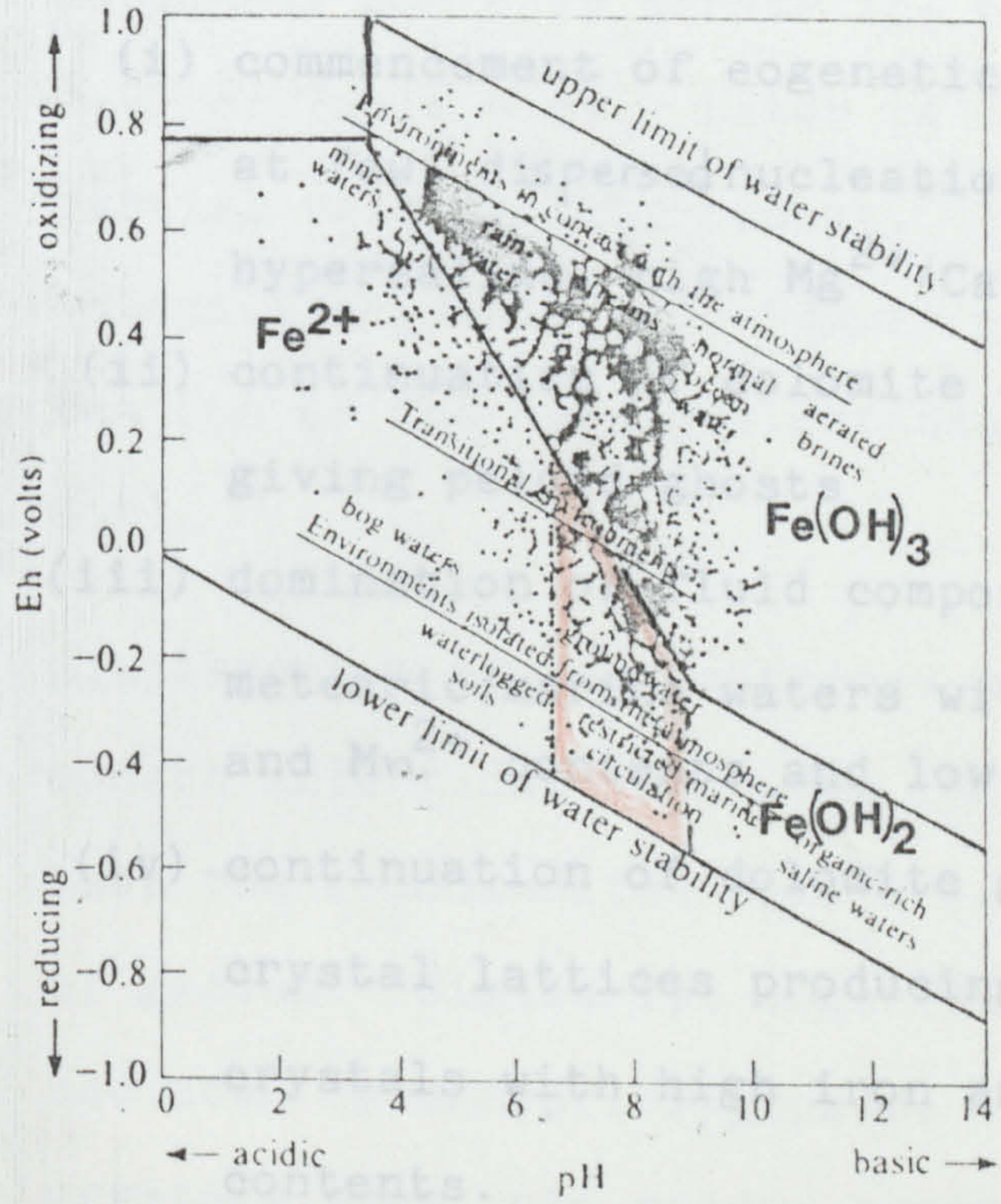
1.0
0.8
0.6
0.4
0.2
0.0
−0.2
−0.4
−0.6
−0.8
−1.0
Eh (volts)
oxidizing
reducing
0
2
4
6
8
10
12
14
pH
acidic
basic
upper limit of water stability
lower limit of water stability
Fe2+
Fe(OH)3
Fe(OH)2
mine waters
rain water
normal aerated brines
bog waters
waterlogged soils
restricted circulation
organic-rich saline waters

or no evidence of replacive evaporites. Their mode of formation can be detailed as follows:-

(i) commencement of eogenetic dolomitisation at few, dispersed nucleation sites in hypersaline, high Mg^{2+}/Ca^{2+} brines.

(ii) continuation of dolomite crystal growth giving peloid ghosts

(iii) domination of fluid composition by mixed meteoric/marine waters with higher Fe^{2+} and Mn^{2+} contents and low Mg^{2+}/Ca^{2+} ratios.

(iv) continuation of dolomite growth on original crystal lattices producing large (500µm+) crystals with high iron and manganese contents.

High iron and manganese contents in the dolomitising fluids may have been further enriched by early diagenesis of the overlying red beds (Walker, 1976). Patchy higher siliciclastic contents formed zones of higher porosity and permeability, promoting formation of larger crystals in those areas (Figs. 4-19 a+b). Similar porosity controls may partially be responsible for zones of dolomite alteration in these sucrose dolomites (Chapter 5).

4.5.10 Limpid dolomite overgrowths

Limpid dolomite overgrowths are found at a few locations. In patterned carbonates, limpid dolomites overgrow dolomicrites (Figs. 3-17 b,

4.22 a+b). Although apparently zoned (Fig. 4.23 b) there is little difference in iron and manganese contents across the crystal (Fig. 4.22 c; Table 4.9). Later calcite forms a partial void filling cement. Rare limpid dolomite crystals (100-500μm) occur in vugs at the top of the ooid grainstones (Fig. 4.23; Table 4.8).

Similarities of the patterned carbonates to some modern intertidal laminates (32.13) indicate that the dolomicrites were originally surrounded by gypsum. Similarly, vugs (Fig. 4.23) were occluded by anhydrite/gypsum. Euhedral limpid crystals grew into voids; evaporite dissolution must have occurred before limpid dolomite growth. Low iron and manganese contents (Table 4.7) show no relation to the coarse sucrose dolomites (4.5.9). Large clear crystals indicate slow growth with few nucleation sites.

Formation of these dolomite crystals is the last episode of dolomitisation apparent in the Cadeby Formation; it post dates earlier eogenetic dolomitisation and dissolution of evaporites. It is thus much later. The reasons for the occurrence of these crystals and the origin of the precipitating solutions is unknown.

TABLE 4.8

Electron microprobe analysis of dolomite overgrowths, Wistow Wood borehole, (SE 567356)

		$MgCO_3$	$CaCO_3$	$FeCO_3$	$MnCo_3$
1	centre dolomicrite	46.08	50.19	2.08	0.15
2	margin dolomicrite	50.70	48.45	0.44	0.07
3	inner margin limpid dolomite	47.83	51.15	0.38	0.11
4	centre limpid dolomite	52.71	50.86	0.33	0.04
5	outer margin limpid dolomite	46.63	49.30	3.27	0.20

see also Fig. 4.22c

Electron microprobe analyses of dolomite overgrowths, New Edlington

6	ooid grainstone	46.40	48.86	0.00	0.10
7	margin ooid grainstone	42.34	48.95	0.09	0.10
8	inner margin limpid dolomite	47.05	48.31	0.19	0.10
9	centre margin limpid dolomite	47.21	49.26	0.70	0.13

see also Fig. 4.23

Figure 4.22 a , b + c Limpid dolomite overgrowths on dolomicrite, Wistow Wood (SE 567356).

a Dolomicrites have many inclusions; limpid dolomite in practically inclusion-free. Opaque mineral is marcasite which grew after formation of limpid dolomite overgrowths. Later calcite pore cement. Field of view is 1.45mm.

b Cathodoluminescence view of same area, showing zoning in limpid dolomite overgrowths and pore-filling calcite. Field of view is 1.45mm.

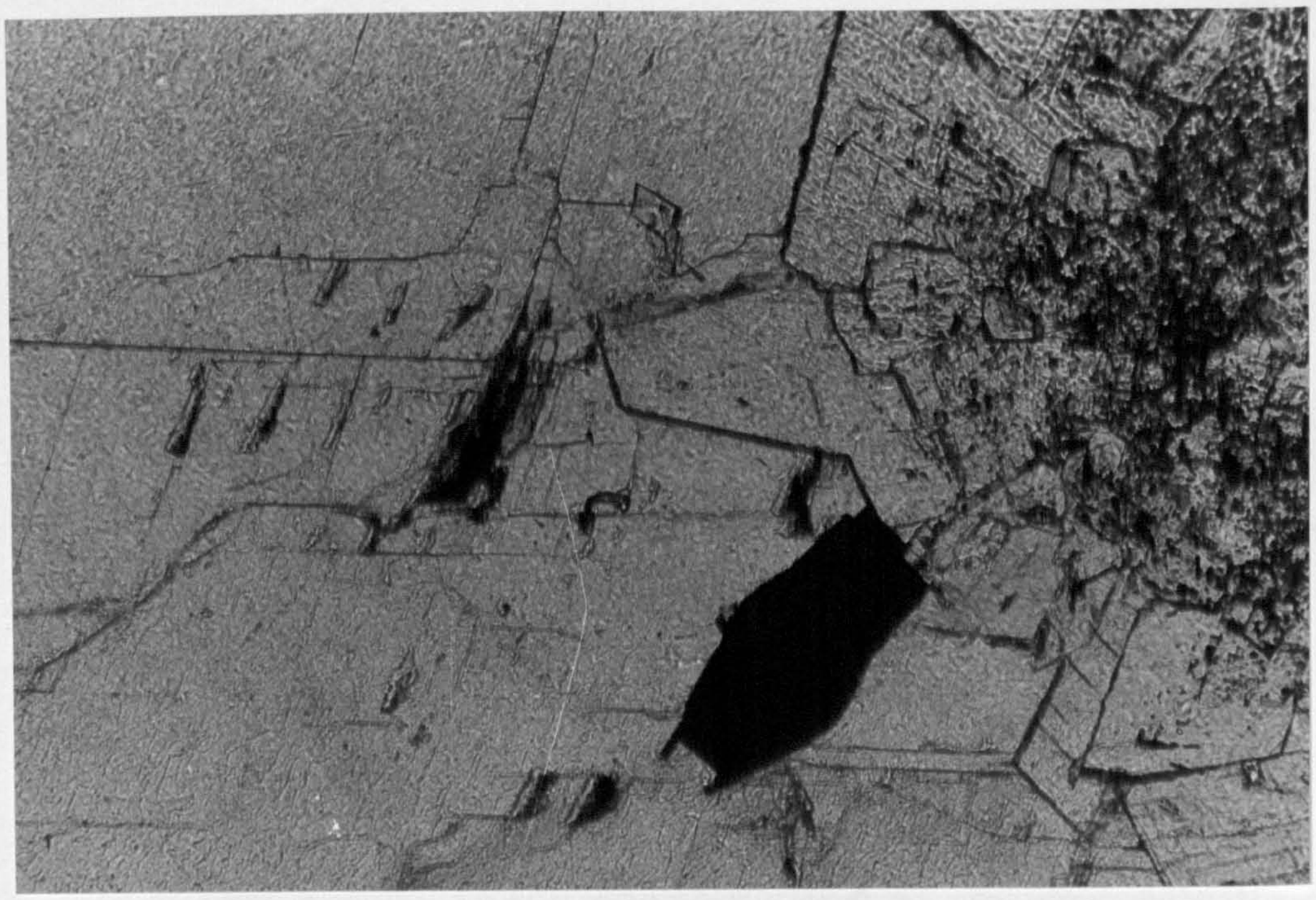

Figure 4.22 c Semi-quantitative scan across limpid dolomite overgrowths (from Table 4.8).

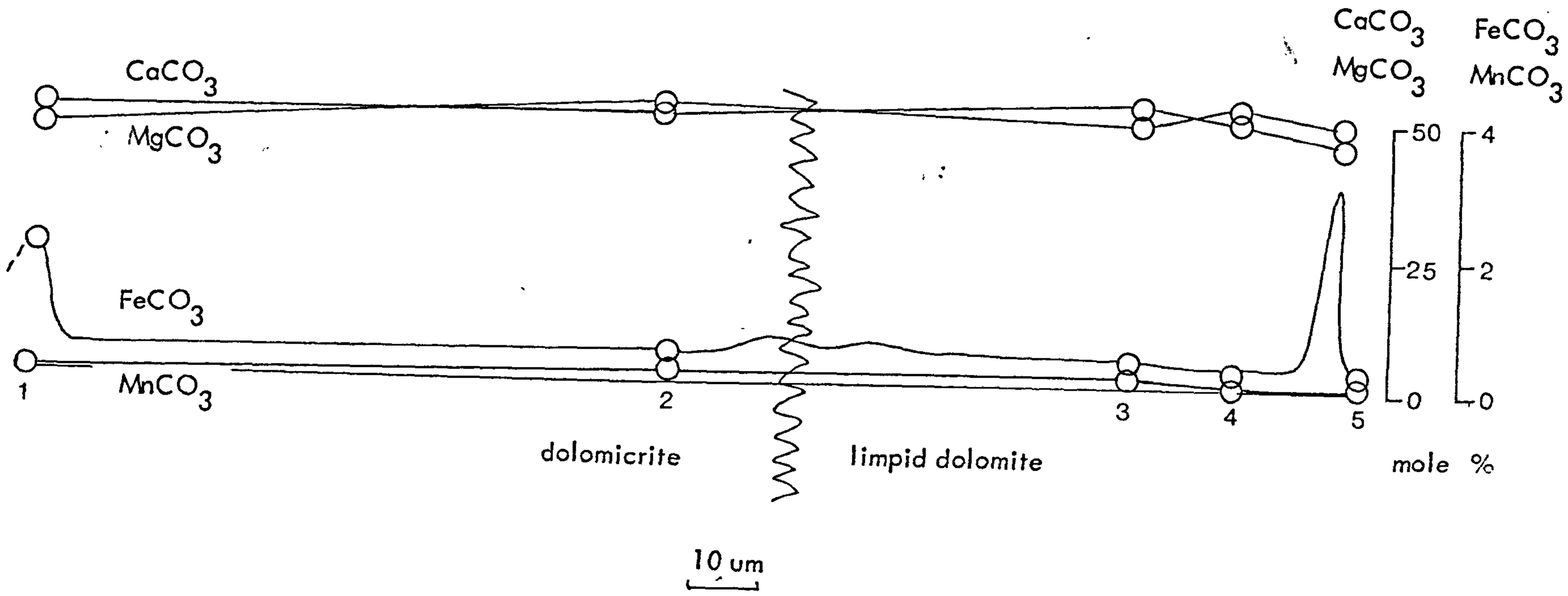
CaCO3
MgCO3
FeCO3
MnCO3
CaCO3
MgCO3
FeCO3
MnCO3
50
25
0
4
2
0
1
2
3
4
5
dolomicrite
limpid dolomite
mole %
10 um

Figure 4.23 Small limpid dolomite crystals partially occluding vuggy porosity, New Edlington Brick Works Quarry (SK 532986). Limpid crystals are euhedral (arrowed). Vug filled by later calcite spar. Field of view is 0.9mm.

4.6 Summary of dolomitisation in the Cadeby Formation

Dolomitisation in the Cadeby Formation continued throughout the diagenetic history from penecontemporaneous, through eogenetic to mesogenetic diagenesis. The major dolomitisation event was eogenetic, due to probable large scale seepage reflux. Other dolomites were formed in associated with penecontemporaneous evaporites and by mixed water fluids. A summary of the different dolomitisation episodes, their major characteristics and their origin is given in Table 4.9. Their relation to other events in the diagenetic history is discussed in Chapter 6.

TABLE 4.9

SUMMARY OF DOLOMITISATION CHARACTERISTICS AND MODELS IN THE CADEBY FORMATION

TYPE	CHARACTERISTICS	CARBONATE PRECURSOR	FLUID CHARACTERISTICS	MODEL	DEPENDENCE ON ORIGINAL FACIES
Perecontemp-oraneous (4.5.2 + 4.5.3)	small crystal size texture destroying intimately associated with evaporites	aragonite + HMC	high Mg^{2+}/Ca^{2+} hypersaline/ continental brine mixing	modified sabkha periodic flooding/ exposure in restricted lagoons	lagoon facies only
Eogenetic - clastic dependent (4.5.4)	small crystal size high clastic organic content texture destroying	aragonite + HMC	high Mg^{2+}/Ca^{2+}	Distal reflux	clastic-rich facies at base of Lower Member only
Eogenetic (4.5.5, 4.5.6 + 4.5.7)	variable crystal size mostly texture destroying pervasive low Fe^{2+} + Mn^{2+} Main dolomitis-ation event	aragonite > HMC>>LMC	high Mg^{2+}/Ca^{2+}	Large scale seepage reflux	Largely facies independent
Fringing cements (4.5.8)	isopachous small limpid dolomites growth into void low-moderate Fe^{2+} + Mn^{2+} after or during eogenetic dolomitisation	----	High Mg^{2+}/Ca^{2+} brine with meteoric influence	modified seepage reflux	Areas near or having subaerial exposure
Sucrose dolomite (4.5.9)	Large euhedral crystals High Fe^{2+} + Mn^{2+} associated with siliciclastics	aragonite > HMC>>LMC but dissolution during dolomit-isation	initial high Mg^{2+}/Ca^{2+} but continued growth in low Mg^{2+}/Ca^{2+}	seepage reflux but later mixed water fluid modified by red bed diagenesis	near shore siliciclastic facies - no overlying evaporites
limpid dolomites (4.5.10)	rare large euhedral clear crystals post evaporite dissolution low Fe^{2+} + Mn^{2+}	----	?hypersaline high Mg^{2+}/Ca^{2+}	?	?

CHAPTER 5

Replacement of dolomite

5.1 Introduction and definitions

Replacement of pre-existing dolomite crystals involves chemical changes within the crystals and crystal modification and leaching by pore fluids from different sources. The result is often, although not always, a more porous rock. "Dedolomitisation", the replacement of dolomite by calcite is often only one stage in an alteration/replacement sequence and may mask earlier alteration characteristics. The aim of this chapter is to demonstrate the replacement sequences occurring in dolomites of the Cadeby Formation, discuss the role of "dedolomitisation" in this alteration and hence demonstrate the varying compositions of pore fluids.

Several authors have noted clear (limpid) dolomite rims surrounding more cloudy, inclusion-rich crystal centres (e.g. Khvorava, 1958; Fritz and Jackson, 1972; Zenger, 1972b; Chillingar et al., 1979; Sibley, 1980). Zenger (in Chillingar et al., 1979) comments that "the rims may be much younger than the dolomite cores" and that Khvorava's dolomites were 'altered during epigenesis' (= mesogenesis) but does not discuss the alteration in detail. Land et al., (1975, p 1605) comment on the re-equilibration of Eocene dolomites by fresh water diagenesis but do not relate this to crystal morphology. I can find no detailed published discussion of formation of the limpid dolomite margins. In the Cadeby Formation, the formation of such margins

is associated with the development of ferroan dolomites (5.2.1). This takes place before "dedolomitisation". Alteration of dolomites thus comprises (i) formation of ferroan dolomites and partial remobilisation of pre-existing dolomite crystals and (ii) "dedolomitisation", with or without subsequent leaching. Other evidence shows different types of "dedolomitisation" within the formation.

The term "dedolomitisation" was first used by Von Morlot (1847) and included all replacement of dolomite by calcite using the general equation

$$Ca\ Mg\ (CO_3)_2 + Ca^{2+}(aq) \rightarrow 2CaCO_3 + Mg^{3+}(aq) \quad (5\text{-}1)$$

In a summary of recent research on "dedolomitisation" Frank (1981) gives two major causes of "dedolomitisation":

(i) alteration of ferroan dolomite by oxygenated meteoric fluids and

(ii) reaction of dolomite with calcium sulphate-rich solutions.

Several authors (e.g. Smit and Swett, 1969; Kinsman, 1981) argue that the term "dedolomitisation" should be abandoned in favour of "calcitisation of dolomite". "Dedolomitisation" is, however, well entrenched in the literature; calcitisation includes the replacement of other minerals than dolomite (4.5.2 + 4.5.3). In this thesis calcitisation and dedolomitisation are defined as follows:-

CALCITISATION : replacement of a mineral by calcite. This may be direct crystal-for-crystal replacement of evaporites (4.5.2 + 4.5.3) or replacement forming a mosaic texture (5.4.1). Minerals replaced are calcium sulphate minerals and some dolomite in this formation; in other formations calcite may replace quartz or chert.

DEDOLOMITISATION : replacement of dolomite by calcite where not associated with concurrent evaporite mineral replacement.

The enhanced susceptibility of ferroan dolomites to dedolomitisation was noted by Katz (1971) and Frank (1981). Evidence below (5.2.4) shows fluids causing dedolomitisation are not necessarily meteoric; they are, however, oxic. Thus Frank's causes of dolomitisation may be re-defined:-

(i) alteration of ferroan dolomite by oxic fluids

(ii) dolomite-calcite dissolution-reprecipitation/ replacement by calcium sulphate-rich fluids.

Cause (ii) does not necessitate former ferroan dolomite.

The replacement of dolomite by calcite is summarised in Figure 5.1. This chapter includes evidence of both types of "dedolomite" and of gypsum/dolomite calcitisation. Direct crystal-for-crystal calcitisation is covered in 4.5.2, 4.5.3 and Harwood (1980).

Figure 5.1 Summary of replacement of dolomite by calcite.

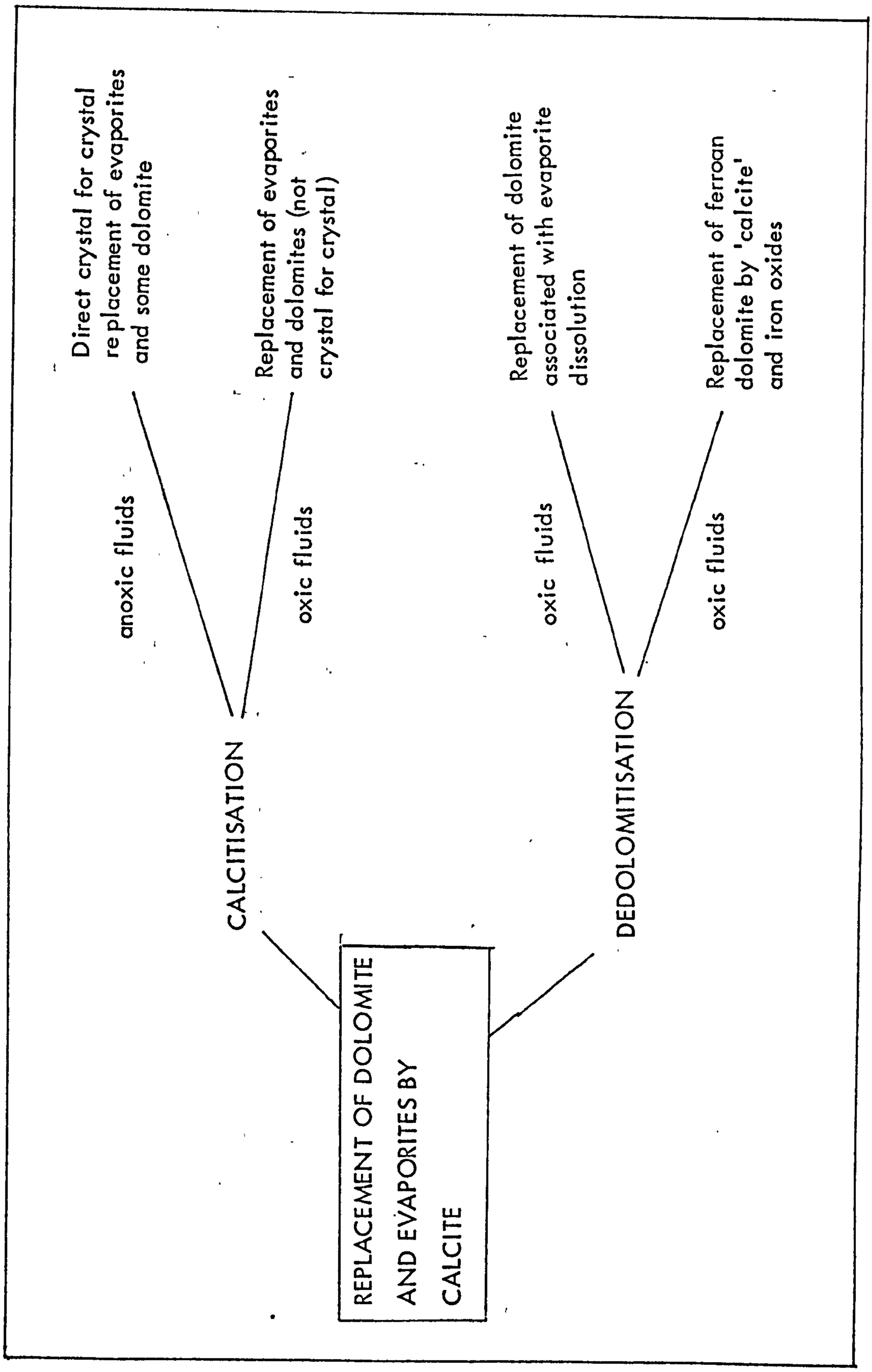
REPLACEMENT OF DOLOMITE AND EVAPORITES BY CALCITE
CALCITISATION
anoxic fluids
Direct crystal for crystal replacement of evaporites and some dolomite
oxic fluids
Replacement of evaporites and dolomites (not crystal for crystal)
DEDOLOMITISATION
oxic fluids
Replacement of dolomite associated with evaporite dissolution
oxic fluids
Replacement of ferroan dolomite by 'calcite' and iron oxides

5.2 Dolomite alteration

5.2.1 Anhedral to euhedral crystals

Much of the Cadeby Formation, especially the grainstone and packstone facies (3.2.4, 3.2.7 and 3.4.2) comprises anhedral dolomite crystals of various sizes (Figs. 4.13 a, b + d). In some areas crystals are subhedral and, in others, predominantly euhedral (Figs. 4.19, a + b; 4.5.9). The change in crystal shape may occur on a regional scale (3.2.6, 3.4.3 and 4.5.9) or in narrower areas, down to a metre of centimetre scale. Rarely this transition is visible across one thin section, or a series of adjoining thin sections. Ferric oxides often mask the alteration sequence.

The change from anhedral calcium dolomites, with negligible iron content, to euhedral/subhedral ferroan or dedolomitised crystals can be demonstrated in several localities of the Cadeby Formation from broad areas to narrow margins adjoining linear voids, including sheet cracks. No alteration of this style has been noticed adjacent to tectonic fractures.

Traversing such a transition area, alteration commences at crystal triple junctions and/or crystal centres. Ferric oxides and "calcite" at triple junctions are shown in Figure 5.2 a+b; cloudy centres and triple junction alteration

in Figure 5.3 a+b. The "calcite" associated with the ferric oxides is ferroan and magnesian; it is termed FM calcite in this chapter to distinguish it from later pore filling non ferroan calcites. Further across the transition area ferric oxide and FM calcite proportions increase and crystals tend towards subhedral from (Fig. 5-2 a+b, Fig. 5.3 c+d). In the subhedral crystals an outer limpid zone with few inclusions contrasts with an inclusion-rich centre (Fig. 5.3 c+d). Similar crystals were described as 'grumelease' texture by Evamy (1967, Fig.6). Both the volume of ferric oxides and the total iron percentage are higher in these opaque areas (Table 5-1, analyses 1-10). The ferric oxides occur in small aggregates (<10μm) similar to the stellate aggregates, or "hedgerows", of Frank (1981). The FM calcite visibly corrodes the surrounding dolomite (Fig. 5.2 b); its composition may approach ankerite. Analyses (Table 5-2, analyses 3, 11) include patches of ferric oxide and good totals are difficult to achieve because of this (see Appendix 10).

Prolonged alteration results in euhedral or subhedral crystals with opaque centres (Figs. 5.2 a and 5.3 d). Microprobe scans and analyses (Fig. 5.4 a-c; Tables 5-1 and 5-2) show large total iron variations; manganese contents show less, but parallel, variation. FM calcite and ferric oxides occur in the centre, poorly

Figure 5.2 Dolomite alteration and ferroan dedolomitisation, Bedale Quarry, Well (SE 257812).

a + b Commencement of alteration at triple crystal junctions (arrow 1), now opaque iron oxides. Further into alteration zone crystals have more subhedral form and become zoned (arrow 2). Anhedral crystals are not zone; sub- and eu-hedral crystals show inner moderately luminescing zone, a dark zone, a brighter zone with outer dark zone along crystal boundary (arrow 2). Crystal centres in subhedral dolomites are opaque in (a) but (b) shows calcite corroding dolomite surrounds
Field of view is 2.25mm.

a : transmitted light

b : cathodoluminescence

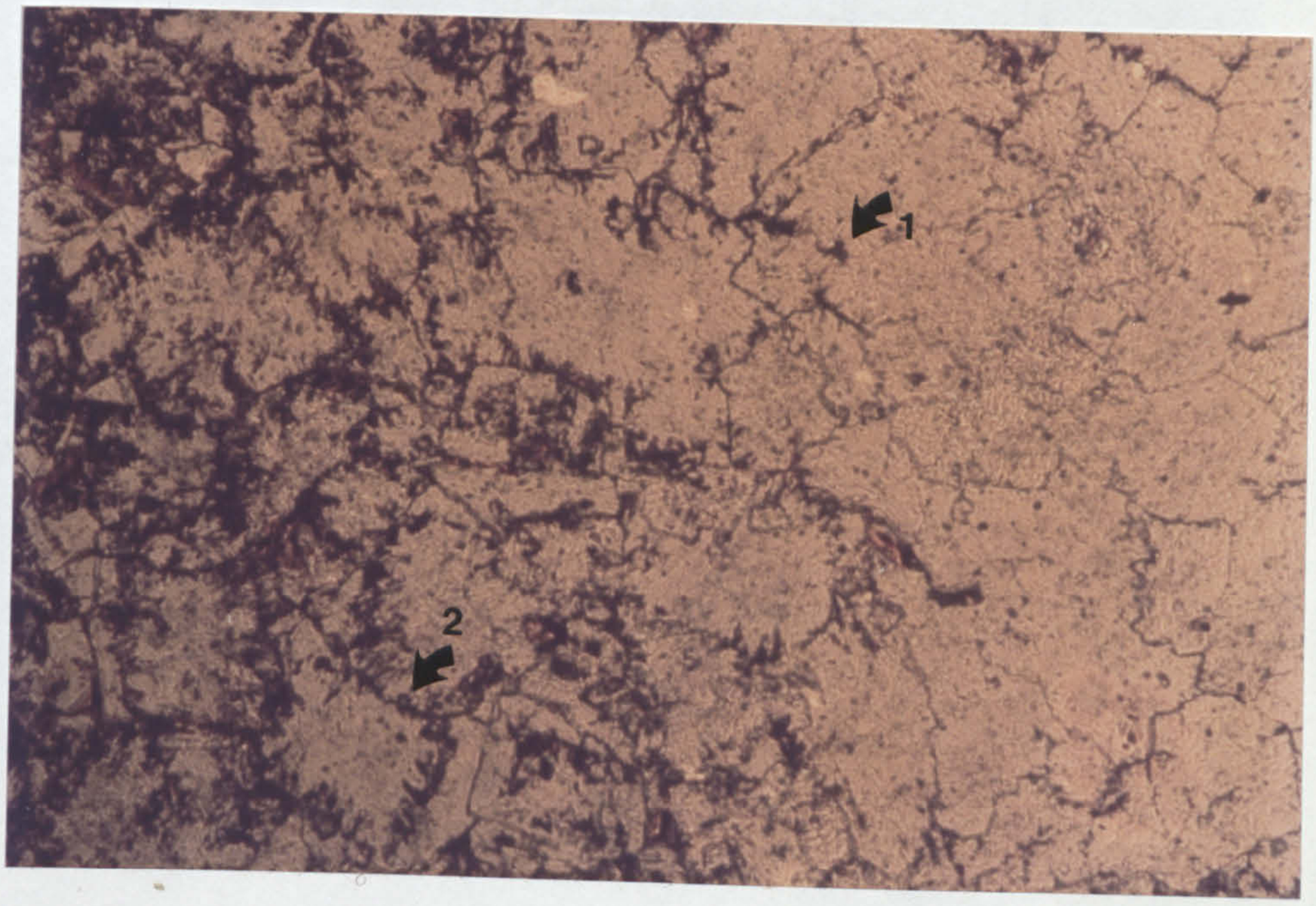
1
2

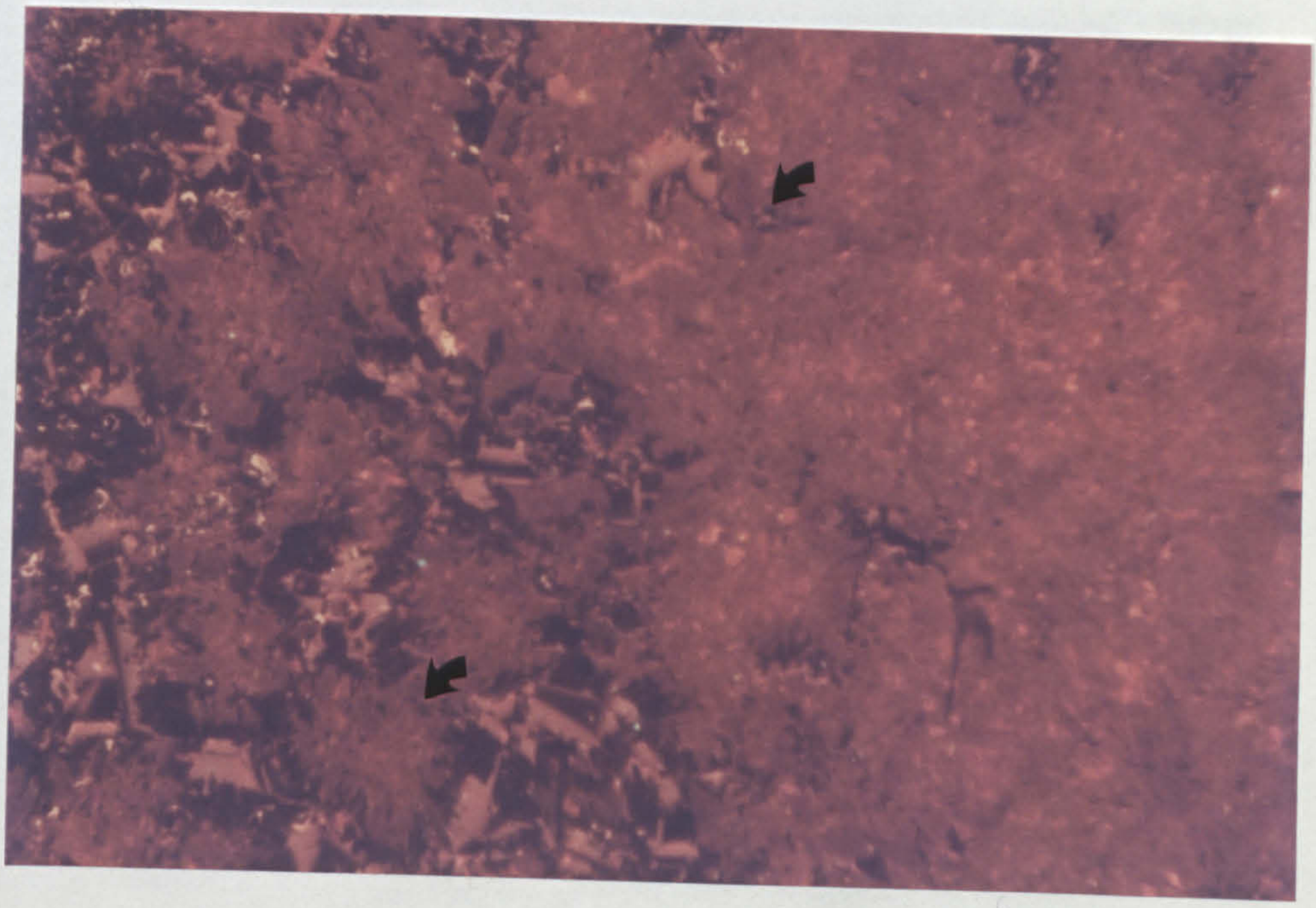

Figure 5.2 c + d Sub- and eu-hedral dolomites.

Dolomites have opaque centres (c) of ferric oxides which show corrosion of dolomite by calcite with cathodoluminescence. Where dolomite crystals do not include ferric oxides there is no calcite (arrow 1). Outer limpid dolomite rims are zoned (d). Dolomite is not corroded by later pore filling calcite (p) which contains small fluorite inclusions (arrow 2). Field of view is 2.25mm.

a : transmitted light

b : cathodoluminescence

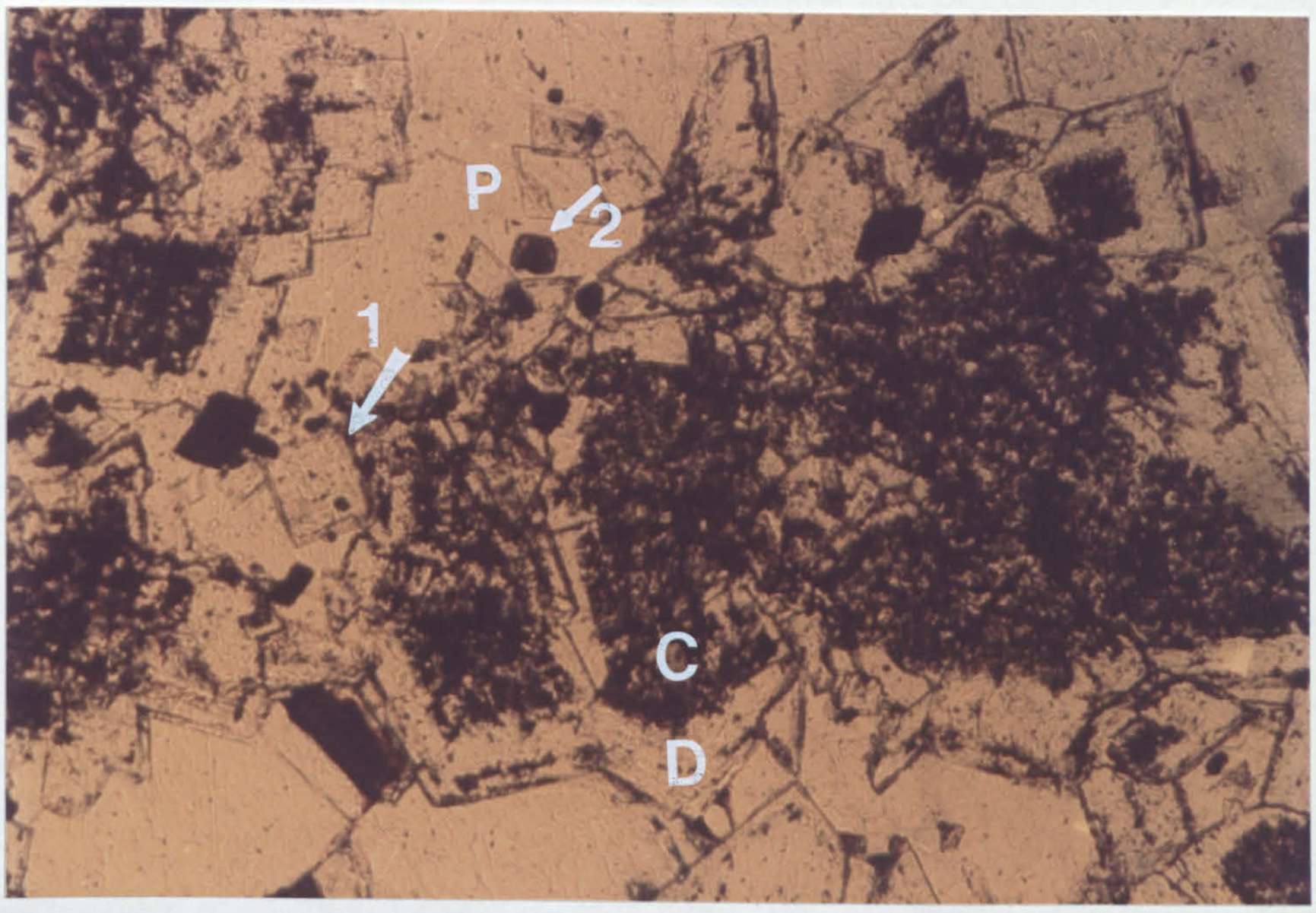
P
2
1
C
D

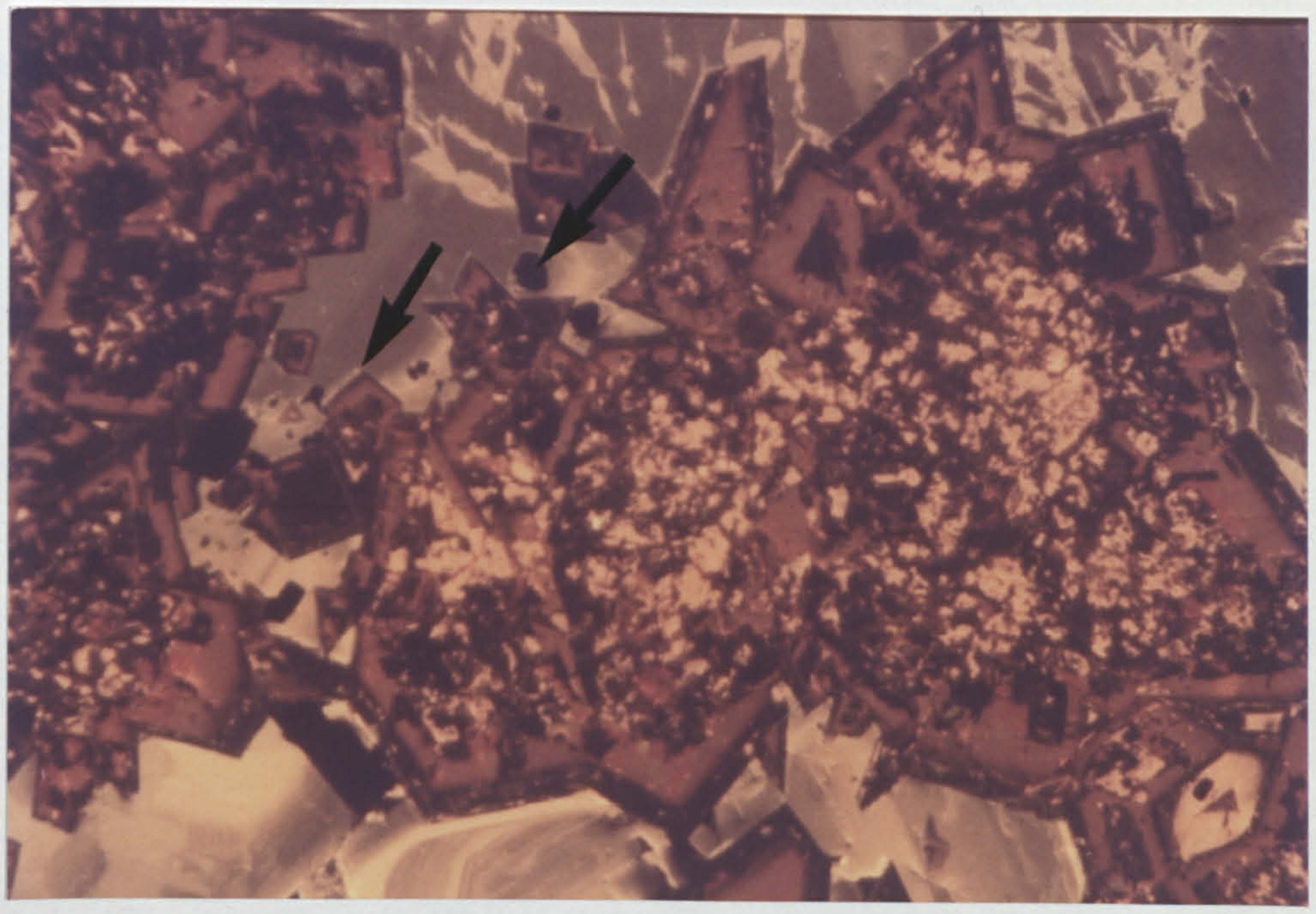

Figure 5.3 Alteration sequence and ferroan dedolomitisation in dolomites, Stanton Hill (SK 482608)

a Anhedral dolomite crystals with no alteration. Crystals contain few inclusions. Field of view is 0.55mm.

b Iron oxide formation at triple crystal junctions (arrowed) and along some crystal boundaries. Field of view is 0.55mm.

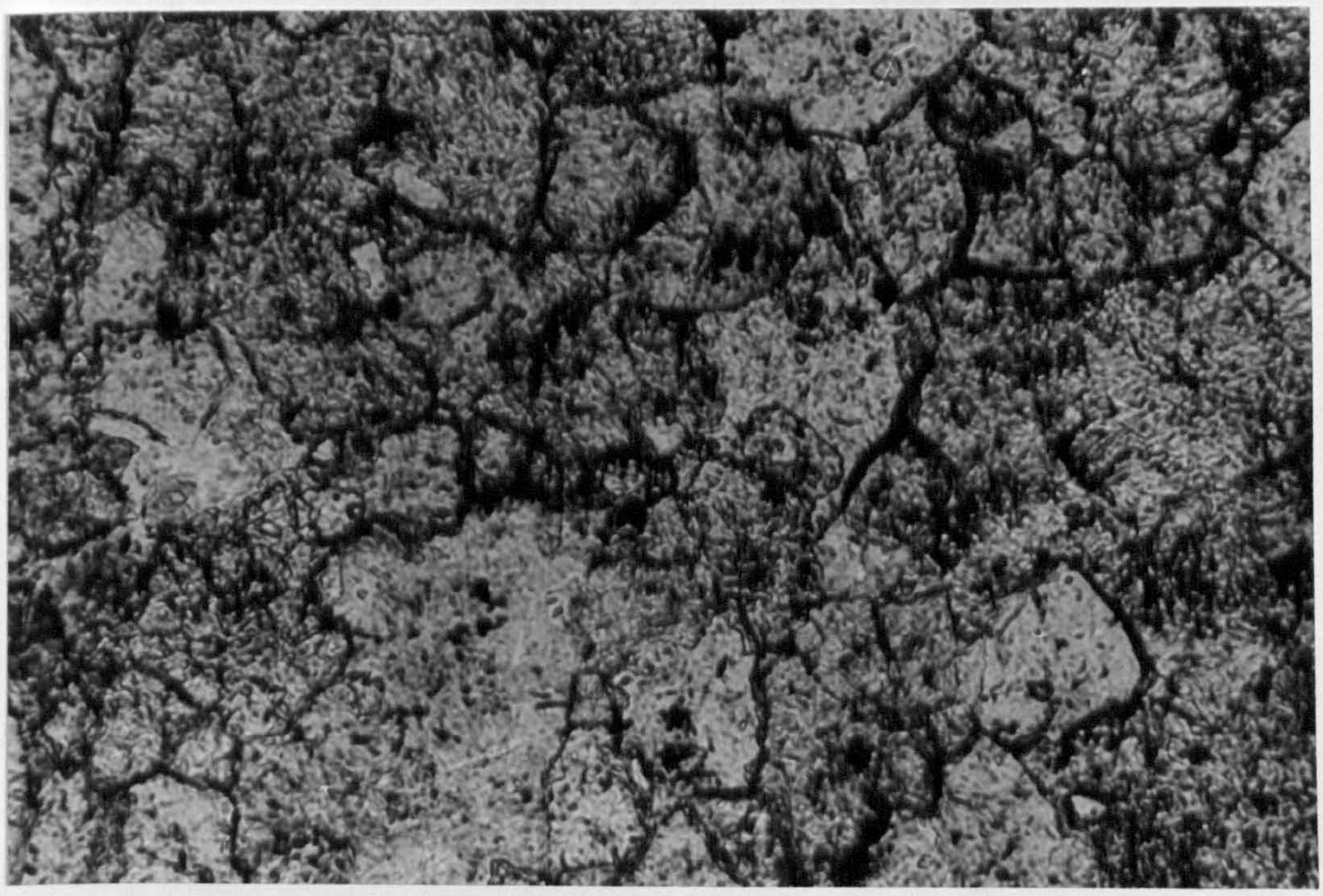

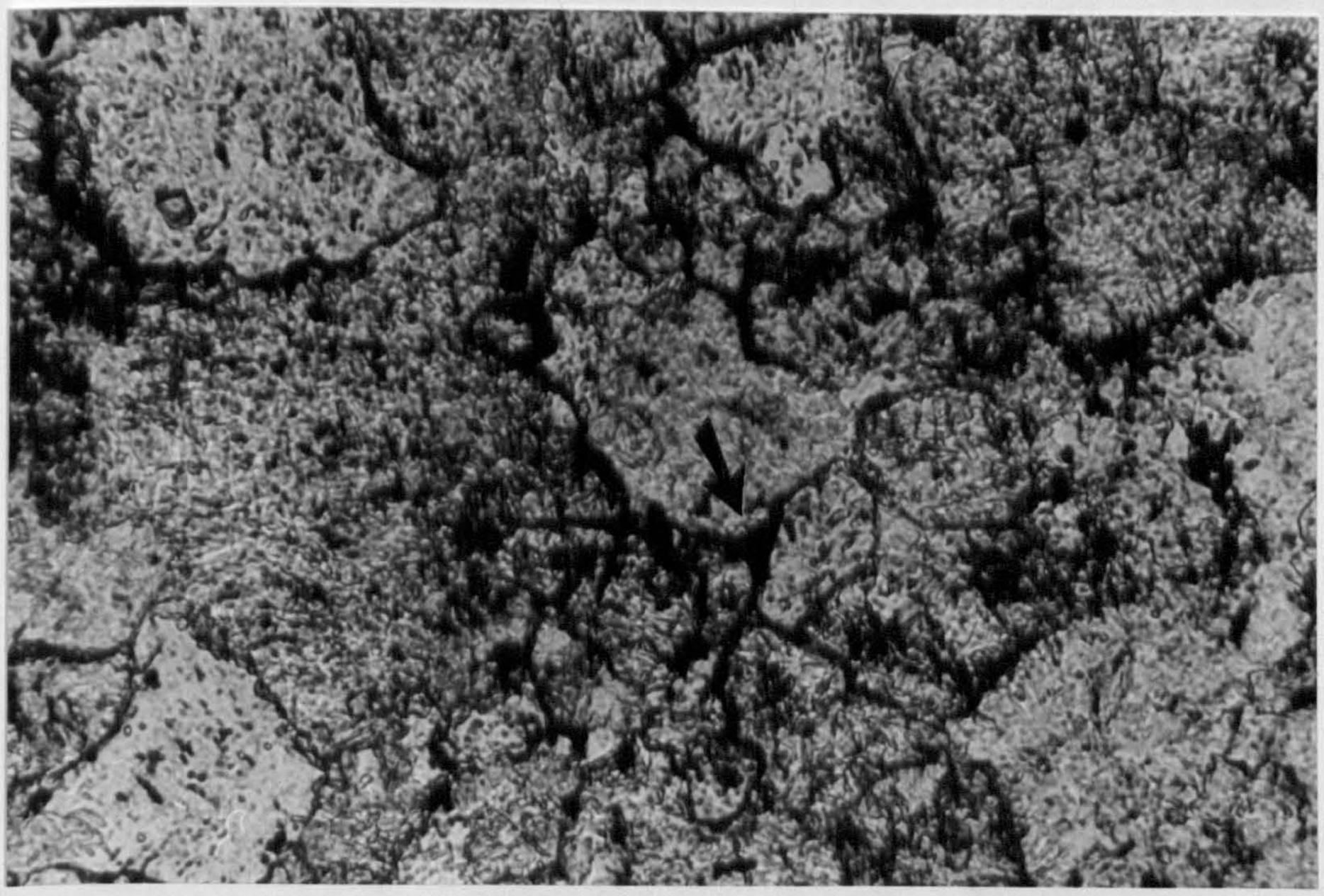

Figure 5.3 c Iron oxides along crystal boundaries increase and centres of crystals are rich in opaque, ferric oxide inclusions. Crystals have more subhedral form with outer, inclusion poor, zone. Field of view is 0.55mm.

d Crystal form is near euhedral with opaque, ferric oxide-rich centres and outer limpid rim. Some FM calcite (F) in crystal centres. Other calcite pore-filling cement (c). Field of view is 0.55mm.

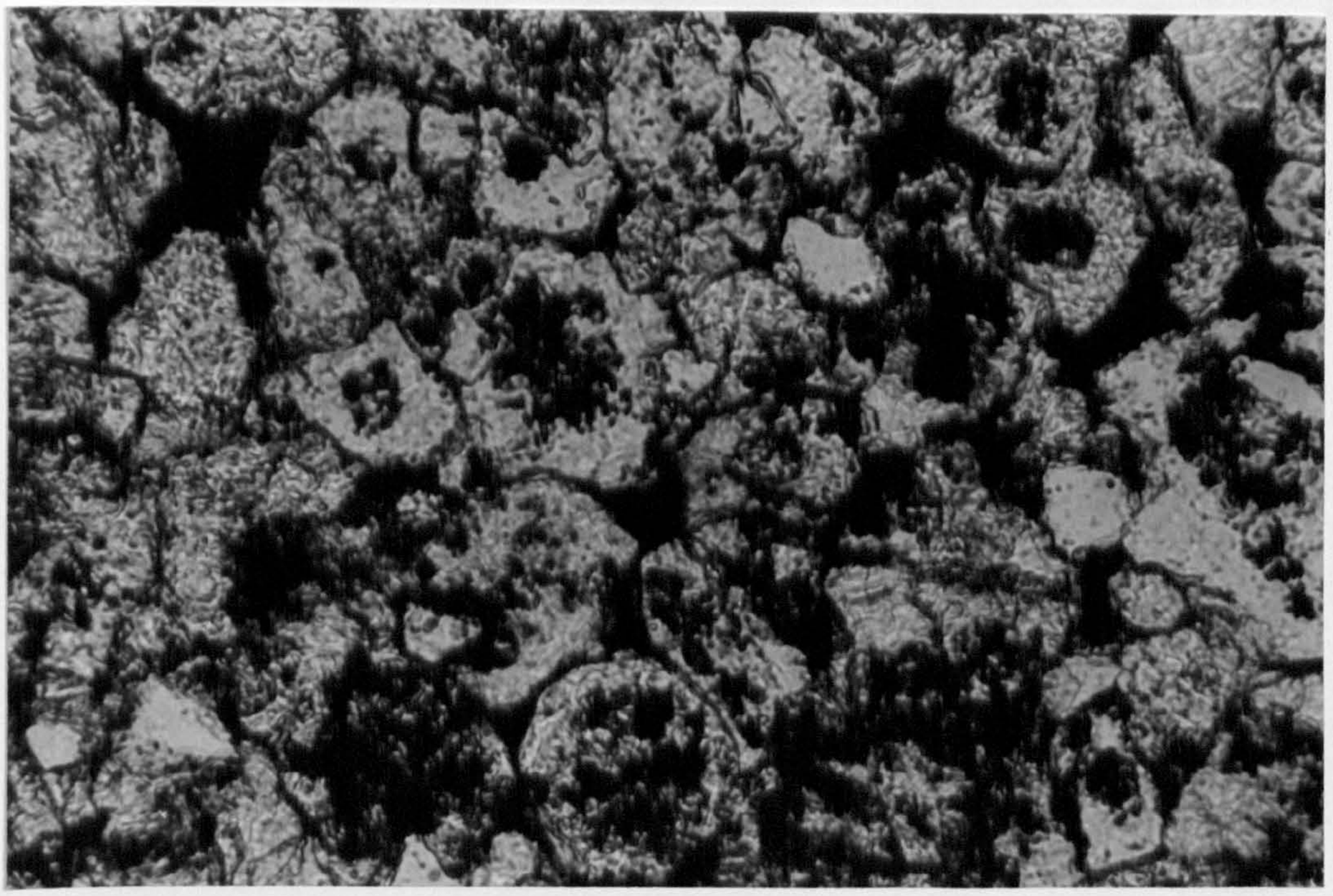

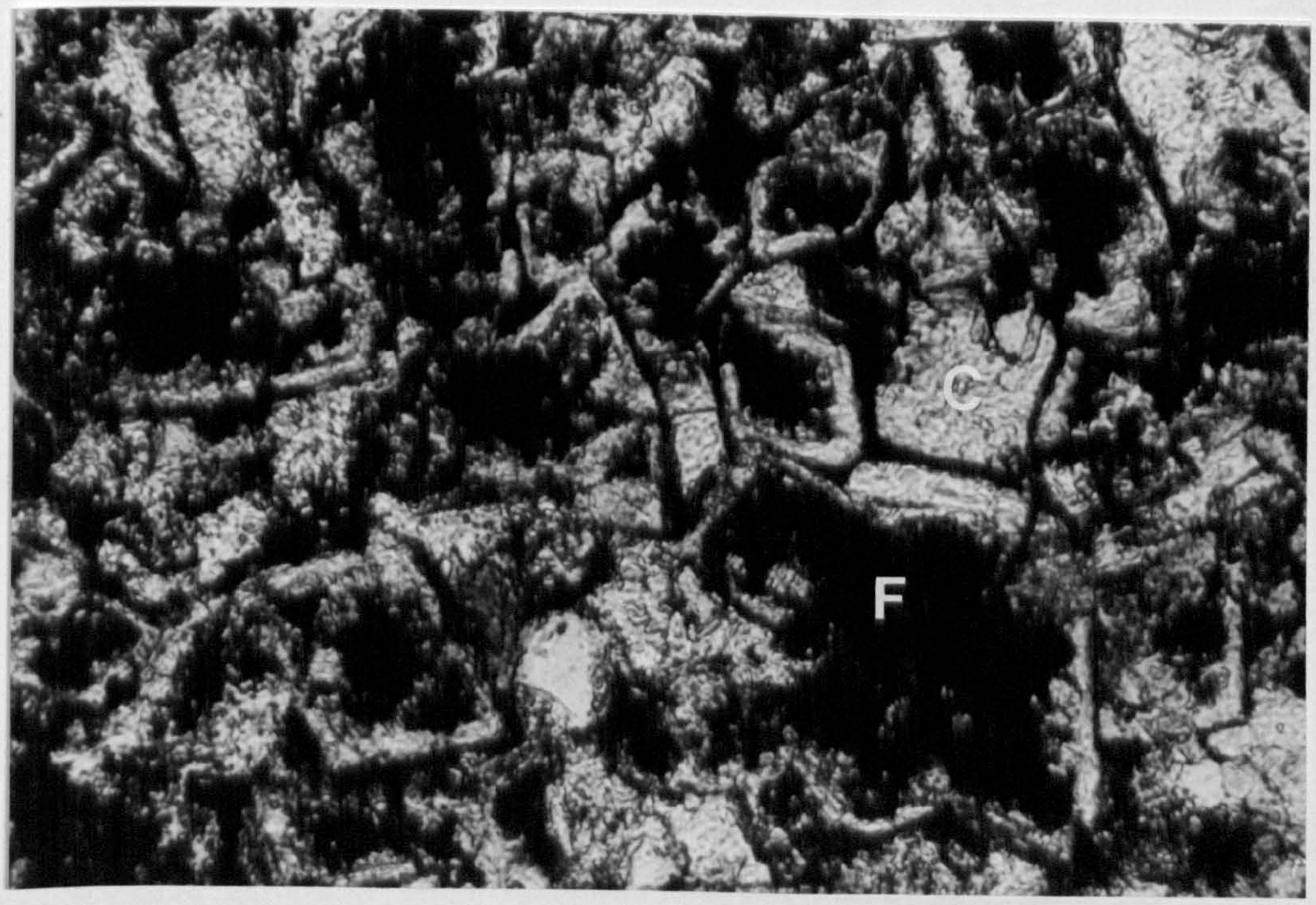
C
F

Figure 5.3 e Euhedral crystals now completely replaced by ferric oxides and FM calcite. Other crystals are 'ghosts' (arrowed) in calcite pore filling cement (c). Field of view is 0.55mm.

f Rhombic pores (R) from preferential leaching of FM calcite and ferric oxides (replaced dolomites) in calcite cement. Field of view is 0.55mm.

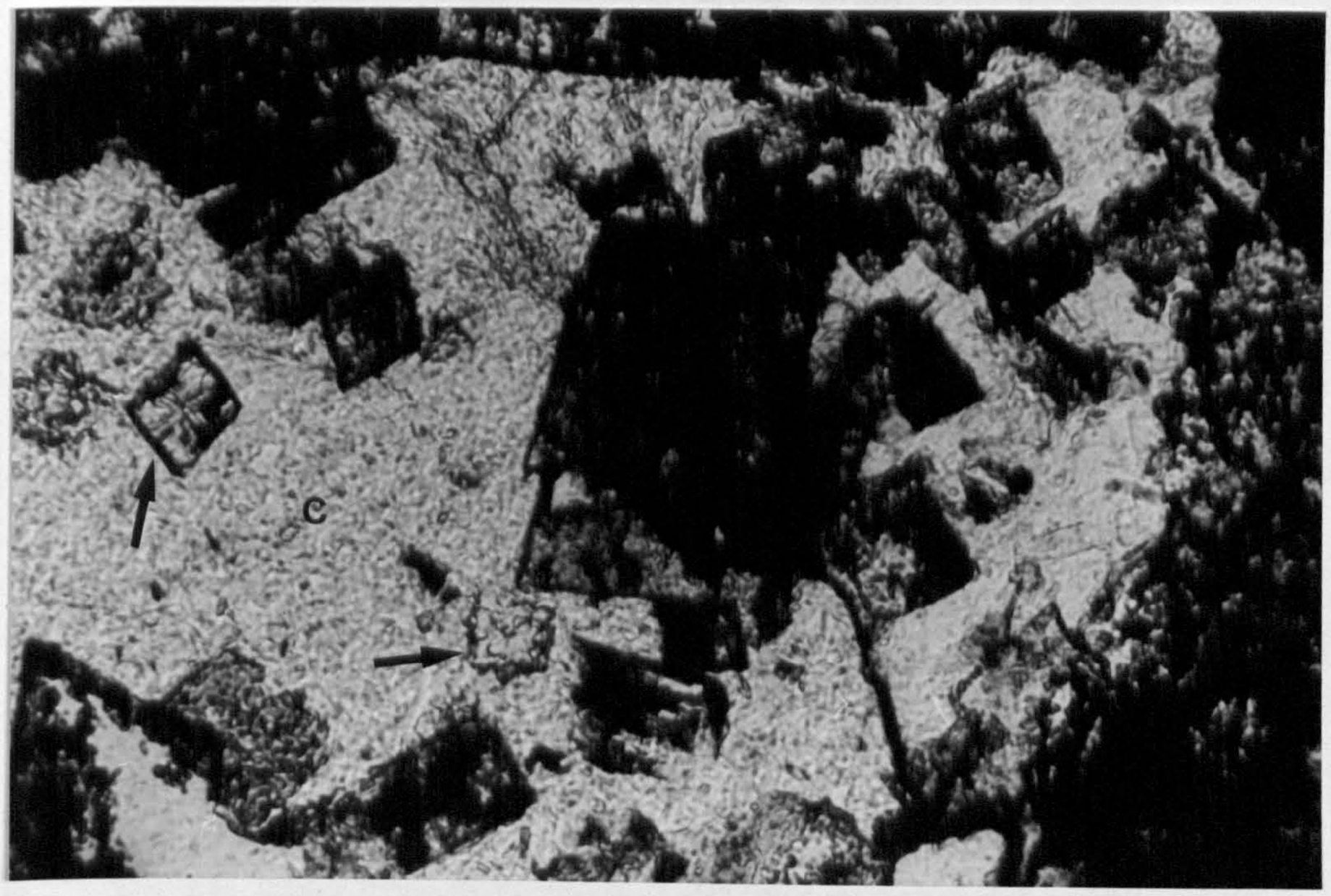
C


R
R

TABLE 5-1

ALTERATION OF DOLOMITES - CLOWNE, NOTTINGHAMSHIRE (SK 486757)

Mole % analysis no.		$MgCO_3$	$CaCO_3$	$FeCO_3$	$MnCO_3$	$\frac{(MgFe)Co_3}{CaCO_3}$
	Unaltered anhedral dolomite					
1	centre	46.59	49.95	0.46	0.17	0.94
2	margin (eg. Fig. 5.3a)	46.07	49.17	0.44	0.13	0.95
	Subhedral dolomite: starting to alter (eg. Fig. 5.3c)					
3	centre of crystal	45.53	49.16	1.50	0.21	0.96
4	ooid ghost in crystal centre	45.78	49.52	1.33	0.29	0.95
5	near margin crystal centre	40.92	50.15	4.33	0.67	0.90
6	inner margin limpid zone	47.00	49.88	0.42	0.16	0.95
7	outer margin limpid zone	47.30	49.40	0.91	0.13	0.98

	Highly altered crystal (eg. Fig. 5.3e)	$MgCO_3$	$CaCO_3$	$FeCO_3$	$MnCO_3$	$\frac{(MgFe)Co_3}{CaCO_3}$
8	translucent area in crystal centre	46.72	49.74	0.97	0.41	0.96
9	opaque area	42.58	45.66	4.27	0.43	1.03
10	opaque hear margin	33.23	37.60	10.06	0.49	1.15

TABLE 5-2

ALTERATION OF DOLOMITES ADJACENT TO SHEET CRACK, WELL, N. YORKS (SE 257812)

Mole % Analysis No.		$MgCO_3$	$CaCO_3$	$FeCO_3$	$MnCO_3$	$\frac{(FeMgMn)Co_3}{CaCO_3}$
1	anhedral dolomite	46.59	48.70	0.73	0.24	0.97
2	grain boundary where alteration starts	44.62	50.24	2.47	0.37	0.94
3	near grain boundary; more altered area	24.83	59.24	12.41	1.53	0.65
	Euhedral dolomite with no Fe oxides					
4	centre	34.45	51.03	11.77	1.66	0.94
5	margin	43.53	49.41	4.56	0.39	0.97
	Zones altered euhedral dolomites with Fe oxides					
6	clear area on crystal unaltered centre	33.48	57.45	2.99	0.50	0.64
	brown opaque area					
7	inner	43.43	53.15	1.33	0.13	0.84
8	centre	19.81	45.64	23.01	1.02	0.96
9	outer	40.79	53.45	2.53	0.34	0.81

		$MgCO_3$	$CaCO_3$	$FeCO_3$	$MnCO_3$	$\frac{(FeMgMn)CO_3}{CaCO_3}$
10	Limpid zone - luminescent zone	39.04	56.49	2.41	0.41	0.73
11	outer non-luminescent area	25.40	61.16	8.98	0.32	0.57
	surrounding calcite void fill					
a		1.66	96.93	0.25	0.00	
b		0.64	98.56	0.12	0.07	
c		0.74	93.35	0.75	0.25	
d		0.69	95.40	0.39	0.28	

Relative positions of analyses 1-11 shows n on Figs. 5 2 a+c.

Figure 5.4 a Semi-quantitative scan across dolomite crystal starting to alter at crystal boundaries, Bedale Quarry, Well (SE 257821).

b Semi-quantitative scan across altered subhedral crystal subject to ferroan dedolomitisation, Bedale Quarry, Well (SE 257812).

c Plot of point analyses across altered subhedral crystal subject to ferroan dedolomitisation, Bedale Quarry, Well (SE 257812).

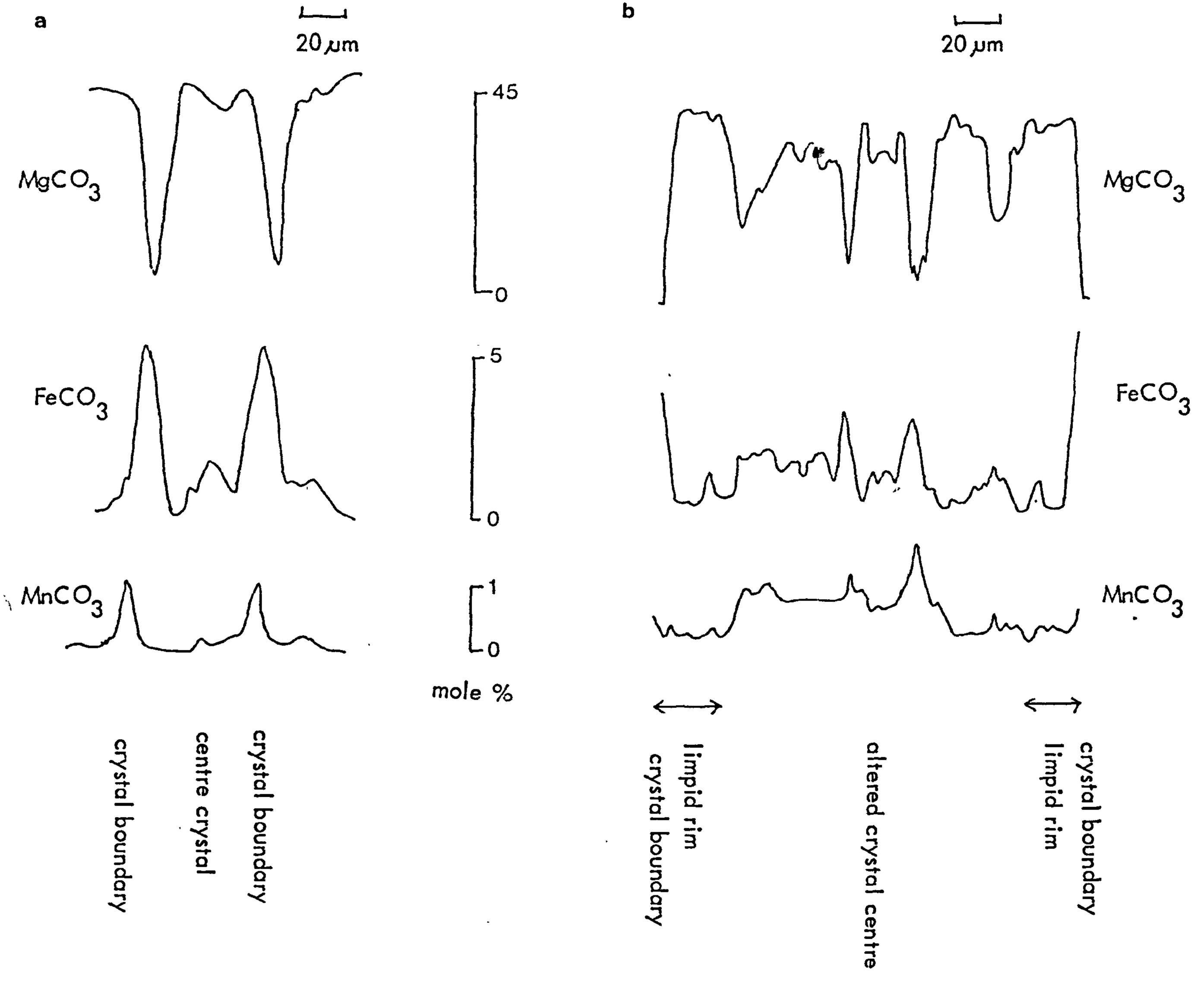
a
20 µm
MgCO3
45
0
FeCO3
5
0
MnCO3
1
0
mole %
crystal boundary
centre crystal
crystal boundary
b
20 µm
MgCO3
FeCO3
MnCO3
limpid rim
crystal boundary
altered crystal centre
crystal boundary
limpid rim

c

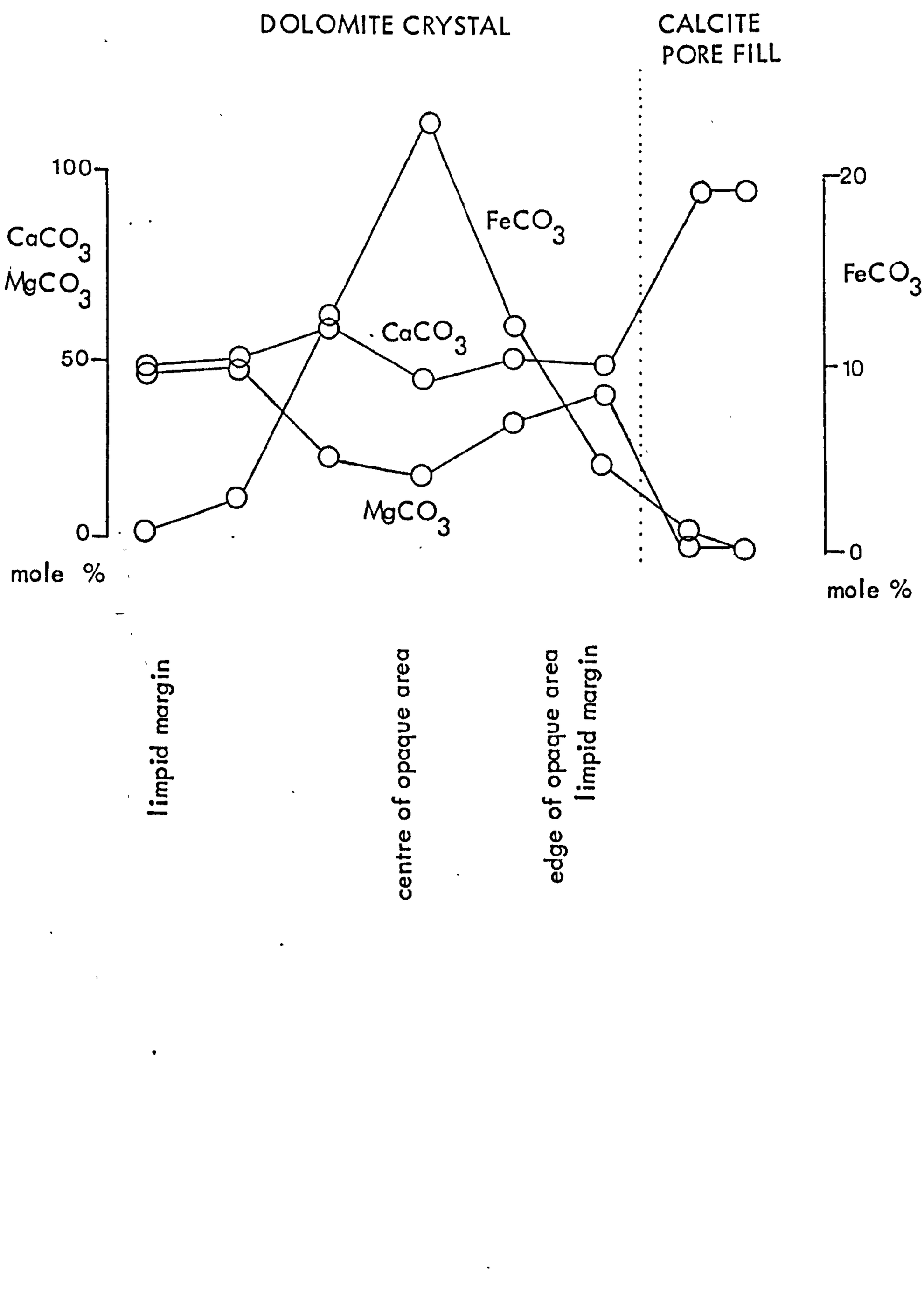
DOLOMITE CRYSTAL
CALCITE PORE FILL
100
50
0
$CaCO_3$
$MgCO_3$
mole %
$FeCO_3$
$CaCO_3$
$MgCO_3$
20
10
0
$FeCO_3$
mole %
limpid margin
centre of opaque area
centre of opaque area
limpid margin

luminescent zones of the dolomite crystals (Figs. 5.2 b, d, Table 5-2, analysis 6). The outer margins of the euhedral crystals are also ferroan but translucent (Fig. 5.2 c, d, Table 5-2, analysis 11). It is noticeable that anhedral, or slightly altered dolomites have neither the poorly-luminescent nor the brighter zones of the subhedral/euhedral crystals (Fig. 5.2 b-d). There is only one central ferric oxide zone in these crystals, unlike the zoned dolomites of Katz (1971) and Frank (1981).

In some areas euhedral/subhedral dolomites are translucent with no ferric oxides or calcite (Fig. 5.2 c, d, Fig. 5.5 a). These dolomites are ferroan, with changes in composition across the crystal (Table 5-2, analyses 4+5; Fig. 5.5 b). Other thin sections show partial development of ferroan dolomites within crystals. Many ferroan dolomite margins here are diffuse; no dissolution/ reprecipitation boundaries are visible within the crystal in transmitted light or cathodoluminescence (Fig 5 6).

Few examples show alteration past the formation of limpid crystal rims and opaque centres (Fig. 5.3 d). Rarely the whole crystal may be altered (Fig. 5.3 e; Table 5-1, analyses 9+10). The total dolomite (or altered dolomite) volume has decreased in these areas; non-ferroan calcite may occlude the resultant porosity (Fig. 5.3 e).

Figure 5.5 a+b Translucent euhedral, zoned dolomites from same thin section as dolomites subject to ferroan dedolomitisation (Figs 5.2 and 5.4). Later centripetal calcite pore cement is brightly zoned. Field of view is 1.00mm across.

a : transmitted light

b : cathodoluminescence

c Semi-quantitative scan across translucent euhedral dolomite crystal.

a

b

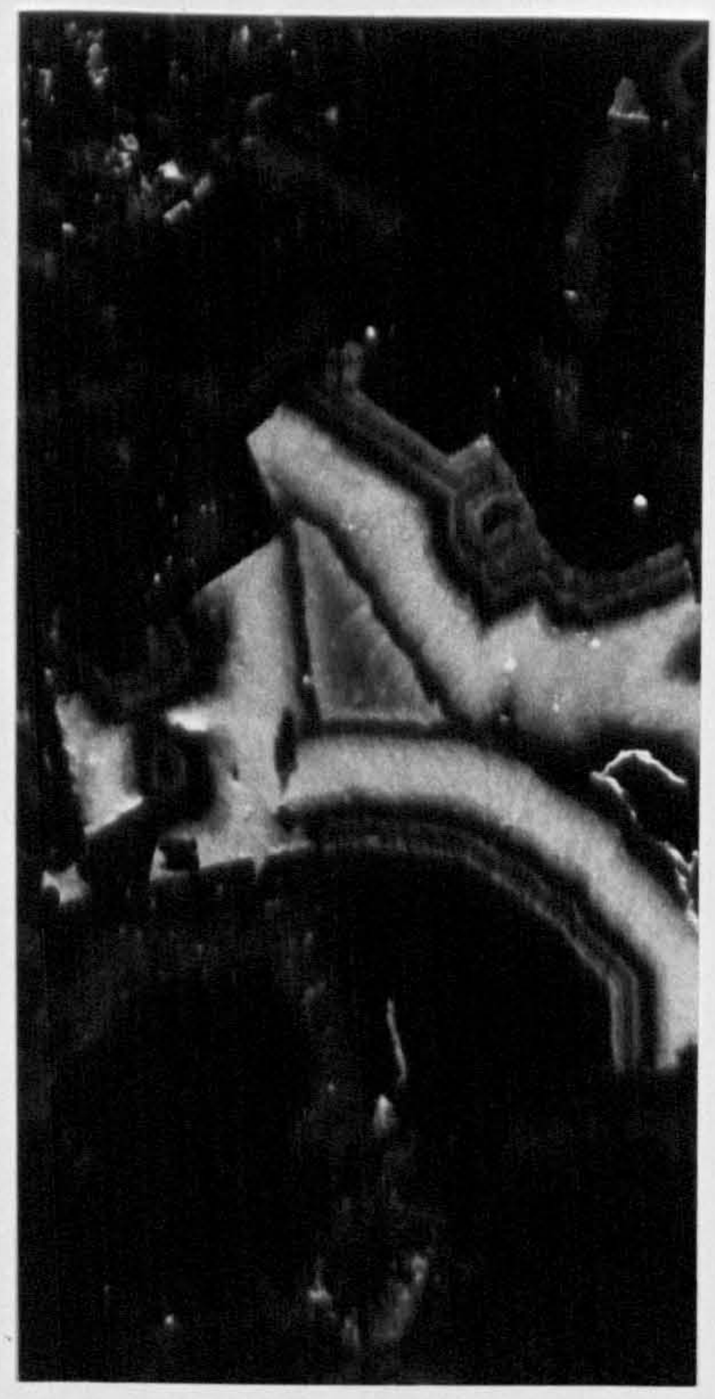

c

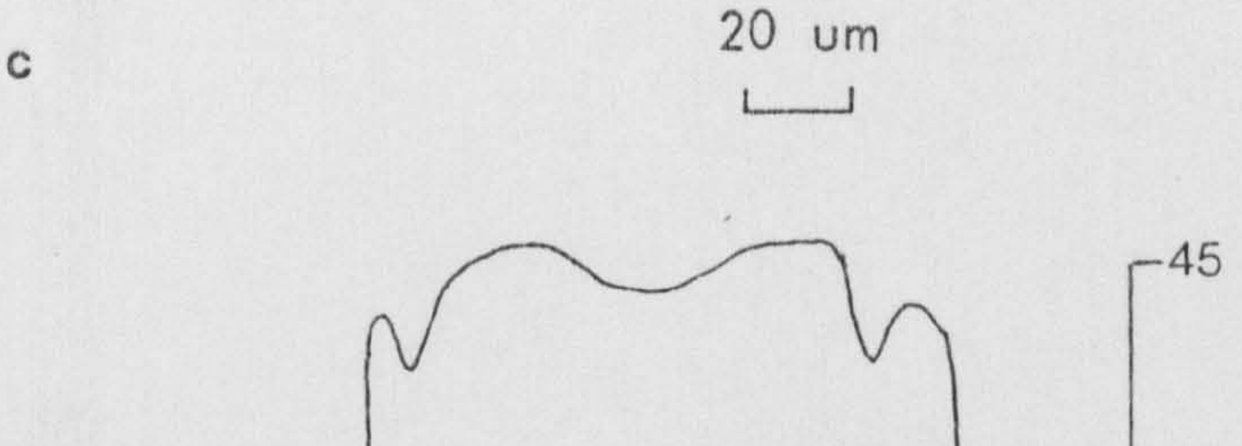

Figure 5.6 Diffuse ferroan dolomite boundary with non-ferroan dolomite, Clowne (SK 486756). Ferroan dolomite (arrowed) is stained so darker than non-ferroan dolomite. No clear boundary is visible between the two. Field of view is 0.55mm.

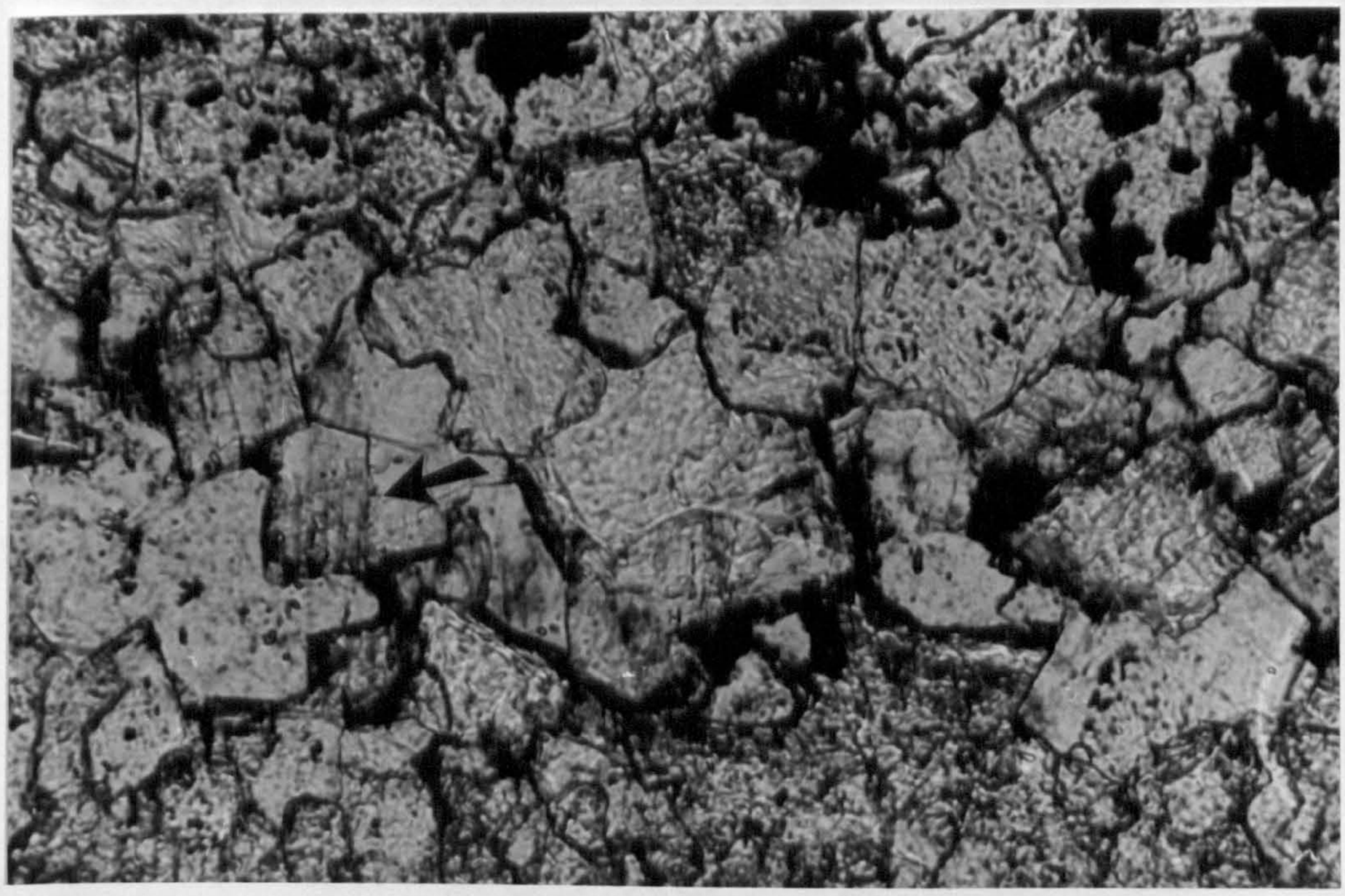

Subsequent leaching of the FM calcite, in zones or of entire crystals (Fig. 5.3f), leads to an effective porosity. Leaching of rhombs in calcite cements (Fig. 5.3f) (leaving rhombic pores) shows higher solubility of the FM calcites. Prolonged leaching can remove all traces of both ferric oxides and FM calcite.

5.2.2 Interpretation of processes

The composition of the FM calcite, its corrosion of the surrounding dolomite and the inclusion of ferric oxide aggregates show this to result from dedolomitisation, called here "ferroan dedolomitisation". The high iron contents of both the FM calcite, with its included ferric oxides, and the surrounding dolomite zones (Table 5-1, analyses 3, 4 and 5), the concentration of dedolomites within the non-luminescent dolomite centres (Fig. 5.2 c+d) demonstrate that ferroan dedolomitisation was of original ferroan dolomites (5.1). The presence of this type of dedolomite can therefore be taken as an indication of original ferroan dolomite.

Katz (1971) and Frank (1981) explain the element variation of zones euhedral/subhedral dolomite crystals by changes in fluid composition during crystal growth. This hypothesis can be applied in isolation to crystals similar to those of Figures 5.2 c+d; it cannot, however, account

for the presence of ferroan dolomite at triple boundaries (Fig. 5.2 a+b, Fig. 5.3 b). Neither does it have any relation to the change in crystal morphology (5.2.1). Katz (1971) states that dedolomitisation occurred during crystal growth. This does not explain the close association of dedolomitised and translucent crystals in the Cadeby Formation (Figs. 5.2 c+d). Ferroan dedolomitisation must post-date crystal growth; it is thus after formation of subhedral/ euhedral crystals.

Two separate processes have therefore taken place in these dolomites in the Cadeby Formation:-

(i) formation of ferroan dolomite, limpid rims and changes in crystal morphology

(ii) ferroan dedolomitisation of most of the ferroan dolomite.

5.2.3 Formation of ferroan dolomite

The formation of ferroan dolomite may be written:

$$Ca\ Mg\ (CO_3)_2 + {}_yFe^{2+}\ (aq) \rightarrow Ca\ Mg_{1-y}\ Fe_y\ (CO_3)_2 + {}_yMg^{2+}\ (aq) \quad (5\text{-}2)$$

Iron is supplied in pore water solutions as Fe^{2+} and as such is incorporated in the carbonate lattie where it substitutes for magnesium. This is apparent from Table 5-2 where the ferroan dolomites (analyses 4+5) have the same degree of stochiometry as the non-ferroan dolomites (Table 5.1,

analysis 1; Table 5-2,analyses 1+2). Thus, in an initially calcium dolomite, iron preferentially substitutes for magnesium and calcium remains virtually constant. Note high $MnCO_3$ contents also in one ferroan dolomite (Table 5-2, analysis 4).

Transport of Fe^{2+} (aq) requires a moderate-low pH and relatively low Eh fluid (Fig. 5.7a). Formation of pure iron carbonate (siderite) occurs in a narrow field (Fig. 5.7 a). Experimental work on the stability of ferroan dolomite has been done for high temperature , thermodynamically stable assemblages (Bickle and Powell, 1977); ferroan dolomites in the Cadeby Formation (e.g. Table 5-2, analyses 4+5) are far out of thermodynamic equilibrium at the temperatures approached during shallow burial (Chapter 10). I can find no publications relating to the conditions of their formation or their chemical properties. Similarly, information on FM calcite properties was lacking. Thus, although the field of formation of ferroan dolomites and FM calcite has been often assumed to coincide with that of pure siderite, it is not possible to be more precise than to state they lie somewhere in the same region (Fig. 5.7 b).

In an ideal solution, the standard free energy change for reaction (5.2) is near zero for ferroan dolomites of low-moderate iron content

Figure 5.7 a Eh-pH diagram for natural waters, carbonate stability fields and Fe^{2+} (aq) stability field.

..... $FeCO_3$ field

-.-.- $MnCO_3$ field

—— Fe^{2+} (aq) field

b Eh-pH diagram showing approximate fields of ferroan dolomite formation, ferroan dedolomitisation and surface leaching. Large arrow indicates change in pore water composition on uplift.

—·—·— Approximate field of ferroan dolomite formation

—··—··— Approximate field of ferroan dedolomitisation

—···—··· Approximate field of surface leaching

a

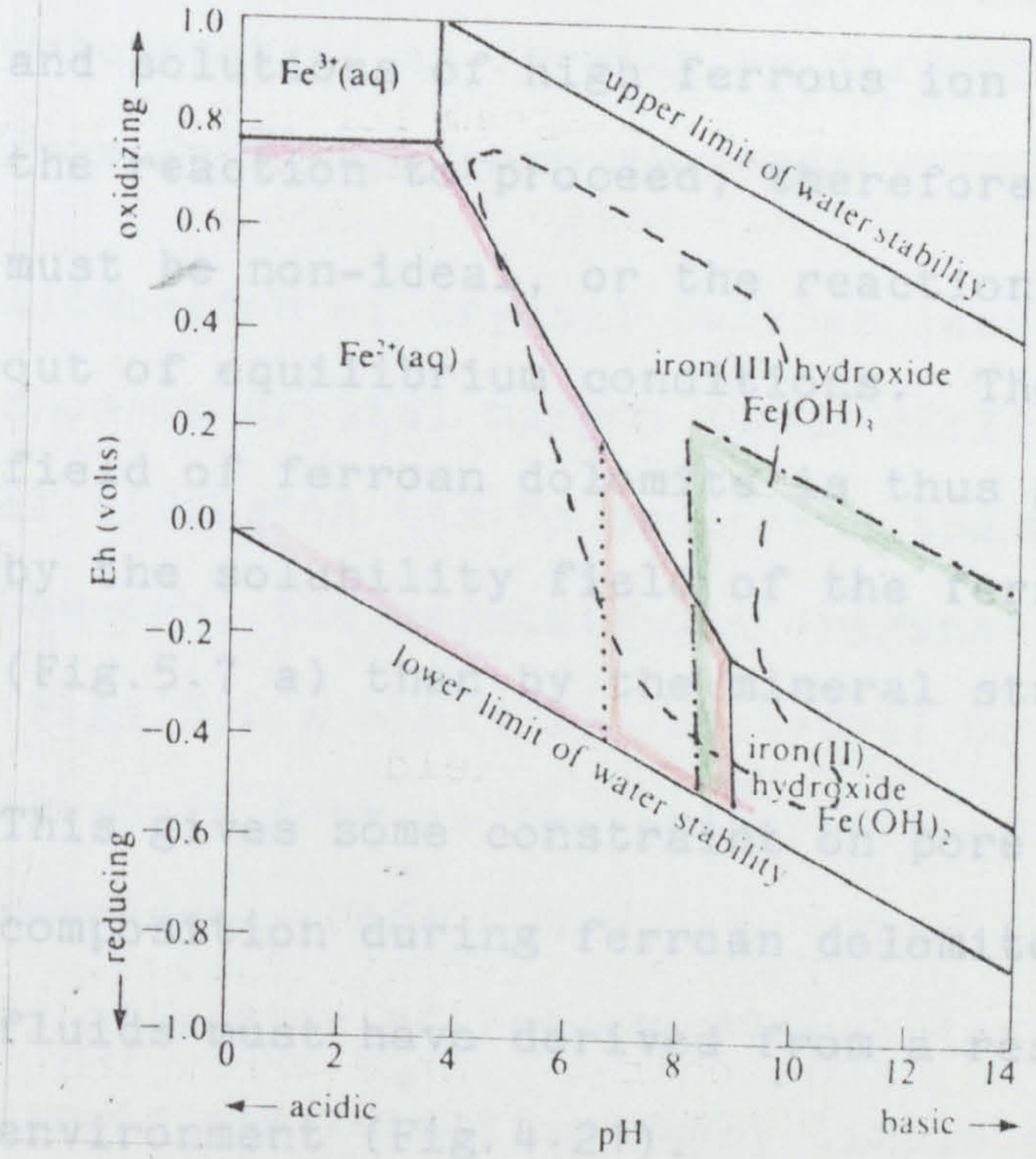

field of natural waters (see Fig. 4.21)

b

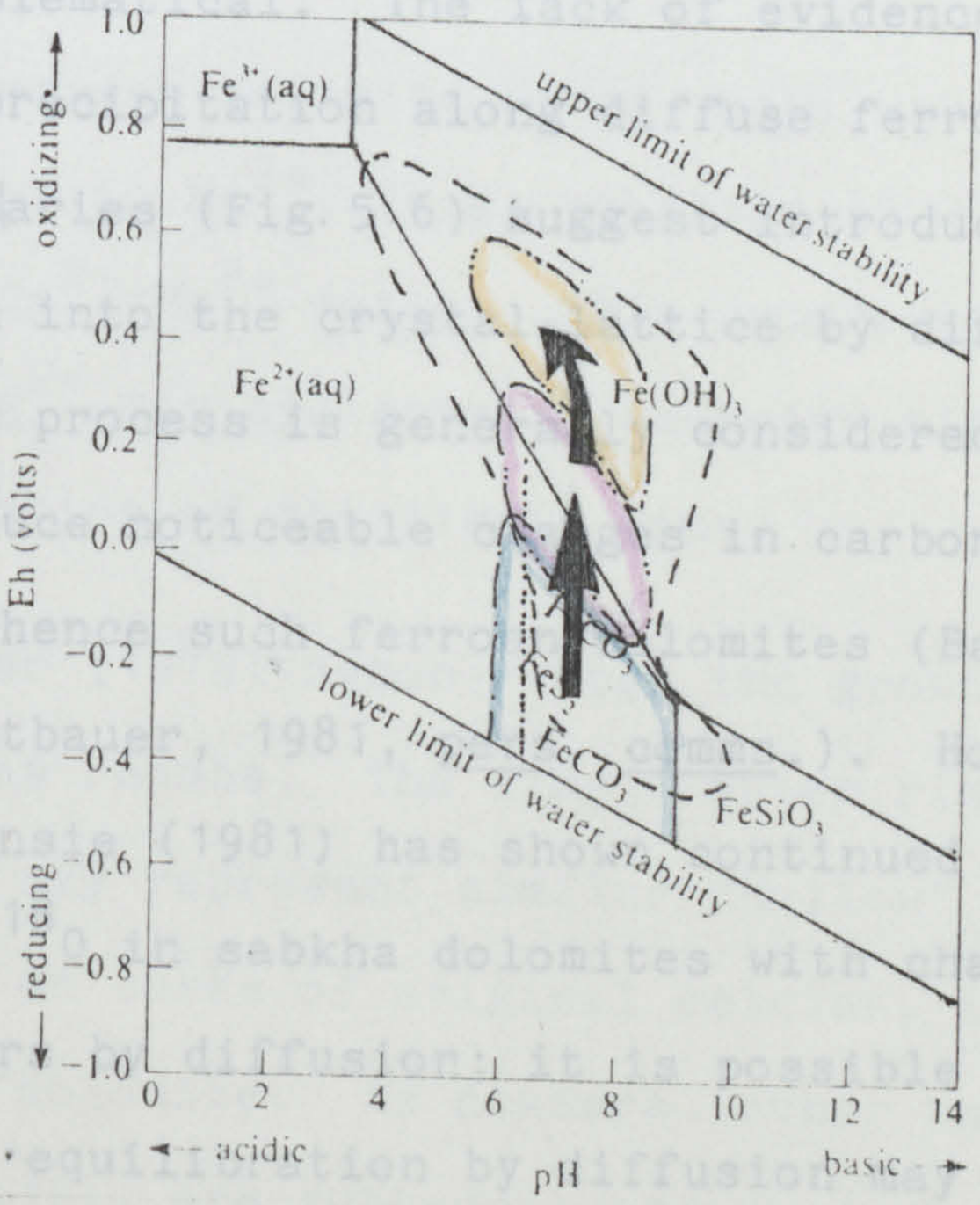

($y < 10\%$) (data from Berner, 1971). This implies equilibrium between non-ferroan dolomite and solutions of high ferrous ion content. For the reaction to proceed, therefore, pore solution must be non-ideal, or the reaction must proceed out of equilibrium conditions. The stability field of ferroan dolomite is thus governed more by the solubility field of the ferrous ions (Fig.5.7 a) than by the mineral stability.

This gives some constraint on pore fluid composition during ferroan dolomites formation; fluids must have derived from a restricted environment (Fig. 4.21).

Actual formation of the ferroan dolomite is problematical. The lack of evidence of dissolution/ re-precipitation along diffuse ferroan dolomite boundaries (Fig. 5.6) suggest introduction of the iron into the crystal lattice by diffusion. This process is generally considered too slow to produce noticeable changes in carbonate composition and hence such ferroan dolomites (Bathurst and Fuchtbauer, 1981, pers. comms.). However, McKensie (1981) has shown continued equilibration of $\delta^{18}O$ in sabkha dolomites with change pore waters by diffusion; it is possible that similar Fe^{2+} equilibration by diffusion may take place around dolomite margins and in crystal centres. K. Schofield (1981, pers. comm.,) finds that, in Derbyshire Viséan carbonates, ferroan dolomites

only form adjacent to, or in the vicinity of, a ferroan calcite pore cement. These are also interpretted as forming by diffusion of Fe^{2+} from Fe^{2+} rich pore fluids.

Alteration of crystal centres leaving a limpid rhombic crystal margin seems difficult to achieve if diffusion has to penetrate the margin. However, the crystals are originally anhedral (Figs.5.2 a + 5.3 a); subhedral or euhedral crystals form as the proportion of ferroan dolomite increases (Figs. 5.3 b, c). This is accompanied by migration of crystal boundaries and, often, limpid rim formation; many limpid rims are non-ferroan (Table 5-1, analyses 6+7) and may be near stochiometric.

As ferroan dolomite forms, pore waters become richer in Mg^{2+}, (e.g. reaction [5-2]), decreasing the Ca^{2+}/Mg^{2+} ratio. This progressive increase in Mg^{2+} may aid crystal boundary migration and formation of the limpid rims.

Weaver (1975) demonstrates the growth of incomplete hollow rhombs. The limpid outer rims (Fig 5.3, c+d) may represent similar "hollow" rhombs which grew on cores of original calcian, inclusion-rich dolomite. As nowhere, other than void linings (4.5.10), are subhedral or euhedral crystals developed without ferroan dolomite (or later dedolomitisation), ferroan dolomite formation and dolomite remobilisation to form subhedral/

euhedral crystals are probably concurrent. The two concurrent reactions are therefore:-

(a) formation of ferroan dolomite (equation 5-2) and

(b) remobilisation of some of the existing dolomite to form near-stochiometric, limpid rhombic overgrowths.

The amount and composition of the ferroan dolomite formed is dependent on:-

(i) Fe^{2+} content of the pore waters

(ii) rate of flow of pore waters (i.e. amount of flushing)

(iii) length of time that the two reactions (a + b above) proceed.

Thus, when Fe^{2+}-bearing pore waters are channelled in open cracks, these pore waters do not penetrate far into the surrounding dolomites and the reactions take place in narrow areas adjacent to the void (Fig.5.2), but where pore fluids permeate broader areas of dolomite, a more diffuse altered area results. The penetration zone may be partially controlled by porosity/permeability barriers from sedimentalogical features. It is possible that the coarse sucrose dolomites (4.5.9) were formed by remobilisation of existing dolomites and development of ferroan dolomite on a much larger, regional scale.

5.2.4 Dedolomitisation of ferroan dolomite

Ferroan dedolomitisation may take place at any stage during the alteration process; nowhere is there evidence of ferroan dolomite formation recommencing after dedolomitisation. Ferroan dedolomitisation therefore "freezes" alteration at a particular stage.

Previous authors have related petrographically similar dedolomitisation of dolomite rhombs or individual zones to the instability of ferroan dolomite in oxic pore waters (Katz, 1971; Al Hashimi and Hemingway, 1973; Frank, 1981). Such dedolomitisation has long been considered a surface phenomenon related to weathering and percolation and leaching of meteoric fluids (Shearman et al., 1961; Schmidt, 1965; Goldberg, 1967; Folkman, 1969; Braun and Friedman, 1970 and others). Near-surface conditions are also implied by the experimental work of Yanat'eva (1955) and De Groot (1967). (De Groot's paper was based on a sample of the Cadeby Formation from Shirebrook, Notts. - Upper Member ooid grainstones?). Neither Yanat'eva nor De Groot used ferroan dolomites and both used $CaSO_4$ -bearing fluids. Their combined results demonstrate that dedolomitisation of non-ferroan dolomites takes place at low Pco_2 and temperatures of less than $50^{o}C$. No published results of dedolomitisation in non-$CaSO_4$- bearing fluids

have been found, although Al Hashimi and Hemingway (1973) reported oxidation of ferroan dolomites under dripping tap water for several months. Thus the range of conditions of dedolomitisation of ferroan dolomite have not been defined; it may be much wider than the range obtained by Yanat'eva and De Groot, particularly as the limpid dolomite rims are not dedolomitised. A possible stability field is shown on Fig 5-7 b). It must be stressed that this argument applies only to dedolomites formed from ferroan dolomite; it cannot consequently be assumed that such dedolomites are necessarily representative of exposure and unconformities.

Dedolomitisation of ferroan dolomite can be expressed as:-

$$2\ CaMg_{1-y}\ Fe_y(CO_3)_2 + Fe^{2} + {}_xCa^{2+} \rightarrow 2Ca_{1+x}Mg_{1-(y+z)}Fe_{(y-w)}\ CO_3$$

$$_{(v+w)}Fe\ \text{oxides} + Mg^{2+}\ (aq) \quad (5\text{-}3).$$

Compositions of both ferroan dolomite and FM calcite are variable (5.2.1).

Due to lack of knowledge of the stability fields of these carbonate minerals (5.2.3, 5.2.4) the pore water composition causing dedolomitisation cannot be precisely determined. Pore water must be of higher pH and/or Eh for formation of ferric oxides (Fig. 5.7 a+b). Where anoxic micro-environments remain, ferroan dolomites are not

dedolomitised. The necessity for the presence of $CaSO_4$ in solution has not been proved; ferroan dolomites are unstable in oxic $CaSO_4$-free environments.

Ferroan dedolomitisation is therefore dependent on:-

(i) formation of ferroan dolomite

(ii) later breakdown of ferroan dolomite in more oxic pore waters.

Ferroan dedolomitisation alters the distribution of both iron and magnesium within the crystal. It was concluded that both dolomite crystals in Fig. 4.20 a+b grew concurrently; crystals in Fig. 5.4 and Fig. 5.5 also were remobilised at the same time. Peaks in iron distribution and loss of magnesium occur in dedolomitised zones (Figs. 4.20 b+c, 5.4 b and 5.5 b); manganese follows iron. The extremely high iron peaks in dedolomitised zones imply some further addition of iron during, or immediately preceding, dedolomitisation. This iron may substitute for calcium (note the stochiometry of analyses 9 and 10, Table 5-1) in the ferroan dolomite lattice forming a "super-ferroan" dolomite and thus trigger dedolomitisation. Equation (5-3) may thus be subdivided:

$$Ca\,(Mg\ Fe)\,(CO_3)_2 + Fe^{2+} \rightarrow (Ca\ Fe)\,(Mg\ Fe)\,(CO_3)_2 + Mg^{2+}\,(aq)$$

super-ferroan dolomite (5-4)

and (Ca Fe) (Mg Fe) $(CO_3)_2$ + $Ca^{2+} \rightarrow$ 2(Ca Mg Fe) CO_3 +

Fe oxides + Mg^{2+} (aq) (5-5)

Langmuir (in Chillingar et al., 1979) suggests pyrite oxidation may promote dedolomitisation:

$$Fe\ S_2 + 7/2_{02} + H_2O \rightarrow Fe^{2+} + 2SO_4^{2-} + 2H^+ \quad (5\text{-}6)$$

$$\text{and } Fe^{2+} + \tfrac{1}{2}O_2 + 5/2H_2O \rightarrow Fe\ (OH)_3 + "H^+ \quad (5\text{-}7)$$

The acidic fluids formed in these reactions then attack the dolomites

$$CaMg\ (CO_3)_2 + 2H^+ \rightarrow CaCO_3 + Mg^{2+} + CO_2 + H_2O \quad (5\text{-}8)$$

Partial oxidation of pyrite (equation 5-6) releases Fe^{2+} ions. These are available to form "super ferroan" dolomite (equation 5-4) which then breaks down to FM calcite and iron oxides (equation 5-5) when conditions become more oxidising. Thus Langmuir's reactions (5-6, 5-7 and 5-8) may not be adequate explanation of pyrite oxidation and ferroan dedolomitisation in these dedolomites.

5.2.5 Leaching of dedolomites

FM calcite and ferric oxides are selectively leached in dolomite or calcite (Figs. 5.2 c and 5.3 f). The enhanced solubility of dedolomitised carbonates has been noted by many (e.g. Evamy, 1967; Al Hashimi and Hemingway, 1973; Frank, 1981). Evamy (1967) attributes the selective

leaching of dedolomite, and hence its greater solubility, to initial production of HMC or aragonite during dedolomitisation. He infers that rhombohedral pores only occur where leaching follows soon after dedolomitisation, before a more stable LMC can form. It is unlikely that HMC or aragonite would form in conditions where dedolomitisation of ferroan dolomite occurs; both HMC and aragonite are more typical of marine waters than the pore fluids causing dedolomitisation (Fig. 5.7 b).

Selective leaching of 'dedolomite' is independent of crystal size. Examples from Evamy (1973) were in a finely crystalline calcite matrix whereas those in Figure 5.3 f are in coarsely crystalline, poikilitic calcite. I propose that selective leaching here is due to the enhanced solubility of the FM calcite formed during dedolomitisation. This would explain the formation, or partial formation, of rhombhedral pores or individual leached zones within the subhedral/euhedral dolomites; it would also explain the presence of iron oxides lining these pore spaces.

5.2.6 Timing of alteration

The dependence of dedolomitisation on oxic pore fluids has led to the association of dedolomitisation with uplift and unconformities (5.2.4) although this generalisation has recently been questioned

by Margaritz and Kafri (1981). Lack of definition of relevant carbonate chemistry also introduces further queries.

Pore-filling baryte and sphalerite are present in some altered dolomites (Figs. 5.8 a+b). Both are adjacent to subhedral/euhedral crystals and limpid margins. Dolomite remobilisation and concurrent formation of ferroan dolomite must thus have occurred before mineralisation. Figure 5.8 a indicates dedolomitisation also took place before baryte mineralisation. Pore-filling sphalerite mineralisation is unlikely to take place near surface; there is no evidence of uplift and later burial in these rocks.

Dolomite alteration, including dedolomitisation, must have occurred at depth. This shows not only the presence of oxic pore solutions circulating at depth but also the presence, prior to mineralisation, of an effective secondary porosity at depth.

Surface weathering is responsible for some dedolomitisation; freshly exposed quarry faces turn from grey to brown in several months. Weathered specimens show iron oxide development and leaching (Figs. 5.9 a+b). In dry periods, surfaces of the Cadeby Formation show magnesium sulphate efflorescence indicating the progression of dedolomitisation (Sorby, 1856; Chillingar, 1956). Intensely weathered exposures may be

Figure 5.8 a Pore-filling baryte in altered dolomite, Skegby (SK 495608).

Dolomite crystals have altered margins with thin limpid rims (arrowed) adjacent to baryte (B). Baryte must thus have been crystallised after alteration of dolomites. Fine siliciclastic content and possible peloid cores and ghosts (small arrows). Field of view is 2.2mm.

b Pore-filling sphalerite in altered dolomite, Linby (SK 537523). Sphalerite corrodes some dolomite, but other crystals show altered margins (arrowed). Field of view is 0.9mm.

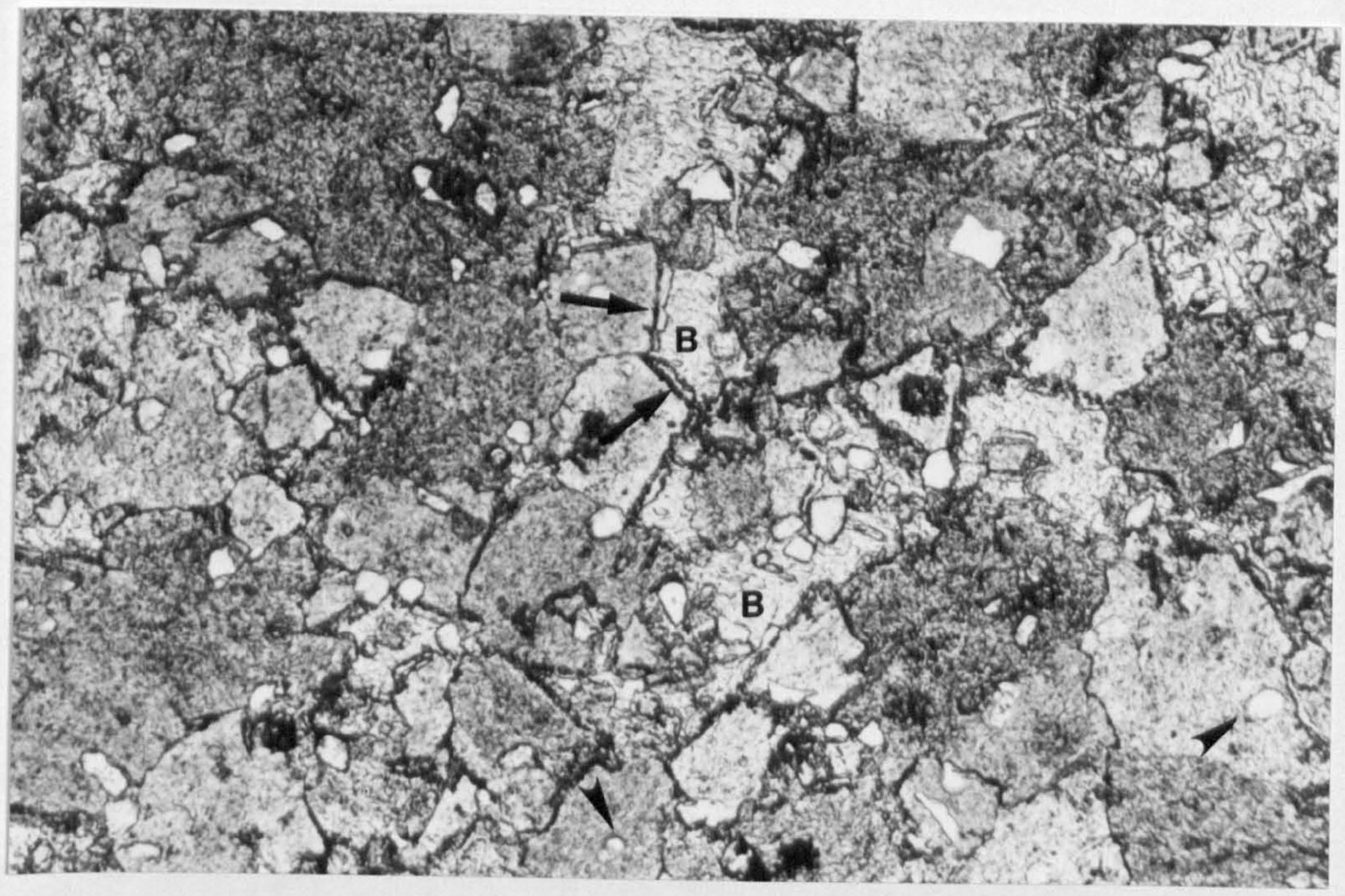
B
B

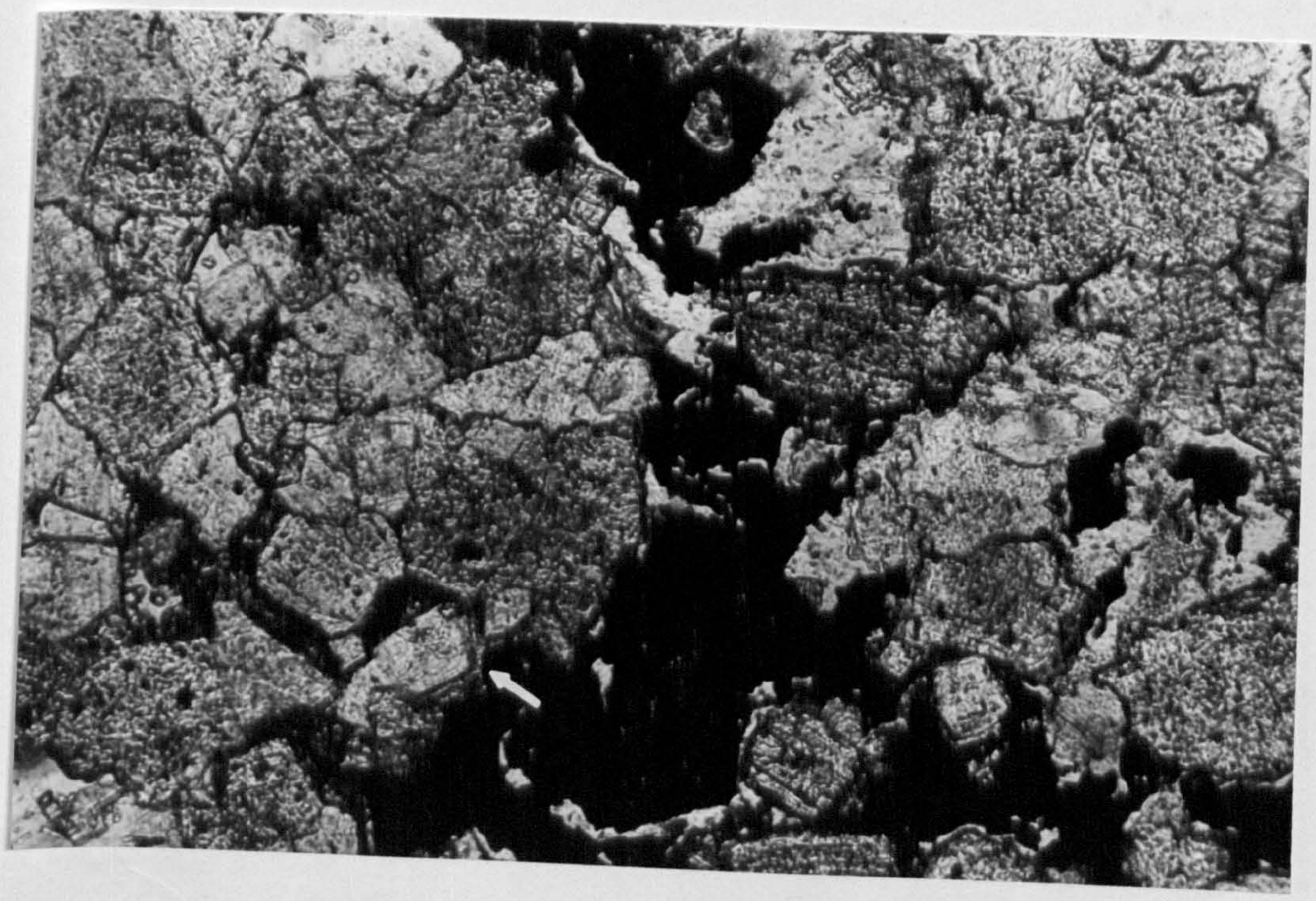

Figure 5.9 a Slightly weathered skeletal wackestone with moldic porosity, Clowne (SK 486756). Dolomite immediately adjacent to void is ferroan and stains darker (arrowed). Remainder is non-ferroan dolomite. Field of view is 0.9mm.

b More weathered skeletal wackestone with moldic porosity, Clowne (SK 486756). No ferroan dolomite remains but pore space is lined with iron oxides (opaque). Field of view is 2.2mm.

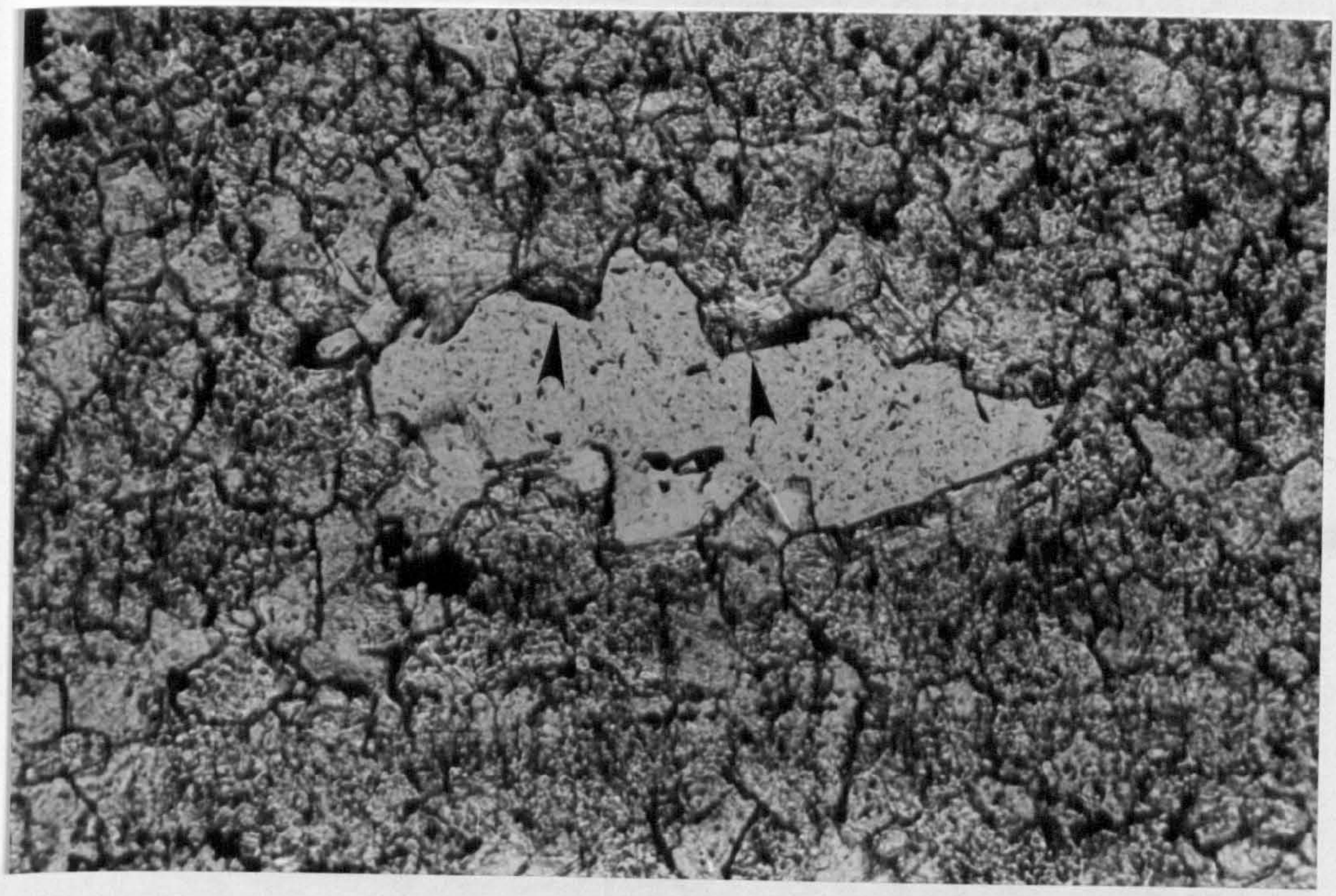

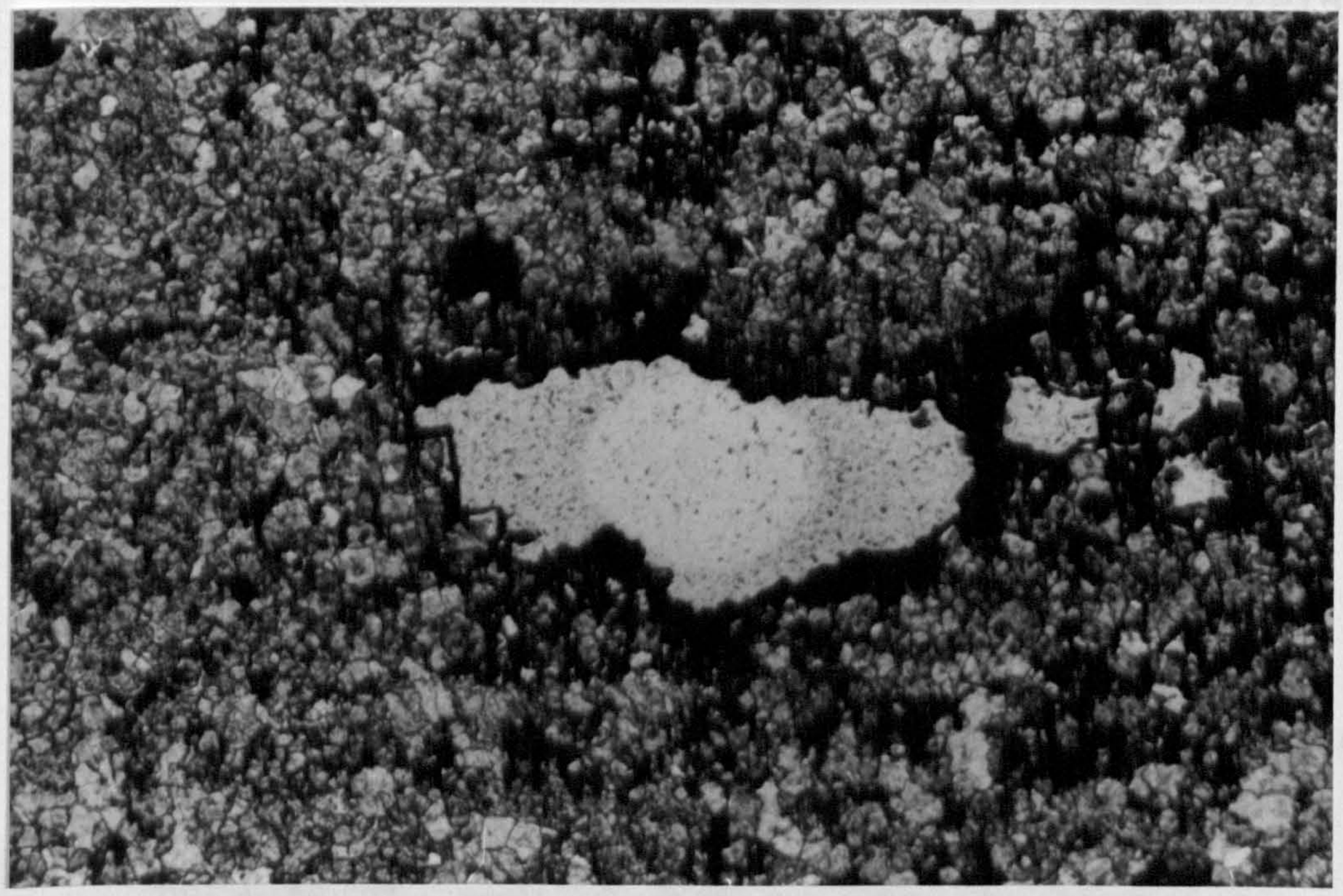

extremely soft and porous due to a combination of dedolomitisation and leaching. The pre-existing ferroan dolomite may have formed during deep ground water circulation before considerable uplift (Fig. 5.7 b). As uplift proceeds, dedolomitisation and leaching become prevalent (Fig. 5.7 b).

5.2.7 Summary of dolomite alteration

Dolomite alteration comprises two main processes:

(i) partial remobilisation of dolomite and formation of ferroan dolomite in anoxic pore fluids

(ii) dedolomitisation of ferroan dolomite in oxic pore fluids.

The former process commences at crystal triple junctions and may continue to produce subhedral and euhedral zoned dolomite crystals. The remobilisation of dolomite and change in crystal form is summarised in Figure 5.10.

Dedolomitisation takes place with the introduction of oxic pore fluids; it effectively 'freezes' remobilisation. Dedolomitisation of ferroan dolomite is not necessarily a near surface process; precise chemical constraints cannot be defined because of lack of data on similar carbonate compositions. The FM calcite produced during dedolomitisation is demonstrably more soluble than neighbouring non-ferroan calcite. The

Figure 5.10 Summary diagram of dolomite remobilisation formation of ferroan dolomite

1. Anhedral dolomite crystals

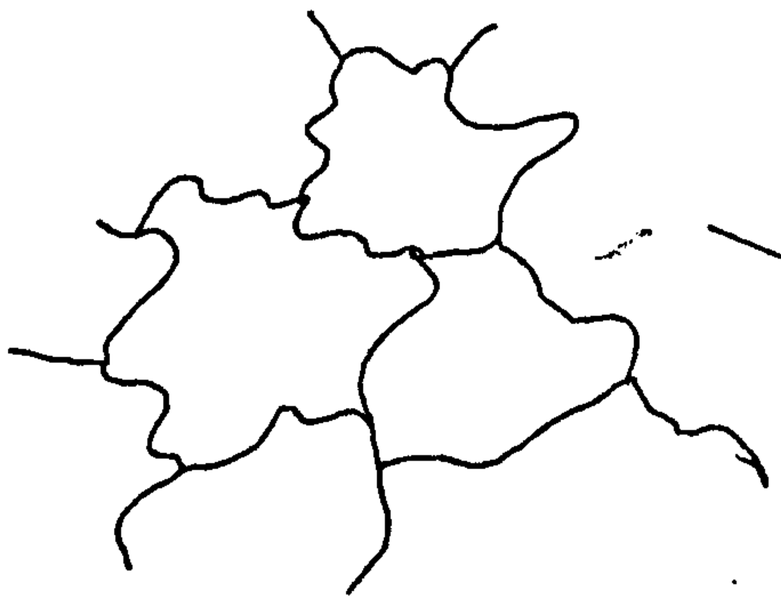

2. Alteration at crystal triple boundaries

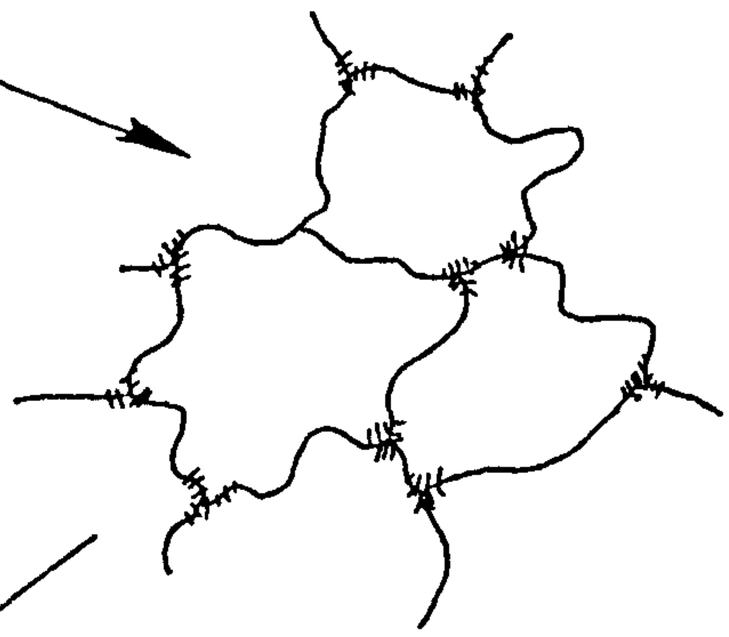

3. Continued alteration at triple junctions and crystal boundaries

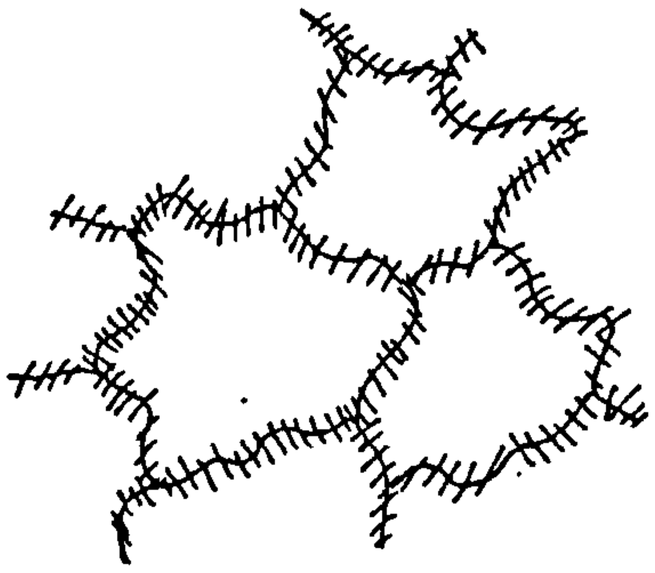

4. Remobilisation around ferroan zones with migration of crystal boundaries

5. Dedolomitisation

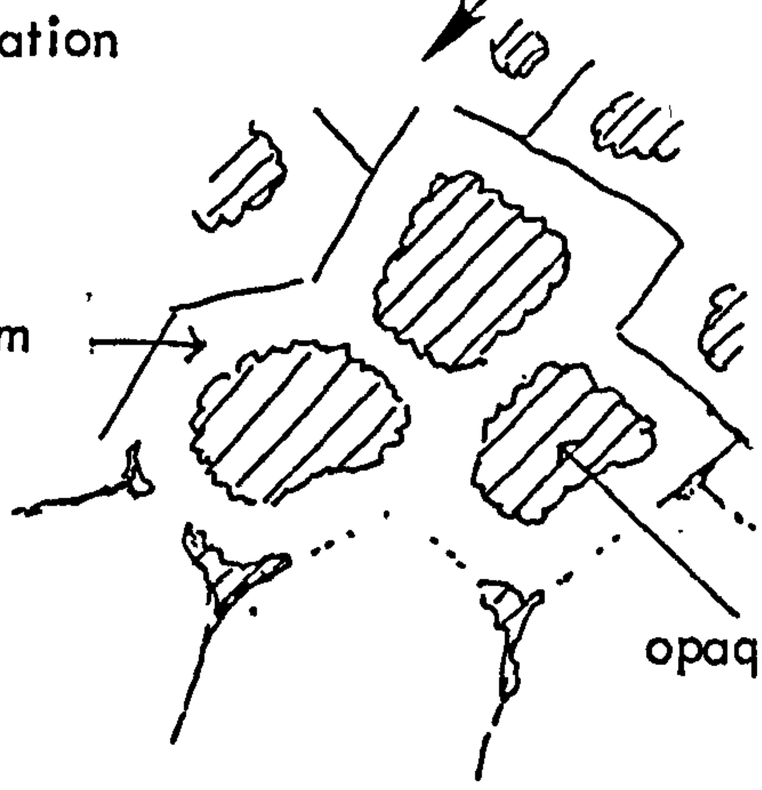

necessity for calcium sulphate-rich fluids in this dedolomitisation is questionable. Although the association of dedolomitisation and ferroan dolomites has been recorded elsewhere, the importance of earlier ferroan dolomite formation and dolomite remobilisation has not previously been demonstrated.

5.3 Dedolomitisation associated with calcium sulphate-bearing pore waters

The presence of dedolomites at the top of the Upper Member has already been noted (2.4.1; Figs. 2.6 a+b). These dedolomites may grade into underlying dolomitised ooid/peloid grainstones (Appendix 5, analyses 101-109) or, elsewhere, demonstrate abrupt contacts (as drawn by Sedgwick, 1829; Fig. 2 5) with cryptalgal laminites. The dedolomites, or secondary limestones, have low base metal contents (2.4.3; Figs. 2.8 f+g) and are of irregular thickness (Fig. 2.5).

Evidence remains of their original grainstone or laminite composition (Figs. 2.6 a+b). Textures are very different from altered dolomites; there are no euhedral or subhedral dolomite, or ferroan dolomite, rhombs; remaining dolomite crystals are corroded. There is no evidence of formation of ferroan dolomite before dedolomitisation; iron oxides are lacking or of low content. No detailed cathodoluminescence or micro-probe work has yet been carried out on these dedolomites; there is no associated mineralisation.

Their irregular form, their position immediately below former evaporites, their compact, recrystallised nature and low base metal contents all suggest these dedolomites result from the dissolution of the overlying evaporites. No such dedolomites occur where the Cadeby Formation was overlain by continental strata. Dissolution and associated dedolomitisation probably occurred with uplift in the Late Tertiary or Quaternary. Descending pore waters had high Ca^{2+}/Mg^{2+} ratios and were at low temperatures and low P_{co2}, promoting incongruent dissolution of dolomite, in accord with experimental evidence of Yanat'eva (1955) and De Groot (1967). These dedolomites therefore appear to have had a separate origin from those associated with ferroan dolomite.

5.4 Calcitisation where not crystal-for-crystal replacement

5.4.1 Occurrence of calcitised gypsum and dolomite

In the Lower Member a progressive sequence of calcitisation of lagoon carbonates can be followed at Sutton Grange, North Yorks. (SE 285744). A calcite mosaic now replaces crystals interpreted as displacive discoid gypsums (Figs. 5.11 a, 3.13). Calcite also replaces the dolomicrite matrix. This calcitisation of dolomicrites commences in irregular patches (Fig. 5.11 a) but grades laterally into poikilitic calcite crystals (Fig. 5.11 b). The rock has a "bubbly"

Figure 5.11 a Pseudomorphed discoid gypsum crystal in lagoon wackestones, Sutton Grange (SE 285744). Gypsum is indicated by crystal morphology, now calcite. Surrounding dolomicrites are enclosed in poikilitic calcite (p) in some areas. Field of view is 2.2mm.

b Poikilitic calcite crystals containing corroded dolomicrites, Sutton Grange (SE 285744). Calcite crystals have 'rounded' margins with fewer dolomicrite includions. Field of view is 2.2mm.

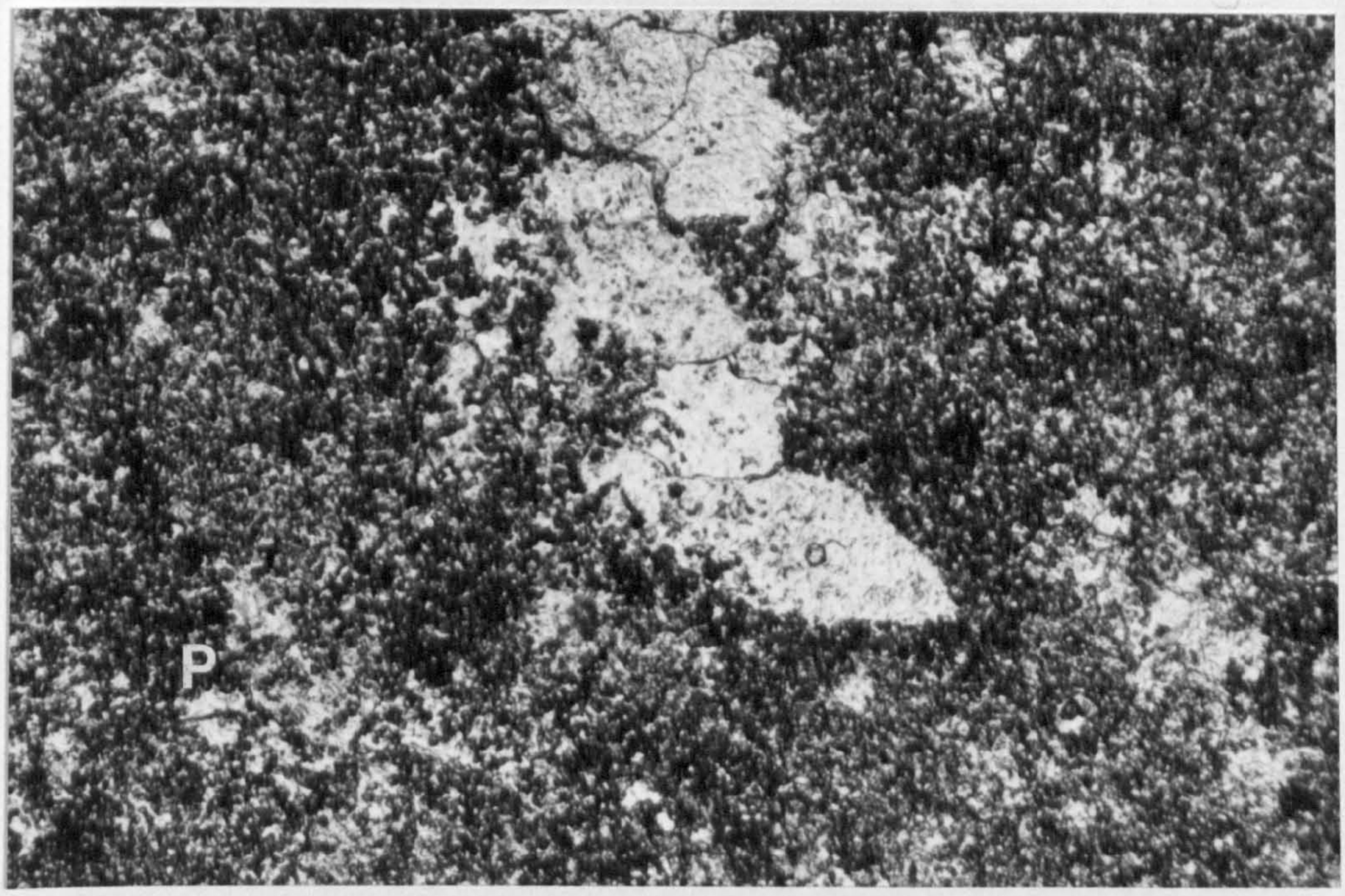
P

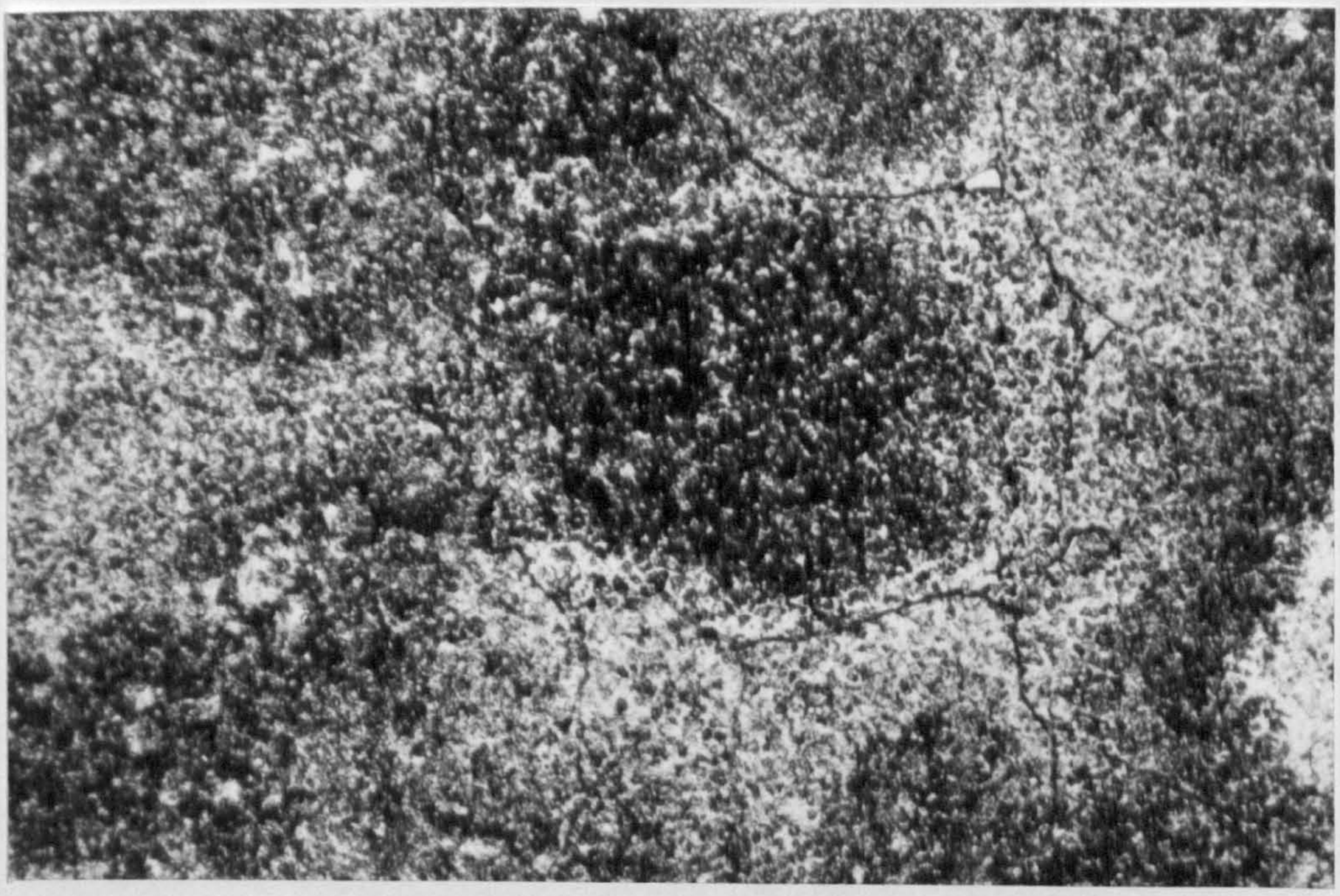

Figure 5.11 c Sub-rounded calcite crystals with concentric dolomite inclusions (arrowed), Sutton Grange (SE 285744). Radial-fibrous bladed calcite cement (B) has grown towards rounded calcites. Field of view is 2.2mm.

d Poikilitic calcite with calcite microspar and bladed calcite cement, Sutton Grange (SE 285744). Large poikilitic calcite (P) contains some dolomicrites; radial fibrous bladed calcite cement (B) has grown on calcite microspar. Field of view is 2.2mm.

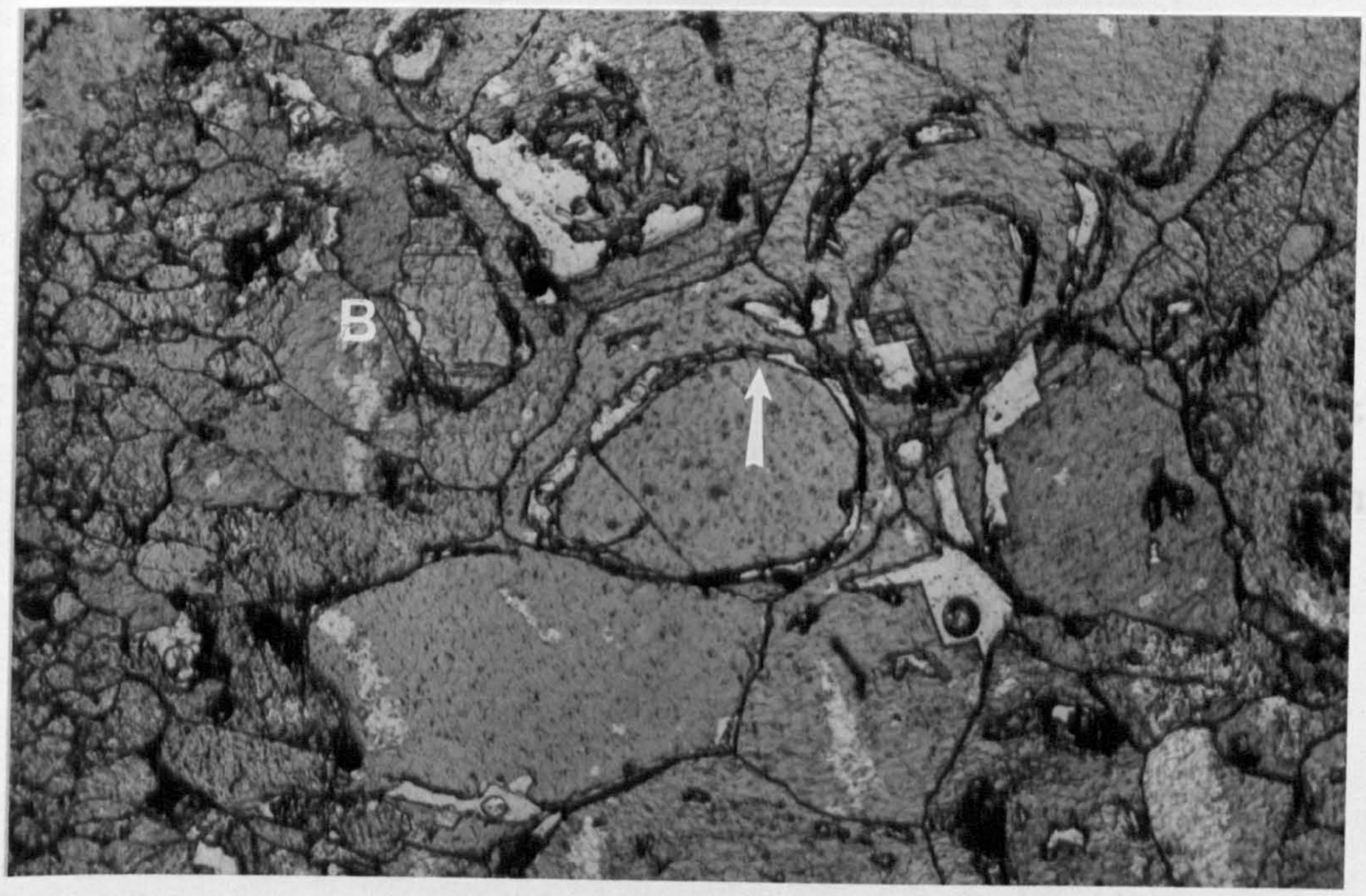
B

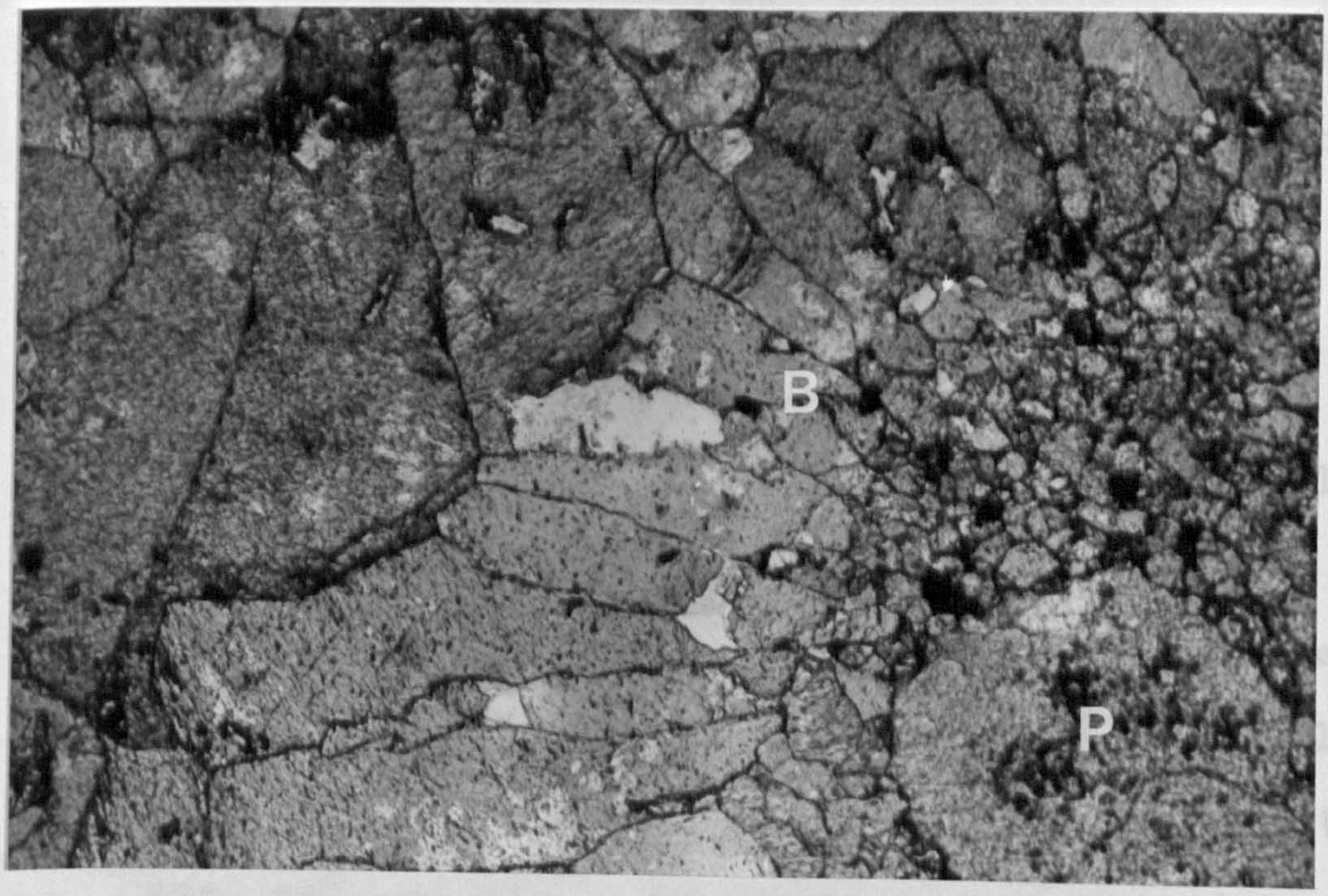
B
P

dedolomite texture (Fig 5 12 a). With further calcitisation, sub-rounded calcite crystals with concentric dolomite inclusions are found (Fig. 5.11 c). Sub-rounded or poikilitic calcites are surrounded by calcite microspar in places (Fig. 5.11 d). The microspar has sutured crystal boundaries. Bladed calcite cements (Fig. 5.11 c+d) are the last stage recognised. The resulting secondary limestone has large voids, lined with the bladed calcite cement (Fig. 5.12 b). These limestones have a similar appearance to the Devonian Pine Point host dolomites (e.g. Dunsmore, 1973; Beales and Jackson, 1975).

Field relationships show little change of volume where only gypsum has been calcitised; lateral changes to secondary limestones show some vertical expansion with more massive, structureless units where bedding is hardly discernable. Voids percentage increases with calcitisation. The overlying ooid grainstones of the Upper Member show no calcitisation. Replaced gypsum crystals may be truncated by stylolites. Whole rock XRF analysis show iron to remain below 1%, much less than in the altered dolomites (5.2); base metal contents are also low (Appendix 5, analyses 591, 573, 597 and 600). No detailed cathodoluminescence or microprobe research has yet been carried out on these calcitised dolomites, although specimens

Figure 5.12 a "Bubbly" dedolomite texture, Sutton Grange (SE 285744).

b Secondary limestone with large voids (V), Sutton Grange (SE 285744). Dolomicrite inclusions are present in some areas (d). Bladed calcite spar cement (s) lines voids.

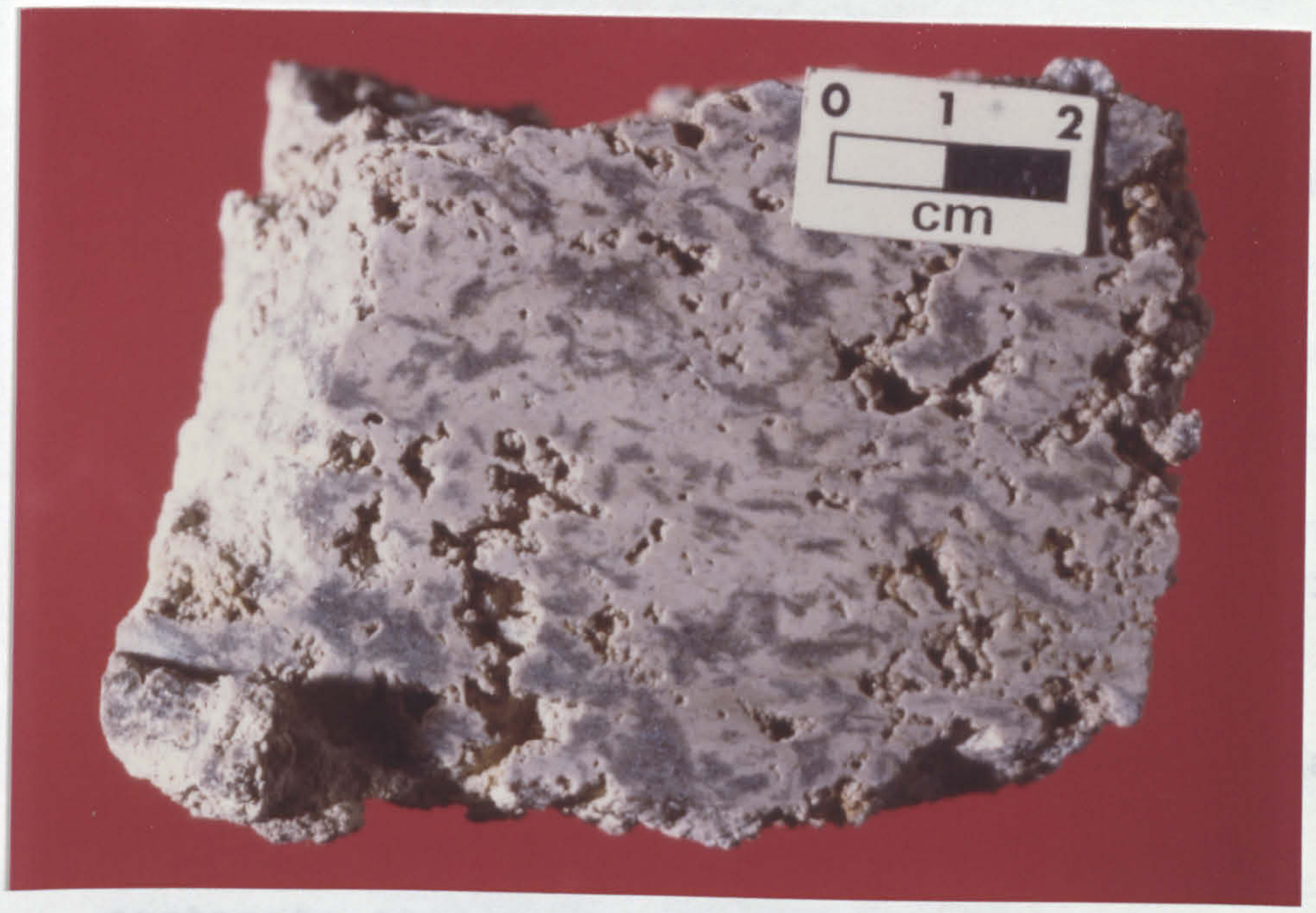
0 1 2
cm

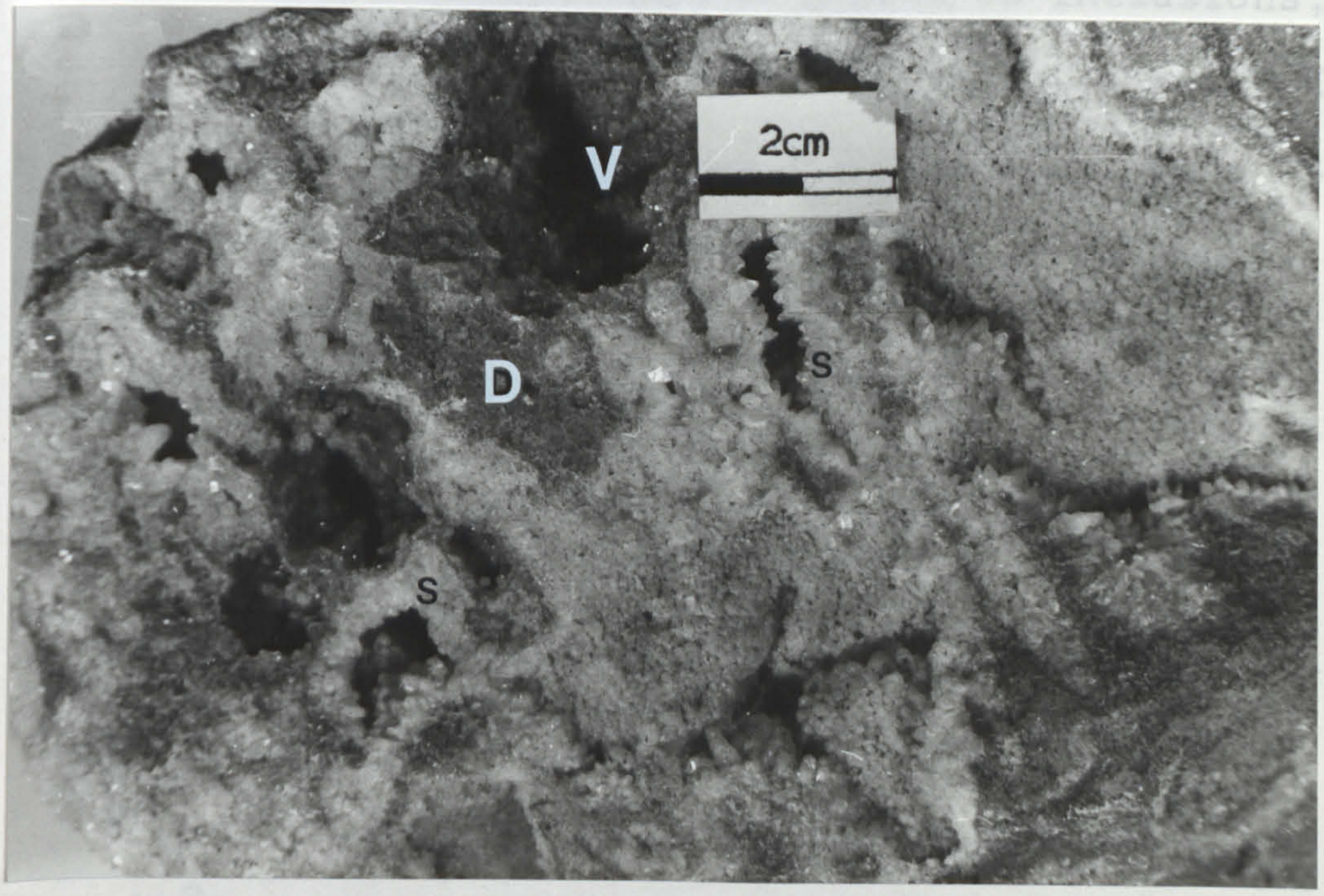
V
2cm
D
S
S

are now in preparation.

5.4.2 Mode of formation

These calcitised dolomites are characterised by their close association with evaporites and by the complete destruction of the original fabric as calcitisation proceeds.

Calcitisation here must have occurred before considerable burial and chemical compaction (i.e. pressure solution). Replacement commences with calcitisation of individual gypsum crystals (Fig. 5.11 a). Calcite growth on original carbonate inclusions within the gypsum results in the mosaic texture; the dedolomites of Evamy (1967 , Figs 3H and 4C) are envisaged to be due to similar calcite growth on inclusions, although Evamy's inclusions are of dolomite. In these Cadeby Formation sediments, more substantial evaporite and dolomite calcitisation has taken place. This may be due to a higher original evaporite content and/or some degree of evaporite dissolution. Remaining dolomite crystals are corroded. The origin of concentric dolomite inclusions in rounded calcites, and the form of of calcites themselves, (Fig. 5.11 c) is yet unknown. Pore fluids must have had high Ca^{2+}/ Mg^{2+} ratios to (i) corrode dolomites and (ii) form massive secondary limestones albeit over a small area. The lack of ferroan dolomite and low

manganese and base metal contents indicates oxic pore fluids. These are likely to have had a meteoric origin (4.5.2 and 4.5.3) although there is no evidence of associated or anoxic conditions here. Their high Ca^{2+}/Mg^{2+} ratio may result from some evaporite dissolution; voids show a volume decrease during calcitisation. These fluids could not have been derived from the overlying Fordon evaporites as the Upper Member grainstones remain dolomites; textures are also very different from the dedolomites at the top of the Upper Member (5.3). The bladed calcite cement may be of recent origin from "recent" groundwater (Harwood, 1980; Coleman and Harwood, 1980) (9.2.3).

5.5 Summary of replacement in the Cadeby Formation

Four distinct types of replacement have been recognised in the Cadeby Formation:

(1) Calcitisation of evaporites by crystal for crystal replacement

(2) Calcitisation of evaporites and dolomites with formation of mosaic calcite and some secondary limestones (5.4)

(3) Dedolomitisation by calcium-sulphate bearing fluids (5.3)

(4) Alteration of dolomites, including formation of ferroan dolomites and subsequent dedolomitisation.

The characteristics of each replacement process, the

pore fluids involved and the time of replacement is summarised on Table 5-3. Insufficient research has yet been done to apply this classification to other described 'dedolomites'. More detailed work on specimens from the Cadeby Formation is planned, although other 'dedolomites' may have mixed, or different, origins.

TABLE 5-3

SUMMARY OF DOLOMITE AND EVAPORITE REPLACEMENT

	TYPE OF REPLACEMENT	CHARACTERISTICS	FLUID	TIME OF REPLACEMENT
CALCITISATION	crystal- for crystal calcitisation (4.5.2 + 4.5.3)	Direct replacement of gypsum, anhydrite and halite by calcite Crystal peusdo-morphs slight dolomite replacement may have associated sulphide formation. Some ferroan dolomite original texture pseudomorphed.	Meteoric origin Anoxic $\frac{Ca^{2+}}{Mg^{2+}} \leqslant 1$	Penecontemporaneou
	Evaporite + dolomite calcitisation (5.4)	Mosaic replacement of gypsum Corrosion and replacement of dolomicrites. No ferroan dolomite and low Fe, Mn contents. Complete calcitisation destroys original texture and forms porous secondary limestone. Water bladed calcite void lining	Meteoric origin ?oxic $\frac{Ca^{2+}}{Mg^{2+}} > 1$	?Penecontemporaneo - Eogenetic?
DEDOLOMITISATION	Dedolomitisation by $CaSO_4$-rich fluids	Close association with overlying evaporites. Forms compact secondary limestones with few voids. Remnants of original texture preserved. Corroded dolomite cyrstals. Low base metal and FeMn contents.	Meteoric origin oxic $\frac{Ca^{2+}}{Mg^{2+}} \gg 1$	Telogenetic
	initial stage Altered dolomites	Change of crystal form from anhedral to subhedral or euhedral. Remobilisation to limpid crystal rims and ferroan dolomite centres - 'grumeleuse' texture. Partial destruction of original fabric High Fe Mn content.	anoxic High Fe^{2+} $\frac{Ca^{2+}}{Mg^{2+}} \geqslant 1$	Mesogenetic
	later stage	Dedolomitisation of rhombs or zones with rhombs. Formation of Fe oxides and FM calcite in opaque zones with high solubility. Possible later leaching. High Fe + Mn content Destruction of original texture	Anoxic/ oxic some Fe^{2+} content $\frac{Ca^{2+}}{Mg^{2+}} > 1$	Mesogenetic + Telogenetic

CHAPTER 6

DIAGENETIC HISTORY OF THE CADEBY FORMATION

6.1 Evidence from previous chapters

The aim of this chapter is to combine evidence of the previous two chapters and, with some new evidence, present the succession of events that took place, and are taking place, during the diagenesis of the Cadeby Formation. Figure 6.1 summarises the evidence from Chapters 4 and 5; it also provides the basic framework of this chapter. Diagenetic environments are classified as penecontemporaneous, eogenetic, mesogenetic and telogenetic (Fig. 4.1). The main processes in each environment are (i) cementation and replacement (ii) dissolution and leaching and (iii) compaction, both mechanical and chemical (pressure solution). These processes control porosity and permeability of the sediments, excluding fracture porosity. Porosity occluding and porosity forming events are indicated on Figure 6.1.

6.2 Penecontemporaneous processes

6.2.1 Cementation and replacement

Penecontemporaneous cementation and replacement were reviewed in 4.5.2, 4.5.3 and 5.4. They include displacive evaporite formation, dolomitisation and evaporite calcitisation.

Figure 6.1 Summary diagram of diagenetiC events

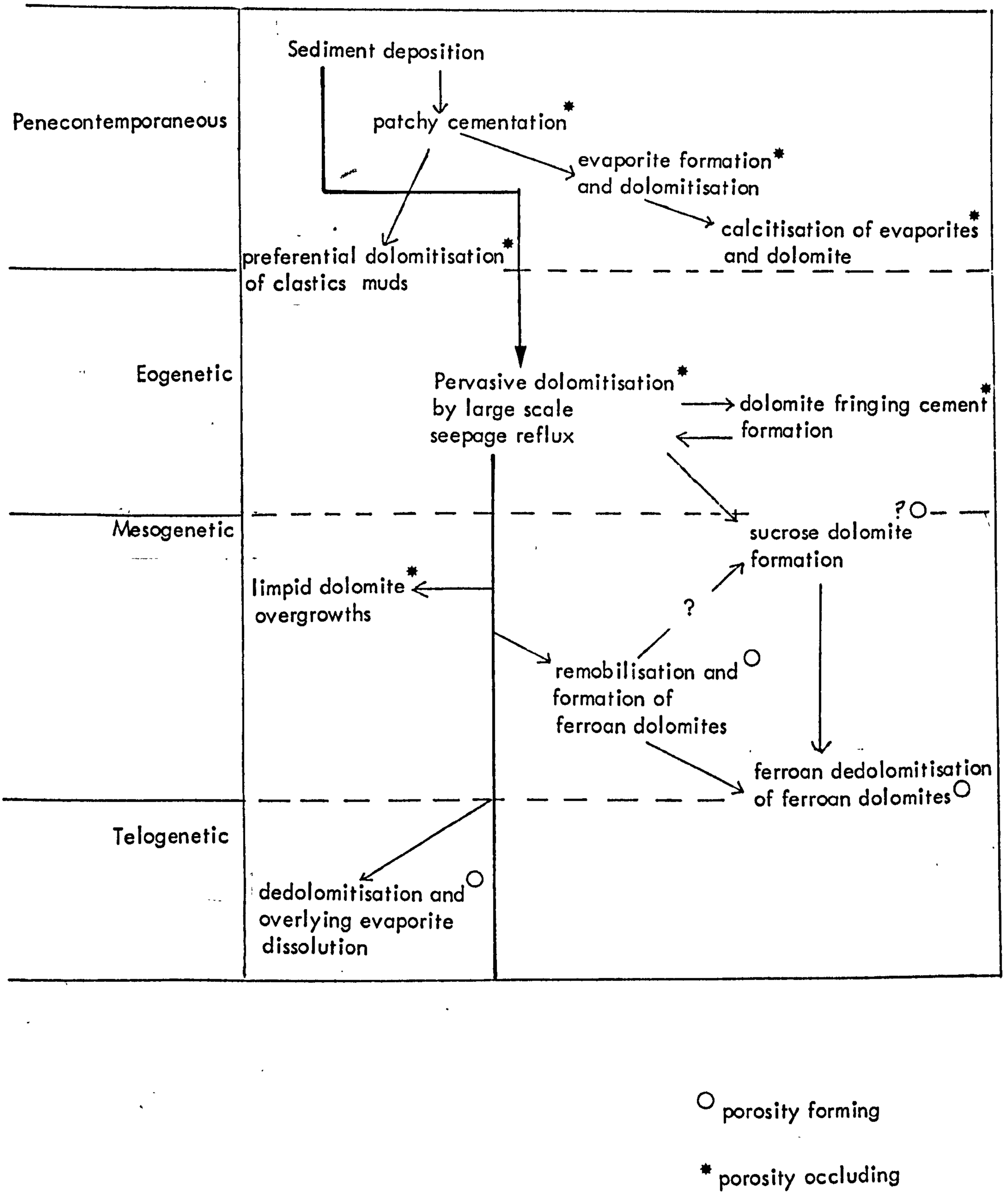
Penecontemporaneous
Sediment deposition
patchy cementation*
evaporite formation* and dolomitisation
calcitisation of evaporites* and dolomite
preferential dolomitisation* of clastics muds
Eogenetic
Pervasive dolomitisation* by large scale seepage reflux
dolomite fringing cement* formation
?O
Mesogenetic
sucrose dolomite formation
limpid dolomite* overgrowths
?
remobilisation and O formation of ferroan dolomites
ferroan dedolomitisation of ferroan dolomites O
Telogenetic
dedolomitisation and O overlying evaporite dissolution
O porosity forming
* porosity occluding

Penecontemporaneous dolomitisation is facies dependent and affects only a small volume of the Cadeby Formation (4.5.2, 4.5.3 and 4.6) Few original limestones are preserved in the Cadeby Formation, calcite wackestones in the Lower Member (Appendix 6, Log 10) owe their preservation to penecontemporaneous cementation (4.5.4) and their position at the base of the formation (4.5.7).

6.2.2 Dissolution and leaching

Dissolution and leaching in the pene-contemporaneous environment is difficult to detect. Early events are masked by dissolution and leaching later in the sediment history (6.3.3, 6.4.2 and 6.5.2).

6.2.3 Compaction

Compaction during penecontemporaneous diagenesis is predominantly mechanical. Burial is minimal; thin walled skeletons fracture from the pressure of over-burden with little displacement of clasts (Fig. 6.2). Soft peloids are compacted in many areas (Fig. 6.3d) although early cementation can prevent this (Fig. 4.13d). Ooids and pisoids are rigid (Fig. 6.3c). Compaction takes place within soft sediments and may result in a porosity decrease of 30%-40% (Shinn et al., 1977).

Figure 6.2 Mechanical composition of thin-walled ?mollusc shell in dolomite skeletal wackestones, Gebdykes Quarry (SE 237823). Shell fragments show little displacement. Field of view is 2.2mm.

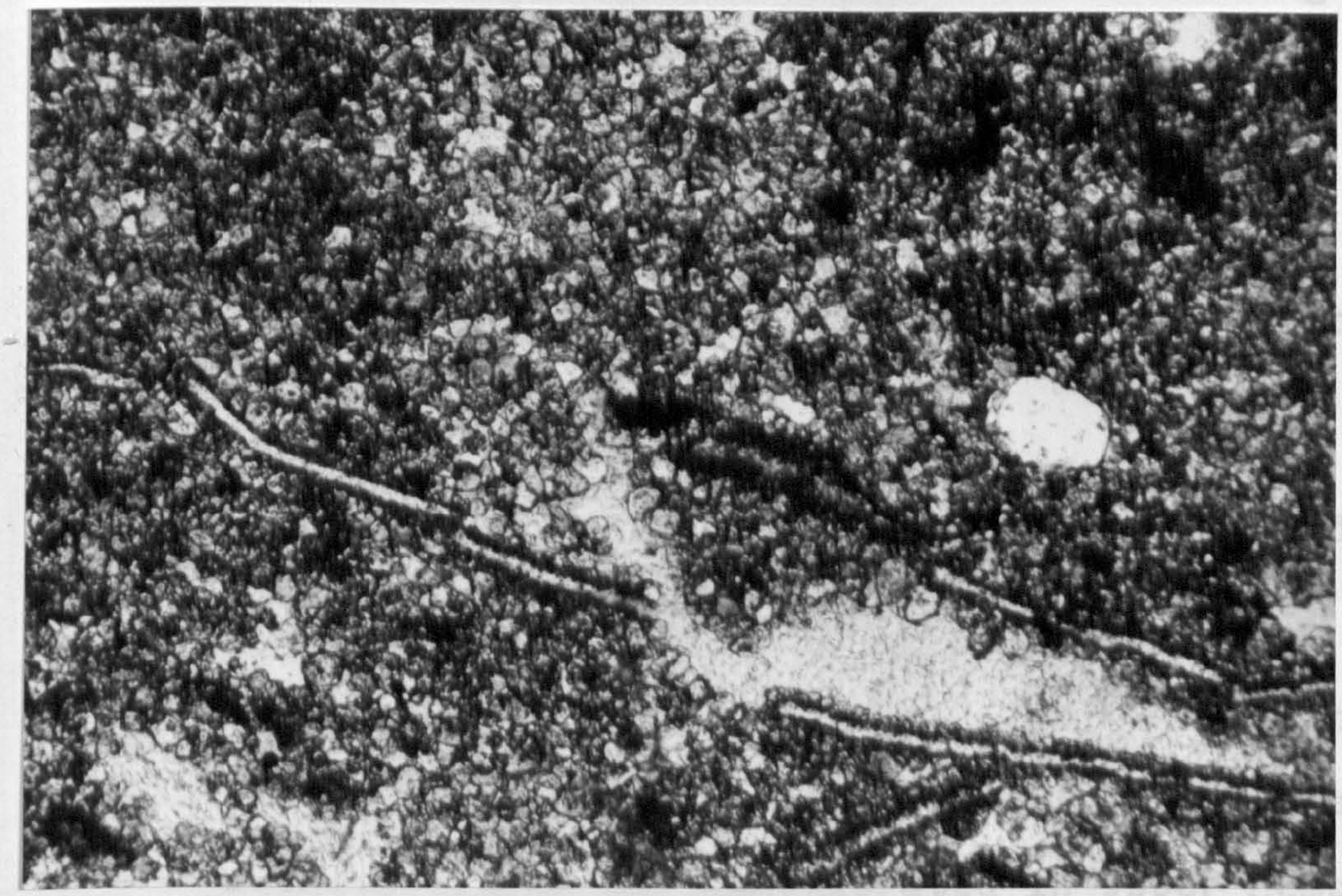

6.3 Eogenetic processes

6.3.1 Cementation and replacement - dolomitisation

Eogenetic dolomitisation is prevasive (4.5.5 - 4.5.7, 4.6); it demonstrably occludes porosity as peloid grainstones become an interlocking mosaic of dolomite crystals (Figs. 4.13a, b + d). Eogenetic dolomitisation is largely independent of facies. It is the main dolomitisation event but has had little effect on previously dolomitised carbonates.

6.3.1 Comentation and replacement - replacive and pore-filling evaporites

Core sections throughout the Cadeby Formation contain replacive (or metasomatic) evaporites although these are concentrated in Upper Member grainstones. No replacive evaporites occur in the more siliciclastic facies in the south of the area. Cores from the Selby coalfield (e.g. Appendix 6, Log 11) show almost complete replacement of the top few metres of cryptalgal laminites of the Upper Member (Fig. 6.3a). Clark (1980) has noticed replacement in subsurface sections of the Z1 and Z2 carbonates in the Netherlands and Denmark. Evaporite-filled peloid and pisoid centres also occur (Fig. 6.3 b + c). Irregular clusters of evaporite crystals, with outlines

Figure 6.3 a Replacement of peloids near to of Upper Member by evaporites, Wistow Wood borehole (SE 567356). Evaporite is now gypsum after anhydrite; anhydrite inclusions (arrowed) are corroded. Evaporite has totally replaced much of peloid grainstone. Field of view is 2.75mm.

b Gypsum after replacive anhydrite in peloid centres in Upper Member packstone, Wistow Wood borehole (SE 567356). Field of view is 2.2mm.

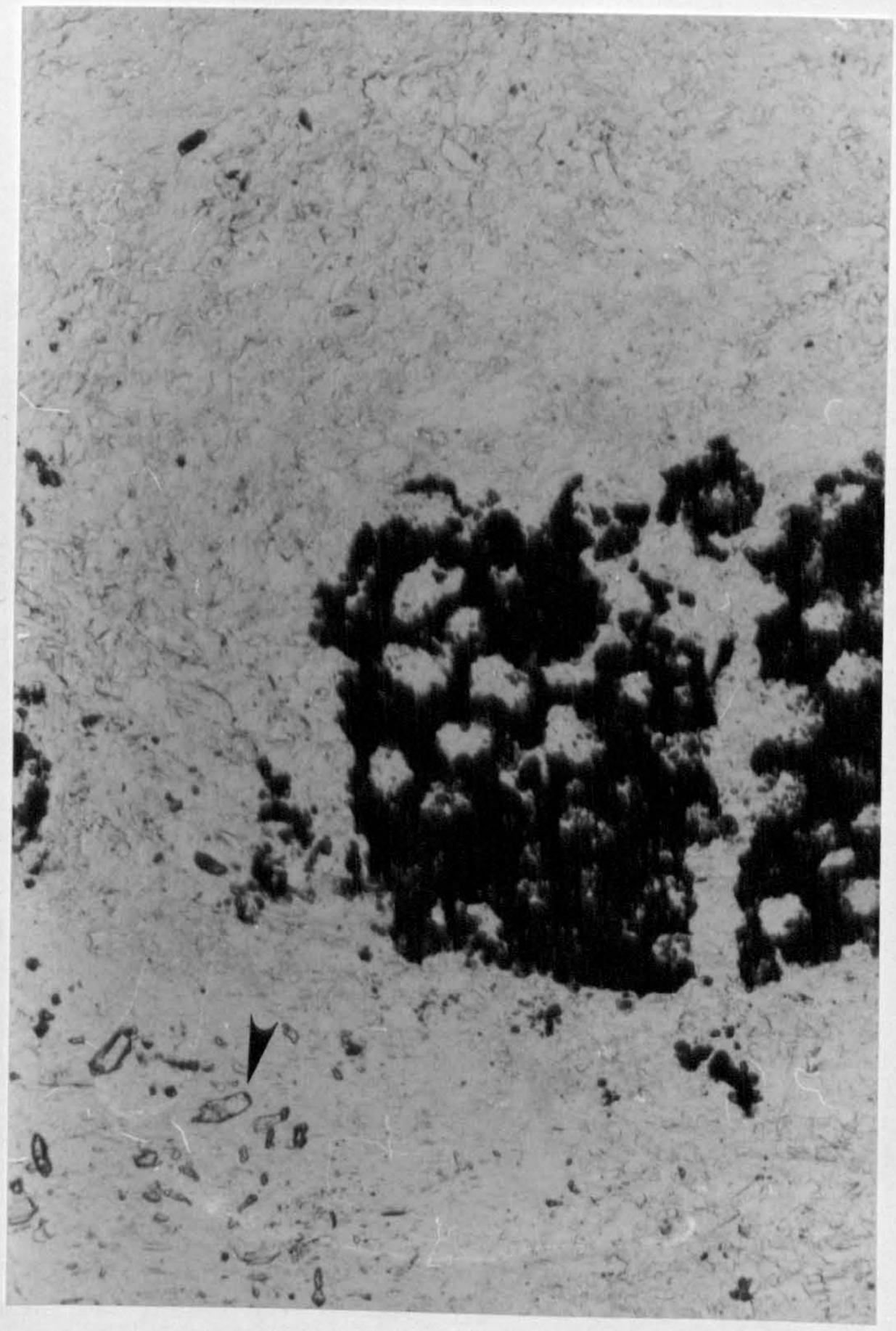

Figure 6.3 c Gypsum after anhydrite replacing pisoid centres in Upper Member packstone, Wistow Wood borehole (SE 567356). Some pisoid centres have remained as evaporite (E) whereas others have been calcitised (C). Field of view is 3.45mm.

d Irregular cluster of replacive evaporite crystals in Upper Member peloid grainstone, Wistow Wood borehole (SE 567356). Evaporite now gypsum after anhydrite. Fabric of compacted peloids is continuous across replacive cluster. Some crystal outlines are rectilinear, indicating original evaporite was anhydrite. Field of view is 2.2mm.


C
C
E

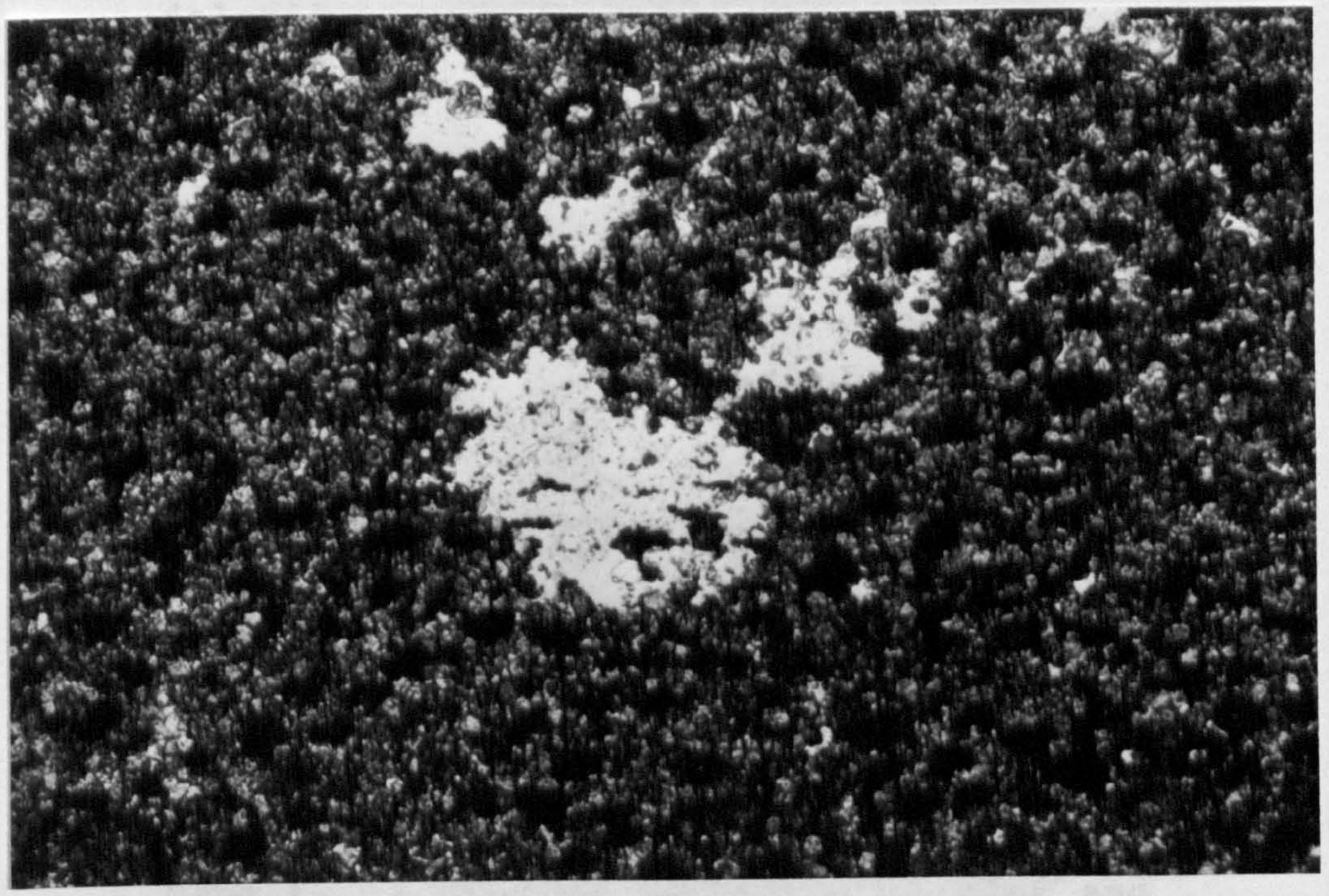

in part irregular, in part rectilinear, reach up to several centimeteres in diameter (Fig. 6.3d); Harwood, 1980, Fig 3). Corroded dolomite crystals "float" in the evaporites (Fig. 6.4a). In the more clastic, nearer basin, nodular carbonates (3.2.2) (Fusezy, 1970; 1980; Kaldi, 1908b) compaction has occ-urred around the replacive evaporites (Fig. 6.4b).

The replacive nature of these evaporites is shown by: (i) presence of rectilinear crystal boundaries, indicating original replacement was by anhydrite (Figs. 6.3d, 6.4; Harwood 1980) (ii) inclusion of corroded dolomite crystals within the evaporites (Fig. 6.4a; Clark, 1980, Fig. 5c) (iii) continuation of sedimentary laminations through the evaporites without distortion (Harwood, 1980, Fig. 3; Clark, 1980, Fig. 6A).

Fowler (1944), Raymond(1953) and Jones (1969) have noted "replacement" anhydrite evaporites in English subsurface cores. Clark records metasomatic evaporites from the subsurface Zechstein carbonates of the Netherlands and Denmark, including replacive nodular and enterolithic anhydrite (Clark, 1980; Clark and Tallbacka, 1980). No replacive nodular or enterolithic anhydrite was noticed in core

Figure 6.4 a Corroded dolomite crystals in replacive evaporite, Wistow Wood borehole (SE 567356). Gypsum (after anhydrite) contains corroded dolomite redicts. Evaporite outline in dolomite shows rectilinear and castellated margins (arrowed), showing original evaporite was anhydrite. Field of view is 0.55mm.

Page scanned as
original

Figure 6.4 b Compaction of siliciclastic mud-rich dolomites around replacive evaporite crystals, Bank End borehole (SK 706972).

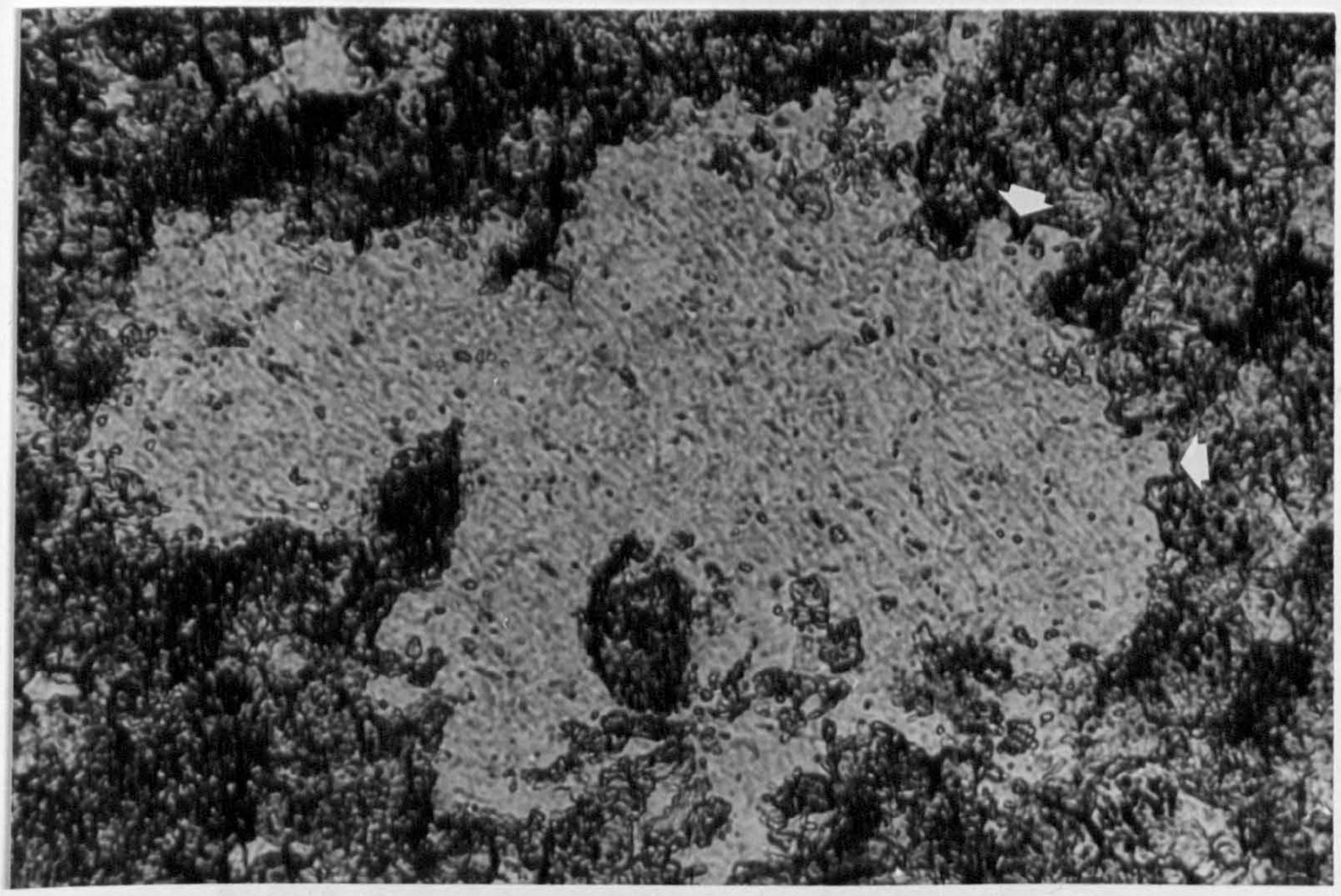

sections studied from the Cadeby Formation; nodular anhydrite was restricted to marl-rich beds within evaporite sequences where formation of both nodules and the few enterolithic structures present appeared pene-contemporaneous, Shearman (written communication, 1977) noticed similar replacive anhydrite in the Mississippian Madison Lime-stone of SE Saskatchewan; peloids were partially replaced. Anhydrite clusters also have rectilinear and irregular outlines. Moore (1981, Fig.7a) shows similar replacive anhydrite.

Clark (1980, Fig.5a) attributes anhydrite in peloid centres to meteoric leaching and subsequent pore-filling evaporites. In the Cadeby Formation peloids with evaporite cores are found throughout several metres near the top of the Upper Member. In places peloid walls are also replaced (Figs.6.3a + b). Leaching with later pore-filling evaporites is not feasible here, as peloid walls would fracture and collapse throughout this thick-ness. No fracturing of peloid walls is observed. The occurrence of some dolomite inclusions within the evaporites (Figs.6.3a-c) also indicates replacement here rather than

a later evaporite cement. Pore-filling evaporites do, however, occur; they occlude any porosity remaining after dolomitisation. Pore-filling evaporites were present further south and west (i.e. towards the basin margin) than replacive anhydrite. Approximate boundaries are shown in Figure 6.5.

Evaporite replacement occurred after dolomitisation (Fig. 6.4a) but before final compaction (Fig. 6.4b). Calcium sulphate-rich fluids were derived from, or were groundwaters associated with, the overlying evaporites as (i) replacement is more common near the top of the Cadeby Formation and (ii) no replacive evaporites occur where the Cadeby Formation is overlain by continental sediments. The calcium sulphate-rich fluids could result from the conversion of original gypsum in the Hayton Anhydrite to anhydrite. The large volume of crystal water expelled in this transition could be forced downwards through the underlying porous carbonates (Clark, 1980). Reflux brine flow, causing dolomitisation perhaps during deposition of the Hayton Anhydrite (4.5.7) was in the same direction; a similar "re-flux" movement may have promoted circulation of the calcium

Figure 6.5 Map showing the approximate extent of replacive evaporites, pore-filling evaporites and possible areas free of later evaporites within the Cadeby Formation.

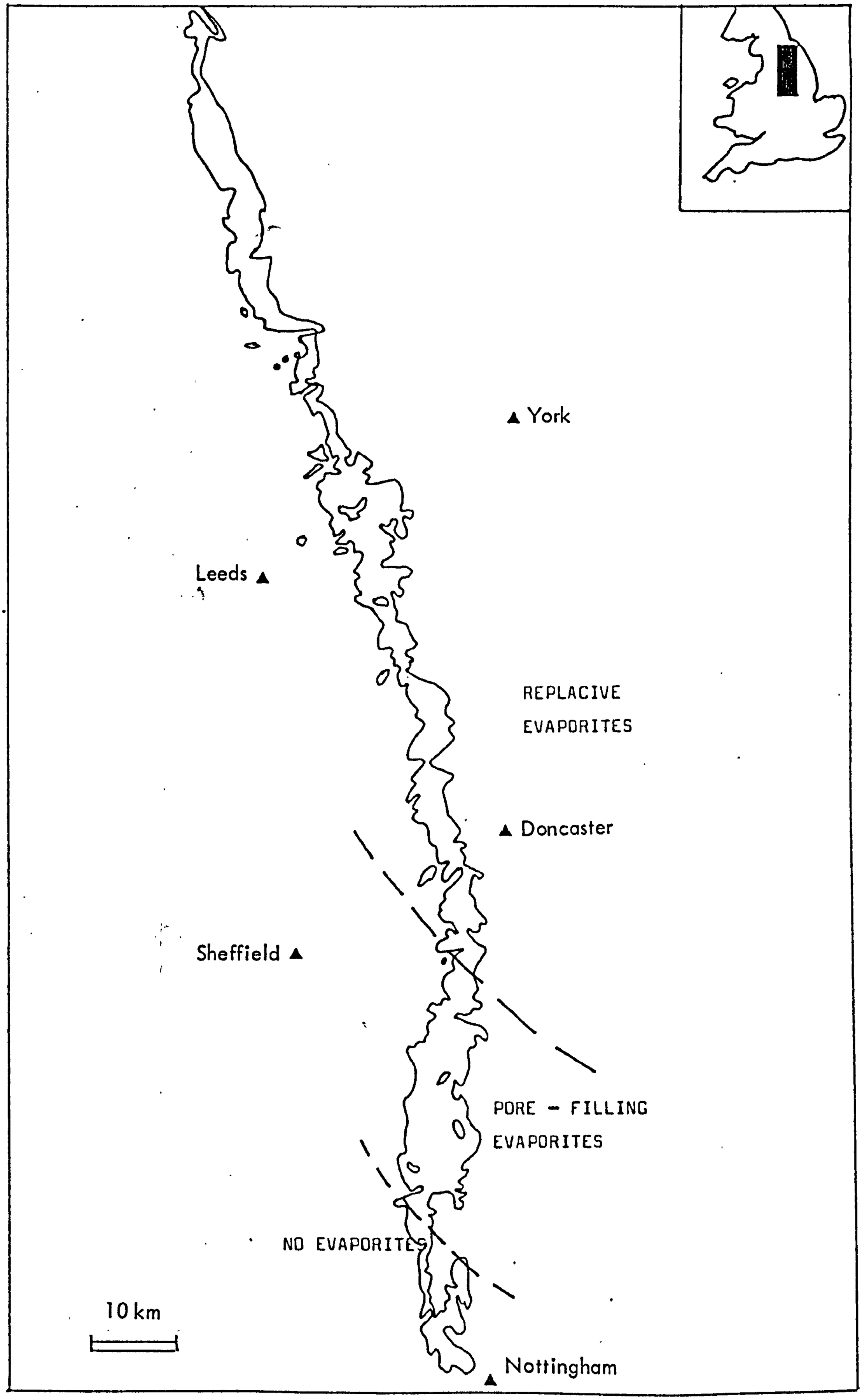
York
Leeds
REPLACIVE
EVAPORITES
Doncaster
Sheffield
PORE - FILLING
EVAPORITES
NO EVAPORITES
10 km
Nottingham

sulphate-rich fluids responsible for replacement by evaporites. Replacement of dolomite by anhydrite may thus be caused by both reflux flow and expulsion of crystal water from overlying evaporites.

Rectilinear outlines and castellated margins indicate that replacement was by anhydrite. The gypsum-anhydrite transition takes place above 42°C at low pressures under equilibrium conditions (Deer et al., 1962). With surface temperatures perhaps averaging 20°C and an average geothermal gradient of $25^{\circ}Ckm^{-1}$, this temperature would be reached in less than one kilometre burial. Present subsurface transition of anhydrite to gypsum takes place between five and three hundred metres in Eastern England today, although throughout the French Alps anhydrite is found at 200m (A. Siddans, pers. comm., 1981). Thus, extrapolating, the gypsum-anhydrite transition in the Cadeby Formation took place at depths of less than 500m during sediment burial; this includes formation of anhydrite in near surface environments. Expulsion of crystal water must have accompanied this transition; replacement by evaporites thus occurred near this depth range. Clark (1980) obtained a narrower (300-600m) range on temperature considerations only. A

consequence of this is that the preceding dolomitisation must have occured at similar, or shallower, depths, reinforcing the hypothesis that most dolomitisation was eogenetic.

Sulphur isotope determinations (9.2.2) show the replacive anhydrite to have sulphur isotope values derived from Upper Permian sea water sulphate. The replacive evaporites are therefore of Upper Permian age, or represent remobilised Upper Permian evaporites which have had no isotopic modification.

Although Clark (1980) records the presence of replacive halite post-dating replacive anhydrite in cores from the Netherlands and Denmark, no unequivocable evidence of replacive halite has been found in the Cadeby Formation. Replacive halite may be more common in the basin centre; it formed during mesogenesis.

6.3.3 Dissolution and leaching

In most of the Cadeby Formation there is no evidence of dissolution and leaching during eogenesis. The predominant processes were dolomitisation and replacement by anhydrite; tight carbonates with porosities below 5%

resulted. Supratidal and exposed environments contain leached peloid cores (4.5.8) showing evidence of little meteoric fluid circulation at the top of both Members.

Dissolution took place in the patterned carbonates (3.2.13). It combined with sulphate reduction in interbedded evaporites to produce anoxic dolomicrites with high porosites (Appendix 6, log 11; Fig. 3.17a). Formation of patterned carbonates was eogenetic (Dixon, 1976; Kendall, 1977); later limpid dolomite overgrowths reinforce this hypothesis in the Cadeby Formation (4.5.10). A belt of porous patterned carbonates extends for several kilometres within the area of the Selby coalfield (Appendix 7, Fig. A7.3); they are found at the base of the formation and are underlain by Permian Basal Sands which in places attain over 20 metres in thickness (Appendix 7, Fig. A7.1). The Basal Sands today form an overpressured aquifer; overpressuring by anoxic ground waters during eogenesis of the Cadeby Formation may have triggered sulphate reduction and formation of the patterned carbonates. This occurred within a narrow, facies-controlled belt (Appendix 7, Fig. A7.3); pore waters were more

saline higher in the formation. The high degree of overpressuring in this belt today has presented engineering problems during coalfield exploitation.

6.3.4 Compaction

Evidence for compaction during eogenesis is apparently restricted to the fractured ooid envelopes described by Kaldi (1980a, Fig 7. 10). Lack of planar or sutural boundaries in the ooid and peloid grainstones show dolomitisation occurred before substantial burial (4.5.5) and produced a lithified carbonate rock resistant to both mechanical and chemical compaction during eogenesis.

6.4 Mesogenetic processes

6.4.1 Cementation and replacement

Replacement by evaporites may have continued in early mesogenesis, along with the formation of sucrose dolomites (4.5.9). The growth of these large, subhedral/subhedral rhombs was initiated during eogenesis (4.5.5). Alteration of some crystals to ferroan dolomite and associated dolomite remobilisation occurred within restricted zones (5.2.3). Limpid dolomite overgrowths, not associated with the above events, formed in

few places (4.5.10).

Cementation and replacement during mesogenesis was minor compared with that which had occurred earlier (6.3.1 and 6.3.2).

6.4.2 Dissolution and leaching

Dissolution and leaching during mesogenesis was mainly associated with dolomite alteration, both with dolomite remobilisation and with dedolomitisation (5.2.3 and 5.2.4). Increase in porosity with increased remobilisation is shown by the presence of intercrystalline cements (5.2.3; Figs. 5. 3d + e). Leaching of FM cal and iron oxides appears to have been restricted to the telogenetic environment. Dolomite alteration is confined to certain restricted areas and thus is only important as a porosity-creating process within those areas.

Some leaching of anhydrite also took place in a few areas during mesogenesis since limpid dolomite overgrowths are found in some voids (4.5.10; Fig. 4.23) and baryte occupies the site of displacive anhydrite nodules (see 8.5.1).

6.4.3 Compaction

Compaction during mesogenesis is predominantly chemical. Pressure solution has generally a small effect throughout most of the Cadeby

Formation at outcrop with a possible 5% volume loss (D. B. Smith, pers. comm., 1981). Low amplitude stylolites and non-sutured seam solution (Wanless, 1979) are dependent both on facies and diagenetic history. Stylolites often follow the base of beds in peloid grainstones and siliciclastic packstones and grainstones, often above clay drapes. Estimates of amount of compaction here are impractical as original clay thicknesses are unknown. In cores, stylolite amplitudes seldom exceed one or two centimetres; subvertical stylolites also occur. Fusezy (1970) describes stylolite configuration in some detail. Kaldi (1980a) shows authigenic kaolinite displaced by late dolomite rhombs (? mesogenetic) in some sutures; he relates this to microenvironments in and around the stylolites. Where preferential cementation has occurred, non-sutured seam dissolution has taken place in the surrounding, non-cemented areas (Figs.6.6a, 4.12a). Similar non-sutured seam disssolution occurs in dolomite mudstones around some replacive evaporites (Fig.6.4b).

The combined cover of Mesozoic sediments over the Cadeby Formation probably never exceeded

Figure 6.6 Non-sutured seam dissolution around areas of early cement, Bank End borehole (SK 706972). Carbonaceous fragments (opaque) show little preferential compaction in cemented zone, but are compacted along seams in areas of non-sutured seam dissolution. Note also compaction around bryozoan fragment (B). ▲Field of view is 3.45mm.


B

one or two kilometres in the outcrop area. Pressure solution therefore had a minor effect on these carbonates. Chemical compaction increases towards the basin centre with lithological changes and increased pressure of overburden.

6.5 Telogenesis

6.5.1 Dissolution and leaching

Dissolution and leaching are the major processes within the telogenetic environment; they are hence described before cementation and replacement.

As uplift proceeds, anhydrite is hydrated to gypsum in the shallow subsurface (6.3.2). Near the surface, gypsum is subsequently leached within the zone of fluctuating groundwaters. Gypsum leaching results in (i) exhumation of earlier moldic and intergranular porosities and burrow forms (Figs. 6.7a), (ii) production of vugs from displacive evaporites (Fig. 6.7b), (iii) vug formation from replacive evaporite dissolution (Harwood, 1980, Fig. 3), (iv) formation of dedolomites from dissolution of thick evaporite sequences (5.3) and (v) combined with meteoric water, leaching of FM calcite and ferric oxides.

The Cadeby Formation is well known for the high

Figure 6.7 a Moldic porosity in skeletal wackestone/packstone "Bakevellia bed", Well (SE 257812). Porosity is occluded by calcite (stained) (arrowed) although there is still effective leached porosity (L). Field of view is 2.2mm.

b Open vugs resulting from dissolution of displacive evaporites, Vale Road Quarry, Mansfield Woodhouse (SK 532648). Hammer is 0.4m long.

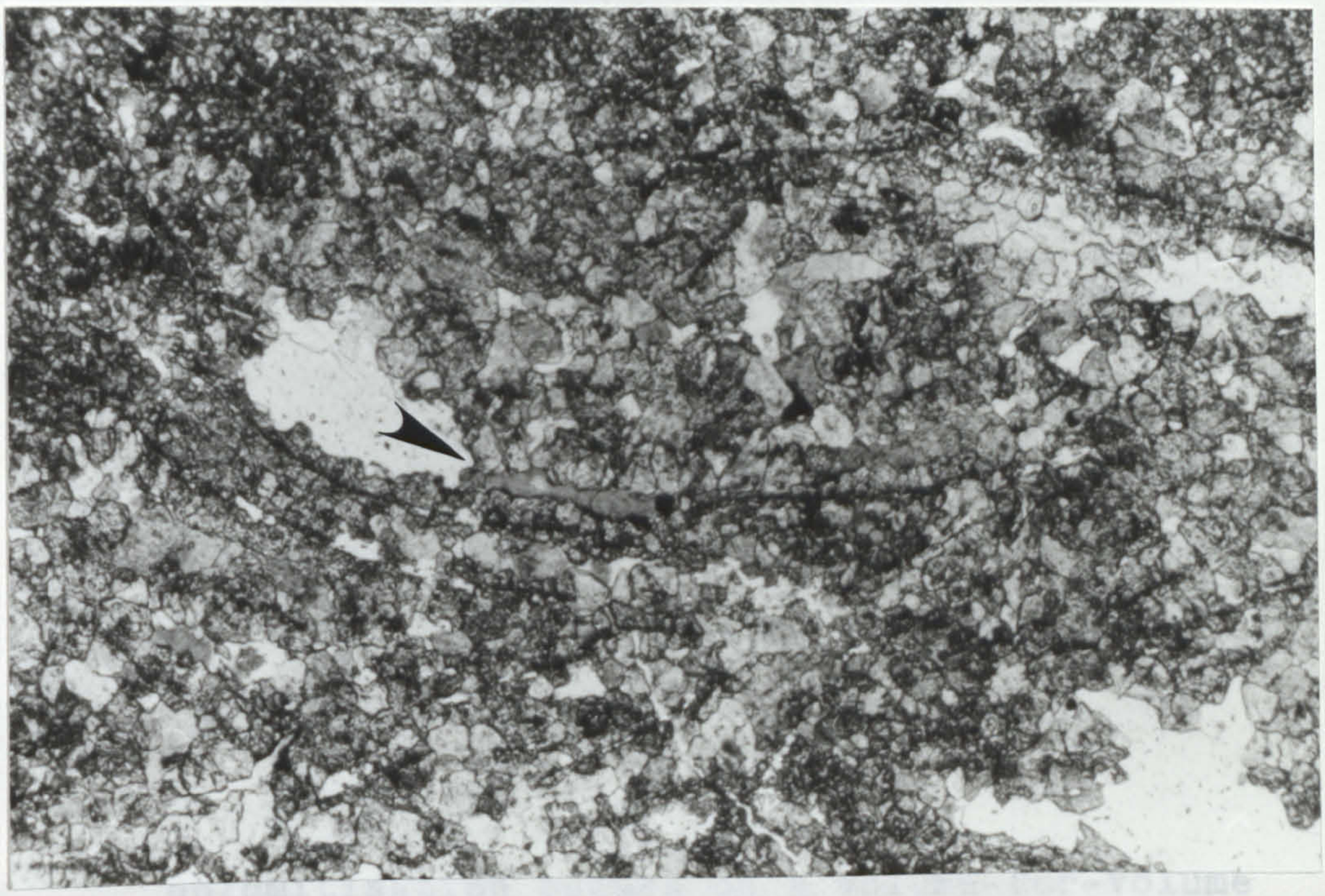

proportion of voids at outcrop. Guy (1911) first proposed these voids resulted from evaporite dissolution, although he did not comprehend the replacive nature of many of the evaporite occurrences. Later authors, including several general handbooks, related vug formation to volume decrease during dolomitisation of calcite. There is a high possibility that much of the Cadeby Formation was still aragonite during dolomitisation (4.5.5). Petrographic evidence shows no volume decrease during dolomitisation; initial dolomitisation occurs on a volume-for-volume basis with some later volume increase from pore-filling dolomite (4.5.5). These factors, with the existence of replacive evaporites in the subsurface (6.3.2), favour Guy's interpretation of the vug origins (Guy, 1911), although it is now well known that these result from dissolution of both replacive and displacive evaporites (Harwood, 1980).

Shearman (written comm., 1977) has commented that other examples of replacive evaporites are rich in inclusions; leaching of these results in a layer of internal sediment on the vug floors, as in the Jurassic limestones of the Lot Valley, S.W. France. This geopetal

sediment is lacking on most floors of the vugs formed by dissolution of replacive evaporites in the Cadeby Foramtion. However, inclusions of corroded dolomites within the metasomatic evaporites of the Cadeby Formation are not abundant. Replacement of dolomite by anhydrite is perhaps more efficient than replacement of calcite; this could be due to the presence of magnesium in the carbonate lattice. Consequently, geopetal sediment within these vugs would be slight.

The dedolomites at the top of the Upper Member are often compact (5.3) but, in the lower levels of the Hayton Anhydrite, dissolution and leaching of interbedded dolomites and evaporites result in cavernous dedolomites, many re-cemented by calcite and similar to the cargneules of the French Alps. Dissolution of the Hayton Anhydrite creates engineering hazards along much of the strike, with formation of collapse funnels and structures, many incorrectly described as sink holes on ord-nance survey maps (3.4.7). Foundering of the overlying Brotherton Formation (EZ 3Ca) is severely affecting buildings in Ripon today (Fig. 6.8)

Leaching and dissolution of dolomites produces the buff appearance of many exposures (5.2.6).

Figure 6.8 Distortion of building from foundering Brotherton Formation, Ripon. Evaporite dissolution in the Ripon Formation leads to foundering of overlying strata.

Leaching of FM calcite and ferric oxides results in effective inter-and intra-crystalline porosities in a soft, friable rock. This leaching is a pervasive process which only usually takes place within one or two metres of the exposed surface. Intense weathering during the Pleistocene, however, has penetrated further, producing a deeply weathered rock. This took place in the Wharfe Valley, south of Wetherby (SE 395470) where excavations for a new sewerage scheme showed considerable weathering of the dolomites along the valley margins at depths in excess of five metres.

6.5.2 Cementation and replacement

Both types of dedolomite formed in the telogenetic environment involve replacement (5.2.4 + 5.3). Ferroan dolomites are replaced by FM calcites and ferricoxides susceptible to leaching (5.2.5); dedolomites formed from $CaSO_4$-rich fluids are more compact and contain purer calcites (5.3).

The dissolution of evaporites and leaching of dolomites produces a calcium-saturated groundwater. This may precipitate calcite spar into vugs formed by evaporite dissolution; these calcites have negative $\delta^{13}C$ values and $\delta^{18}O$ values typical of Late Tertiary to

present day meteoric waters (9.2.3), (Harwood, 1980, Fig 3; Coleman and Harwood, 1980). These calcite cements may occlude small vugs; in large vugs individual calcite spar crystals may exceed two centimetres. The bladed spar of the calcitised dolomites (5.4) may result from this "recent" precipitation.

Many exposures have "hairline" cracks now cemented by calcite. These calcites are also of "recent" origin. These irregular small fractures may result from fracturing with release of overburden. They may also be formed by hydraulic fracturing associated with growth of fibrous gypsum. This fracturing may result in an "auto brecciated" texture.

6.6 Diagenetic history of the Cadeby Formation

The diagenetic history of the Cadeby Formation is summarised in Figure 6.9. The major processes were eogenetic dolomitisation and replacement by metasomatic anhydrite; both these processes occlude porosity. During mesogenesis, alteration of dolomite led to formation of secondary porosity within certain areas. Uplift into the telogenetic environment did not take place until late Tertiary in Eastern England; inclusion of blocks of ooid

Figure 6.9 Summary diagram of the diagenetic history of the Cadeby Formation.

PENECONTEMPORANEOUS

TELOGENESIS

Sediment Surface

DEPOSITION

MECHANICAL COMPACTION

patchy cementation

evaporite formation

dolomitisation

(calcitisation)

exposure and leaching

*LEACHING OF CARBONATES

secondary calcite cements

*dedolomitisation

*PERVASIVE DOLOMITISATION

formation of fringing dolomite cements*

*Gypsum

EOGENESIS

sucrose dolomite formation*

*PORE FILLING and REPLACEMENT BY ANHYDRITE

*Anhydrite

*ferroan dedolomitisation

leaching and later limpid overgrowths*

*ferroan dolomite formation and dolomite alteration

Depth of Burial (log scale)

PRESSURE SOLUTION

MESOGENESIS

continued burial

Actions of differing fluids

- ✦ hypersaline
- ✧ meteoric
- * mixed water
- • deep circulating waters

★ facies dependent

* dependent on diagenetic enviroment

grainstones within Pleistocene glacial gravels show this had occurred by late Quaternary. Ground water percolation caused, and is causing, evaporite dissolution with pervasive alteration of exposed carbonates. Secondary limestones at the top of the formation result from the dissolution of the Hayton Anhydrite. Later calcite cements occlude some leached porosity.

6.7 Control on porosity

Porosity control is dependent on the diagenetic processes. No primary porosity has been observed in the Cadeby Formation apart from modified primary porosity within patch reefs in some burrow traces (Fig.3.25) and exhumed fenestra-e (Fig.4.16a). Porosity cannot in general be related to depositional environments, although some facies, particularly the ooid/peloid grainstones, are more likely to contain secondary leached porosities. No examples of effective fracture porosity have been found in exposures.

Figure 6.10 summarises the diagenetic history and its relation to porosity, whereas dolomite alteration and evaporite dissolution during mesogenesis enhance porosity in certain restricted areas. Uplift creates an effective leached porosity although formation of secondary limestones (dedolomites) from evaporite dissolution produces local permeability barriers. Late calcite cements

also occlude vuggy porosity and seal small fractures.

Figure 6.10 Relative formation or occlusion of porosity by the different diagenetic events.

Process	Primary Porosity		Porosity Occlusion		Secondary Porosity	
	0	+	0	+	0	+
Deposition						
Early cementation						
Displacive evaporite formation						
Associated dolomitisation						
Pervasive dolomitisation						
Dolomite remobilisation and ferroan dolomite formation						
Replacement by evaporites						
Evaporite dissolution						
Dedolomitisation						
Near-surface leaching						
Secondary calcite cements						
Exposure and leaching						

CHAPTER 7

Whole Rock Geochemistry - Relationships to Facies and Diagenesis

7.1 Introduction

Results of XRF whole rock analyses from the Cadeby Formation and insoluble residue determinations are in Appendix 5; methods of preparation, standards and calibration in Appendices 2, 3, and 4. Results are tabulated in five rock groups; primary limestones, dolomites, secondary limestones, dolomites with evaporites and evaporites. Analyses and degree of calibration of evaporite samples were insufficient for use of precise values. Clastic mudstones were analysed for comparative study only.

Computer plots correlating elements were obtained for all five rock groups; dolomite and limestone analyses were subdivided on facies and results were later manually plotted. Several authors (Billings and Ragland, 1968; Chester, 1965; Jones and Hirst, 1972; Till, 1971) have related whole rock analyses to facies and energy of the depositional environment; Weber (1964) distinguished between "primary" and "secondary" dolostones. The aim of this chapter is to see if facies and/or diagenesis can be related to chemical analyses of specimens from the Cadeby Formation. Sampling was mainly for the initial project; specimens analysed are mainly from the Upper Member and consequently some facies are poorly represented.

7.2 Results

7.2.1 Non-carbonate fraction

Insoluble residue shows excellent correlation with Al_2O_3 plus SiO_2 (correlation factor 0.972) (Fig. 7.1). The slope is steeper than 45° due to insufficient calibration of SiO_2 percentages which are consistently lower than their true values.

Al_2O_3 plus SiO_2 also correlate with TiO_2 (correlation factor 0.83) showing this element to be mainly concentrated in the non-carbonate fraction (Fig. 7.2). The breccia facies shows systematically higher TiO_2 than other facies (correlation factor 0.99); TiO_2 correlates equally with SiO_2 and Al_2O_3 in this facies. This, plus some correlation with Al_2O_3, suggests TiO_2 is present as detrial rutile and in some clay minerals.

No correlation with the non-carbonate fraction nor with Al_2O_3 is shown by the base metals analysed; barium shows a minimal correlation with non-carbonates (Fig. 7.3) (approx. 50 ppm Ba for 10% Al_2O_3 + SiO_2 or 15% insoluble residue) and with Al_2O_3. Jones (1969) and Hirst (1972) found both barium and lead to correlate with clay minerals in the basin facies of the Raisby and Ford Formations (EZ1 carbonates) in County Durham; both elements were further enriched in the platform

Figure 7.1 Plot of Al_2O_3 + SiO_2 v. Insoluble Residue (I.R.).

Key for Figures 7.1 to 7.10

primary limestones		✦
grainstone barriers	dolomite	○
	dolomite (core sample)	◇
	dedolomite	●
siliciclastic carbonates	dolomite	◊
	altered dolomite	◈
breccia facies		△
lagoon mudstones and wackestones		□
lagoon mudstones and wackestones with evaporites		■
dedolomitised lagoon mudstones and wackestones		■
patterned carbonates and anoxic facies from cores		*
dolomites with evaporites		⌖
evaporites with dolomites		☼

oxides are measured in wt.% and elements in ppm.

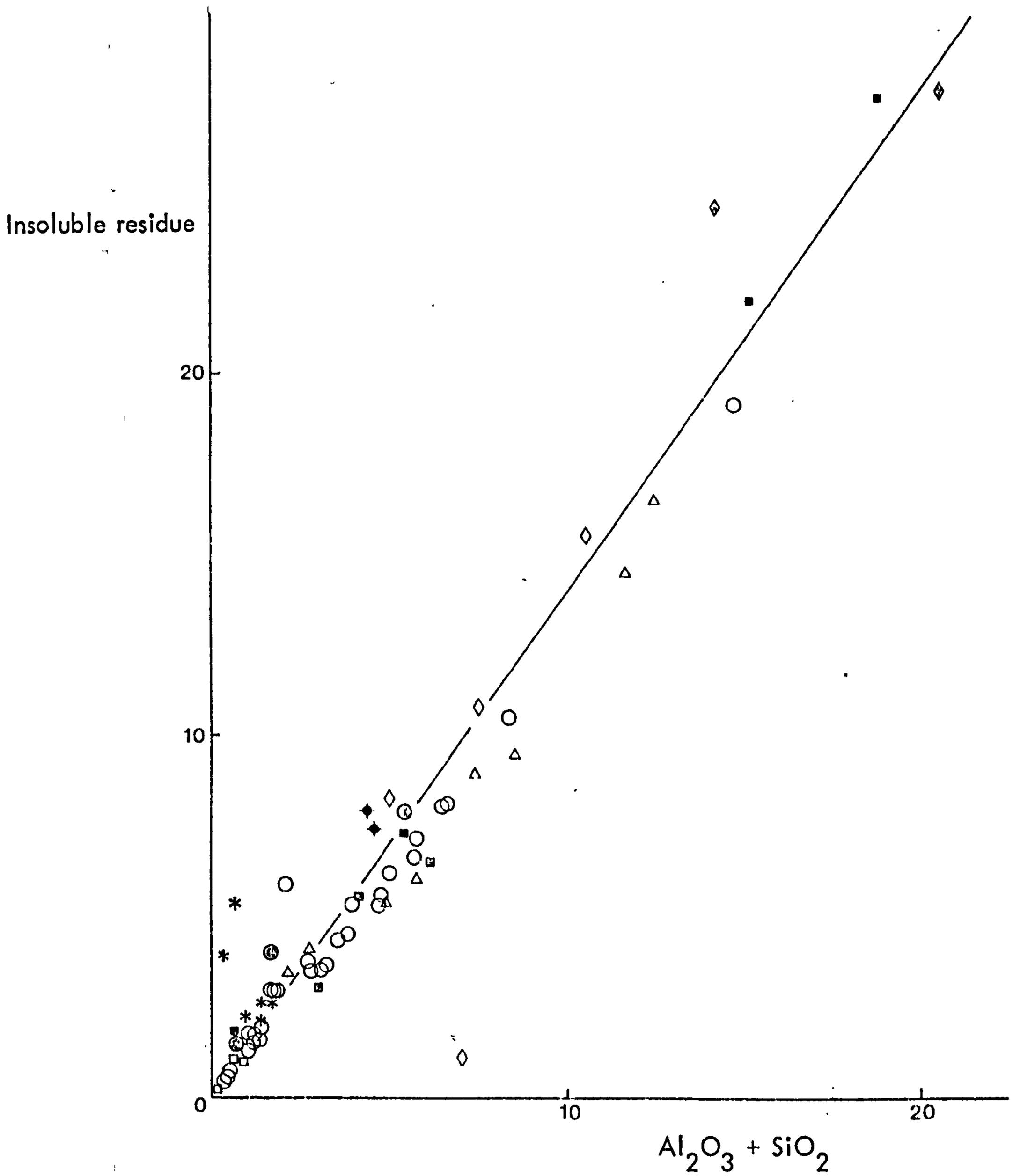
Insoluble residue
20
10
0
10
20
$Al_2O_3 + SiO_2$

Figure 7.2 Plot of Al_2O_3 v. TiO_2

Key for Figures 7.1 to 7.10

primary limestones		✦
grainstone barriers	dolomite	○
	dolomite (core sample)	◇
	dedolomite	◉
siliciclastic carbonates	dolomite	◊
	altered dolomite	◆
breccia facies		△
lagoon mudstones and wackestones		□
lagoon mudstones and wackestones with evaporites		▣
dedolomitised lagoon mudstones and wackestones		■
patterned carbonates and anoxic facies from cores		*
dolomites with evaporites		⌖
evaporites with dolomites		☼

oxides are measured in wt.% and elements in ppm.

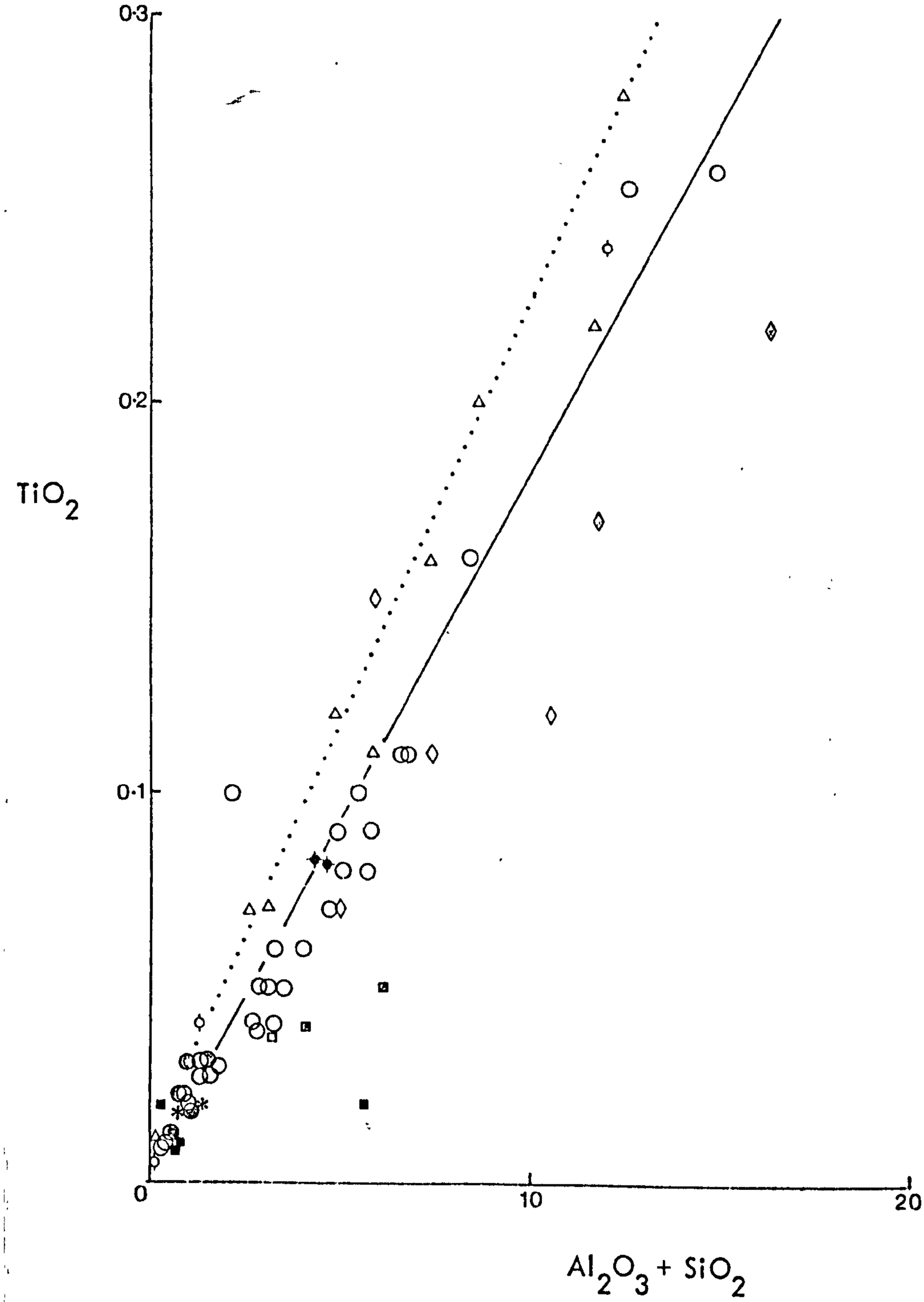
0·3
0·2
0·1
0
10
20
TiO2
Al2O3 + SiO2

Figure 7.3 Plot of $Al_2O_3 + SiO_2$ v. Ba.

Key for Figures 7.1 to 7.10

primary limestones		✦
grainstone barriers	dolomite	○
	dolomite (core sample)	◇
	dedolomite	●
siliciclastic carbonates	dolomite	◊
	altered dolomite	♦
breccia facies		△
lagoon mudstones and wackestones		□
lagoon mudstones and wackestones with evaporites		■
dedolomitised lagoon mudstones and wackestones		■
patterned carbonates and anoxic facies from cores		*
dolomites with evaporites		⌖
evaporites with dolomites		☼

oxides are measured in wt.% and elements in ppm.

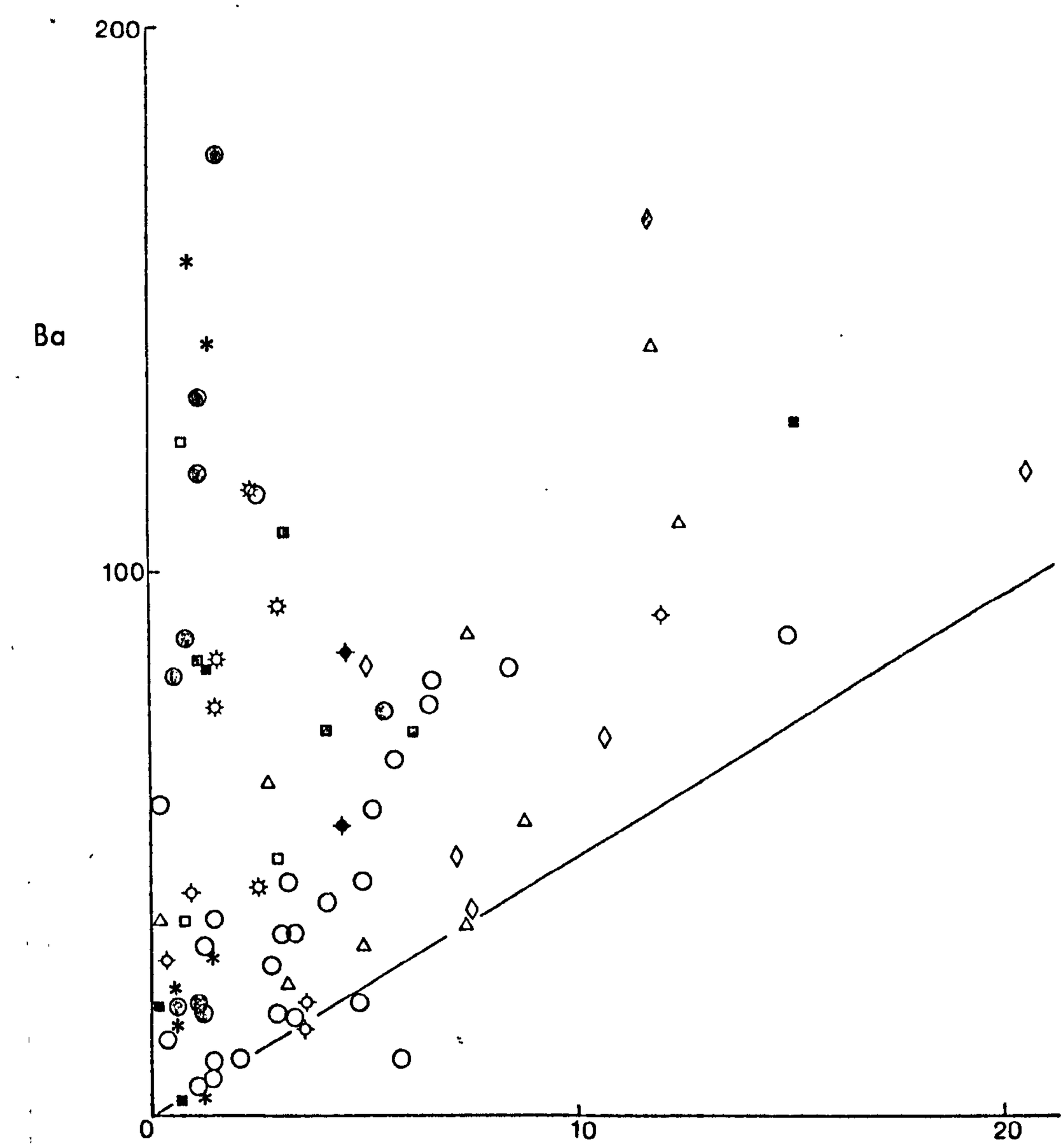
200
100
Ba
0
10
20
$Al_2O_3 + SiO_2$

facies. Only a proportion of the barium in the Cadeby Formation is associated with the non-carbonate fraction (Fig.7.3); both lagoon facies and dedolomites have significantly higher barium contents. Baryte mineralisation is found in lagoon facies (Chapter 8; Harwood, 1980 and in press) but not in the dedolomites; barium concentration here seems related to dedolomitisation processes (7.2.4).

Although some proportion of total iron (as Fe_2O_3)is related to Al_2O_3 plus SiO_2 (Fig. 7.4) and to Al_2O_3 alone, manganese shows no correlation with either. Both sodium and strontium show a minimal correlation with the non-carbonate fraction; some of these elements are therefore present in clay minerals.

Analysis of a stylolite-rich specimen (593) and an adjacent specimen with the stylolite residue removed (591) demonstrated increased Al_2O_3, SiO_2, Na_2O and Zn within the stylolites; other elements showed minimal differences.

7.2.2 Iron and manganese

The range of total iron values is greater in dedolomites than dolomites (Fig.7.4); manganese, in contrast has a higher range in dolomites (Fig.7.5). Both iron and manganese are low in evaporite-rich samples

Figure 7.4 Plot of $Al_2O_3 + SiO_2$ v. Fe_2O_3

Key for Figures 7.1 to 7.10

primary limestones ✦

grainstone barriers
- dolomite ○
- dolomite (core sample) ◇
- dedolomite ●

siliciclastic carbonates
- dolomite ◊
- altered dolomite ♦

breccia facies △

lagoon mudstones and wackestones □

lagoon mudstones and wackestones with evaporites ■

dedolomitised lagoon mudstones and wackestones ■

patterned carbonates and anoxic facies from cores *

dolomites with evaporites ⊹

evaporites with dolomites ☼

oxides are measured in wt.% and elements in ppm.

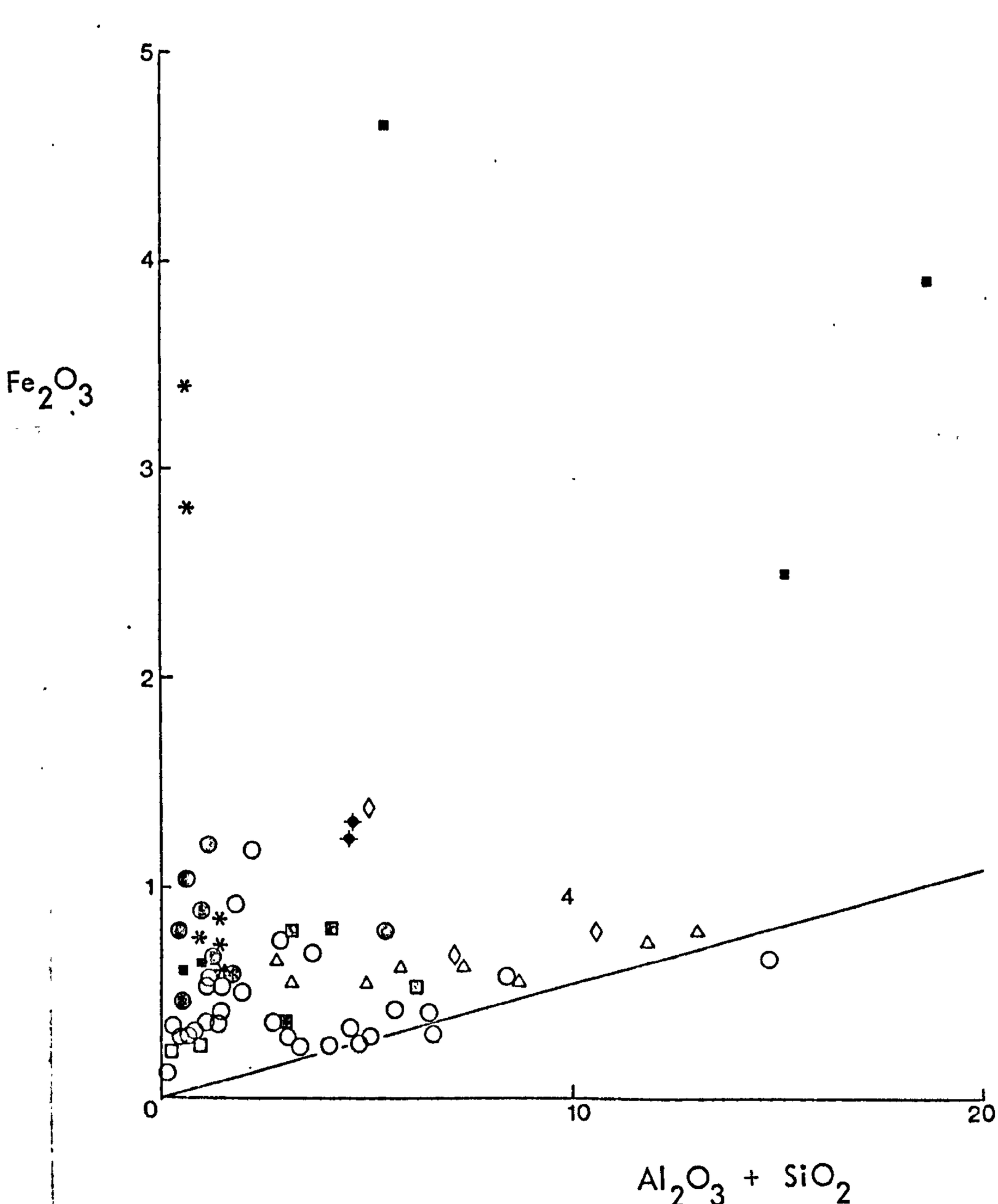
Fe_2O_3
5
4
3
2
1
0
10
20
4
$Al_2O_3 + SiO_2$

Figure 7.5 Plot of Fe_2O_3 v. MnO_2.

Inset shows approximate fields of dolomites, evaporites and secondary limestones.

Key for Figures 7.1 to 7.10

primary limestones

grainstone barriers — dolomite ○
dolomite (core sample) ◇
dedolomite ●

siliciclastic carbonates — dolomite ◇
altered dolomite ◆

breccia facies △

lagoon mudstones and wackestones □

lagoon mudstones and wackestones with evaporites ■

dedolomitised lagoon mudstones and wackestones ■

patterned carbonates and anoxic facies from cores *

dolomites with evaporites ⊙

evaporites with dolomites ☼

oxides are measured in wt.% and elements in ppm.

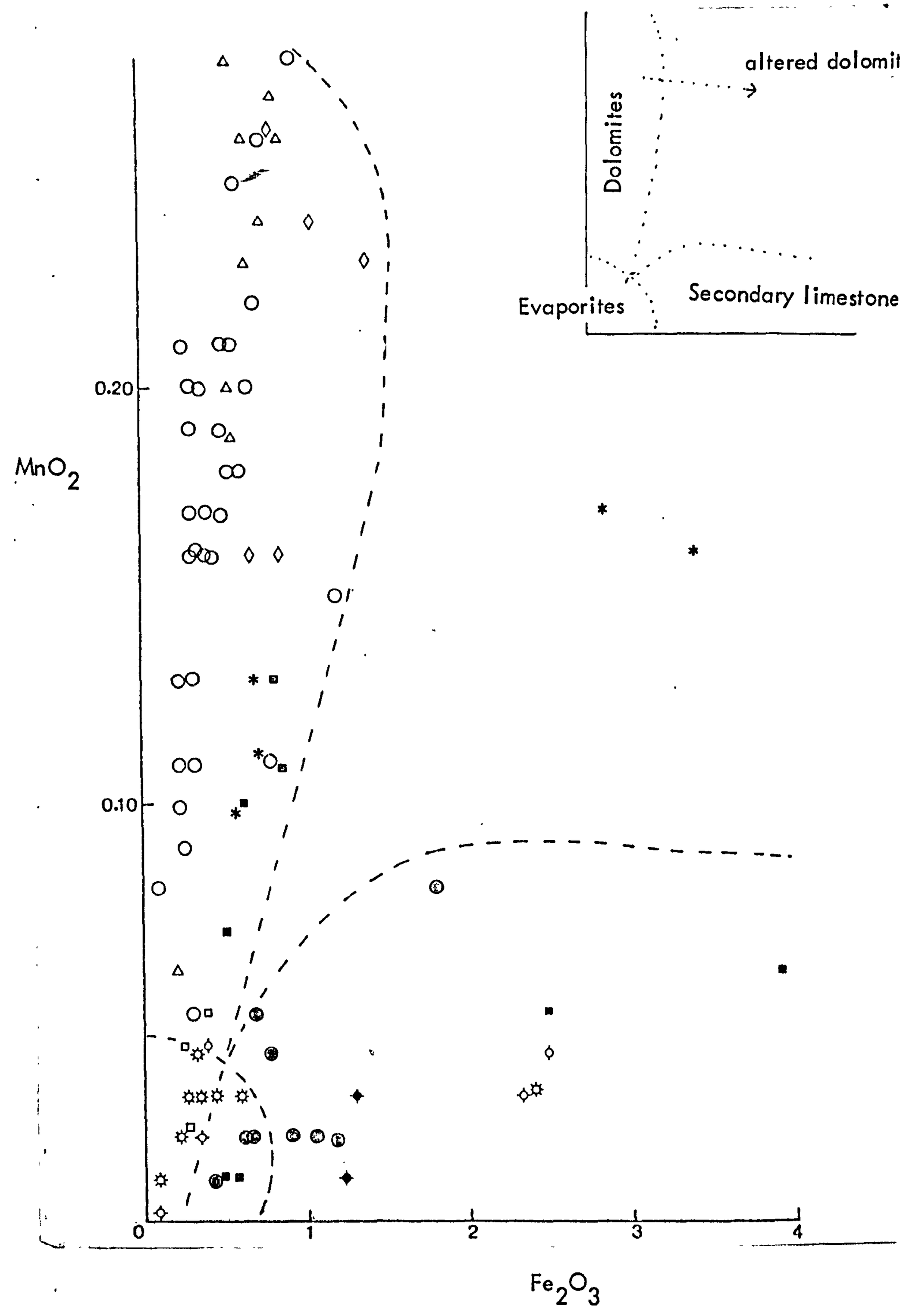
altered dolomites
Dolomites
Evaporites
Secondary limestones
0.20
0.10
MnO_2
0
1
2
3
4
Fe_2O_3

(Fig.7.5). The iron-manganese plot broadly defines the fields of evaporites, dolomites and dedolomites (Fig.7.5) although this breaks down for anoxic facies (Fig.7.5). There is no gradation between dolomites with high manganese contents and dedolomites. This suggests (i) the fluids causing dedolomitisation (5.3) had little or no manganese and (ii) manganese was acquired by the dolomites after formation of the dedolomites, perhaps from surface exposure and weathering of the more porous dolomites. Subsurface samples with low manganese reinforce this hypothesis. Ferroan dedolomites (5.2) have high manganese values and extremely high total iron (Appendix 5); they are easily distinguishable from dedolomites by analysis of these elements.

7.2.3 Strontium

Strontium content is known to vary with carbonate mineralogy; Sr^{2+} substitues for Ca^{2+} within the carbonate lattice. Strontium contents have been used as an indication of the amount of recrystallisation within carbonates (Kinsman, 1969). Subsequent research has shown that (i) the distribution coefficient for strontium (and for barium) increases during rapid crystallisation

(Kitano et al., 1971) and (ii) strontium content in dolomites may decrease with increase in crystal size (Mattes and Mountjoy, 1980; M'Rabet, 1981). Strontium content decrease with increase in crystal size has not been demonstrated in the Cadeby Formation (e.g. specimens 131 and 134, Fig. 4 13 a+b) although the dolomicrites do contain more strontium. However, the dolomicrites are from lagoon facies (Fig 7-6); strontium here may be derived from original evaporites (4.5.2 + 4.5.3).

Anhydrite and gypsum have much higher strontium contents than carbonates (Butler, 1973; Dean and Tung, 1974; Dean, 1980, Table 5-1) (Appendix 5). Specimens from dolomicrites with some replaced evaporites (Appendix 5, specimens 462, 463 and 470) have significantly higher strontium contents; they also have much higher strontium than later calcite spar which fills some vugs after evaporite dissolution (Appendix 5, specimens 451 and 465) (Coleman and Harwood, 1980; Harwood, 1980). Calcitised evaporites, therefore apparently maintain a trace of their origin in these high strontium contents.

Shearman and Shirmohammadi (1969) showed a decrease in strontium in their dedolomites

Figure 7.6 Plot of $MgCO_3$ v. SrO.

Key for Figures 7.1 to 7.10

primary limestones		✦
grainstone barriers	dolomite	○
	dolomite (core sample)	◇
	dedolomite	◉
siliciclastic carbonates	dolomite	◊
	altered dolomite	◆
breccia facies		△
lagoon mudstones and wackestones		□
lagoon mudstones and wackestones with evaporites		■
dedolomitised lagoon mudstones and wackestones		■
patterned carbonates and anoxic facies from cores		*
dolomites with evaporites		☼
evaporites with dolomites		☼

oxides are measured in wt.% and elements in ppm.

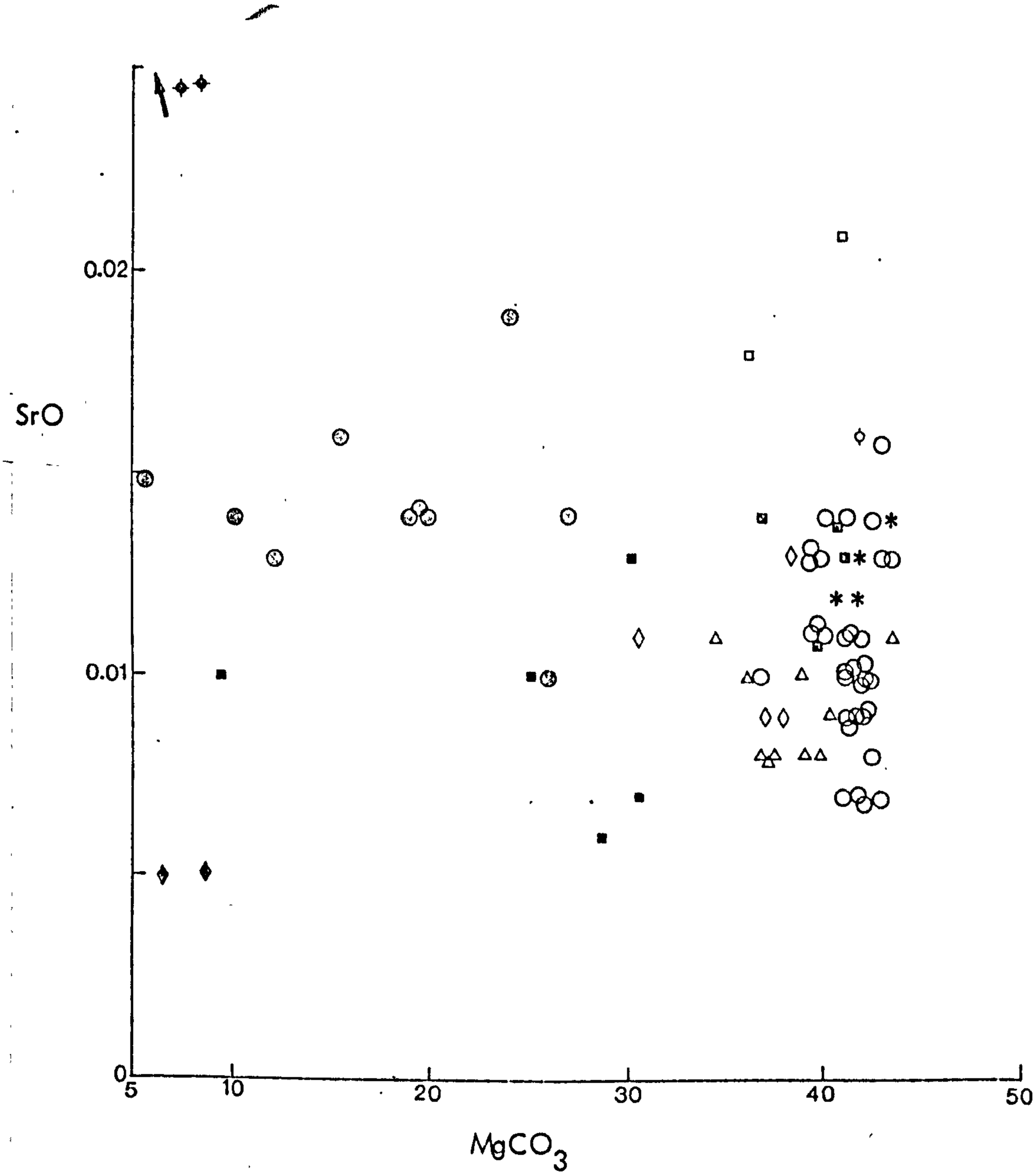
SrO
0.02
0.01
0
5
10
20
30
40
50
MgCO3

compared to nearby dolomites. The two analyses of altered dolomites (Appendix 5, specimens 643 and 644) (5.2) show a very low strontium content; dedolomites (5.3) have similar or higher strontium values than dolomites (Fig.7.6). Jones (1969) demonstrated similar strontium contents in dedolomites from the EZ1 carbonate in County Durham; more recent analyses from the Ford Formation (G. Aplin, pers. comm., 1981) show dedolomites to have higher strontium contents than dolomites. Clark (1980) shows increase in strontium during formation of secondary limestones in the subsurface; secondary limestones formed at the surface have little change in strontium content. The similar of higher strontium values reinforce the earlier conclusion (5.3) that dedolomites (sensu stricto) in the Cadeby Formation were formed by reaction with fluids resulting from evaporite dissolution; altered dolomites analysed are distinct from dedolomites (Fig.7.6). Because, on average, dedolomites and ferroan dedolomites possess higher strontium and/or higher iron contents a broad distinction can be made between dolomites and replaced dolomites by plotting strontium and iron values (Fig.7.7).

Figure 7.7 Plot of Fe_2O_3 v. SrO.

Approximate fields are of primary limestones, secondary limestones and dolomites.

Key for Figures 7.1 to 7.10

primary limestones ✦

grainstone barriers
- dolomite ○
- dolomite (core sample) ◇
- dedolomite ●

siliciclastic carbonates
- dolomite ◊
- altered dolomite ♦

breccia facies △

lagoon mudstones and wackestones □

lagoon mudstones and wackestones with evaporites ■

dedolomitised lagoon mudstones and wackestones ■

patterned carbonates and anoxic facies from cores *

dolomites with evaporites ⌖

evaporites with dolomites ☼

oxides are measured in wt.% and elements in ppm.

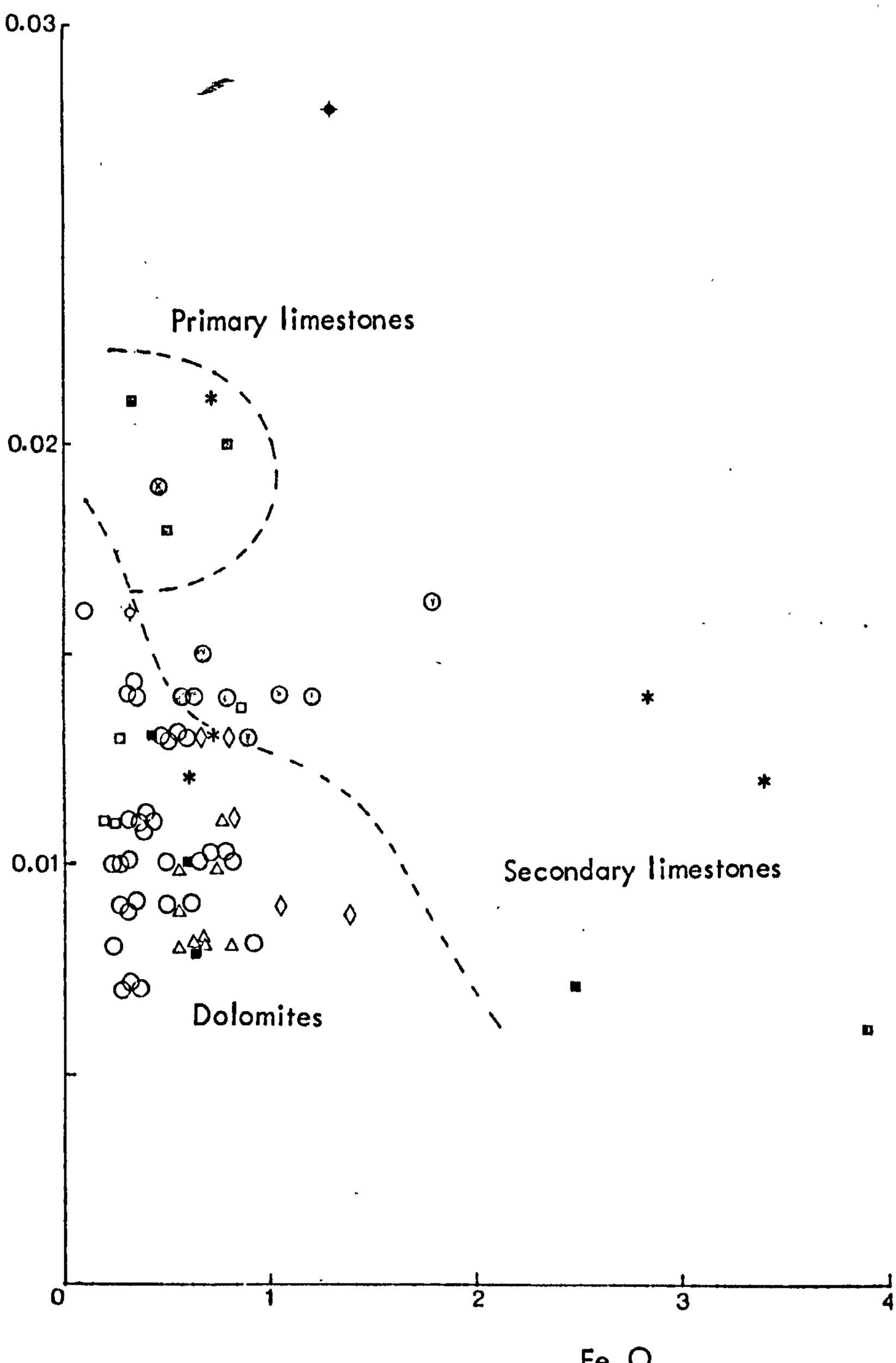
0.03
0.02
0.01
SrO
Primary limestones
Secondary limestones
Dolomites
0
1
2
3
4
Fe2O3

7.2.4 Barium

Barium has a greater range in dedolomites than dolomites; it is also, on average, higher within evaporites (Appendix 5).

Barium shows no facies relationships except for higher values in lagoon mudstones and wackestones. This may be because of barium inclusion within the lattices of former evaporites (Harwood, in press). Evaporite- and eogenetic dolomite fields are defined on a barium/manganese plot (Fig. 7.8); dedolomites fall within the evaporite field or between the two. This again suggests dedolomite origin in evaporite dissolution.

Lagoon mudstones and wackestones subject to penecontemporaneous dolomitisation also plot near evaporites. Friedman (1969) uses barium/manganese and barium/iron plots to distinguish lagoonal (brackish) and marine recent carbonates. His total values are one or two orders of magnitude less than in Cadeby Formation carbonates so such plots cannot be applied here. There is no simple relationship between barium and iron contents in the Cadeby Formation.

7.2.5 Sodium

Sodium values are low in carbonate specimens and are subject to large errors (Appendices 4 and 5). There appears some correlation

Figure 7.8 Plot of MnO_2 v. Ba.

Insert shows approximate fields of evaporites and eogenetic dolomites.

Key for Figures 7.1 to 7.10

primary limestones ✦

grainstone barriers
- dolomite ○
- dolomite (core sample) ⊙
- dedolomite ⊛

siliciclastic carbonates
- dolomite ◇
- altered dolomite ◈

breccia facies △

lagoon mudstones and wackestones □

lagoon mudstones and wackestones with evaporites ▣

dedolomitised lagoon mudstones and wackestones ■

patterned carbonates and anoxic facies from cores *

dolomites with evaporites ⌖

evaporites with dolomites ☼

oxides are measured in wt.% and elements in ppm.

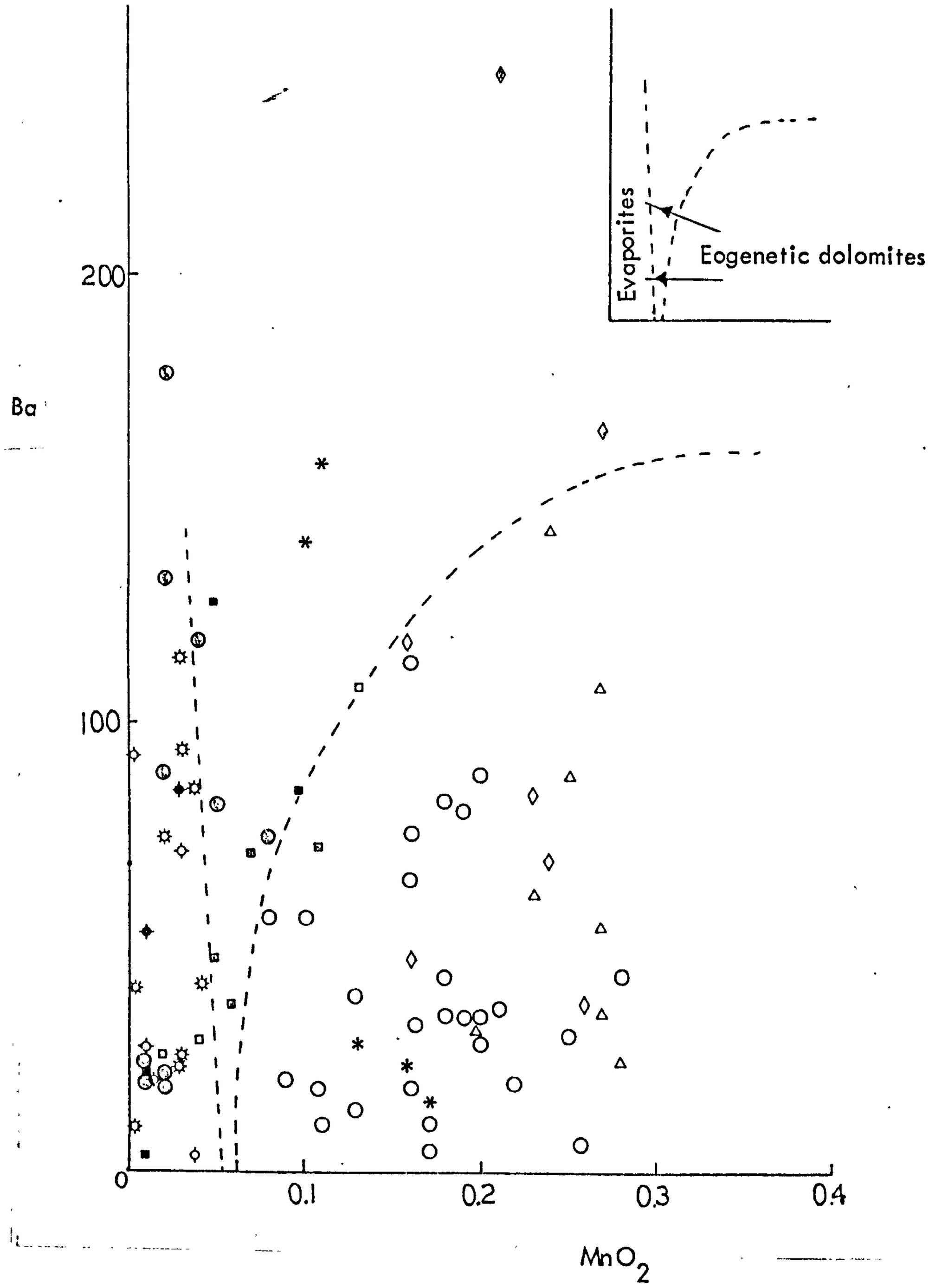
Evaporites
Eogenetic dolomites
Ba
200
100
0
0.1
0.2
0.3
0.4
MnO2

between sodium and strontium, and with Al_2O_3; sodium is partially contained in clay minerals (7.2.1) and therefore shows some relationship with similar elements (e.g. Ba, Fe_2O_3 and TiO_2). Sodium has been used as an indication of facies salinity (Land and Hoops, 1973). However, its inhomogeneous distribution within crystals (Fritz and Katz, 1972; Fritz and Jackson, 1972) and its presence in inclusions (M'Rabet, 1981) lend arguments against its use as a precise determining factor of paleosalinity, in spite of the regional variations displayed by Veizer et al., 1977).

7.2.6 Base metals (Zn, Pb + Cu)

Although initial analyses included chromium, nickel and cobalt with some rare earths (Nb,Y) and zirconium, values determined were very small and differences between specimens few. Remaining specimens were only analysed for zinc, lead and copper.

Base metal contents show no relation to facies, the non-carbonate fraction nor each other. Dedolomites have lower base metal contents than dolomites (Appendix 5); therefore discriminant plots with other elements which show differences between dolomite and dedolomites can be compiled. Zinc is the best

base metal discriminator (Fig.7.9). Loss of base metals with progressive dedolomitisation can be demonstrated by a series of samples (Fig.7.10). Specimens from Skelbrooke (SE 501124) show a linear decrease in zinc with loss of magnesium carbonate (Fig.7.10). Dedolomitisation therefore appears to "flush" base metals from the original dolomite.

7.3 Discussion and conclusions

7.3.1 Facies dependence

Although earlier research suggested reef and other platform facies might be distinguished by trace element contents (Chester, 1965; Billings and Ragland, 1968), Till (1971) found elemental concentrations could only be related to the energy of deposition and hence, indirectly, to the non-carbonate fraction. Thus low energy lagoon and basin facies had both higher trace element contents and higher clay mineral fractions than high energy bafflestone or ooid grainstone facies (Till, 1971).

Jones (1969) and Jones and Hirst (1972) discriminated between basin and platform facies using insoluble residue, barium and base metals. No basin facies were analysed in this study. These results show it is rarely possible to discriminate between

Figure 7.9 Plot of MnO_2 v. Zn.

Key for Figures 7.1 to 7.10

primary limestones		✦
grainstone barriers	dolomite	○
	dolomite (core sample)	◌
	dedolomite	◍
siliciclastic carbonates	dolomite	◇
	altered dolomite	◈
breccia facies		△
lagoon mudstones and wackestones		□
lagoon mudstones and wackestones with evaporites		⊠
dedolomitised lagoon mudstones and wackestones		■
patterned carbonates and anoxic facies from cores		*
dolomites with evaporites		⌖
evaporites with dolomites		☼

oxides are measured in wt.% and elements in ppm.

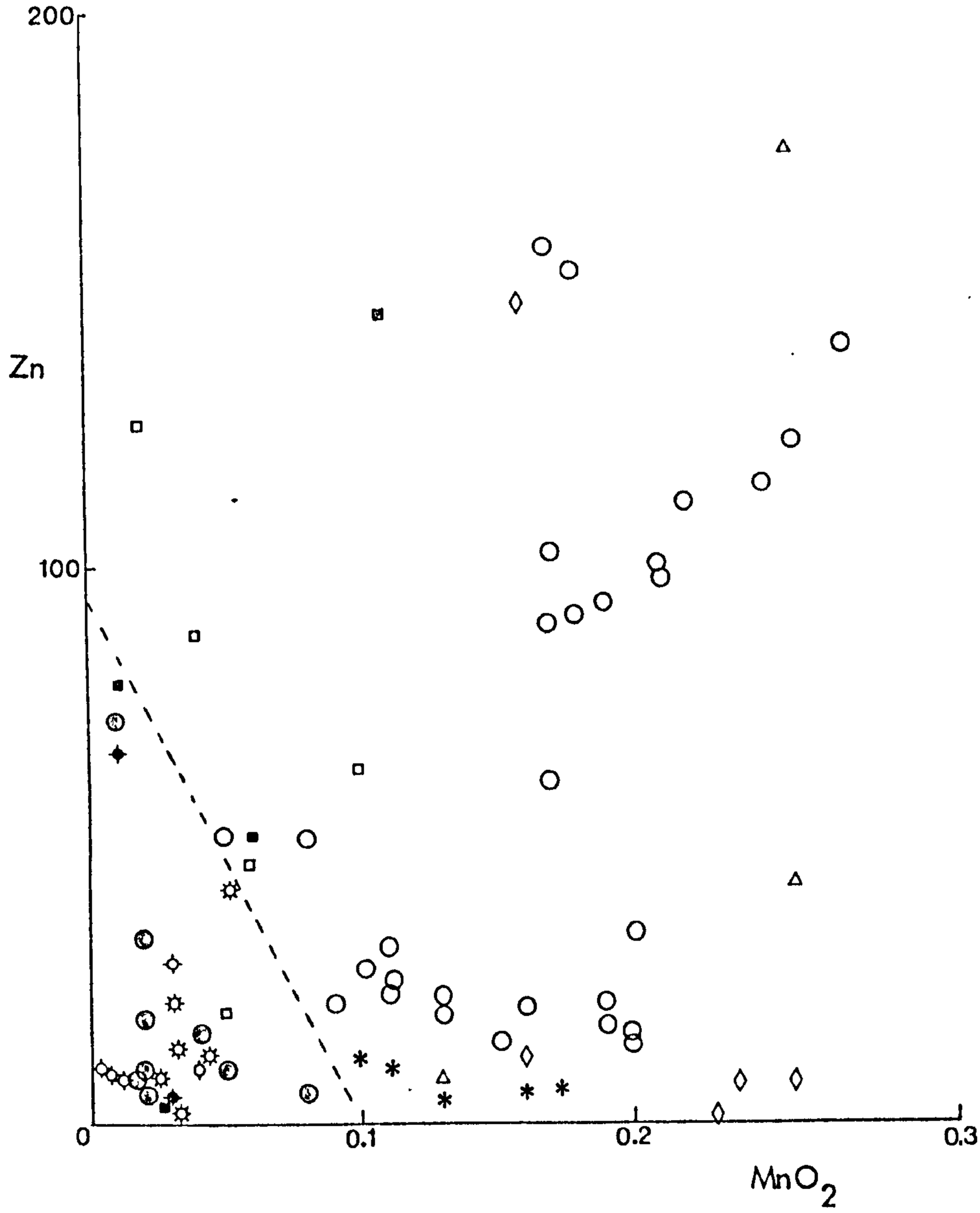
200
100
Zn
0
0.1
0.2
0.3
MnO2

Figure 7.10 Plot of $MgCO_3$ v. Zn.

Dotted line shows change through Skelbrooke section from dolomite (109) to dedolomite (101).

Key for Figures 7.1 to 7.10

primary limestones		✦
grainstone barriers	dolomite	○
	dolomite (core sample)	○
	dedolomite	⊕
siliciclastic carbonates	dolomite	◇
	altered dolomite	◈
breccia facies		△
lagoon mudstones and wackestones		□
lagoon mudstones and wackestones with evaporites		⊟
dedolomitised lagoon mudstones and wackestones		■
patterned carbonates and anoxic facies from cores		*
dolomites with evaporites		☼
evaporites with dolomites		☼

oxides are measured in wt.% and elements in ppm.

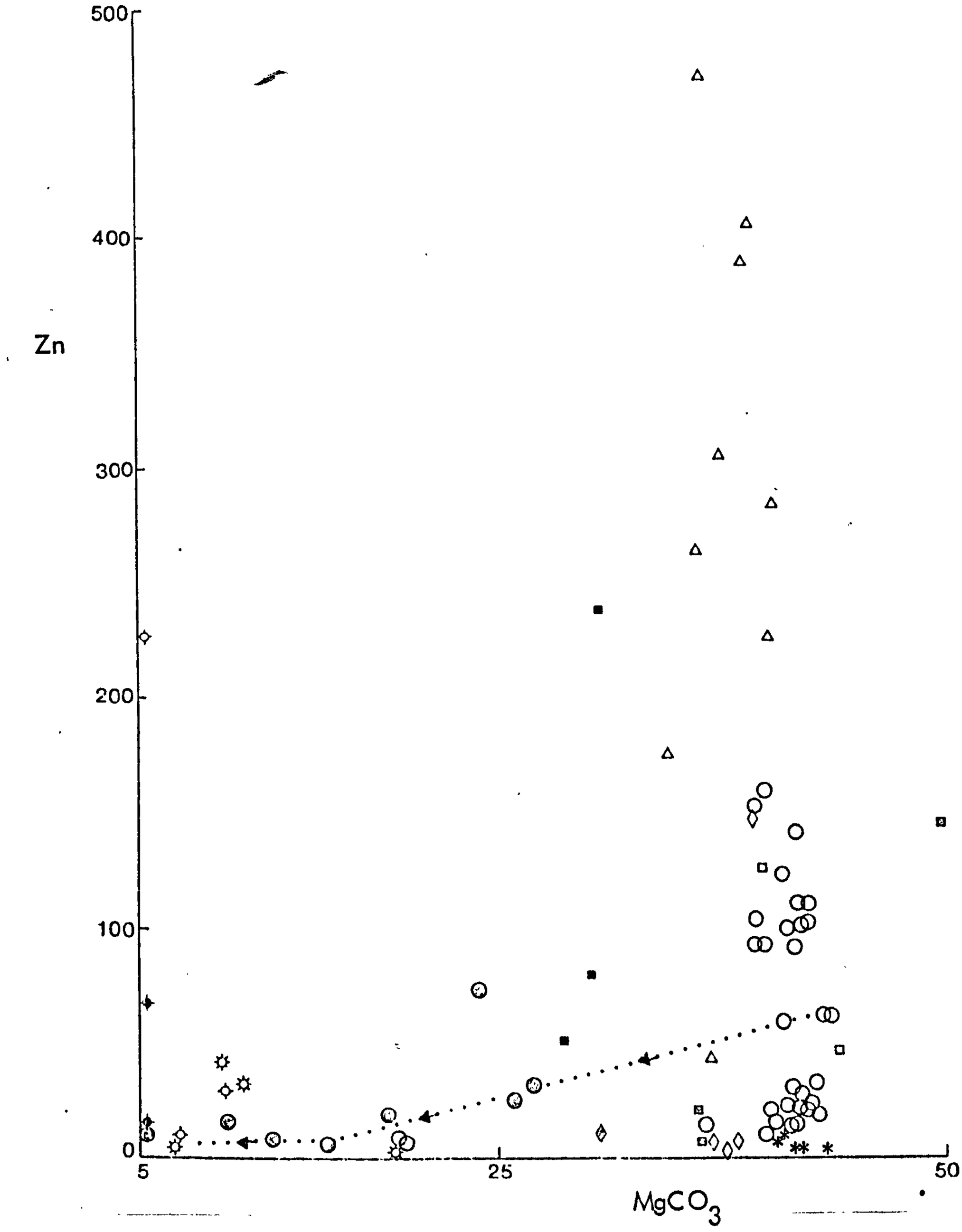
500
400
300
200
100
0
Zn
5
25
50
MgCO3

individual platform facies on geochemistry; the breccia facies (Fig.7.2) and lagoon carbonates (Figs.7.2, 7.5a, 7.6, 7.7 and 7.8) are the major exceptions. However, analyses of the lagoon wackestones and mudstones were few and differences are also probably related to diagenetic history (7.3.2).

7.3.2 Dependence on diagenetic history

Weber (1964) showed higher concentration of Al, Ba, Fe, Zn and Na (with K and Li) in "primary" dolostones, whereas Sr was higher in "secondary" dolostones. No dolomites within the Cadeby Formation are primary (Chapter 4); whole rock analyses do, however, seem to distinguish penecontemporaneous dolomites, the lagoon wackestones and mudstones (4.5.2 + 4.5.3) with an average higher Sr, Ba and Zn and lower Na than other, eogenetic dolomites. More analyses of penecontemporaneous dolomites are necessary to support this hypothesis.

Whole rock analyses also show distinctions between ferroan dolomites (high Fe and Mn, low Sr), dedolomites (average Sr + Fe, high Ba and low base metals) and calcitised evaporites (high Sr). The distribution of the elements in these three secondary

limestones reinforces the hypothesis of their diverse origins presented in Chapter 5 (Table 5-3).

7.3.3 Conclusions

Whole rock XRF analyses of the Cadeby Formation are of little use in facies determination but they may possibly distinguish different diagenetic events. Analyses suggest:

(1) Penecontemporaneous dolomites can be discriminated from eogenetic dolomites

(2) Dedolomites demonstrably result from evaporite dissolution and consequent reaction with sulphate-rich fluids. A few analyses of calcitised evaporites suggest these can also be discriminated by their high strontium content.

(3) Ferroan dedolomites are geochemically distinct from dedolomites.

There is further scope for following these results using more specimens from each facies and relating these more closely to diagenetic history. Many of the aspects included in Chapter 6 have not been covered in this study. However, whole rock analysis is a

clumsy tool in carbonate geochemistry as it amalgamates the many different values shown by more detailed petrography and analysis. Examples are the element variations within single crystals (e.g. Fig. 5.4a, b + c) and the differences in composition between constituent allochems (Brand and Veizer, 1980).